Influence of cooling rate on residual stresses and chipping of porcelain on zirconia restorations

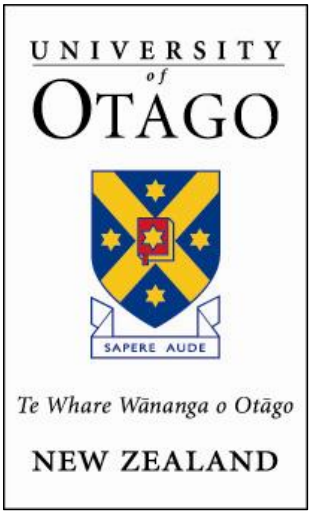

Basil Al-Amleh
BDS (Otago)

A thesis submitted in partial fulfilment for the degree of

Doctor of Clinical Dentistry in Prosthodontics

At the Department of Oral Rehabilitation
University of Otago, Dunedin
New Zealand
2011

PUBLICATION AND PRESENTATION

Publication arising from this thesis

Al-Amleh B., Lyons K., and Swain M. (2010), 'Clinical trials in zirconia: A systematic review', *J Oral Rehabil*, 37, 641-652.

Poster presentation:

Al-Amleh B., Waddell N., Lyons K., Jansen Van Vuuren L., He C., Swain M., 'Influence of cusp veneering porcelain thickness and cooling rate on residual stresses in zirconia crowns' **International College of Prosthodontists**, 14th Biennial Meeting, Big Island of Hawaii, September 8th – 12th 2011

ABSTRACT

Cohesive failure of veneering porcelain, or chipping, has been recognised as the main disadvantage of zirconia-based restorations. This is believed to be due to a propensity to develop large thermal gradients within the veneering porcelain layer when the restoration cools from the sintering temperature to room temperature. Recent literature draws attention to the vastly different thermo-physical properties of zirconia compared to other core materials, in particular to its very low thermal conductivity.

When the veneering porcelain in a zirconia restoration is cooled at a fast rate from above to below the glass transition temperature during the final firing cycle, high residual tensile zones develop within the veneering porcelain. These tensile zones act as weakness zones within the veneering porcelain that increase the risk of fracture. Thus slow cooling protocols are currently recommended for zirconia-based restorations to reduce the development of high residual tensile zones, and therefore reduce the risk of chipping fractures.

In addition to the cooling rate, the thickness of the veneering porcelain has also been identified as a contributing factor by further increasing thermal gradients from the outer cooling surface of the veneering porcelain to the inner porcelain close to the zirconia core. So far there are no studies that have integrated the relationship between veneering porcelain thickness, cooling rates, and differences in surface residual stresses on anatomical zirconia molar crowns.

This research is composed of three parts: Part I (chapter 2) is a comprehensive review of the published clinical trials on zirconia-based restorations. Part II (chapter 3) investigates residual stresses on the cusp tips of fast cooled and slow cooled zirconia molar crowns with various cusp thicknesses. In part III (chapter 4), fast and slow cooled molar zirconia crowns were tested under static loading-to-failure in order to qualitatively compare differences in failure modes and fracture features using fractographic analysis. Furthermore, quantitative assessment of the maximum load-to-failure in both groups was also undertaken to establish any strengthening effects developed by the tempering process on the fast cooled zirconia crowns.

Methods & Materials:

Part I:

A comprehensive review of *in vivo* trials involving zirconia-based restorations featuring in MEDLINE and PubMed between 1950 and June 2011 was completed. A manual hand search of relevant dental journals was also completed.

Part II:

Six identical Procera zirconia copings (Procera, Nobel Biocare), pressed with IPS e.max ZirPress (Ivoclar Vivadent) and layered with IPS e.max Ceram (Ivoclar Vivadent) based on a mandibular molar form, were divided into 3 groups to the following flattened cusp heights: 1mm, 2mm, and 3mm. Half the samples were slow cooled during the final glazing cycle and the other half fast cooled. To determine residual surface stresses, 4 cusps on each crown were indented using a Vickers microhardness indenter under a load of 10N. Crack measurements were made on calibrated photographic images taken immediately after each indentation using an optical light microscope and a mounted digital camera.

Part III:

Ten identical Procera zirconia copings, pressed with IPS e.max ZirPress based on a mandibular molar form, were divided into 2 groups. Half the samples were slow cooled during the final glazing cycle and the other half fast cooled. Following cementation of the zirconia crowns to epoxy resin abutments using Rely-X Unicem (3M ESPE), the disto-lingual cusp of each crown was subjected to a simulated occlusal adjustment prior to loading-to-failure using a universal testing machine. This was done using a 4mm diameter stainless steel ball at a cross-head speed of 0.1mm/min. Qualitative fracture analysis of each fractured sample was initially carried out by a visual interpretation. Two samples from each group were chosen for examination by scanning electron microscopy.

Results:

Part I:

Nineteen clinical trials involving zirconia-based restorations were found. Fifteen were conducted on fixed partial dentures, and 4 on single crowns, of which 14 were based on soft-milled zirconia, and 5 on hard-milled zirconia. Chipping of veneering porcelain was a common occurrence, and framework fracture was only observed in soft-milled zirconia.

Part II:

Residual surface compressive stresses were recorded for all fast cooled crowns. In contrast, surface residual tensile stresses were recorded on the cusp tips of all slow cooled zirconia crowns. The highest residual compressive stresses were found on fast cooled 1mm thick porcelain cusps (-13.08 MPa) which was significantly higher than the 2mm and 3mm fast cooled crowns ($P < 0.05$). There was a significant linear trend for residual stress to decrease as thickness of the veneering porcelain increased in the fast cooled group ($P < 0.05$). There was no statistical significant difference between the 2mm fast cooled and 3mm fast cooled samples ($P > 0.05$). The highest residual tensile stresses were recorded for the 2mm thick cusp crown in the slow cooled group (5.36 MPa), however there were no significant statistical differences in the various cusp heights for the slow cooled group ($P = 0.05$).

Part III:

The average maximum load-to-failure for the fast cooled group was slightly lower than that recorded for the slow cooled group (901.54 N and 1013.00 N respectively), however this difference was not statistically significant ($P > 0.05$). Fractographic analyses confirmed the presence of differential residual stress profiles in the veneering porcelain of fast cooled zirconia crowns by the presence of high concentrations of twist hackles, compression curls, and multi-plane fractures, which were not observed in the slow cooled zirconia crowns.

Conclusions:

Part I:

Based on the limited number of short-term *in vivo* studies involving zirconia-based restorations, there is a high incidence of veneering porcelain chipping, affecting every brand of zirconia, in both single crowns and fixed partial dentures. These clinical trials report on restorations fabricated before the implementation of the modified manufacturers' recommendation of slow cooling zirconia-based restorations. Further long-term prospective studies that address the cooling protocol around the glass transition temperatures of the veneering porcelains are necessary to establish the best manufacturing process for zirconia-based restorations.

Part II:

The results confirm that residual surface compressive stresses at the cusp tips were significantly higher in the fast cooled crowns than the slow cooled crowns. Increasing the thickness of the veneering porcelain in zirconia molar crowns did not cause an increase in the resultant surface residual stresses possibly due to variation in the anatomical contours of veneering porcelains. Moreover, a reverse trend was found when decreasing the thickness of veneering porcelain from 2mm to 1mm cusp tips in fast cooled crowns.

Part III:

Fast cooling zirconia crowns did not improve fracture resistance under static loading-to-failure. In addition, crack propagation and fracture patterns were highly influenced by the cooling protocols used.

ACKNOWLEDGEMENTS

"*Alhamdulillah*" for blessing me with more than just strength and health to do this work until it was complete.

I have the pleasure to thank the many people who made this thesis possible. It is difficult to overstate my gratitude to my supervisors, especially to Prof Michael Swain, for his patience, motivation, enthusiasm and immense knowledge. I am indebted to him more than he knows. I would like to also thank Karl Lyons, for convincing me a few years ago to come back to the School of Dentistry and do a Clinical Doctorate in Prosthodontics, in addition to his "hawk eye" while reading my thesis. Thank you to Neil Waddell, Chris He, and Ludwig Jansen van Vuuren for always being accessible and willing to help with this research, but most importantly, in problem solving the often encountered challenges. I could not have imagined having a better group of supervisors and mentors for my Doctorate research. My sincere thanks go to Dr Vincent Bennani for his help and guidance during my first research topic which unfortunately never took off due to technical difficulties.

I would also like to thank Ms. Sawsan Al-Shamaa, lecturer in quantitative analysis, AIS St Helens, Auckland, and Dr Momen Atieh for the statistical analyses; Liz Girvan for her assistance with the scanning electron microscope; Wendy Jansen van Vuuren for the Procera scanning; Steve Swindells for equipment used during sample preparations; Husain Al-Badry, Zeyad Swaid and Tony Chiu for the IT support; as well as Nobel Biocare and Sir John Walsh Research Institute, University of Otago, for their generous research grants.

My time as a postgraduate student could not have been more enjoyable without the friendship and support of my fellow postgraduate colleagues, including my classmate Constance Law, along with many others. Special thanks go to Mike Smith, for the endless debates which we entertained each other with, in matters outside our patients' care. Those days will be greatly missed. I also would like to acknowledge Dr Don Schwass, for not

only being a thorough clinical supervisor, whom I have learned immensely from, but also for his encouragement and friendship over the past two years.

My wife and I have always been extraordinarily fortunate in making great friendships wherever we went. A special thank you goes to all our friends whom we missed while in Dunedin, such as Arif, Noor, Mazen, Ghassan and Fady, and the Al-Badry, Swaid, Al-Jouborys, Al-Hassani, Moharam, and Lotfy families and many more. We are also grateful for all the new friendships made while in Dunedin, such as Khalid Musaad, Rami Farah and family, Momen Atieah and family, Ghassan Hamid and family, Nabeel Al-Sabeeha and family, and the Al-Tamimi family, to name a few. You've all been our family away from home. Thank you to Ahmad Mustafa and Abdulla Mustafa for the weekly get together too.

Finally, I would like to express my sincere gratitude to my wonderful parents-in-law and the rest of the family, for their support with our decision which took us away from them.

DEDICATION

Where would I be without of my family?

To my parents. I thank you, mum and dad, for believing in me more than I did myself, every step of the way. Your endless prayers, support, and love are a gift I could never repay.

To Osama and Mohammed, my best friends and caring siblings, thank you for always being supportive and full of encouragement no matter what I do.

Words fail me to express my appreciation to my beautiful wife and best friend Nada, whose dedication, love and persistent confidence in me, has taken the load off my shoulders. I owe her for unselfishly letting her intelligence, passions, and ambitions collide with mine. Thank you for understanding my constant absences, thank you for our beautiful children, Saleh and Maryam, and most importantly, thank you for making it easy for me by making it hard on yourself.

TABLE OF CONTENT

LIST OF TABLES

LIST OF FIGURES

LIST OF ACRONYMS & ABBREVIATIONS

BSD	back scatter electron detector
CAD/CAM	computer aided design/computer aided manufacture
CTE	coefficient of thermal expansion
DB	disto-buccal
DL	disto-lingual
DR	distal ridge
FEA	finite element analysis
FPD	fixed partial denture
GIC	glass ionomer cements
HIPed	hot isostatic pressed
IRFPD	inlay retained fixed partial dentures
LTD	low temperature degradation
MB	meiso-buccal
Mg-PSZ	magnesium doped partially stabilised zirconia
ML	mesio-lingual
PJC	porcelain jacket crown
SBS	shear bond strengths
SEM	scanning electron microscope
TIF	tagged image file
Tg	glass transition temperature
UV	ultraviolet
Y-TZP	yttria stabilised tetragonal zirconia polycrystalline
ZTA	zirconia-toughened alumina

α	coefficient of thermal expansion
ΔT	temperature difference
q	cooling rate
l	half thickness of plate
k	thermal diffusivity
$\rho\ max$	maximum stress
K	function of specimen geometry
E	modulus of elasticity
K_{IC}	fracture toughness
H	hardness
c	length of radial crack
P	load applied
κ	constant
Y	half-penny surface crack
σ	residual stress

CHAPTER 1
LITERATURE REVIEW

1.0 A BRIEF HISTORY OF DENTAL CERAMICS

The first known ceramic article dates back to 23,000 B.C. (Savage 1965). The earliest pottery vessels however, were found in the Yuchanyan cave in South China and date from 16,000 B.C (Boaretto et al. 2009). These ceramic items were made of earthenware and stoneware ceramics, primarily composed of a mix of clay, kaolin, quartz and feldspar. These ceramics were fired at relatively low temperatures and were easily chipped. They were also opaque and usually coloured grey or brown because of impurities in the clay used for their manufacture (Dodd et al. 1994). Translucent porcelain on the other hand, was first pioneered during the King-te-chin's dynasty in China about 1000 A.D (Savage 1965). This porcelain material was much stronger than the earlier earthenware and stoneware ceramics, and more importantly, they were used to produce white translucent vessels with very thin walls of only 2 to 3mm.

Porcelain was first suggested for use in dentistry by the French dentist Fauchard in 1728 (Capon 1927). In his publication "Art of Dentistry" (1728), he writes: "... I might from this not only perfectly imitate the enamel of teeth, but the gum, in cases where it is necessary to replace the teeth in whole or parts of sets". These early dental porcelains were used in the fabrication of porcelain denture teeth and porcelain dentures (Jones 1985). The following two centuries saw great leaps in the development of dental porcelains. This is largely due to the interest in porcelain because of its favourable properties, such as fracture toughness, wear properties, biocompatibility, corrosion resistance, nonporous surface, cleansability and hygiene, as well as resistance to staining and odours compared to other available materials at that time. It has been recorded that to overcome the foul taste and odour of his ivory dentures, George Washington used to soak them in an alcoholic beverage, namely port (Guerini 1909).

Using burnished gold and platinum foils in order to make a matrix for high fusing porcelains, Land in 1886 was the first to introduce fused feldspathic porcelain inlays and crowns, for which he was granted a patent a year later (Jones 1985). Nevertheless, the brittle nature of feldspathic porcelain and its inability to withstand deformation strain of more than 0.1 – 0.3% without fracture has limited the widespread use of Land's porcelain jacket crowns (PJC). It was almost 80 years later when McLean and Hughes (1965) introduced their alumina oxide-reinforced ceramic in order to overcome the low strength of the conventional PJCs, that all-ceramic restorations re-emerged into the dental scene (McLean et al. 1965). At that time however, the technique for fusing porcelain to cast-metal cores was being developed, and produced restorations of superior strength and clinical performance compared to PJC restorations, in addition to acceptable aesthetics (Johnston et al. 1958). The role of the metal substructure is to strengthen the veneering feldspathic porcelain by providing support, as well as to suppress internal crack propagation (Kelly 2004). It wasn't long until the metal-ceramic system was used in almost all aspects of fixed prosthodontics, such as single crowns, as well as anterior and posterior long-span fixed partial dentures (FPDs) with high long-term success (Creugers et al. 1994; Walton 1999; Tan et al. 2004). Indeed, metal-ceramic restorations remain the gold standard in terms of predictability and long-term success (Raigrodski 2004b). Despite that however, the interest and demand for non-metallic restorations has increased for clinicians and especially patients.

Other than the aesthetic advantages of all-ceramic restorations, there are a number of benefits to eliminating the metal substructure in fixed restorations. The possibility of violating the biological width and iatrogenic periodontal disease can be reduced by maintaining slightly supragingival margins in all-ceramic restorations, instead of placing the finish line of the preparation at the free gingival margin or slightly below as is necessary for metal-ceramic restorations in order to hide the dark shadow produced by the metal (Crispin et al. 1981). Furthermore, metal-ceramic restorations are more prone to overcontouring than all-ceramic restorations due to the increased need for facial reduction (Yuodelis et al. 1973; Donovan et al. 2004). Finally, metal-free ceramic systems eliminate the problem of alloy hypersensitivity found in a small percentage of the population (Gökçen-Röhlig et al. 2010).

1.1 ALL-CERAMIC SYSTEMS

Ceramics are a composite of metallic and non-metallic elements that are mixed in various amounts to form a glassy matrix that is either lightly or heavily filled with particles (Anusavice 2003; Kelly 2008). Currently, dental ceramics fall into three main categories, depending on the glass and filler content:

- Predominantly glass
- Particle-filled glass
- Polycrystalline

Dental ceramics that are predominantly glass, such as feldspathic porcelains, best mimic the optical properties of both enamel and dentine. Glasses are three-dimensional networks of silica (SiO_2) and potash feldspar ($K_2O \bullet Al_2O_3 \bullet 6SiO_2$) or soda feldspar ($Na_2O \bullet Al_2O_3 \bullet 6SiO_2$), or both (Anusavice 2003). They do not have any regular pattern, and therefore they are amorphous structures. Optical effects that enhance their aesthetics and give vitality to the restorations, such as opalescence, colour, and opacity are usually controlled by small amounts of filler particles such as pigments and opacifiers. These also alter important properties of the glass, namely the firing or fusion temperature, and thermal coefficient of expansion. Feldspathic porcelains have low flexural strengths and fracture toughness, and therefore must be reinforced by a core substructure in order to prevent catastrophic bulk fractures under occlusal loads (Etemadi et al. 2006). Guazzato et al. demonstrated that in bilayered dental ceramics, the property of the layer on the bottom surface dictates the ultimate strength of the specimen. This is because it is this layer that is subjected to the peak tensile stresses during loading (Guazzato et al. 2004c). In other words, feldspathic porcelains are more suitable as the aesthetic layer veneered on a core substructure (ceramic or metallic) which provides the support and strength to the bilayered system.

Ceramic cores in bilayered all-ceramic restorations are either particle-filled glasses or polycrystalline ceramics (Kelly 2008). The difference between those two ceramics is that the later contains no glass, and is a matrix of non-translucent alumina oxide or zirconium oxide which must be veneered to create natural-like aesthetics. On the other hand, some particle-filled glass ceramics, such as IPS Empress I and IPS e.max Press (Ivoclar Vivadent, Schaan, Liechtenstein) do not necessarily need to be veneered by feldspathic

porcelain for aesthetics, since they contain sufficient glass to result in semi-translucent restorations with enhanced light transmission (Conrad et al. 2007). Examples of monolithic and bilayered all-ceramic restorations are listed in table 1-1.

Of all the currently available ceramic systems, zirconia is the only ceramic which is indicated for fabrication of all-ceramic crowns and FPDs in both the anterior and posterior of the mouth (Raigrodski 2004b; Conrad et al. 2007). This is because mechanical properties of zirconia are the highest ever recorded for any dental ceramic, thus permitting the reduction of core thickness and the fabrication of long-span fixed prostheses (figure 1-1).

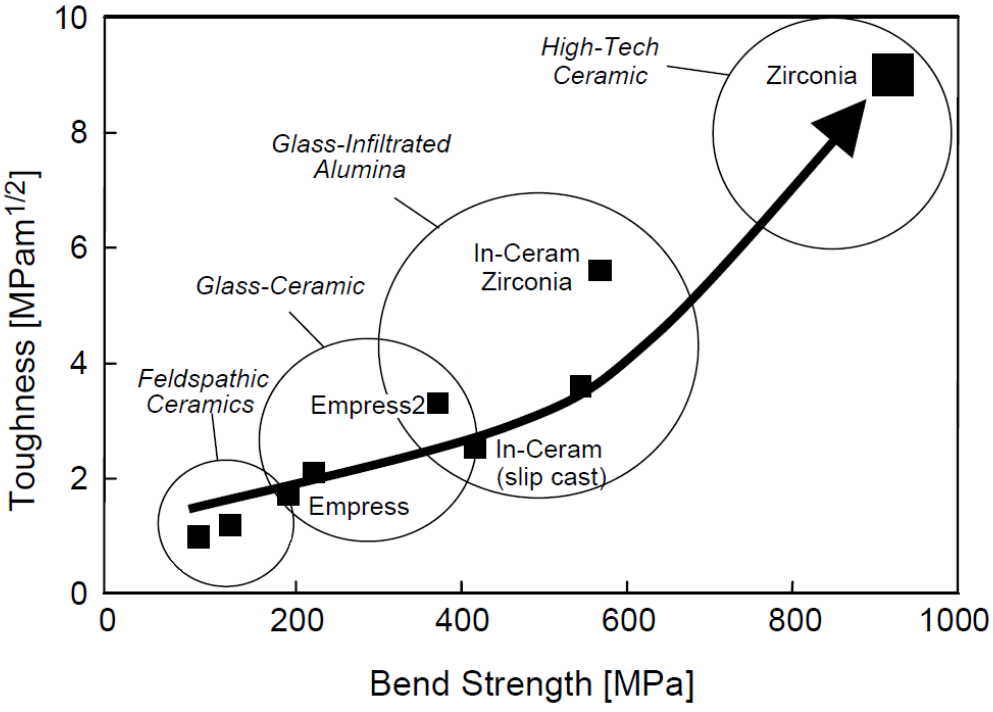

Figure 1-1: Mechanical properties of dental ceramics (modified from Luthy et al. 2005)

Table 1-1- Example of dental ceramics for all-ceramic systems; Ivoclar Vivadent, Schaan, Liechtenstein; Vita, Bad Sackingen Germany; Nobel Biocare, Zurich, Switzerland (from Raigrodski 2004a; Guazzato et al. 2002; Albakry et al. 2003, Kelly 2008)

Type of ceramic	Material	Purpose	Example systems	Manufacturing technique	Flexural strength (MPa)	Fracture toughness ($MPa\text{-}m^{1/2}$)
Predominantly glass	Feldspathic porcelain	Veneering porcelains	IPS e.max Ceram (Ivoclar Vivadent) IPS e.max ZirPress (Ivoclar Vivadent)	Hand layered Heat pressed	100 110	0.7 – 0.93
Particle-filled glass (High glass content)	Leucite reinforced ($SiO_2 \bullet Al_2O_3 \bullet K_2O$)	Monolithic restorations or Core ceramic	IPS Empress (Ivoclar Vivadent)	Heat pressed	182	1.77
(Low glass content)	Lithium disilicate ($SiO_2 \bullet Li_2O$)	Monolithic restorations or Core ceramic	IPS e.max Press (Ivoclar Vivadent) IPS e.max CAD (Ivoclar Vivadent)	Heat pressed, milled	300-400	2.8 - 3.5
	Glass-infiltrated alumina oxide	Core ceramic	In-Ceram Alumina (Vita)	Slip cast, milled	236-600	3 - 4.5
	Glass-infiltrated alumina oxide with 35% partially stabilised zirconia	Core ceramic	In-Ceram Zirconia (Vita)	Slip cast, milled	421-800	6 - 8
Polycrystalline (No glass content)	Alumina Oxide (Al_2O_3)	Core ceramic	Procera Alumina (Nobel Biocare)	Densely sintered	400	4.5 - 6
	Zirconia (3mol%Y-TZP)	Core ceramic	Procera Zirconia (Nobel Biocare)	Milled	900-1200	9 - 10

1.2 POLYCRYSTALLINE ZIRCONIA

1.2.1 Properties of zirconia

Zirconia is unique in its polymorphic crystalline makeup, in that it occurs in three temperature dependant forms that are: monoclinic (at room temperature to 1170^{o}C), tetragonal (1170^{o}C – 2370^{o}C) and cubic (2370^{o}C – up to melting point) (figure 1-2) (Denry et al. 2008). However, when stabilising oxides such as yttria, magnesia, ceria, and calcia are added to zirconia, the tetragonal phase is retained in a metastable condition at room temperature, enabling a phenomenon called phase transformation toughening to occur (Kelly et al. 2008a). The partially stabilised crystalline tetragonal zirconia, in response to mechanical stimuli, such as tensile stress at crack tips, transforms to the more stable monoclinic phase with a local increase in volume of approximately 4%. This increase in volume closes crack tips, effectively impeding crack propagation (figure 1-3). It is this transformation toughening process which gives zirconia its superior strength and toughness, exceeding all of the currently available ceramics (table 1-1 and figure 1-1). Compared to alumina, zirconia has twice the flexural strength, partly due to the higher sintered density, smaller particle size, and transformation toughening process (Piconi et al. 1999).

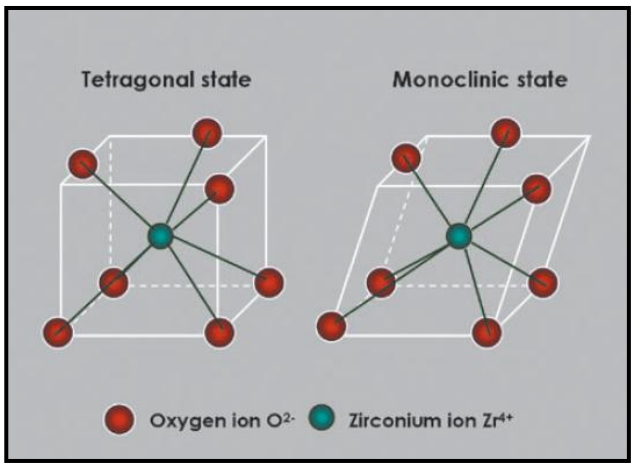

Figure 1-2: Tetragonal (left) and monoclinic (right) crystallographic phases of zirconia (from Vagkopoulou et al. 2009)

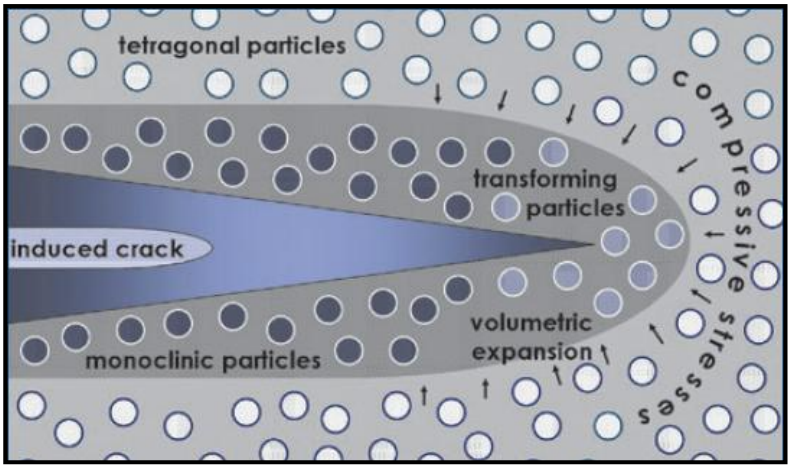

Figure 1-3: Schematic drawing of zirconia phase transformation occurring at a crack tip (from Vagkopoulou et al. 2009)

1.2.2 Types of zirconia ceramics

To date, there are three types of zirconia containing ceramics used in dentistry. Glass-infiltrated zirconia-toughened alumina ceramics (ZTA), magnesium doped partially stabilised zirconia (Mg-PSZ), and 3 mol% yttria stabilised tetragonal zirconia polycrystalline (Y-TZP) (Denry et al. 2008). The latter is the most utilised form in dentistry due to its higher flexural strength reported to range from 900 to 1200MPa (Christel et al. 1989).

In-Ceram zirconia (Vita, Bad Sackingen, Germany) is a commonly used glass-infiltrated zirconia-toughened alumina ceramic, which can be processed by either slip-casting or soft machining using computer aided design/computer aided manufacture (CAD/CAM) technology (Guazzato et al. 2004a). It is only slightly more translucent than Y-TZP due to the glass ceramic infiltration; however, its low mechanical properties are due to its limited zirconia content, presence of glass and porosity, which limits its use to short span FPDs to the anterior and premolar regions of the mouth (Conrad et al. 2007).

Despite extensive testing, Mg-PSZ has found few biomedical applications. At room temperature, the cubic zirconia makes up the major phase of Mg-PSZ, while tetragonal zirconia precipitates as the minor phase (Piconi et al. 1999). It requires higher sintering temperatures and strict cooling cycles compared to other zirconia ceramics, making it more complex and expensive to manufacture. Furthermore, the large grain size of Mg-PSZ (30-

60μm) is associated with residual porosity. In view of these reasons, Denzir-M (Dentronic AB, Skellefteå, Sweden) is the only Mg-PSZ ceramic available to the dental market (Sundh et al. 2006, 2008).

As previously mentioned, Y-TZP is the most utilized zirconia ceramic in dentistry due to its superior mechanical properties, biocompatibility and aesthetic potential (Denry et al. 2008). It has been used in root canal posts (Meyenberg et al. 1995), frameworks for all-ceramic posterior crowns and fixed partial dentures (FPDs) (Sailer et al. 2006; Sailer et al. 2007; Edelhoff et al. 2008; Molin et al. 2008), implant abutments (Glauser et al. 2004; Zembic et al. 2009), and dental implants (Wenz et al. 2008). The mechanical properties of zirconia however, were found to be dependent on its grain size (Garvie 1965; Stichert et al. 1998). This is evident in the spontaneous transformation from the tetragonal phase to the monoclinic phase which occurs above a critical grain size of > 1μm. On the other hand, the transformation toughening process is not possible in zirconia with grain size less than 0.2μm (Becher et al. 1992). Development of larger grain sizes is also dependent on longer and higher sintering temperatures which have a critical role in the final stability and resultant mechanical properties of the zirconia.

1.2.3 Manufacturing of Y-TZP restorations

Advancements in CAD/CAM technology has made it possible to use zirconia in dentistry (Kelly et al. 2008b). Unlike other ceramics, Y-TZP restorations cannot be manufactured in traditional ways, such as the powder-liquid or casting techniques. Zirconia restorations must be milled out of pre-made blanks (or blocks), where the prepared abutment is first scanned, then using appropriate computer software, the desired framework is designed and milled.

There are two types of zirconia milling processes available: a) soft-milling and b) hard-milling (Raigrodski 2004b). Soft-milling involves machining enlarged frameworks out of pre-sintered blanks of zirconia, also called the “green” state. These are then sintered to their full strength, which is accompanied by shrinkage of the milled framework by approximately 25% to the desired dimensions. Hard-milling involves machining the framework directly to the desired dimensions out of densely sintered (higher strength and

more homogenous) zirconia blanks, typically these have been hot isostatic pressed (HIPed). However, due to the extreme hardness of sintered HIPed zirconia, a robust milling system with an extended milling period is required compared to the soft-milling process, which places heavy demands on the cutting instruments. The relative ease and speed of soft-milling as well as the cost advantages may be why more manufacturers chose this method to fabricate their dental zirconia products, while only a smaller number have used HIPed zirconia. Among the common representative systems utilising soft-milling are Lava (3M ESPE, Seefeld, Germany), Procera Zirconia (Nobel Biocare, Zurich, Switzerland), IPS e.max ZirCAD (Ivoclar Vivadent, Schaan, Liechtenstein) and Cercon (Dentsply Degudent, Hanau, Germany). Systems that utilise hard-milling of HIPed zirconia include DC-Zirkon (DCS Dental AG, Allschwil, Germany) and Denzir (Decim AB, Skellefteå, Sweden).

Supporters of soft-milling claim that hard-milling may introduce microcracks in the framework during the milling process which may affect the overall fracture strength of the restoration. In contrast, hard-milling supporters claim a superior marginal fit because no shrinkage is involved in their manufacturing process. They argued that marginal misfit of restorations can lead to the accumulation of plaque and subsequently recurrent caries, periodontal conditions, and unaesthetic margins (Raigrodski 2004a; Sailer et al. 2007). Nevertheless, the clinical fit of soft-milled non-HIPed zirconia was confirmed using 4 unit posterior FPDs (Reich et al. 2008).

Zirconia has an opaque white colour which does pose an aesthetic problem. For this reason, some companies offer their zirconia frameworks and abutments in most of the colour shades in the Vita classic shade range (Vita, Bad Sackingen, Germany) (Raigrodski 2004b). This is to help improve the final aesthetics and colour of the restoration, in addition to reducing the amount of veneering porcelain needed to match the shade of adjacent teeth (Devigus et al. 2004). However there is conflicting evidence in the literature in regards to the effects of staining oxides on the final flexural strength of the zirconia (Pittayachawan et al. 2007; Hjerppe et al. 2008).

1.2.4 Low thermal degradation

Porcelains and most oxide ceramics are prone to moisture induced stress-corrosion caused by a chemical reaction between water molecules and the porcelains ionic-covalent bond at a crack tip (Michalske et al. 1982). In effect, the overall fracture toughness of a ceramic is significantly reduced in the presence of moisture (Gupta et al. 1981; Taskonak et al. 2008c). Zirconia on the other hand, has an additional issue namely an inherent accelerated ageing problem that has also been identified to occur in the presence of water, known as low temperature degradation (LTD). This aging phenomena was first described by Kobayashi and colleagues, where in a humid environment, spontaneous slow transformation from the tetragonal phase to the more stable (but weaker) monoclinic phase occurs in zirconia grains at relatively low temperatures (150 - 400^{o}C) (Kobayashi et al. 1981). This accelerated ageing problem of zirconia has created concern in the dental community and has instigated a large number of studies to determine the extent of this ageing phenomena and its implication on dental restorations long-term success.

A large number of studies have investigated the percentage of monoclinic phase transformation of different types of zirconia, under various temperatures, in dry and moist conditions, confirming LTD in zirconia samples (Sato et al. 1985a; Sato et al. 1985b; Tsukuma 1986; Li et al. 1996). In one study, aging of Y-TZP conducted under 70^{o}C in wet conditions resulted in more than 50% of monoclinic phase change after 5000 hours; that is equivalent to 208 days, or just over 6 months (Chevalier et al. 1999). At the same time, it has been widely demonstrated that extensive transformation to the monoclinic phase causes a deterioration of the mechanical properties of zirconia, especially bending strengths (Piconi et al. 1999; Lughi et al. 2010).

So far there is no accepted mechanism explaining LTD (Lughi et al. 2010). One theory proposes that water molecules react with yttrium oxide to form clusters rich in yttrium hydroxide; leading to a depletion of the stabiliser in the surrounding zirconia grains which are then free to transform to the monoclinic phase (Lange et al. 1986). The phase transformation of one grain leads to an increase in its volume by 4%, spreading stress to the neighbouring surrounding grains via a domino effect, further inducing phase transformations, and so on. This continues until enough of the monoclinic phase exists in

the bulk of the material, eventually weakening its flexural strength (Piconi et al. 1999). The process is exacerbated by the penetration of water between grains and microcracks (Lughi et al. 2010). The growth of this transformation zone results in severe microcracking, grain pullout and surface roughness of the zirconia; ultimately leading to degradation of the materials strength, putting it at risk of spontaneous catastrophic failure (Kelly et al. 2008b). How great the problem of this ageing process is going to be for zirconia restorations in the long run is currently unknown? The vulnerability of zirconia to ageing is only made worse by the fact that its severity has been shown to differ between different zirconias from different manufacturers, and even in zirconia from the same manufacturer but which have been processed differently (Chevalier 2006).

1.2.5 Treatment effects on zirconia

Unlike other ceramics, different surface treatments, such as particle air-abrasion (Wang et al. 2008), polishing (Zhang et al. 2004), and multiple firing cycles (Guazzato et al. 2005), were found to directly influence the strength of Y-TZP both positively and negatively, demonstrating the unstable and sensitive nature of zirconia.

During the CAD/CAM milling procedure, zirconia is subjected to surface damage, which has been found to significantly reduce its overall flexural strength (Wang et al. 2008). Damage may also be produced in the laboratory during preparation of the zirconia prosthesis either by bur adjustments, or during the veneering process. Air-abrasion with aluminum oxide (Al_2O_3) of different grit sizes has been shown to have different effects on the flexural strength of zirconia. Zhang and colleagues found a reduction in the flexural strength of polished zirconia after air-abrasion with 50 µm Al_2O_3 (Zhang et al. 2004). Wang and colleagues corroborated these results (Wang et al. 2008). In contrast, the flexural strength of ground or as delivered CAD/CAM milled Y-TZP was increased when subjected to 50 µm Al_2O_3 air-abrasion (Wang et al. 2008). It has been reported that the air-abrasion particles increase the flexural strength by creating a residual compressive stress field on the surface as a result of tetragonal to monoclinic transformation, by removing weakly attached surface grains, and eliminating the trace lines produced during the CAD/CAM milling process, thereby reducing surface roughness (Kosmac et al. 1999). However, this process is sensitive to the size and pressure of the air-abrasion procedure.

Severe surface damage in the form of sharp scratches, cracks, and grain pull out, causing an increase in the surface roughness of zirconia, and a decrease in the flexural strength was observed when 120µm particles were used (Wang et al. 2008). This illustrates the strong correlation between flexural strength and severity of surface damage as indicated by surface roughness. Thermal firing of zirconia after air-abrasion has been found to lower the flexural strength, thought to be due to the reversing effect of the monoclinic phase back to tetragonal phase, relieving the compressive fields created by the air-abrasion (Guazzato et al. 2005). Others however reported thermal firing to have no influence on the flexural strength of zirconia (Wang et al. 2008).

Polished zirconia surfaces demonstrate higher flexural strengths than non-polished or rough surfaces (Zhang et al. 2004; Wang et al. 2008). This is due to the reduction in severity and number of surface defects and flaws by the polishing process, were the internal strength of the material becomes the governing factor determining the mechanical strength (Luthardt et al. 2002). For this reason Wang and colleagues suggested a more realistic flexural strength figure for zirconia of 820 MPa rather than the common stated value of 900- 1400 MPa in the literature (Christel et al. 1989; Piconi et al. 1999). This is because these higher values are based on polished zirconia, and the flexural strength of as delivered CAD/CAM milled zirconia was found to be lower. They concluded that surface damage induced by the milling procedure on sintered or pre-sintered blocks should be addressed and further investigated.

1.2.6 Veneering of zirconia substructures

Zirconia has an opaque white colour, and despite being able to produce colour shaded zirconia, it is only a partially translucent material in thin sections. Therefore, just like in metal-ceramic restorations, feldspathic porcelains are veneered to zirconia cores in order to impart natural aesthetics to the restorations.

Currently there are two commercial methods for veneering zirconia restorations: conventional hand layering using the powder liquid technique, and heat-pressing on the veneering porcelain. Heat-pressing ceramics has gained popularity with the success of two particle-filled glass ceramics (leucite reinforced, and lithium disilicates containing

ceramics) (Dong et al. 1992; Guazzato et al. 2004b). This technique has also been successfully used to veneer feldspathic porcelains to zirconia substructures (Aboushelib et al. 2006; Guess et al. 2009). It involves using a special pressing porcelain furnace with a pneumatic ram (Gorman et al. 2000). Using the lost wax technique, ceramics are pressed in a mould at high temperatures under vacuum. A number of benefits have been reported in the literature to heat-pressing as opposed to the more traditional method of sintering, such as excellent marginal fit, and better surface contact between the zirconia core and pressed veneer. Higher bond strength between zirconia core and pressed porcelain has been reported by some (Aboushelib et al. 2006; López et al. 2010), while others found no significant difference between pressing or hand layering to zirconia (Tsalouchou et al. 2008; Guess et al. 2009). Another benefit of pressing is claimed to be reduced porosity within the veneering porcelain (Aboushelib et al. 2006; López et al. 2010). However this has not been corroborated by some studies that found spherical porosities in both pressed and hand layered porcelains to zirconia (Tsalouchou et al. 2008; Guess et al. 2009). Nevertheless, Guess et al. found porosities to be more extensive in hand layered veneers. In the meantime, the adhesive bond between zirconia and veneering porcelain is not yet fully understood, with reports of destabilisation of zirconia grains from the tetragonal phase by application of wet porcelain material (Tholey et al. 2009). Using energy-dispersive x-ray analysis to investigate the chemical structure at the zirconia core/veneer interface, it was found that the veneer elements diffused into the zirconia layer to a depth of 8 – 10 μm (Aboushelib et al. 2006).

Chipping of the veneering porcelain in zirconia-based restorations has been reported to be higher than that reported for metal-ceramic restorations and other all-ceramic restorations. Molin and Karlsson reported an incidence of chipping fractures of 35% in zirconia-based FPDs in 5 years (Molin et al. 2008). Larsson et al. reported an incidence of 54% in 1 year (Larsson et al. 2006). In the mean time, Reuter and Brose reported a chipping rate of 2.5% for metal-ceramic FPDs after 5-years (Reuter et al. 1984), while no veneering porcelain chipping has been reported for glass infiltrated ceramic-based frameworks after 5 years (Vult von Steyern et al. 2001; Olsson et al. 2003).

Zirconia has a coefficient of thermal expansion that is lower than that of metal alloys (Anusavice 2003). Therefore, special veneering feldspathic porcelains that have lower

coefficients of thermal expansion have been developed by manufacturers specifically for veneering zirconia cores (Fischer et al. 2009a; Ozkurt et al. 2010). These porcelains have some compositional and microstructural differences. In light of this, questions have been raised as to whether zirconia-tailored feldspathic porcelains are more prone to chipping than those used for veneering metal alloys. Quinn et al. using an edge chipping test, found similar resistance to chipping between metal/veneering porcelains combinations and zirconia/veneering porcelains (Quinn et al. 2010). Furthermore, the flexural strength values of veneering porcelains for zirconia were also found to be similar to veneering porcelains used for metal-ceramic restorations (Fischer et al. 2008). Therefore the lack of physical differences between the two materials suggests that the differences in clinical behaviour may not be related to fundamental material differences, but rather due to differences in residual stress development within the ceramics during the fabrication process.

It has been established that differences in the coefficient of thermal expansion (CTE) between the core substructure and the veneering porcelain, cooling rate to room temperature of the restoration, and thickness of the veneering porcelain, are the three main influencing factors that determine whether residual stresses in the veneering porcelain will be in compression or tension, thereby influencing the overall fracture resistance of restorations (Anusavice et al. 1988; Coffey et al. 1988; DeHoff et al. 1996). It is now believed that it is residual stress influencing factors that are responsible for the high chipping incidence found in zirconia-based restorations (Swain 2009).

1.3 RESIDUAL STRESSES IN BILAYERED DENTAL RESTORATIONS

Chipping of veneering porcelain has been identified as a major setback for zirconia-based restorations (Al-Amleh et al. 2010). The literature has cited several explanations as to why zirconia-based all-ceramic restorations have a higher incidence of chipping fractures (cohesive rather than adhesive fractures) compared to metal-ceramic and other all-ceramic restorations. These include mismatch of the coefficient of thermal expansion between the zirconia and veneering porcelain (Fischer et al. 2009b), mechanically defective micro-structural regions in the porcelain, areas of porosities (Ohlmann et al. 2008), surface defects or improper support by the framework (Marchack et al. 2008), overloading and fatigue (Coelho et al. 2009a), and low fracture toughness of the veneering ceramic (Beuer et al. 2009b). Nevertheless the most accepted explanation so far is the development of high residual tensile stresses within the veneering porcelain caused by fast cooling zirconia restorations as proposed by Swain (2009). Indeed, slow cooling firing programmes have recently been introduced by zirconia manufacturers in order to reduce the risk of chipping fractures (Göstemeyer et al. 2010).

In the following sections, basic principles involved in glass and ceramic strengthening will be explained using the simple monolayer glass plate model, which will be followed by a more detailed description of how those factors interact in the development of residual stresses in dental bilayered restorations.

1.3.1 Glass strengthening

1.3.1.1 Thermal tempering

At room temperature, ceramics and glasses almost always fracture catastrophically in response to applied tensile loads before any plastic deformation can occur due to their brittle nature (Anusavice 2003). These fractures frequently initiate via crack growth from existing flaws that are present on the surface, in a direction perpendicular to the applied load (Kelly 1995). Although it is virtually impossible to create a ceramic structure

completely free of surface flaws, it is possible to "toughen" a ceramic by intentionally inducing residual compressive stresses within its surface (Rawson 1974). This can be accomplished by a heat treatment process called thermal tempering, a process which involves heating the glass to a critical temperature and then rapidly quenching it to room temperature via air jets or, in some cases, an oil bath (Callister 2007). This technique has been widely used with great success in the glass industry in fabricating "toughened glass" for car windscreens and glass doors. To cause fracture in tempered glass, the magnitude of an externally applied tensile stress must be great enough to first overcome the residual compressive surface stress and, in addition, to stress the surface in tension sufficiently to initiate a crack, which may then eventually propagate to fracture the plate.

Figure 1-4 shows the residual stress distribution over the cross section of a tempered glass plate at room temperature that was cooled at the same rate on both surfaces. The stress distribution that develops is parabolic, with surface compressive stress being double the magnitude of the internal tensile stress, however, the compressive stresses are only within the outer 16% of the thickness of the glass, with the bulk of the internal structure being in tension (Tada et al. 2000). This pattern of stress distribution, compression on the surface and tension in the centre of a plate, is the result of thermo-mechanical properties, namely the glass transition temperature, coefficient of thermal expansion, cooling rate, and thickness of the glass plate. Each of the mentioned parameters will be described and explored in this section, in regards to their influence on a simple plate geometry and more complex crown like geometries.

Figure 1-4: Residual stress distribution over the cross section of a tempered glass plate at room temperature (from Callister 2007*)*

1.3.1.2 Glass transition temperature

During tempering of glass, residual stresses arise from differences in cooling rates of the outer surface and inner regions of the glass. Initially, the glass is heated to a temperature high enough to weaken atomic covalent bonds, changing the glass from a solid state to a viscous-sluggish state (Rawson 1974). As the temperature of the glass at the outer surfaces drops down to a specific temperature, called the glass transition temperature (Tg), it becomes rigid (Fairhurst et al. 1981). At this time, the interior having cooled less rapidly than the outer surfaces is at a higher temperature (above Tg) and therefore is still viscous and able to relax stresses developing because of the thermal gradient within the specimen. Eventually with continued cooling, the interior region cools down to below the glass transition temperature and no further relaxation of stresses is possible. As a consequence, the inside tends to contract more than the outside, and at room temperature, it sustains residual compressive stresses on the outer surfaces, with compensating tensile stresses at interior regions (figure 1-4). This process in effect toughens the glass, because applied tensile loads that may fracture non-strengthened glass, initially have to exceed the surface compressive stresses before surface cracks begin to be placed in tension. That is the strength of the tempered material will be approximately increased by the extent of the surface compressive stresses developed during tempering. However, it is important to note that although the overall "effective" fracture toughness of tempered glass increases, once a crack begins to grow through the thin compressed superficial layer, the glass can spontaneously shatter, as the internal tensile stresses rapidly accelerate and bifurcate cracks (Quinn 2007).

1.3.1.3 Stress distribution pattern

It must be understood that distribution and magnitude of transient stresses (stresses developed above room temperature) and residual stresses (stresses developed at room temperature) are complex in nature. For spherical like objects such as spheres or cylinders (or crowns) the resultant stresses are explained in terms of the three principle stress components: hoop, radial, and axial (Proos et al. 2002; Anusavice 2003). To go beyond the simplistic plate model, these stress components are demonstrated here using the geometry of a dental crown (figure 1-5). The hoop or circumferential stress exists in a circular fashion around the crown. Axial or tangential stress act parallel to the long axis of a crown,

while radial stress radiates horizontally towards the centre of the crown and is perpendicular to the facial surface.

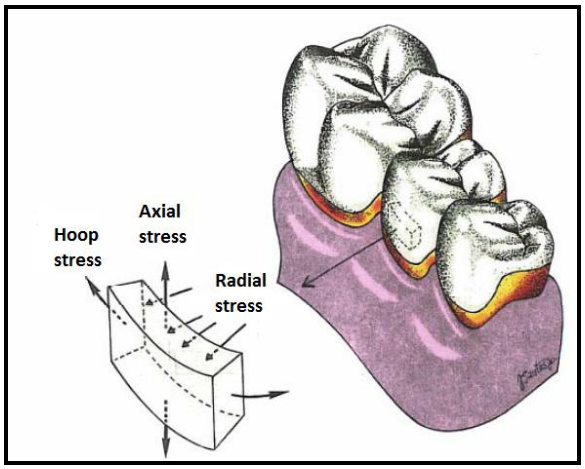

Figure 1-5: Hoop, axial, and radial stresses in the veneering porcelain of a metal-ceramic crown (modified from Anusavice 2003)

The situation for a crown is somewhat more complex as this is a bilayer system involving a core veneered with porcelain. Thus in an extension of both the glass plate situation mentioned previously, the coefficient of thermal expansion of the core and porcelain must be considered, as well as the cooling rate. Thicknesses of the core and porcelain also influence stress distribution in the veneering porcelain in dental crowns and FPDs (Coffey et al. 1988). The complex geometry of dental restorations however, which are composed of various steep changes in the thickness of the veneering porcelain, and have sharp contours, are possibly the most difficult influencing factor to investigate in the development of residual stresses, as there are no simple tests available that are able to definitively record and determine the magnitude and pattern of stress in all three planes at any one point (Mainjot et al. 2011). Most studies on residual stress patterns in dental restorations rely on assumptions for mathematical modelling (Zhang et al. 2010b), finite element analyses (FEA) (Proos et al. 2002; Rafferty et al. 2010), and optical imaging polarising systems measuring polarised light transmitted through thin porcelain sections (Zallat 2006). Nevertheless, basic but definitive global and surface residual stress calculations are possible using plate geometries by means of mechanical testing methods, via fracture mechanics techniques (Taskonak et al. 2008b) and microhardness indentation techniques (DeHoff et al. 1996). However for the time being, laboratory validated FEA studies may be the only means of getting an insight into the magnitude and pattern of stress

development in various test geometries despite their inherent limitation as an investigative method (DeHoff et al. 2008; DeHoff et al. 2009).

1.3.2 Residual stress influencing factors in dental restorations

During the fabrication of bilayered dental crowns and FPDs, differences in the coefficient of thermal expansion (CTE) between the core substructure and the veneering porcelain, cooling rate of the restoration to room temperature, and thickness of the veneering porcelain, are considered to be the main three influencing factors that determine whether the residual stresses in the veneering porcelain is in compression or tension, and thereby influencing the overall fracture toughness of the restorations (Anusavice et al. 1988; Coffey et al. 1988; DeHoff et al. 1996). Over the last 5 decades, a large number of studies have been conducted investigating the above mentioned factors and their influence on manufacturing metal-ceramic restorations, which has resulted in a number of recommendations and techniques to ensure that residual compressive stresses are always introduced in to the surface of the veneering porcelain to strengthen it. Unfortunately, what has been learnt about metal-ceramic systems over the last 50 years does not necessary apply to all-ceramic systems, and in particular to zirconia. In his theoretical model, Swain demonstrated how those three key parameters can contribute to the development of residual tensile stresses in zirconia based restorations, explaining the increase in chipping fractures (Swain 2009).

The following sections will explore each of the mentioned parameters and relate them back to metal-ceramics and all-ceramic restorations in an attempt to highlight any differences between the two systems which may shed light on the chipping problem in zirconia-based restoration and how it can be resolved.

1.3.2.1 Thermal expansion mismatch

The change in length per unit of the original length of a material when its temperature is raised by $1^{o}C$ is called the coefficient of thermal expansion (CTE), α. In other words it refers to how much a material expands upon heating and contracts upon cooling (Craig et al. 2002). It is calculated as follows (equation 1),

$$\propto = \frac{(L_{final} - L_{original})}{L_{original} \times (^{o}C_{final} - {}^{o}C_{original})} \quad (1)$$

Where L_{final} is the final length of the material after heating, $L_{original}$ is the original length, $^{o}C_{final}$ is the final temperature, and $^{o}C_{original}$ is the starting temperature. The units are expressed in units of /^{o}C or /^{o}K, and more frequently in exponential form because the values are usually very small, such as ppm/^{o}K or X10^{-6}/^{o}K, (table 1-2).

Table 1-2: Examples of CTE values at 25 – 500^{O}C for common dental materials (from data sheets)

	Product	**CTE (ppm/^{o}K)**
Zirconia veneering porcelains	IPS e.max Ceram (Ivoclar Vivadent)	9.9
	Rondo zirconia (Nobel Biocare,)	9.7
Alloy veneering porcelains	Super Porcelain AAA (Noritake, Kyoto, Japan)	12.4
	Reflex (Wieland, Pforzheim, Germany)	12.9
Zirconia	Procera Zirconia (Nobel Biocare)	10.4
	Lava Zirconia (3M ESPE)	10.7
Bonding alloys	Olympia (Jelenko, New York, USA)	13.5
	Will-Ceram (Ivoclar Vivadent)	15.5

Every dental ceramic and alloy has its own CTE value. This will change slightly with temperature and is a product of the specific constituents of the material makeup, and is reported by the manufactures in material product data sheets. The ISO Standard 6872 for dental ceramics recommends that CTE values are reported as an average value with standard deviation for expansion of a material at 5^{o}C/min to 10^{o}C/min for two specimens fired twice and two specimens fired four times between 25^{o}C and 500^{o}C (or the glass transition temperature, whichever is lower) (ISO standard 1995). Nevertheless, manufacturers do not seem to adhere to this standard and report CTE values from various other temperatures or even during cooling contraction (DeHoff et al. 2009). Under these circumstances, it would be difficult and even invalid to make direct comparisons of CTE values amongst different products. By the same token, trying to pick the correct combination of CTE between various products can be difficult and may lead to failure of bilayered dental restorations, since differences in CTE values between core and veneering

materials plays a critical role in the stability of the bond between them (Coffey et al. 1988; Anusavice et al. 1989b).

During cooling of a bilayered dental restoration, transient tensile stresses may cause crack formation in the veneering porcelain. If no cracks develop however, then residual stresses develop in the system as its cools down from the firing temperature above Tg, to room temperature, either enhancing or reducing the "effective" fracture toughness of the veneering porcelain (Anusavice 2003). To create favourable residual stresses, the alloy must have a slightly higher thermal contraction value (α) than the porcelain (known as a positive CTE mismatch) (Bagby et al. 1990). This produces axial and hoop compressive stress within the porcelain after cooling to room temperature, and any tensile radial stresses which may develop are assumed to be negligible (Anusavice et al. 1980). Simply put, if the alloy and porcelain are allowed to contract freely, they would no longer fit together since the metal substructure will contract more than the porcelain due to its higher CTE. However since they are bonded together, residual stresses develop within the system, in the form of tensile stress in the metal substructure and compressive stress in the veneering porcelain. Because ceramics are best able to resist crack propagation when they are under compression rather than tension, a small positive mismatch of CTE ($\alpha_{metal} > \alpha_{porcelain}$) is preferred in metal-ceramic restorations to put the veneering porcelain under slight compression (Coffey et al. 1988). However if the CTE of the alloy is much higher than that of the veneering porcelain ($\alpha_{metal} >> \alpha_{porcelain}$), delamination of the porcelain may occur. A negative mismatch of CTE ($\alpha_{metal} < \alpha_{porcelain}$) has been identified as a major contributor to crack formation due to the development of axial and hoop tensile stresses within the porcelain, rendering it less resistant to intraoral forces and the initiation of cracks from the outer surface of the porcelain inwards (Anusavice et al. 1980).

Currently, there is no single test available to manufacturers when developing metal-ceramic and all-ceramic systems to ensure that veneer-core systems will be thermally compatible (Baran 1985). This is despite the number of test designs reported in the literature that have been developed to investigate incompatibility, including bimaterial strips (Tuccillo et al. 1972), split rings (Bertolotti et al. 1982), crowns (Anusavice et al. 1981), semicircular arch specimens (Anusavice et al. 1988), discs (Anusavice et al. 1983), and spheres and cylindrical forms (DeHoff et al. 2008).

While the exact range of compatible values for CTE in metal-ceramic restorations is still unknown, it is generally accepted that the CTE of porcelain should be about 10% lower than that of the metal substructure (Coffey et al. 1988). In the same way, it is also generally accepted that for all-ceramic based restorations, the CTE of the veneering ceramic should also be lower than that of the ceramic core for the establishment of a strong core/veneer bond and veneering porcelain (Coffey et al. 1988; Anusavice et al. 1989b). DeHoff and Anusavice suggest a positive CTE mismatch less than 1 ppm/^{o}K for all-ceramic restorations (DeHoff et al. 2009). Fischer and colleagues investigated the shear bond strength between various veneering porcelains and a zirconia core. They reported spontaneous debonding when zirconia cores were veneered with a metal-ceramic veneering porcelain which had higher CTE than the zirconia core. On the other hand, ten veneering porcelains intended for zirconia and one for alumina, all having a range of CTE's below that of zirconia, showed strong bond strengths and no spontaneous debonding. Interestingly, they noted that the bond strength between zirconia cores and veneering porcelains was much higher than the cohesive strengths of the individual veneering ceramics when there was the recommended small positive mismatch of CTE. As a consequence, the authors concluded that the veneering ceramic is the weakest link, and it is the fracture toughness of the veneering porcelain that should be improved in order to overcome the chipping problem with zirconia-based all-ceramic restorations (Fischer et al. 2009a).

1.3.2.2 Cooling rate

Just as commercial tempering is used to strengthen glass for windscreens and TV sets (Rawson 1974), tempering of metal-ceramic restorations by removing them from the furnace at high temperatures and allowing them to bench-cool in air at ambient temperatures, has been established as common practice by dental laboratories to strengthen the veneering porcelain (figure 1-6) (DeHoff et al. 1990; Asaoka et al. 1992). The ambient-air cooling rate has been reported to approach about 10^{o}C/s, although this rate is not found to be constant during convection cooling (Fairhurst et al. 1989).

Transient and residual stresses of dental porcelain plates cooled at various cooling rates have been investigated by a number authors, using body-porcelain discs (Asaoka et al.

1992), opaque body-porcelain discs (Anusavice et al. 1989b; Anusavice et al. 1991), and metal-porcelain discs (DeHoff et al. 1996); each reporting similar results. Regardless of the exact values reported in each study, surface residual compressive stresses were observed with faster cooling rates, while slow cooled samples exhibited residual tensile stresses (Anusavice et al. 1989b; Anusavice et al. 1991; DeHoff et al. 1996). Consequently, the aforementioned studies concluded that fast cooling metal-ceramic restorations, by allowing them to bench air-cool from high temperatures, is preferable in order to strengthen the veneering porcelain in metal-ceramic restorations.

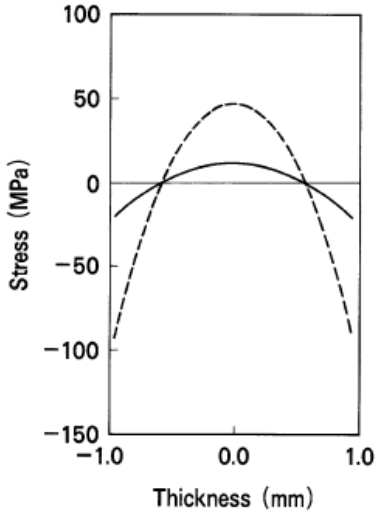

Figure 1-6: Result of simulation of residual stresses (at 30°C) in a porcelain disc, 2mm thick, after ambient-air cooling (solid line) and forced-air cooling (dashed line) (modified from Asaoka & Tesk 1992)

Taskonak et al. determined residual stresses in heat-treated zirconia-based bilayered discs under both fast and slow cooling rates (Taskonak et al. 2008b). They also found fast cooling generated surface residual compressive stresses with an upper compressive limit of -21 MPa, and slow cooling generated residual tensile stresses with the upper tensile limit of +19 MPa. The authors concluded that residual stresses can be altered using different heat treatments, and that these changes are a direct result of the viscoelastic behaviour of the glass veneer during the various cooling rates. The authors did not make any clinical recommendations regarding cooling rates for zirconia-based restorations, however the results may suggest that bilayered zirconia discs behave similarly to metal-ceramic discs during fast and slow cooling protocols. It may be possible to assume that faster cooling of

a zirconia-based restoration, just like metal-based restorations, will likely develop the desired residual compressive stresses in the veneering porcelain, increasing fracture toughness of the veneering porcelain, and the clinical life of the restoration. However, this practice has been recognised as being the offending factor when it comes to the zirconia-based restoration chipping problem (Swain 2009; Göstemeyer et al. 2010).

1.3.2.4 Thickness of veneering porcelain and geometry

It has been well established for metal-ceramic systems, that a thin porcelain layer is stronger than porcelain layers that exceed 1.5 to 2 mm (Miller 1977). Temperature gradients throughout cooling veneering porcelain will result in areas that are above and below the glass transition temperature, and the thicker the porcelain is, the greater are the thermal gradients and residual stresses (Asaoka et al. 1989; Tada et al. 2000). A number of studies examined the relationship of the thickness of the veneering porcelain in various geometries and its influence on residual stress development. Many however, preferred to use simple models to look at this interaction, such as monolayer and bilayer plates, because of their simplicity in explaining complex thermo-mechanical principles. In reality however, crowns and FPDs are more sphero-cylindrical hollow forms with varying thickness of porcelain and framework throughout the anatomical forms, demonstrating far more complex structures than simple plates. What's more, residual stresses are additive in nature, and are geometry-dependent (Anusavice et al. 1989a). As a result, residual stresses may vary at different locations in a restoration. This may be due to variations in the thermal properties of the porcelain resulting from different cooling rates (Coffey et al. 1988), and irregular porcelain/core thickness ratios (Bertolotti 1980). A brief review and discussion about the thickness of the veneering porcelain in plate, spherical and cylindrical geometries follows next.

Asaoka and Tesk (1989) investigated the influence of thickness and cooling rate on tempering stresses developed in monolayer porcelain plates. They found that the temperature difference between the surface and centre of a porcelain plate is proportional to the square of the plate half-thickness, as given in equation 2:

$$\Delta T = \frac{q l^2}{2k} \qquad (2)$$

Where ΔT is the temperature difference, q is the cooling rate, l is half-thickness of the plate, and k is the thermal diffusivity of the porcelain. It must follow that since the temperature difference is greater in a thicker plate, then the surface residual compressive stresses and the central residual tensile stresses are also greater. Asaoka and Tesk reported that thicker plates needed a longer time to complete the liquid-to-glass transformation from the surface to the centre while the layers of porcelain reached Tg during cooling, where a 4 mm thick plate needs 4.0 seconds for liquid-to-glass transformation, whereas a 2 mm thick plate needs only 1.0 seconds.

In his bilayer plate model, using four different ceramic core materials, Swain demonstrated that although the residual stress of the inner veneering porcelain at the interface with the coping was always in compression, the outer surface increased in tension as the thickness of the veneering porcelain increased (assuming a positive CTE mismatch of 1 ppm/^{o}K and Tg of 500^{o}C for all four groups) (Swain 2009). In other words, when keeping everything constant, increasing the thickness of the veneering porcelain increases the residual tensile stress on the surface of the veneering porcelain in a bilayer model. Nevertheless, the author recognises that this is a very simplistic model, as it does not consider a number of important influencing factors such as the complex sphero-cylindrical form of dental restorations, changes in cooling rates over temperature gradients, and the fact that above Tg the thermal expansion value of a material is much higher than below Tg.

Using the classical formula by Timoshenko for calculating thermally induced stresses in bimaterial thermostat strips (Timoshenko 1925); Nielsen & Tuccillo suggested that this stress equation could also be applied to porcelain-metal bilayered dental restorations (Nielsen et al. 1972) (equation 3),

$$\rho\ max = K(\Delta\alpha\Delta T) \qquad (3)$$

where $\rho\ max$ is the maximum tensile or shear stress, $\Delta\alpha$ is the difference in CTE of the two materials, and ΔT is the temperature range through which such stress develops. They claimed that the K factor became a function of specimen geometry and modulus of elasticity (E), formulating K values of 0.5E for discs, 1.13E for cylindrical, and 1.7E for spherical geometries. Thus it would appear that cylindrical and spherical geometries would generate higher stress values than disc geometries for any given differences in CTE. This

influence of veneering porcelain/substructure core ratio and CTE mismatch on spherical and cylindrical geometries has been investigated in a number of studies which support Nielsen & Tuccillo's model. Walton and O'Brien found that metal-ceramic spherical configurations were more sensitive to CTE mismatch than were metal-ceramic discs (Walton et al. 1985). They reported 100% crack development in spheres and discs with positive mismatch value of 1.8 ppm/^{o}K and 3.8 ppm/^{o}K, respectively, when the porcelain/metal ratios was 1:1. On the other hand, 0% cracking was observed when the thickness of porcelain was decreased to 1:4 in sphereical samples and 1:2 in disc samples for all tested CTE mismatches. The authors explained the observed difference was due to differences in thermal gradients between thicker and thinner porcelain veneers. However, sample numbers in this study were very small (2 samples per group for some groups), visual examination after 24 hours was used to assess thermal failure by evidence of checking, cracking, or rupture of the porcelain, without trans-illumination or microscopic examinations being utilised by the authors for crack detection. Therefore there is the possibility that undetected cracks may have existed at the 24 hour mark, especially as they also reported that "some" spherical samples developed cracks 6 weeks later, which may in fact have been undetected cracks which have propagated due to stress corrosion from atmospheric moisture coupled by residual tensile stresses (Gupta et al. 1981). Nonetheless, the influence of increasing the veneering porcelain thickness and faster cooling rates on the development of spontaneous cracks in porcelain/zirconia spheres was statistically confirmed in a more recent study conducted on 5 nominally compatible commercially available porcelains, which did utilise both magnification and UV light for sample examination (Guazzato et al. 2010).

Using finite elemental analysis, DeHoff et al. demonstrated that bilayered ceramic cylindrical and spherical geometries can be used to identify highly incompatible ceramic combinations, however they could not identify marginally incompatible systems (DeHoff et al. 2008). They found that the maximum principal residual stress in the veneer layer adjacent to the core interface of cylindrical and spherical geometries to be relatively constant for CTE mismatch ranging from -0.61 ppm/^{o}K to +1.02 ppm/^{o}K, which then increases rapidly for CTE mismatch less than -0.61 ppm/^{o}K. High tensile stress concentration at the end of the cylinder was noted, as a result, much higher maximum tensile residual stresses where found for the cylindrical geometry compared to spheres

when the CTE mismatch was less than -0.61 ppm/^{o}K, but not for more positive mismatches. Stresses in the cylinder away from the edges were well below the maximum values and more nearly equal to those in spheres. In clinical reality however, only CTE values with a small positive mismatch would be chosen for bilayered dental restorations, thus one would think that the stress concentration effect seen in the cylindrical geometries here should be of minimal concern, however, it is well known that prolonged and repeated firing of porcelain can increase its CTE value due to change to the leucite content of the porcelain, couple that with abrupt changes in shape and thickness in the ceramic contour of a dental crown or FPD (Anusavice 2003), and the potential for tensile stress raisers would certainly be a clinical reality. In another FEA study by the same group, residual tensile stresses ranged from 5.4 MPa in discs and 16.8 MPa to 44.0 MPa in 3-unit FPDs in compatible all-ceramic systems (DeHoff et al. 2009). Thus it has been shown that spherical geometric forms induce maximum thermal stresses in bilayered structures and represent the extreme forms that can occur clinically.

1.3.2.4 Thermal conductivity of core materials

Theoretically, the previous mentioned principles should apply to any core material, whether it be a metal or a ceramic, in terms of the type and magnitude of residual stresses that develop in the veneering porcelain of bilayered dental restorations. So why are zirconia-based restorations experiencing higher adhesive chipping fractures compared to other core based restorations? The answer is now thought to be because of its very low thermal conductivity compared to all other traditionally used core materials, even other ceramic core materials (Guess et al. 2008; Swain 2009). Cascone recognised that thermal conductivity of the core material was also a contributing factor in the development of thermal stresses in metal-ceramic restorations (Cascone 1979). This factor was not, however, previously investigated since most metal-ceramic alloys are good thermal conductors and it is unlikely that differences amongst them had any clinical significance.

Looking back at the monolayer plate model, heat will pass through a heated plate to eventually equilibrate with the surrounding temperature. This heat flux is dependent on the material's thermal conductivity, temperature difference, and the half thickness of the plate, and therefore heat transfer across materials of high thermal conductivity occurs at a faster

rate than across materials of low thermal conductivity (Callister 2007). According to the International System of Units, thermal conductivity is measured in Watts per meter Kelvin ($Wm^{-1}K^{-1}$) (NIST 2008).

For solid materials, heat is transported by free electrons and by vibrational lattice waves, or phonons (Kittel 1986). Of the two heat transfer mechanisms, free moving valence electrons are much more efficient and effective than phonons. Metals are extremely good conductors of heat because of the relatively large number of free electrons that are available to participate in electric current and heat energy conduction. On the other hand, ceramics and polymers are poor thermal conductors because free electron concentrations are low and phonon conduction is primarily responsible for their thermal conduction. Heat transport via the elastic vibration of the materials lattice (phonons) is highly limited due to phonon scattering by lattice imperfections. Therefore glass and amorphous ceramics are low thermal conductors since their atomic structure is highly disordered and irregular (Callister 2007). In fact, ceramics have been widely used as thermal insulators due to their low thermal conductivity, and their inherent resistance to oxidation, corrosion and wear (Cao et al. 2004; Gong et al. 2006).

In order to understand how the thermal conductivity of a core material can influence residual stress formation, we need to first appreciate the considerable difference in thermal conductivity between zirconia and other core materials. Table 1-3 lists the thermal conductivity of some commonly used core materials. Gold alloy is the best heat conductor (200 $Wm^{-1}K^{-1}$), followed by base metals and alumina ceramic (40 $Wm^{-1}K^{-1}$ and 30 $Wm^{-1}K^{-1}$ respectively), while zirconia has a thermal conductivity of 2 Wm^{-1} K^{-1}, which is 100 times less than gold alloys and 15 times less than alumina.

Table 1-3: Thermal conductivity of common dental materials from highest to lowest; (modified from Swain 2009)

Materials	Thermal conductivity ($Wm^{-1}K^{-1}$)
Gold alloys	200
Base metals	40
Alumina	30
In-Ceram alumina	14
Zirconia	2
Feldspathic porcelain	2

As a consequence, when a metal-ceramic restoration is fast cooled by air-bench cooling, the veneering porcelain, which begins at a temperature above Tg, cools rapidly both from the outside and the inside of the restoration. On the other hand, when a zirconia-based restoration is fast cooled, the centre of the veneering porcelain close to the zirconia core remains longer at temperatures above Tg. This is because the zirconia core traps the internal temperature by fault of its very low thermal conductivity, while the surface of the restoration cools at a faster rate. This forms a large thermal gradient between the outer surface of the veneering porcelain and the inner regions, and in effect develops high residual tensile zones within the inner regions of the veneer. In contrast, when zirconia restorations are slow cooled, that is the entire veneering porcelain thickness is allowed to cool down below Tg before the restoration is removed from the furnace, then any residual stresses that develop in the system are the result of CTE mismatch and any geometric influences, such as the core/veneer thickness ratio (Swain 2009). It would appear that since no large thermal gradients develop between the inner and outer regions of the veneering porcelain when the porcelain is above Tg, then only transient tensile stresses develop but no permanent residual stress zones.

1.3.2.5 In vitro studies on fast vs. slow cooling zirconia

The recent recognition that zirconia is a very poor thermal conductor, has prompted zirconia manufacturers to now recommend slow cooling programmes for zirconia restorations, in order to avoid the development of residual tensile stresses within the

veneer layer (Göstemeyer et al. 2010). Interestingly, this recommendation has been made without any clinical trials to back up it up, and only a very small number of *in vitro* studies have looked at the influence of cooling rates on the stability of zirconia-based restorations (Taskonak et al. 2008b; Göstemeyer et al. 2010; Guazzato et al. 2010; Komine et al. 2010; Rues et al. 2010).

Using zirconia spheres and 5 zirconia compatible veneering porcelains, Guazzato et al. found that the incidence of cracking of veneering porcelains increased with a faster cooling rate (Guazzato et al. 2010). The authors state that spherical geometric forms were used since they represent the extreme form that can occur clinically, in addition to the fact that spheres have been found to induce maximum thermal stresses in bilayered structures (Nielsen et al. 1972; Walton et al. 1985; DeHoff et al. 2008).

Komine et al. found that fast cooling significantly decreased the shear bond strength in veneer/zirconia discs in one brand of veneer but not for another (Komine et al. 2010). However, the cooling protocols used in this study are not clear and are not based on the glass transition temperatures of the test veneers. On the other hand, Rues et al. found that an extended cooling time of 6 minutes in the furnace significantly improved the cohesive failure within the veneering porcelain of one brand in anterior crown forms, in both static loaded-to-failure samples and thermocycled samples (Rues et al. 2010). In addition to fast cooling, by removing the crowns out of the furnace to bench-air cool just after the completion of the final glaze firing, they also investigated whether 6 minutes extended slow cooling of every firing cycle had a significant advantage over extended cooling the final glazing cycle only. Their results suggest that slow cooling the final cycle was sufficient to reduce residual tensile stresses within the veneering porcelain. Thus dental technicians need not waste time by slow cooling zirconia restorations after every firing cycle, but only need to do so after the final glaze cycle. Once again however, the glass transition temperatures of the veneering porcelains were not mentioned by the authors, and no specifics were given in terms of the cooling rate used and how much lower than the Tg values did the furnace reach before removing the restorations after the 6 minutes cooling time. In the meantime, mathematical modelling and FEA studies have also confirmed that high residual tensile stresses develop with fast cooling zirconia restorations (Zhang et al. 2009; Zhang et al. 2010b).

In contrast to the previous studies, Göstemeyer et al. found that slow cooling negatively influenced the zirconia/veneer interface adhesion (Göstemeyer et al. 2010). Based on their four-point bending test of notched bilayered samples, they claim that slow cooling would increase the risk of adhesive delamination failures as opposed to chipping fractures. However, the study by Rues et al. does not support these findings, since only cohesive chipping failure was observed in their anterior zirconia crown samples.

1.3.3 Measuring surface residual stresses

Lawn and Marshall (1977) first pioneered the analysis of tempered glass. They demonstrated that contact-induced cracking with a sharp indenter in tempered glass, was initially hard to extend because of the compressive residual stresses at the surface, however, when the indentation-driven crack extended beyond a critical size then the resistance to crack extension decreases (Lawn et al. 1977). Furthermore, spontaneous crack extension occurs when the magnitude of the residual stress and specimen's size exceeds a critical value. They suggested that the magnitude of the residual surface stresses can be quantified by use of a microhardness indenter (such as a Vickers indenter) to induce surface cracks whose size depends on the state of the surface stresses (Marshall et al. 1977).

As previously mentioned, tensile loads create stresses at crack tips, and as the load is increased, the intensity of crack tip stresses rises rapidly. In glasses and ceramics, purely straight opening cracks without sliding or shearing is termed "mode *I*" opening, and the stress intensity caused by this is designated by the letter *K*. Therefore the stress intensity at a crack tip in simple mode *I* opening is written as K_I. At some critical stress intensity, conditions are right for the crack to become unstable and separate the ceramic part into two pieces. Critical stress intensities for mode *I* opening (K_{IC}) are generally not dependent on the condition of the material, that is they are flaw size insensitive, and therefore K_{IC} values can be used to compare the true fracture toughness (or resistance to crack propagation) between different materials, also as an indicator of clinical reliability and serviceability of a ceramic restoration (Kelly 2004).

Table 1-4: K_{IC} values for selected dental materials (modified from Kelly 2004)

Material	K_{IC} (MPa.m$^{0.5}$)
Feldspathic porcelains	~ 0.9 – 1.2
Leucite-reinforced ceramic	~ 1.5 – 1.7
Alumina	~ 4.5
Zirconia	~ 8 – 12
Dental alloys	~ 20 +

The indentation fracture technique is one of the most commonly used methods for evaluating the fracture toughness of ceramics because of its simplicity and convenience, causing negligible surface damage and does not need special sample preparations. As a result, this technique has been used in a large number of studies investigating tempering induced residual stresses in dental monolayer and bilayer porcelains discs (Anusavice et al. 1989b; Anusavice et al. 1991; DeHoff et al. 1996) and in non-dental ceramics (Tatarko et al. 2009; Peitl et al. 2010). Anusavice and colleagues using opaque body-porcelain bilayer discs reported that crack lengths induced on the surface of body porcelain by a microhardness indenter were significantly smaller for specimens tempered by air blasting than those specimens subjected to either slow cooling in a furnace or free convective cooling in air (Anusavice et al. 1989b), and that tempering by forced cooling significantly strengthened bilayered discs (Anusavice et al. 1991). Similar results were reported by DeHoff et al. using metal-ceramic discs (DeHoff et al. 1996). This technique has also been used to measure growth rates of cracks in the presence of stress and moisture in glass (Gupta et al. 1981).

Recently however, this method of measuring fracture toughness in glass and ceramics has been challenged (Quinn et al. 2007). They argued that Vickers indentation fracture toughness tests reveal serious discrepancies in fracture toughness values, and that this technique is not reliable for ceramics and other brittle materials. Nevertheless, even though simple indentation techniques may not be satisfactory for ranking materials between classes, indentation experiments can give extremely interesting information about crack formation and comparative surface residual stress trends in a group of samples within a study, as opposed to comparing actual results among different studies in the literature.

1.4 FRACTURE OF ZIRCONIA-BASED RESTORATIONS

1.4.1 Fracture mechanics

Clinical catastrophic failure of monolithic ceramic restorations, such as Dicor and IPS Empress, and bilayered all-ceramic restorations, such as IPS Empress 2 restorations, has been reported to occur as bulk fracture throughout the entire restoration (El-Mowafy et al. 2002; Fradeani et al. 2002; Chadwick 2004; Kelly et al. 1989). Fractures appear to initiate at the inner surface of the ceramic adjacent to the cement layer. Tensile loads are highest at this point due to the resiliency of the underlying cement and dentinal tooth structure during normal occlusal loading, such that a crack propagates through the material to the outer surface, ultimately leading to bulk fractures (Lawn et al. 2001). In some clinical cases, wear facets were noted directly opposite the failure origin, providing evidence that failure does not originate from damage at the wear facets but from an area below (Kelly et al. 1990; Thompson et al. 1994). Clinical failure of zirconia-based restorations are associated with fracture or chipping of the veneering porcelain (Raigrodski et al. 2006; Molin et al. 2008; Örtorp et al. 2009), and less often fracture of both the zirconia core and veneering porcelain (Sailer et al. 2007; Beuer et al. 2009a; Çehreli et al. 2009). Research into the basic fracture mechanics of brittle dental ceramic crowns has focussed on contact testing with indenters using Hertzian contact mechanics. These tests identified three modes of damage which occur in porcelain veneered all-ceramic restorations: *inner* and *outer Hertzian cone cracking*, microdeformation *quasiplastic yield*, and *radial cracking* (figure 1-7) (Rekow et al. 2007).

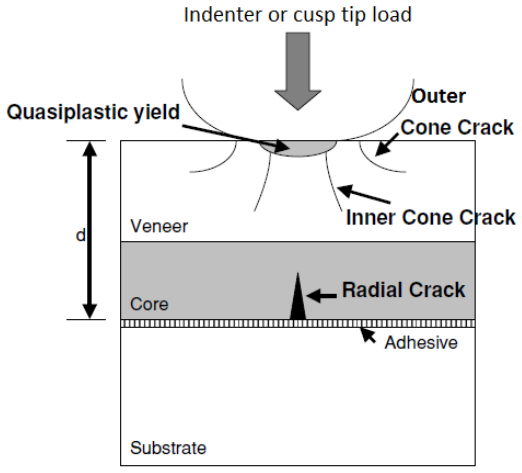

Figure 1-7: Schematic of damage modes in porcelain/ceramic core bilayer (adapated from Rekow & Thompson 2007)

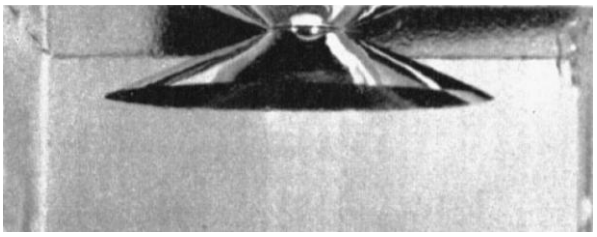

Figure 1-8: Side view of outer Hertzian cone cracking through a glass plate (adapted from Roesler 1956)

Two types of damage occur immediately below the indenter contact area, namely quasiplastic damage which produces grain boundary microcracks within the subsurface "yield" zone, and inner Hertzian cone cracks. In the mean time, outer Hertzian cone cracks develop in the near-contact region of the porcelain veneering layer (figure 1-8), whereas far-field radial cracks develop at the bottom surface of the core material in line with the axis of loading which is the result of tensile stresses generated during loading from yield of the supporting substructure (Lawn et al. 2001; Kim et al. 2007). *In vitro* mouth-motion cyclic loading studies have shown that bulk fracture via radial cracking does not tend to occur in porcelain/zirconia bilayered structures, but cone Hertzian cracking predominates, which stops at the veneer-core interface (Kim et al. 2007; Tsalouchou et al. 2008; Guess et al. 2009). This is not surprising since the fracture toughness of zirconia is reported to be as high as 9 -10 $MPa.m^{1/2}$ (Christel et al. 1989; Luthardt et al. 1999) while toughness values for veneering porcelain are relatively much lower (0.7 – 0.93 $MPa.m^{1/2}$) (Taskonak et al. 2006; Thompson et al. 2004).

Simply put, fracture failure of dental ceramics is associated with crack *initiation* followed by crack *propagation* through the dental restoration, however this process is complex and is directly influenced by the elastic modulus of the chosen materials. This includes the thickness ratio of the core/veneering porcelain, the cement type and thickness, the yield of supporting substructure (dentine or metallic core), the presence of a moist environment, geometry of the restoration, and fatigue resistance of the veneer (Lawn et al. 2001; Thompson et al. 2004). Since long-term clinical studies on zirconia-based restorations are limited (Al-Amleh et al. 2010), a raft of *in vitro* trials have been conducted to identify the various modes of fracture in zirconia-based restorations in order to predict their clinical durability. These studies include loading tests on flat crown-like layered systems (Guazzato et al. 2004c; Kim et al. 2007; Guess et al. 2009), on stylised crowns with cyclic

fatigue type mouth-motion machines (Coelho et al. 2009b; Rosentritt et al. 2009), static load-to-failure tests (Beuer et al. 2008; Akesson et al. 2009), FEA modelling to conduct stress analyses (Oh et al. 2002), as well as fractographic analysis of clinically failed zirconia restorations (Taskonak et al. 2008a; Aboushelib et al. 2009; Bulpakdi et al. 2009).

1.4.2 *In vitro* studies on zirconia-based restorations

Feldspathic porcelains have low flexural strength and fracture toughness, however they are relatively fatigue resistant (Jung et al. 2000), and as a result they have excellent clinical longevity when used to veneer metal substructures (Creugers et al. 1994; Walton 2002). However, the same could not yet be said about all-ceramic systems since their structural performance remains less stable than that of metal-ceramics, with bulk fracture and porcelain chipping estimated to affect 5% - 10% of all-ceramic single-unit prostheses by 6-years of function (Kelly 2004). Nevertheless, zirconia-based restorations are expected to outperform other all-ceramic systems due to the superior mechanical properties of zirconia owing to the inherent transformation toughening mechanism (Piconi et al. 1999). Guazzato et al. demonstrated that in a bilayered sample, the property of the layer on the bottom surface is what dictates the ultimate strength of the specimen. This is because it is this layer that is subjected to the peak tensile stresses (Guazzato et al. 2004c). Lawn et al. believe that using high strength cores for all-ceramic crowns should improve their clinical performance since bulk fracture was the main mode of fracture in all-ceramic crowns (Lawn et al. 2001). One study estimated the probability of fracture of zirconia-based FPDs to be almost 0% after a simulated 10-year clinical service study (Fischer et al. 2003).

The main objective of conventional static load-to-failure and cyclic-fatigue mouth-motion simulated tests is to determine whether the materials used in stylised crown forms, or a particular design, are able to withstand maximal biting forces and selective environmental fatigue conditions in metal-ceramic and all-ceramic systems (Josephson et al. 1985; Pallis et al. 2004; Ghazy et al. 2006; Zarone et al. 2007). Recently this method of testing has also been used for zirconia-based FPDs (Ohlmann et al. 2005; Larsson et al. 2007), and single-unit crowns (Akesson et al. 2009; Coelho et al. 2009a). Direct comparison between these studies is difficult because studies tend to use different experimental set-ups, such as the materials used for the supporting dies, luting cements, cyclic fatigue parameters, moist or

dry conditions, rate of load application (cross-head speeds), angle of loading, and size of loading indenter. To add to the confusion, each of the mentioned parameters have been described in the literature to greatly influence the overall fracture strength and fracture modes in dental ceramics (Kelly 1999; Lawn et al. 2001; Thompson et al. 2004). Table 1-5 lists studies conducted on zirconia-based posterior crown forms, demonstrating this wide variation in study parameters and outcomes.

Quasi-static load-to-failure tests have been widely used primarily because of their relative simplicity and ease of use compared to cyclic-fatigue mouth-motion simulated tests which require more expensive and complex machinery (Kelly 1999). However, fracture toughness and fracture modes of ceramics are closely influenced by the condition of testing, and a recommendation has been made to test dental ceramics under fatigue conditions to create failure modes similar to that seen in retrieved clinical specimens (Kelly 1999). This is because ceramics undergo an abrupt transition of damage mode and strength degradation after cyclic loading compared with static loading conditions (Jung et al. 2000). Furthermore, testing should be conducted in an aqueous environment, since moisture stress corrosion enhances crack growth when water is present at the crack tips (Gupta et al. 1981), and water has been shown to influence dental ceramics strength in static loading-to-failure tests (Jones et al. 1987), and under cyclic fatigue loading (Myers et al. 1994).

Table 1-5- ***In vitro*** **trials on zirconia-based posterior single crown forms; Mg-PSZ, densely sintered magnesia partially stabilised zirconia; SS, stainless steel; TC, tungsten carbide; d, diameter of ball; $, fatigue cyclic testing of some or all samples; $T, thermal cycling; #, core with non-uniform thickness; *, core with 0.5 mm uniform thickness; @, load-to-failure results after fatigue cycling; CnvC, conventionally cemented group; AdhB, adhesive bonding group.**

Study	Crown core/veneer material	Type of dies & cement	Loader & crosshead speed	Load at fracture ± s.d. (N)
Sundh et al. 2004	Denzir zirconia/ IPS Empress 2 #	Stainless steel	5 mm d SS ball	3486 ± 1067
	Denzir zirconia/ IPS Eris #	Zinc-phosphate	0.5 mm/min	4114 ± 321
	Denzir zirconia/ IPS Empress 2 *			2226 ± 553
	Denzir zirconia/ IPS Eri *			2740 ± 272
	IPS Empress			2346 ± 371
Akesson et al. 2009	Denzir zirconia/ Vita VM9	Stainless steel	5 mm d SS ball	
	0.2mm thick	Zinc-phosphate	0.5 mm/min	4521 ± 635
	0.1mm thick			1931 ± 634
	Denzir-M Mg-PSZ/ Vita VM9			
	0.2mm thick			3072 ± 424
Von Steyern et al. 2006	Procera Zirconia/ Cerecon Ceram S ($)	Resin (Duralay)	2.5 mm d SS ball	1108 ± 190 @
	Procera Alumina/ AllCeram ($)	Zinc-phosphate	0.25 mm/min	904 ± 91 @
Coelho et al. 2009a	Lava zirconia/ Lava veneer ($)	Aged composite	6.25 mm d TC indenter	1227 ± 221
	Cercon zirconia/ Vita veneer ($)	Resin cement	1 mm/min	
Zahran et al. 2008	In-Ceram YZ/ Vita VM9	Epoxy resin	3 mm d SS ball	1459 ± 492
	Vita Mark II blocks/ no veneer	Resin cement	1 mm/min	1272 ± 109
Rosentritt et al. 2009	4 zirconia-based systems ($, $T)	Extracted human teeth	12 mm d SS ball	CnvC
	Alumina-based system ($, $T)	Resin cement	1 mm/min	1111 – 2038 @
	Metal-ceramic system ($, $T)	Zinc-phosphate		AdhB
				1181 – 2295 @

In the studies listed in table 1-5 which utilised some form of fatigue testing, no two studies used similar fatigue testing parameters, with maximum loading forces ranging from 300 – 600 N, the number of cycles used ranging from 10,000 – 1,200,000 cycles, and the frequency of loading ranging from 1 – 20 Hz (Von Steyern et al. 2006; Zahran et al. 2008; Coelho et al. 2009a; Rosentritt et al. 2009). Another source of confusion is what can be considered to be an accurate number of cycles which best represents normal function in the oral cavity at a defined period? Wiskott et al. estimated the average individual to chew 2,700 times per day with "active" cycles being calculated by dividing this figure by a factor ranging from 5 and 20 (Wiskott et al. 1995). On the other hand, DeLong and Douglas estimate 1,500 active contacts per day (DeLong et al. 1983). It is not surprising then to find that a large range of set cycles are used in the literature to approximate oral function in a simulated time period in fatigue testing trials. For example, Cibirka et al. consider 5,000,000 cycles to represent 5-years of normal function in the oral cavity (Cibirka et al. 2001). Zahran et al. consider 500,000 cycles to represent 10-years of function, while for the same number of cycles, Kelly estimates about half a year of continuous bruxism (Kelly 1999).

As would be expected, complete bulk fracture of test crowns through the zirconia core and veneering porcelain was more commonly reported in load-to-failure tests which did not follow any form of fatigue cyclic conditions (Akesson et al. 2009; Coelho et al. 2009a). However not all load-to-failure studies exclusively report bulk fractures, chipping fractures of the veneering porcelain were also reported in all the samples by Zaharan et al. On the other hand, the main mode of fracture for cyclically fatigue tested zirconia crowns was chipping of the veneering porcelain (Von Steyern et al. 2006; Rosentritt et al. 2009), with two studies reporting veneer chipping fractures for all fatigue tested zirconia samples (Zahran et al. 2008; Coelho et al. 2009a). These results corroborate the findings that the reported failure mode with mouth-motion fatigue testing of crown-like geometries initiated cracks from the point of load application in the form of inner and outer Hertzian cone cracks, which commonly propagated to the veneer/core interface (Rekow et al. 2007), and that load-to-failure tests produce results which may not reflect true clinical failures (Kelly 1999).

With the exception of the study by Rosentritt and colleagues, bulk fracture was significantly higher in other all-ceramic controls than in zirconia-based specimens (Sundh et al. 2004; Von Steyern et al. 2006; Zahran et al. 2008), although no significance was found in the overall fracture strengths. These results also support the clinical observation that ceramic monolithic restorations and some zirconia-based all-ceramic bilayered restorations are prone to bulk fracture, rather than chipping fractures (Kelly et al. 1989; El-Mowafy et al. 2002; Fradeani et al. 2002; Chadwick 2004).

In a fatigue testing study investigating In-Ceram YZ crowns veneered with Vita VM9, and Vita Mark II all-ceramic crowns, chipping was only seen in the veneering porcelain of the zirconia crowns. All the Vita Mark II crowns survived the same fatigue testing conditions with no evidence of chipping or cracking (Zahran et al. 2008). On the other hand, when samples were loaded-to-failure without prior fatigue cycling, only the Vita Mark II crowns catastrophically failed by bulk fractures, while zirconia crowns had chipping fractures of the veneer. Vita Mark II is a feldspathic porcelain which comes in blocks for CAD/CAM milling of restorations, and has relatively similar mechanical properties to the veneering porcelain Vita VM9 (Krejci et al. 1994). These results confirm that conditions created by load-to-failure testing and fatigue cyclic testing are indeed very different, producing vastly different failure mechanisms, even in samples from the same study.

Some studies used dies made of high modulus materials, such as stainless steel, to support test crowns, while others used low modulus materials such as resins or extracted teeth (table 1-5). It has been recognised that high modulus dies dramatically increase the fracture strength of test specimen compared with those supported by low modulus materials. This is because the higher the elastic modulus of the supporting die material, the lower the flexion that will occur in the inner surface of the crown core at the cement interface during normal loading, thus reducing the tensile stresses which would cause radial bulk fractures (Lawn et al. 2001; Thompson et al. 2004). This relationship was observed clinically in a retrospective study that found that the longevity of Dicor crowns doubled with gold tooth cores compared to dentine cores (Malament et al. 2001; Malament et al. 2010). Furthermore, the stainless steel dies used by Sundh et al. and Akesson et al. may account for the very high fracture loads reported in those two studies (table 1-5)

compared to the other studies that used low modulus dies (Von Steyern et al. 2006; Zahran et al. 2008; Coelho et al. 2009a; Rosentritt et al. 2009).

Another factor which could negatively influence the support offered by the tooth substrate for ceramic crowns is the thickness and type of cement used because of their low elastic modulus (Scherrer et al. 1994; Kelly 1999). Consequently, increasing the thickness of cement can have a large effect on reducing flexural failure loads. Similarly, voids in the cement layer can also have a negative influence on the overall fracture strength of ceramic crowns (Anusavice et al. 1992) In reality, both dentine and metallic cores routinely make up the supporting structure underneath fixed prostheses, likewise a number of luting cements are also available to the clinician (Rosenstiel et al. 2006). For these reasons, *in vitro* testing of all-ceramic crown forms may benefit from using both types of materials to reproduce more clinically relevant results, provided that reported results are specified to the core and cement type. Admittedly, it is difficult to extrapolate from *in vitro* studies if these factors influence the overall fracture strengths, or mode of failure, of zirconia-based restorations compared to other all-ceramic restorations. In one study for example, the method of luting (adhesive bonding vs. conventional cementation using zinc-phosphate) did not have any significant influence on the fracture force and fracture mode in artificially aged zirconia crowns (Rosentritt et al. 2009).

1.4.3 Fractographic analysis of clinically failed restorations

Although the aim of any laboratory test is to mimic the clinical situation where a prosthesis is designed to function, many intra-oral variables remain difficult to be reproduced *in vitro* (Kelly 1999). As a result, some authors have conducted fractographic analyses on retrieved clinically failed zirconia restorations in order to analyse failure mechanisms, identify origins of fracture, and to determine the probable cause of failure (Taskonak et al. 2006; Taskonak et al. 2008a; Aboushelib et al. 2009; Bulpakdi et al. 2009). Researchers are then able to determine whether the failure was caused by a processing defect, by contact damage, or by overloading.

Zirconia-based FPDs were found to fail at the connector sites from the gingival surface where tensile stresses were greatest due to occlusal loading (Taskonak et al. 2008a;

Bulpakdi et al. 2009). In contrast, clinical failure of lithium disilicate FPDs were mostly initiated from the occlusal surface of the connector sites as a result of repeated contact damage (Taskonak et al. 2006). Aboushelib and colleagues compared the fracture type and the stress at failure of clinically fractured zirconia-based crowns and FPDs with replicas tested under static axial loading in a universal testing machine (Aboushelib et al. 2009). They found that critical cracks in failed zirconia crowns were associated with veneer delamination, at the core/veneer interface, with generation of hoop stresses and radial cracking, while cone cracking was the dominant failure type in statically loaded replica crowns. They argued that cone cracking required specific loading conditions, which are virtually impossible to generate intra-orally. This is because normal chewing cycles apply loads over a large surface area over the slopes of the functional cusps, with peak loads only occurring for a fraction of a second, as opposed to critical small contacts generated by an indenter, with a sustained increased load for a relatively long time. Nevertheless, the authors did not address the fact that cyclic fatigue testing may have resulted in a more realistic outcome compared to the static load-to-failure test which they adopted.

The value of fractographic analysis of clinically failed restorations comes from the fact that these restorations were subjected to multifactorial influences in corrosive oral environment, created by moisture, with abrupt thermal changes, and functional and parafunctional masticatory activity, all of which are almost impossible to replicate accurately in laboratory settings. This is because the main cause of fatigue failure of dental ceramics is subcritical crack growth in corrosive conditions (Drummond et al. 1991). However, none of the studies mentioned reported the clinical age of the retrieved prostheses, and only a small number of specimens were reported in each study. Finally, not all of the specimens clinically retrieved had intact fracture surfaces on which to perform fractographic analyses. What is more, methods of retrieval were not described, leaving the reader to wonder about the reliability of this method and the relevance of the data reported.

1.4.4 Shear bond strength of veneering porcelains to core substructures

Ceramic dental prostheses are primarily bilayered (Kelly 2004). It is therefore important to quantify the bond strength between the veneering porcelain and the underlying substructure is order to determine the weakest link in the layered structure, and more importantly, address possible ways to improve their clinical longevity.

The literature has conflicting conclusions whether the bond strength between veneering porcelains and zirconia core is the weakest link in the layered structure, or if it is the ultimate strength of the veneering porcelain (Ozkurt et al. 2010). Benchmark shear bond strengths (SBS) of zirconia core to the veneer layer are based on metal-based systems. This is despite that fact that metal-based systems are vastly different to zirconia-based systems. For metal-ceramics, bonding veneering porcelain to metal alloy is accomplished by mechanical interlocking (Shell et al. 1962), van der Walls forces (O'Brien et al. 1964), and chemical bonding via a metal-oxide interface (Knap et al. 1966). The result is a strong and stable bond that has lead to the successful use of this type of restoration in dentistry over the last five decades. In contrast, little is known about the bond interface between veneering porcelains and zirconia (Tholey et al. 2009).

For metal–ceramics, bond strength measurement was standardised by the International Organisation of Standardisation using the Schwickerath crack initiation test (three-point-bending test), and it has been established that a fracture stress of 25 MPa is the minimum adequate bond strength for metal-ceramic combinations (ISO standard 1999). In the meantime, adequate bond strengths for all-ceramic materials have not been determined, presumably because three-point-bending tests cannot be applied to all-ceramic multilayered systems due to the brittleness of ceramic core materials (Guess et al. 2008). To date, diverse test methodologies have been used to assess core-veneer bond strengths in all-ceramic systems, ranging from SBS tests (Al-Dohan et al. 2004; Guess et al. 2008; Ozkurt et al. 2010), microtensile bond strength (MTBS) tests (Aboushelib et al. 2005; Aboushelib et al. 2006, 2008), and biaxial flexural strength tests (Guazzato et al. 2004a). Unfortunately however, there is no form of standardisation.

A SBS test is defined as a test in which two materials are connected via an adhesive agent and loaded under shear until separation occurs. The bond strength is calculated by dividing the maximum applied force by the bonded cross-sectional area (Craig et al. 2002). The SBS test has been widely used because of its relative simplicity and ease of use compared to the MTBS test. Some of the advantages of SBS testing are ease of specimen preparation, a clear test protocol, and rapid production of test results (Ozkurt et al. 2010). Nevertheless, when using an *in vitro* method to estimate the clinical performance of materials, some critical aspects must be taken into account. Firstly, *in vitro* results cannot be extrapolated directly to the clinical situation, and secondly, large variations in SBS *in vitro* test results have made the test questionable (Hadavi et al. 1993). For this reason, efforts must be made to standardise SBS test methods to improve the clinical value of this *in vitro* test. In particular, consideration should be given to the storage conditions, type of substrate, specimen preparation, rate of load application (cross-head speed), and the cross-sectional surface area of the test samples. Examples of some recent zirconia core/veneer SBS test studies demonstrating the various shapes and cross-sectional areas of specimens, as well as testing conditions and cross-head speed of loading are shown in table 1-6.

Table 1-6: SBS test results of zirconia core/veneer bond strengths and applied test methods; ®, manufacturer recommended veneering porcelain used; *, veneering porcelain not recommended by manufature used; n, group not significantly different to control; sl, group significantly lower than control group; sh, group significantly higher than control group; TC, results after thermocycling; SD, standard deviations; Coh-V, cohesive failure through veneering porcelain; Coh-C, cohesive failure through core material; Adh, adhesive failure or delamination; VP, veneering porcelain; C, core; d, diameter; h, height; w, width; l, length; CHS; cross-head speed

Study	Core Materials	Veneering Porcelain	Range of SBS values (MPa ± SD)	Predominant type of Failure	Geometry of samples and cross-head speed
Al-Dohan et al. 2004	Metal alloy (control)	Noritake ®	30.16 ± 5.88	Coh-V	VP: cylinder d: 2.4mm, h: 3mm C: cylinder d: 10mm, h: 8mm CHS: 0.5 mm/min
	IPS Empress 2	IPS Eris ®	30.86 ± 6.47 n	Coh-V + Coh-C	
	Procera AllZircon	Cerabien CZR ®	28.03 ± 5.03 n	Coh-V	
	DC-Zircon	Vita D ®	27.90 ± 4.79 n	Coh-V	
	Procera AllCeram Alumina	Degussa-Ney AllCeram ®	22.40 ± 2.40 sl	Coh-V	
Guess et al. 2008	Metal alloy (control)	Vita VM13 ®	27.6 ± 12.1 26.4 ± 13.4 TC	Coh-V	VP: rectangle block h: 3mm, w: 5.4mm, l: 4mm C: rectangle block h: 13mm, w: 5.4mm l: 5mm CHS: 5 mm/min
	Vita In-Ceram YZ Cubes	Vita VM9 ®	12.5 ± 3.2 sl 9.7 ± 4.2 TC sl	Adh	
	DC-Zirkon	IPS e.maxCeram ®	11.5 ± 3.4 sl 11.5 ± 1.7 TC sl	Adh	
	Cercon	Cercon Ceram ®	9.4 ± 3.2 sl 9.6 ± 4.2 TC sl	Mixed: Coh-V & Adh	
Fischer et al. 2009a	Vita In-Ceram YZ Cubes	*Zirconia porcelains:@* 7 brands of veneering porcelains	21.9 ± 6.2 - 31.0 ± 7.1	Coh-V	VP: rectangle blocks h: 5mm, w: 10mm, l:5mm C: Cube blocks 10 mm^3 CHS: 1 mm/min
		*Alumina porcelain: ** Allux	27.7 ± 4.0	Coh-V	
		*Metal porcelain: ** Reflex	0.00	Spontaneous debonding	

Study	Core Materials	Veneering Porcelain	Range of SBS values (MPa ± SD)	Predominant type of Failure	Geometry of samples and cross-head speed
López et al. 2010	Metal alloy (control)	d.SIGN ®	13.45 ± 3.80	-	VP: disk-shaped d: 8mm h: 2mm C: cylinders d: 8mm h: 15mm CHS: 0.5mm/min
	IPS e.maxPress	IPS e.maxCeram ®	24.19 ± 3.73 sh	-	
	IPS e.maxZirCad	IPS e.maxZirPress ®	12.69 ± 2.14 n	-	
		IPS e.maxCeram ®	7.85 ± 2.50 sl	-	
	Lava	Lava Ceram ®	10.20 ± 5.08 n	-	
		IPS e.maxCeram *	4.62 ± 3.13 sl	-	
Ozkurt et al. 2010	Zirkonzahn	Ice Keramik ®	24.46 ± 3.72	Mixed: Coh-V & Adh	VP: disk-shaped d: 5mm h: 3mm C: disk-shaped d: 7mm h: 3mm CHS: 1 mm/min
		IPS e.maxCeram *	26.04 ± 4.01	Mixed: Coh-V & Adh	
		Vita VM9 *	26.52 ± 6.32	Mixed: Coh-V & Adh	
	Cercon	Cercon Ceram ®	20.19 ± 5.12	Adh	
		IPS e.maxCeram *	24.17 ± 4.54	Mixed: Coh-V & Adh	
		Vita VM9 *	21.67 ± 7.80	Mixed: Coh-V & Adh	
	Lava	Lava Ceram ®	27.11 ± 2.72	Mixed: Coh-V & Adh	
		IPS e.maxCeram *	23.05 ± 4.88	Adh	
		Vita VM9 *	18.66 ± 2.73	Mixed: Coh-V & Adh	
	DC-Zirkon	TriCeram ®	40.48 ± 8.43	Mixed: Coh-V & Adh	
		IPS e.maxCeram *	21.38 ± 5.99	Mixed: Coh-V & Adh	
		Vita VM9 *	31.51 ± 8.15	Mixed: Coh-V & Adh	

From the studies listed in table 1-6, the shear strengths for metal-ceramic systems ranged from 13.45 – 30.16 MPa when the metal alloys were tested against their recommended veneering porcelains, while zirconia-based samples tested against their recommended veneering porcelains ranged from 9.4 – 40.48 MPa. It is important to note that none of the studies listed used the ISO 9693:1999 standard for their SBS tests, thus values below the recommended 25 MPa for minimal bond strength cannot be applied as a cut off limit for determining the compatibility of core and veneer materials. In these studies the shear strengths of zirconia and their corresponding recommended veneers are comparable to metal alloys controls (Al-Dohan et al. 2004; López et al. 2010), with the exception of one study (Guess et al. 2008). Guess and colleagues used a much faster cross-head speed of 5 mm/min for loading their samples compared to others that used 0.5 mm/min (Al-Dohan et al. 2004; López et al. 2010). This may have contributed to the very low SBS values for zirconia samples reported by Guess et al.. When investigating the method of veneering to zirconia, Lopez et al. found that the SBS for pressed samples did not show a significant difference to metal controls, while layered samples showed significantly lower SBS values (López et al. 2010). Pressed lithium disilicate porcelain samples and their veneers consistently achieved the highest shear strengths compared to other materials, significantly better than metal controls (López et al. 2010). This is most likely due to the pure chemical bond that is possible between this type of core and its veneer, by virtue of their glass phase content (Kelly 2004). Nevertheless, the SBS between zirconia and its veneering porcelains are comparable to strengths produced by metal-ceramic systems.

The predominant type of failure in SBS studies is a mix between cohesive failure through the veneer, and adhesive failure (delamination) between the veneer and zirconia substrate. While it is important to report the type of failures in shear bond studies, no clinical correlation should be made because failure mechanisms of all-ceramic restorations are directly related to the testing methods and surrounding environment (Kelly 1999). Failure mechanisms for zirconia-based restorations should be determined by well established long-term clinical trials.

1.5 Summary of literature review

The high fracture toughness of zirconia has made it a suitable core material for all-ceramic single crowns and fixed partial dentures in the posterior of the mouth. However there are no long-term clinical data on zirconia-based restorations, yet studies have identified a chipping problem that mainly involves the veneering porcelain. One of the reasons for this high incidence of chipping with zirconia-based restorations is believed to be due to zirconia's propensity to develop large thermal gradients within the veneering porcelain layer that results in high residual stresses within the veneer. This is because of its very low thermal conductivity.

There are a number of factors that influence the residual stress profile within veneering porcelains in a bilayered structure, namely CTE mismatch, cooling rate, and the thickness of veneering porcelain. From examination of the literature, it would appear that other than FEA studies, *in vitro* studies which investigate these factors are mostly based on simple flat geometries, with some authors using spherical geometries to mimic the contours of dental restorations, because of their simplicity in explaining complex thermo-mechanical principles. In reality however, crowns and FPDs are more complex sphero-cylindrical hollow forms with varying thickness of porcelain and framework throughout their anatomy, with potential stress concentration areas that influence the stress profile within the bilayered restoration. So far, there are no studies that investigate the direct effect of veneering porcelain thickness or cooling rates on residual surface stresses, and fracture features in actual zirconia crown forms.

1.6 AIM OF RESEARCH

1.6.1 Outline of thesis

This thesis has three parts that investigate the chipping problem in zirconia-based restorations. To confirm that chipping of the veneering porcelain is a problem, a comprehensive systematic review of all published clinical trials on zirconia was undertaken and is the subject of chapter 2. This chapter is based on a paper published in the Journal of Oral Rehabilitation (Al-Amleh et al. 2010), that includes an updated review on the subject. Chapter 3 investigates the influence of veneering porcelain thickness and cooling rates on residual stress development in zirconia crowns. This *in vitro* study utilised Vickers hardness indentation testing to determine the residual surface stresses on 1mm, 2mm and 3mm veneering porcelain flattened cusp tips. The aim of the second *in vitro* study, chapter 4, was to explore differences in the fracture mechanics of statically loaded-to-failure fast and slow cooled zirconia crowns. An occlusal adjustment, just below the loading contact was created on one of the cusps on each sample to replicate a clinical reality of often needed occlusal adjustments undertaken post crown cementation. It has been well established that static load-to-failure tests, also called "crunch the crown" tests (Kelly 2004; Swain 2009), do not mimic clinical conditions or represent clinical failures. However, this method has been chosen to investigate evidence of residual stress differences in veneering porcelain on tempered crown samples using fractography. The features found on a fractured porcelain sample can tell much regarding the presence of residual stresses (Quinn 2007), and therefore this method may prove to be a simple and direct method to confirm the presence (or absence) of residual stresses in crown samples.

1.6.2 Significance of the research projects

In recent years zirconia restorations have been marketed by manufacturers despite limited long-term scientific evidence. A search of the literature has highlighted some concerns with chipping problems and a risk of spontaneous framework fracture that may be due to low temperature degradation of zirconia in the presence of moisture. Therefore, the systematic review on published clinical trials conducted on zirconia will summarise the clinical behaviour and clinical problems reported by the dental profession.

Furthermore, a search of the literature has identified three critical factors influencing the development of residual stresses within the veneering porcelain of bilayered restorations; CTE mismatch, thickness of the veneering porcelain and cooling rates. Most importantly, fast cooling of zirconia restorations has been identified to develop residual tensile zones within the veneering porcelain, thought to be one of the contributing factors in the high incidence of chipping experienced with zirconia-based restorations (Swain 2009). Currently there are no simple methods for determining the magnitude and pattern of residual stresses within the veneering porcelain in the complex geometries of dental restorations (Mainjot et al. 2011). The Vickers indentation technique has been used to investigate residual surface stresses influenced by cooling rates and thickness of veneering porcelain in flat plate and disc samples only (Anusavice et al. 1989b; Anusavice et al. 1991; DeHoff et al. 1996). This study will use this method to investigate differences in residual surface stresses caused by cooling rates on various veneering porcelain thicknesses in actual zirconia crown forms. Because this method has not been utilised beyond the flat model, before it is important to correlate results from previous studies with results obtained under various complex geometric influences found in crown forms.

Finally, static load-to-failure tests do not produce results that correlate with clinically failed restorations, nevertheless, a large number of researchers continue to use this method due to simplicity in preparing and carrying out this type of study. Using fractography, this simple method of testing will be utilised to confirm the presence of residual stresses within tempered crown samples.

1.6.3 Null hypotheses

The following null hypotheses were investigated:

1. Residual surface stresses on cusp tips of zirconia crowns are not influenced by the thickness of the veneering porcelain.
2. Residual surface residual stresses on cusp tips of zirconia crowns are not influenced by the cooling rate of the restoration during the final firing cycle.
3. The fracture mechanisms and fracture features of fast and slow cooled zirconia crowns are the same during static load-to-failure testing.

CHAPTER 2
CLINICAL TRIALS IN ZIRCONIA: A SYSTEMATIC REVIEW

2.0 INTRODUCTION

In dentistry, gold and metal-alloys have passed the test of time, and are recognized as predictable and well-established clinical materials for the restoration of various fixed prostheses (Spear 2001). Indeed, metal-ceramic systems require relatively little special knowledge for their routine use which has led to their worldwide acceptance and use since their inception. Nevertheless, increasing esthetic demand influencing dentistry has driven the development of a number of ceramics for their esthetic capability, biocompatibility, colour stability, wear resistance and low thermal conductivity (Studart et al. 2007). In 1885, porcelain jacket crowns were first used for single crowns for the anterior teeth because of their aesthetic and natural appearance (McLean et al. 1965). However, ceramics cannot withstand deformation strain of more than 0.1-0.3% without fracturing, and are susceptible to fatigue fracture (Callister 2007). It is this brittleness, due to the ionic-covalent atomic bonding, which limited their use in dentistry for decades (Vult von Steyern et al. 2005).

The most recently introduced dental ceramic is zirconia, with 3 mol% yttria containing tetragonal zirconia polycrystalline (Y-TZP) being the most utilised form of zirconia in dentistry. This is due to its high flexural strength, reported to range from 900 to 1200 MPa (Christel et al. 1989). Y-TZP has been used in root canal posts (Meyenberg et al. 1995), frameworks for all-ceramic posterior crowns and fixed partial dentures (FPDs) (Molin et al. 2008; Sailer et al. 2007), implant abutments (Glauser et al. 2004; Zembic et al. 2009), and dental implants (Wenz et al. 2008).

Advances in CAD/CAM technology has made it possible to more readily use zirconia in dentistry. This technology enables complex shapes to be milled out of HIPed and non-

HIPed zirconia blanks (or blocks), where the prepared abutment is first scanned, then using computer software, the desired framework is designed prior to milling (Raigrodski 2004b). Supporters of soft-milling claim that hard-milling may introduce microcracks in the framework during the milling process. In contrast, hard-milling supporters claim a superior marginal fit because no shrinkage is involved in their manufacturing process. Nevertheless, *in vitro* studies support the use of both HIPed and non-HIPed zirconia for all ceramic FPDs, crowns and implant abutments for the posterior of the mouth due to their high flexural strength and fracture toughness (Guazzato et al. 2004a).

However, early clinical findings show that there is one main drawback for zirconia restorations compared to metal-ceramics, that is a high incidence of veneering porcelain fracture, manifesting clinically as chipping fractures. Furthermore, concern has been raised regarding the inherent accelerated ageing problem that has been identified to occur in zirconia in the presence of water, known as low temperature degradation (LTD), which causes a decrease in physical properties by spontaneous phase transformation of the zirconia crystals from the tetragonal phase to the weaker monoclinic phase, putting zirconia frameworks at risk of spontaneous catastrophic failure (Kelly et al. 2008b).

Case reports of large multi-unit tooth and implant zirconia FPDs suggest that the dental community may have some confidence in zirconia as a restorative material, with some authors restoring full mouth rehabilitations using zirconia-based restorations despite limited scientific evidence (Chang et al. 2007; Dunn 2008; Nam et al. 2008).

The objective of this systematic review was to report on the clinical success of HIPed and non-HIPed Y-TZP based restorations (single crowns and FPDs), focusing on the incidence of framework fracture and chipping of the veneering porcelain in both groups.

2.1 MATERIALS AND METHODS

A search was performed in MEDLINE and PubMed for *in vivo* trials on zirconia restorations published between 1950 and June 2011. The keywords used for the search, and the numbers of articles produced were:

1. "zirconia AND clinical"- 483 articles
2. "zirconia AND fixed partial dentures"- 199 articles
3. "zirconia AND FPD"- 32 articles
4. "zirconia AND single crowns"- 111 articles

In addition, a manual hand search of the literature was conducted to identify clinical trials on Y-TZP that were not listed on MEDLINE or PubMed. Articles found were read to identify that they satisfied the following inclusion and exclusion criteria:

Inclusion Criteria:

1. Human *in vivo* only
2. Conducted on Y-TZP
3. Fixed prosthetics (single crowns and FPDs)
4. In the English language

Exclusion Criteria:

1. Case reports
2. *In vitro* trials
3. Animal studies
4. Trials less than 12 months

The search yielded 19 articles and abstracts involving clinical trials of Y-TZP restorations that satisfied the inclusion criteria. Following this, a final search was conducted by inspecting the bibliographies of the 19 reviewed articles to identify any additional studies, however, none were found.

2.2 RESULTS

In total, 19 clinical trials involving Y-TZP based restorations were found in the literature, of which only 2 were randomized control trials (Larsson et al. 2006; Çehreli et al. 2009). The majority of studies investigated all-ceramic FPDs in the posterior mouth (Bornemann 2003; Pospiech et al. 2003; Vult von Steyern et al. 2005; Larsson et al. 2006; Raigrodski et al. 2006; Sailer et al. 2006; Sailer et al. 2007; Crisp et al. 2008; Edelhoff et al. 2008; Molin et al. 2008; Ohlmann et al. 2008; Tinschert et al. 2008; Beuer et al. 2009a; Schmitter et al. 2009; Wolfart et al. 2009; Roediger et al. 2010), while a small number investigated single crowns (Çehreli et al. 2009; Örtorp et al. 2009; Groten et al. 2010; Schmitt et al. 2010), and only one study was available on implant supported zirconia FPDs (Larsson et al. 2006). Seven different brands of Y-TZP were identified among the 19 studies with Cercon (Dentsply Degudent, Hanau, Germany) zirconia being the most investigated brand (table 2-1).

The longest follow-up period found was five years, where two papers reported results on patients restored with zirconia all-ceramic FPDs (Sailer et al. 2007; Molin et al. 2008). Both studies involved 3 to 5-unit FPDs on natural teeth in the premolar and molar regions, except for one 3-unit FPD that replaced a lateral incisor (Molin et al. 2008). The survival rate of Y-TZP FPDs was between 74% (Sailer et al. 2007) and 100% (Molin et al. 2008) over 5 years. In the earlier study, a 5-unit FPD framework fracture occurred, reportedly due to accidental biting of a stone in a piece of bread. While the incidence of chipping of the veneering ceramic was 15.2%, in this study, secondary caries was found to be the most common cause of failure (21.7%). This was attributed to the poor marginal fit produced by the prototype milling technique used to fabricate the zirconia restorations in this particular study.

Three studies reported data with 1-year follow-up periods for three different treatment modalities. These were: zirconia FPDs on natural teeth (Crisp et al. 2008), FPDs restored on titanium implant abutments (Larsson et al. 2006), and inlay retained FPDs (Ohlmann et al. 2008). The highest incidence of framework fracture and chipping veneering porcelain were both reported in 1-year follow-up studies (10% and 54% respectively) compared to longer follow-up periods.

Table 2-1: List of *in vivo* trials conducted in yttria stabilised tetragonal zirconia polycrystalline; HIPed, hot isostatic pressed zirconia; FPD, fixed partial denture; IRFPD, inlay retained fixed partial denture; Ti abut, titanium implant abutment; +C, cantilevers included

Type of zirconia	Brand	Study	Follow-up periods	Type of restorations	Sample size	Framework fracture %	Veneer fracture %
Non-HIPed	Cercon (Dentsply)	Sailer et al. 2007	5 years	3-5 units FPD	33	8	15
		Wolfart et al. 2009	4 years	3-4 units FPD +C	58	0	11
		Roediger et al. 2010	4 years	3-4 units FPD	99	1	14
		Beuer et al. 2009	3 years	3 units FPD	21	5	0
		Cehreli et al. 2009	2 years	Single crowns	15	7	0
		Schimitter et al. 2009	2 years	4-7 units FPD	30	3	3
		Groten et al. 2010	1.75 years	Single crowns	71	0	4
		Bornemann et al. 2003	1.5 years	3-4 units FPD	59	0	3
	Lava (3M ESPE)	Schmitt et al. 2010	3 years	Single crowns	19	0	5
		Raigrodski et al. 2006	2.5 years	3 units FPD	20	0	25
		Pospeich et al. 2003	2 years	3 units FPD	38	0	3
		Crisp et al. 2008	1 year	3-4 units FPD	38	0	3
	Procera (Nobel Biocare)	Ortrop et al. 2009	3 years	Single crowns	204	0	2
	IPS e.max Zir/CAD (Vivadent-Ivoclar)	Ohlmann et al. 2008	1 year	IRFPD	30	10	13
HIPed	Denzir (Cadesthetics AB)	Molin & Karlsson 2008	5 years	3 units FPD	19	0	36
		Larsson et al. 2006	1 year	2-5 units FPD/Ti abut	13	0	54
	DC- Zirkon (DCS Dental AG)	Tinschert et al. 2008	3 years	3-10 units FPD +C	65	0	6
		Vult von Steyern et al. 2005	2 years	3-5 units FPD	23	0	15
	Digizon	Edelhoff et al. 2008	3 years	3-6 units FPD	21	0	9.5

2.2.1 Zirconia single crowns

Single crowns have a small representation in published clinical trials on Y-TZP. In a 2-year randomized control trial, 1 of 15 Cercon zirconia crowns fractured in half, only 1 month after cementation on a maxillary second molar (Çehreli et al. 2009), so that the success rate for this study was 93% after 2-years. There was no significant difference in soft tissue health adjacent to the Cercon crowns and the control crowns made with In-Ceram zirconia (Vita, Bad Sackingen, Germany). No chipping of the veneering porcelain was reported after 2-years. In contrast, despite no framework fractures being reported in 54 Cercon single crowns after 21 months by Groten et al., 2 crowns sustained chipping fractures which required replacement of the entire restorations (Groten et al. 2010).

No framework fractures were reported after 3-years in a study of 204 single crowns fabricated with Procera zirconia (Nobel Biocare, Zurich, Switzerland) in a private practice setting (Örtorp et al. 2009). However, 16% of the crowns had some type of complication, and 6% were recorded as a failure. Loss of retention (12/204= 6%), extraction of abutment tooth (5/204= 2.5%), persistent pain (10/204 = 5%), and chipping of veneering porcelain (4/204 = 2%) were some of the complications reported in this study which had a cumulative survival rate of 93% at 3 years.

Another study involved nineteen severely decayed anterior teeth, restored with 0.3mm thick Lava zirconia copings (3M ESPE, Seefeld, Germany) having feather-edged margins (Schmitt et al. 2010). In the 3-year follow-up period, no framework fractures were reported, nevertheless, one crown sustained a chipping fracture in the veneering porcelain.

2.2.2 Zirconia fixed partial dentures

The most investigated treatment modality are zirconia fixed partial dentures, with 15 different clinical trials reporting data on FPD spans ranging from 3 to 10-units. Except for one study, the FPDs used natural teeth as abutments; the exception used titanium implant abutments. Zirconia FPDs demonstrated favourable results, exhibiting a high success rate in most studies. A relatively small number of framework fractures were reported in the clinical trials, and do not appear to have occurred spontaneously, but rather an initiating factor was determined to have contributed to the fractured frameworks. The longest FPD

spanned 10-units (5 pontics on 5 abutments) involving a framework made with DC-Zirkon (DCS Dental AG, Allschwil, Germany) and the veneering porcelain was Vita D (Vita, Bad Sackingen, Germany) (Tinschert et al. 2008). This study also included two cantilever posterior FPDs. No framework fractures were reported after 3-years of follow-up; however, chipping of the veneering porcelain was reported in 4 posterior FPDs of the 65 FPDs placed in the anterior and posterior regions.

2.2.3 Zirconia framework fracture

Fracture of Y-TZP substructures mostly occurred in FPDs, nevertheless this was found to be rare, and was only reported in 6 studies involving two zirconia brands (table 2-2). The incidence of framework fracture was directly related to the design of the FPD, where inlay retained FPDs showed the highest failure rate of 10% after only 12 months. These inlay retained FPDs were made with IPS e.max ZirCAD (Ivoclar Vivadent, Schaan, Liechtenstein), where debonding of the inlay pontic was concluded to be the cause of the framework fractures. In the review, Cercon zirconia suffered the majority of framework fractures compared to the other zirconia brands investigated; however it must be kept in mind that it is also the most investigated brand (8 out of 19 trials), followed by Lava (3M ESPE) (4 out of 19 trials). Both IPS e.max ZirCAD and Cercon zirconia are a non-HIPed zirconia manufactured by the soft-milling process.

Table 2-2: *In vivo* studies which reported Y-TZP framework fracture and the time until fracture; NS, not specified; IRFPD, inlay retained FPD.

Study	Brand of zirconia	Type of restoration	Time until fracture	Number of units fractured	Incidence %
Sailer et al. 2007	Cercon zirconia	3-5 unit FPD	38 months	1 out of 13	8
Roediger et al. 2010	Cercon zirconia	3 unit FPD	NS (< 4 years)	1 out of 91	1
Beuer et al. 2009	Cercon zirconia	3 unit FPD	30 months	1 out of 21	5
Schimitter et al. 2009	Cercon zirconia	4-7 unit FPD	1 month	1 out of 30	3
Cehreli et al. 2009	Cercon zirconia	Single crowns	1 month	1 out of 15	7
Ohlmann et al. 2008	IPS e.max ZirCAD	IRFPD	NS (< 1 year)	3 out of 30	10

2.2.4 Veneering porcelain fracture

The most common complication observed in zirconia-based restorations was fracture of the veneering porcelain, manifesting clinically as chipping fractures of the veneering ceramic with or without exposing the underlying Y-TZP framework. All seven of the zirconia brands investigated exhibited chipping fractures, even when using specifically manufactured veneering porcelains with modified coefficients of thermal expansions compatible with zirconia (Raigrodski et al. 2006; Sailer et al. 2007). These chipping fractures were also found to occur in non-load bearing areas, such as the mesio-lingual cusps on a mandibular second molars (Schmitter et al. 2009), and the lingual aspect of FPD pontics (Sailer et al. 2007). Possible trends in the location of chipping were identified by some authors and included the premolar and molar regions (Örtorp et al. 2009), particularly the second molars on FPDs (Raigrodski et al. 2006) and the connector area in mandibular posterior FPDs (Tinschert et al. 2008).

Denzir zirconia (Cadesthetics AB, Skellefteå, Sweden) frameworks veneered with Triceram (Dentaurum, Ispringen, Germany), demonstrated the highest incidence of veneering porcelain fracture at 1-year (54%) when FPDs were restored on titanium implant abutments (Larsson et al. 2006). In addition, there was a 36% incidence of roughness/pitting on occlusal surfaces of 3-unit FPDs on natural teeth after 5-years with Denzir zirconia frameworks veneered with either a feldspathic porcelain Vita Veneering Ceramic D (Vita) or leucite reinforced pressed ceramic IPS Empress (Ivoclar Vivadent) (Molin et al. 2008).

2.2.5 Cementation and bonding

Due to its high flexural strength, zirconia can be conventionally cemented, just like metal-ceramic restorations, without need for any pretreatment; although bonding of zirconia is possible provided special conditioning treatment of the zirconia is carried out first because zirconia is not etchable. Indeed, cementation of zirconia all-ceramic restorations is a simpler process compared to other all-ceramic systems that require additional steps for bonding. This was evident in the range of cements used by the various authors in the published clinical trials; zinc phosphate cement (Bornemann 2003; Vult von Steyern et al. 2005; Larsson et al. 2006; Molin et al. 2008; Tinschert et al. 2008; Örtorp et al. 2009;

Roediger et al. 2010), glass-ionomer cements (GIC) (Pospiech et al. 2003; Beuer et al. 2009a; Çehreli et al. 2009; Wolfart et al. 2009; Schmitter et al. 2009; Schmitt et al. 2010), resin-modified GIC (Raigrodski et al. 2006; Edelhoff et al. 2008), and resin cements (Sailer et al. 2006; Sailer et al. 2007; Crisp et al. 2008; Edelhoff et al. 2008; Molin et al. 2008; Ohlmann et al. 2008; Tinschert et al. 2008; Örtorp et al. 2009; Groten et al. 2010).

Loss of retention was seen in 11 out of 19 studies involving cementation of zirconia restorations. One 3-unit FPD cemented with Panavia F (Kuraray, Okayama, Japan) lost retention after 12-months (Molin et al. 2008), a 4-unit FPD cemented with Variolink (Ivoclar Vivadent) lost retention after 33.3 months in service (Sailer et al. 2007), while two 3-unit FPDs in the molar region cemented with zinc phosphate lost retention at 17 and 32 months (Tinschert et al. 2008). Ketac Cem (3M ESPE) glass ionomer cement had 1 posterior 3-unit FPD decemented after 38 months (Beuer et al. 2009a), in addition to 2 long-span FPDs at 8.8 and 14.2 months in service (Schmitter et al. 2009). All debonded zirconia restorations were recemented successfully for the duration of the follow-up period in each of the studies.

In contrast, 6 cases of debonded inlay retained zirconia FPDs were seen with Panavia F (dual-cured resin cement) and Multilink (automix self-curing resin cement), despite pretreatment of the zirconia with tribochemical air abrasion (Rocatec , 3M ESPE). Fracture of the framework occurred in 3 of 6 debonded restorations (Ohlmann et al. 2008). Similarly, in a study involving single Procera zirconia crowns, 12 out of 204 crowns lost retention of which 4 could not be recemented (Örtorp et al. 2009). Unfortunately, the type of cement used for the crowns which lost retention was not reported, as both zinc phosphate and resin cement (Rely-X Unicem, 3M ESPE) were used.

Despite the encouraging retentive capacity of zinc phosphate cemented zirconia restorations, after 5-years follow-up of 3-unit FPDs that were cemented with either resin cement (Panavia F) or zinc phosphate (De Trey Zinc, Dentsply), visible evidence of ditching along the margins was only seen in the zinc phosphate cemented group (Molin et al. 2008). Ditching was reported in 5% of mesial abutments and 26% of distal abutments in this study, however this problem was not reported in other trials using zinc phosphate cement.

2.3 DISCUSSION

With the limited number of published clinical trials, one can conclude that Y-TZP has potential for acceptance as a suitable material for fixed prosthodontic dental treatment, however larger sample sizes and longer *in vivo* studies are needed. The majority of published studies are prospective clinical trials, with the longest follow-up period being 5-years. In addition, only two randomised controlled trials exist, with 1 to 3-year follow-up periods. Long-span multi-unit FPDs have also been included in a number of studies, demonstrating confidence in the structural potential of zirconia frameworks (Vult von Steyern et al. 2005; Larsson et al. 2006; Sailer et al. 2007; Edelhoff et al. 2008; Tinschert et al. 2008; Schmitter et al. 2009).

The majority of the published clinical trials demonstrate a careful and meticulous approach in their treatments, with steps taken to ensure that the zirconia frameworks are delivered at their best possible condition before final cementation. Furthermore, it was interesting to note that the majority of studies included bruxism in their exclusion criteria, and therefore this should alert to a potential limitation of this all-ceramic system that is not being investigated clinically.

2.3.1 Zirconia framework fracture

The probability of fracture of zirconia FPDs has been estimated to be almost 0% in a simulated 10-year clinical service study (Fischer et al. 2003), however, framework fracture was reported in several *in vivo* trials of less than 5-years (Sailer et al. 2007; Ohlmann et al. 2008; Beuer et al. 2009a; Çehreli et al. 2009; Schmitter et al. 2009; Roediger et al. 2010). Five out of 8 studies involving Cercon zirconia reported framework fractures both in single crowns and FPDs. In an *in vitro* trial it was reported that a force of 379 to 501 MPa was needed to load Cercon zirconia 4-unit FPDs to failure, which is higher than the average human bite, confirming its suitability as a substructure framework for FPDs (Taskonak et al. 2008a). Cercon zirconia is a non-HIPed Y-TZP, and it is too early to say whether it is a weaker brand of zirconia compared to others due to the limited number of trials published so far, bearing in mind that Cercon zirconia is the most clinically investigated brand of Y-TZP.

A 5-unit Cercon zirconia maxillary FPD fractured at the connector between two pontics at the first and second premolars after 38 months in service (Sailer et al. 2007). The dimension of the fractured connector was 19.28mm^2, well above the recommended connector area of 9 – 16mm^2 (Raigrodski 2004a). Accidental biting on a stone was reported to be the primary reason for failure. Scanning electron microscopy (SEM) analysis revealed the primary crack initiation site on a Cercon zirconia FPD that failed 29 days after insertion to be from the gingival aspect of the connector, which was around 10.5 mm^2 in surface area (Schmitter et al. 2009). It was claimed by the authors to be due to inappropriate alteration done by a dental technician during the veneering of the FPD. This confirms reports that the most susceptible part to fracture in all-ceramic FPDs is the connector area (Kelly et al. 1995; Oh et al. 2002). In fact, fractographic analyses of five failed 4-unit Cercon zirconia FPDs confirmed all the connector failures were initiated from the gingival surface; where tensile stresses were the greatest (Taskonak et al. 2008a). In contrast, lithium disilicate-based FPDs were found to fracture from the occlusal surface of the failing connector (Taskonak et al. 2006). Framework fracture was also reported in a load bearing site, at the cervical margin of a maxillary premolar (Roediger et al. 2010). Reduced thickness of the framework was proposed to be the reason for this fracture.

As for single crowns, one Cercon zirconia crown used to restore a nonvital maxillary 2nd molar, fractured in half after 1 month of service (Çehreli et al. 2009). This tooth did not have a post, and although bruxism was part of their exclusion criteria, the patient reportedly had nocturnal bruxism, for which he had been undertaking muscle-relaxation splint therapy.

Despite the promising results reported *in vitro* (Ohlmann et al. 2005), inlay retained FPDs made with IPS e.max ZirCAD (Ivoclar Vivadent), also a non-HIPed Y-TZP, demonstrated the highest incidence of fractured frameworks in just 1-year, with a survival rate of 57% (Ohlmann et al. 2008). These FPDs had inlays, partial and full-crowns as retainers with at least one retainer being an inlay. Debonding of 20% of the retainers resulted in 10% framework fractures primarily when one retainer debonded, which subsequently over loaded the connectors to failure. Bonding procedures in this study used the generally recommended bonding method for Y-TZP, namely using tribochemical silica-coating air abrasion (Rocatec, 3M ESPE) pretreatment of the inner surface of the copings, followed by silanisation and cementation using phosphate monomer resin cements, Panavia F

(Kuraray) and Multilink Automix (Ivoclar Vivadent). Debonding was explained by the reduced area of adhesion, either due to the small surface area of the inlay retainers or due to voids in the resin cement. No other *in vivo* studies investigated the longevity of inlay retained FPDs, and furthermore, The study by Ohlmann al. 2008 was the only *in vivo* study conducted on IPS e.max ZirCAD. The physical properties of IPS e.max ZirCAD are no lower than the average Y-TZP (Giordano 2006), hence the high failure rate seen could only be explained by the design of the inlay retained framework. Wolfart & Kern reported two case studies involving inlay retained FPDs. These inlay retained FPDs had modified wrap-around wing retainers resembling metal winged resin-bonded retainers in order to increase the bonding surface area. These also had full thickness zirconia that omitted any veneering ceramic for maximum strength (Wolfart et al. 2006). Nevertheless, in contrast to other treatment modalities, Y-TZP IRFPDs cannot yet be recommended and should not be clinically prescribed until improvements in bonding of zirconia are achieved and further long-term clinical trials are published.

An *in vitro* study of five framework designed cantilever zirconia FPDs made of Lava (3M ESPE) showed poor fracture resistance, where most fractures occurred at the distal wall of the terminal abutment (Ohlmann et al. 2009). As a consequence, cantilever FPDs made of zirconia were not recommended by the authors; nevertheless, a 3-unit, and a 4-unit cantilever Y-TZP FPDs survived 3-years in function in the posterior region of the mouth (Tinschert et al. 2008). These cantilever FPDs were made from DC-Zirkon (DCS Dental AG) HIPed densely sintered blanks, and cemented with zinc phosphate cement. Further larger sample sizes and longer follow-up periods are necessary before zirconia cantilever FPDs can be recommended.

2.3.2 Chipping of veneering porcelain

Zirconia has a white opaque color, which needs masking by veneering it with a more translucent, and aesthetic porcelain to achieve an acceptable aesthetic result, as with porcelain-fused-to-metal restorations (PFM). The most striking finding reported in the literature is the high incidence of cohesive failure of veneering porcelain, manifesting clinically as chipping of veneering ceramic with or without exposing the underlying Y-TZP framework. The incidence of chipping fractures ranged from 0% in two studies, both on Cercon zirconia at 2-years (Çehreli et al. 2009) and 3-years (Beuer et al. 2009a), to as

high as 54% in just 1-year (Larsson et al. 2006). No brand of Y-TZP has escaped this problem and it has been reported in all seven brands of zirconia investigated for crowns and bridges as follows: Cercon [15% in 5-years (Sailer et al. 2007), 14% in 4-years (Roediger et al. 2010), 11% in 4-years (Wolfart et al. 2009), 3% in 2-years (Schmitter et al. 2009), 4% in 1.75-years (Groten et al. 2010), 3% in 1.5-years (Bornemann 2003)]; Lava [5% in 3-years (Schmitt et al. 2010), 25% in 2.5-years (Raigrodski et al. 2006), 3% in 1-year (Crisp et al. 2008), and 3% in 2-years (Pospiech et al. 2003)]; IPS e.max ZirCAD [13% in 1-year (Ohlmann et al. 2008)]; Procera [2% in 3-years (Örtorp et al. 2009)]; DC-Zirkon [6% in 3-years(Tinschert et al. 2008), 15% in 2-years (Vult von Steyern et al. 2005)]; Denzir [36% in 5-years (Molin et al. 2008), 54% in 1-year (Larsson et al. 2006)] and Digizon (Amann Girrbach, Pforzheim, Germany) [9.5% in 3-years (Edelhoff et al. 2008)]. In some occasions they occur at non load-bearing areas, and no set pattern has been identified so far, although the second molars have been reported to have a higher incidence than the rest of the dentition due to higher forces found in the posterior of the mouth (Raigrodski et al. 2006; Tinschert et al. 2008).

It is important to appreciate that a large number of reported chip fractures were undetected by patients and were an incidental finding during review appointments (Vult von Steyern et al. 2005; Larsson et al. 2006; Crisp et al. 2008). Some patients were satisfied with simply polishing the rough margins (Sailer et al. 2007; Crisp et al. 2008; Schmitter et al. 2009; Roediger et al. 2010), or repairing the fracture with composite resin (Edelhoff et al. 2008; Wolfart et al. 2009). While in some cases, the patients chose not to have them polished at all (Raigrodski et al. 2006). Nevertheless, some restorations did require total replacement due to major chipping fractures that could not be polished because they posed aesthetic concerns (Sailer et al. 2007; Örtorp et al. 2009; Groten et al. 2010).

Chipping fractures can be a disappointment to both the clinician and patient, and it has been noted in the literature as a serious problem (Marchack et al. 2008), instigating a large number of studies investigating this phenomenon in an attempt to solve it. Numerous reasons have been suggested, such as mismatch of the CTE between the veneering porcelain and the zirconia substructure (Fischer et al. 2009a), mechanically defective micro-structural regions in the porcelain, areas of porosities (Ohlmann et al. 2008), surface defects or improper support by the framework (Marchack et al. 2008), overloading and fatigue (Coelho et al. 2009a), low fracture toughness of the veneering porcelain (Beuer et

al. 2009b), and finally the low thermal conductivity of zirconia (Swain 2009). Delamination, as opposed to chip fractures has also been proposed as a cause of failure. Delamination is the adhesive failure between the veneering ceramic and zirconia, manifesting clinically as the complete loss of porcelain partially exposing the substructure. Ohlmann et al. (2008) argued that delamination can only be confirmed after microscopic examination, which is impossible if the restoration remains in situ, and therefore it is quite possible that many fractures that have been classified as delamination may in fact be chipping fractures. This speculation is supported by evidence that the bond strength between zirconia and a large number of veneering porcelains with varying CTEs were higher than the cohesive strength of the porcelain itself (Al-Dohan et al. 2004; Tsalouchou et al. 2008; Fischer et al. 2009a). Consequently it has been concluded that the veneering porcelain is the weakest link, and improving its strength could reduce the incidence of veneering porcelain chipping (Ashkanani et al. 2008; Fischer et al. 2009a). This was attempted by using high strength heat-pressed ceramics that have been shown to have better bond strengths to zirconia frameworks compared to traditional layering ceramics, receiving support in the literature (Aboushelib et al. 2006). Aboushelib and colleagues described a "double veneering" technique which combines the high bond strength of heat-pressed ceramics with the superior aesthetics of layered porcelain in an effort to improve the overall strength and aesthetics of the veneering porcelain (Aboushelib et al. 2008). Unfortunately, chipping fractures have also been reported to affect pressed porcelain in clinical trials on zirconia FPDs and does not appear to have solved this chipping problem (Molin et al. 2008; Ohlmann et al. 2008).

Improper design of the zirconia framework has also been suggested to be a contributing factor in chipping fractures, due to inadequate support provided by thin zirconia copings commonly milled. Recently, an improved customised zirconia coping design has been recommended by bulking out the substructure to provide adequate support for the veneering porcelain. This was demonstrated in a case report by Marchack and colleagues (Marchack et al. 2008), where the design of their zirconia crowns was taken from the conventional PFM technique of a full contour wax-up, which was then cut back to allow for the veneering porcelain. An aesthetic drawback would be the visible opaque white zirconia along the palatal or lingual surfaces, however the authors argue that patient acceptance is high as soon as they are given the choice between the appearance of a metal margin or a white ceramic. Tinschert and co-workers (Tinschert et al. 2008) adopted this

modified framework design in their FPDs, however chipping fractures still occurred in 4 of 65 FPDs in their clinical trial spanning 3-years. Alteration of the zirconia crystalline structures during sandblasting prior to the veneering process was suggested by the authors as possible reason why they had chipping fractures, however if that was the case, then complete delamination of the porcelain would be expected rather than chipping fracture of the superficial porcelain.

It is important to note, that none of the clinical trials reviewed mention whether slow cooling protocols were implemented during the final glaze cycles in order to avoid the development of high residual tensile stresses within the veneering porcelains. That is not surprising since these papers report the outcome of restorations that have been fabricated at a time when the issue of fast cooling causing high residual stresses had not yet been raised and brought to the attention of researchers (Guess et al. 2008; Swain 2009). Therefore, it is safe to assume that a slow cooling protocol, tailored around the veneering porcelain Tg, was probably not carried out by those researchers, and it is quite likely that these restorations were fast cooled. Nevertheless, it is not possible to make the assumption that the high incidence of chipping fracture in zirconia-based restorations is due to cooling rates, since this factor has not been addressed in any of the published clinical trials so far.

2.3.3 Low temperature degradation

Catastrophic failure of zirconia restorations has been a major concern due to the inherent spontaneous ageing of zirconia in the presence of water via low temperature degradation. The vulnerability of zirconia to ageing is exacerbated by the fact that its severity has been shown to differ between different zirconias from different manufacturers, and even in zirconia from the same manufacturer but which have been processed differently (Chevalier 2006). This may be reflected clinically, for example, in the higher incidence of fractured zirconia frameworks reported with Cercon zirconia. This suggests a possible weakness of this brand compared to others, or that it may be prone to low temperature degradation. However, before this can be confirmed, further studies with larger sample sizes and a longer review period must be completed, especially given that each case of framework fracture was caused by an initiating factor, such as accidentally biting a stone, improper laboratory technique, insufficient thickness of the zirconia coping, and poor design, which if avoided, longer restoration life-time may have been expected.

2.3.4 HIPed vs. non-HIPed zirconia

The type of blanks from which zirconia restorations are milled have been suggested to affect the final outcome of restorations. Supporters of soft-milling using non-HIPed zirconia claim that hard-milling of HIPed zirconia could introduce microcracks in the framework during the milling process, reducing its overall physical strength and the longevity of the prosthesis (Raigrodski 2004b). This has not been evident in published clinical trials; in contrast zirconia catastrophic fractures have only been reported in non-HIPed zirconia, and not in HIPed zirconia. On the other hand HIPed zirconia supporters claim superior marginal fit because no shrinkage is involved in the manufacturing process, and precise margins are not possible with non-HIPed zirconia, giving rise to the risk of recurrent caries, periodontal conditions, and unaesthetic margins. Sailer et al. (2007) reported the highest incidence of secondary caries (22%) in a non-HIPed zirconia (Cercon zirconia) FPDs after a 5-year follow-up, suggested to be due to using a prototype soft milling method which has since been improved. Notably, no other study reported a high incidence of caries, even when using non-HIPed zirconia. Reich and colleagues (Reich et al. 2008) examined the clinical fit of 4-unit posterior FPDs made by non-HIPed zirconia and found a median marginal gap of 77µm in 24 FPDs, well within the clinically acceptable marginal gap limit of 100-120µm (McLean et al. 1971). Further *in vivo* studies with larger sample sizes and longer follow-up periods are needed to establish any significant differences between HIPed and non-HIPed zirconia restorations, and although more dental zirconia manufacturers supply non-HIPed Y-TZP, so far clinical results favor HIPed zirconia due to the absence of any framework failures in the short-term.

2.4 CONCLUSIONS

1. Based on the limited short-term studies available, zirconia can be said to be suitable for fabrication of all-ceramic posterior single crowns, and long-span FPDs.
2. Inlay retained FPDs cannot be recommended in light of published *in vivo* trials.
3. Chipping of veneering porcelain is confirmed to be an ongoing problem with zirconia- based all-ceramic restorations, and is reported in every clinically tested zirconia brand.
4. Zirconia framework fractures have only been reported in soft milled non-HIPed zirconia, with a possible advantage being seen in hard milling HIPed zirconia.
5. Zirconia based all-ceramic restorations can be cemented with conventional luting cements, however bonding to tooth structure is also possible (but with limited success).
6. So far, no clinical trials have specifically implemented slow cooling protocols for their restorations as part of their study.

CHAPTER 3
INFLUENCE OF CUSP VENEERING PORCELAIN THICKNESS AND COOLING RATE ON RESIDUAL STRESSES IN ZIRCONIA CROWNS

3.0 INTRODUCTION

Residual tensile stresses within the veneering porcelain of zirconia-based restorations have been suggested as the main cause of chipping fractures of veneering porcelain (Swain 2009). Zirconia is a very poor thermal conductor and therefore it traps heat in the veneering porcelain, causing the formation of high thermal gradients within the veneer during cooling of the restoration after the final firing cycle. The rate at which a zirconia restoration is cooled has a direct influence on the development of high compressive residual surface stresses and compensating central residual tensile stresses (Swain 2009; Zhang et al. 2009; Guazzato et al. 2010; Zhang et al. 2010b).

Currently there are no simple techniques to directly measure residual stresses within the veneering ceramic. This is because residual internal stresses are locked within the porcelain, resulting in three dimensional stresses that are axial, hoop and radial (Mainjot et al. 2011). As a result, past studies relied on indirect means to determine residual stress formation in the veneering porcelain, using mathematical modelling (Asaoka et al. 1989; Zhang et al. 2010b), finite element analyses (Proos et al. 2002; DeHoff et al. 2008; DeHoff et al. 2009), fracture mechanics (Taskonak et al. 2008b), optical imaging polarising systems measuring polarised light transmitted through thin porcelain sections (Zallat 2006), and more recently using a hole-drilling method adapted from the engineering industry (Mainjot et al. 2011). Guazzato et al. investigated cracking of veneering porcelains associated with residual stress formation caused by the influence of cooling rate and veneer thickness in zirconia spheres (Guazzato et al. 2010). Basic, but definitive,

global residual surface stresses have been determined using microhardness indentation techniques developed by Marshal and Lawn (1977) (Anusavice et al. 1989b; Asaoka et al. 1992; DeHoff et al. 1996; Taskonak et al. 2008b). This method has been used because of the relative simplicity in sample preparation and testing. Nevertheless, it has been limited to the simple monolayered and bilayered plate model. This is due to the need for a perpendicular flat surface during indentation by the Vickers indenter, which does not suit cuspal inclines and curved surfaces (Anusavice et al. 1989b). The geometry of dental crowns and FPDs, for example are not flat. They have a complex form, being composed of various changes in the thickness of veneering porcelain, sharp contours, and have a sphero-cylindrical form. They are also a bilayered system, involving a core veneered with porcelain. Thus the difference in coefficient of thermal expansion of the core and veneering porcelain, the cooling rate around the veneering porcelains glass transition temperature, and the thickness ratio of core to veneer, have a direct influence on the final residual axial, hoop and radial stress formation within the veneer (Anusavice 2003; Swain 2009). Furthermore, the distribution and magnitude of residual compressive and tensile stresses have a direct influence on the fracture resistance of the veneering porcelain and its clinical serviceability (DeHoff et al. 2009).

The aim of this study was to investigate the influence of cooling rate on the residual surface stresses in zirconia crowns with flattened cusps of different heights. Cusp heights of 1mm, 2mm, and 3mm were investigated using fast and slow cooling protocols during the final glazing cycle. A Vickers indenter test was used to calculate the residual stresses for each crown and the results compared.

The null hypothesis for this study was that residual stresses would be the same for all cusp heights, and for both cooling protocols.

3.1 MATERIALS AND METHODS

3.1.1 Mandibular molar master model

The zirconia crown preparation was completed on an acrylic replica of an anatomical mandibular right molar obtained from a dental morphology teaching kit (Nissin Dental Study Model Mould 305,Nissin Dental Products, Kyoto, Japan) (figure 3-1).

Figure 3-1: Mandibular right molar selected for the study

The roots of the molar form were imbedded into the top platform of a waxed jig with multiple indexing features. The jig was waxed using pink tray wax (Toughened wax no.4, Komdent, Wiltshire, UK) (figure 3-2). A silicone mould (Deguform, Degudent, Hanau, Germany) was made of the waxed jig and imbedded molar, an epoxy resin material (Masterflow 622 Heavy Duty Epoxy Resin Grout, Degussa, Hanau, Germany) was mixed according to manufacturer's instructions and poured into the mould (figure 3-2).

Figure 3-2: Model tooth in waxed jig (left), epoxy resin duplicate of jig (right)

Zirconia crown preparation was carried out on the resin master model using course and fine-grit diamond burs (Komet Diamonds, Brasseler GmbH & Co. Lemgo, Germany), comprising 2 mm occlusal reduction, 1.5 mm axial reduction, 1.2 mm shoulder, 4 mm height and 8 mm width mimicking an average molar full crown preparation (Rafferty et al. 2010) (figure 3-3).

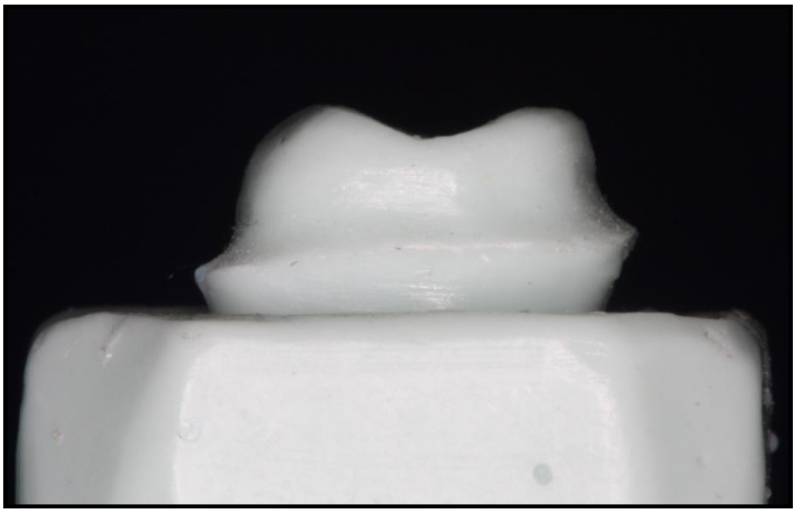

Figure 3-3: Proximal view of full crown preparation

3.1.2 Zirconia crown samples

Using a Piccolo Procera scanner (Nobel Biocare) the master resin abutment was scanned and 50 duplicate 0.7 mm thick Procera zirconia crown copings (Nobel Biocare) were milled, allowing for die spacing of 20 µm. The copings were veneered with a wash layer of IPS e.max ZirLiner (Lot N351534, Ivoclar Vivadent) mixed with IPS e.max ZirLiner Liquid (Lot M32337, Ivoclar Vivadent) and then sintered in a Programat P500 (Ivoclar Vivdent) furnace following manufacturer's instructions (table 3.1). No pre-treatment of the zirconia copings was done, and the first wash firing was done on "as delivered" zirconia (figure 3-4).

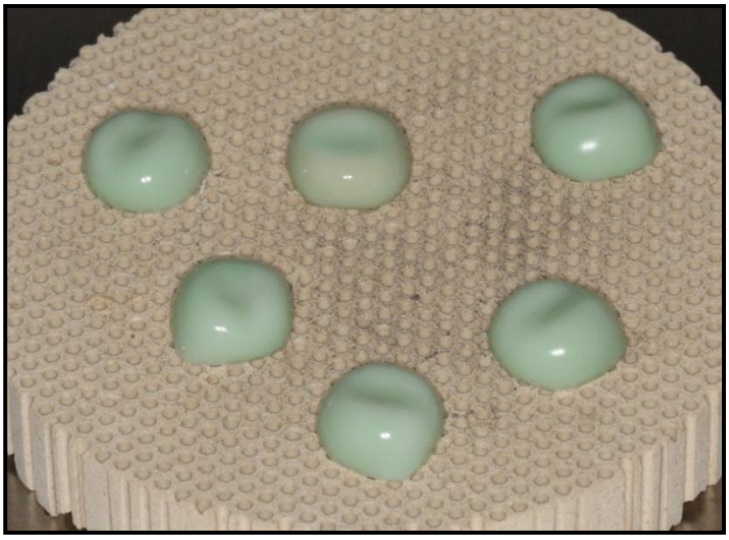

Figure 3-4: Pre-sintered IPS e.max ZirLiner on zirconia copings ready to be sintered

3.1.3 Split putty keys

Using a duplicate of the master resin model, the thickness of the veneering porcelain was modified using blue modelling wax (S-U-Gnatho-Wax Blue, Schuler Dental, Ulm, Germany) to the final anatomy of a flat cusped crown with a 1mm, a 2mm, and a 3mm thick veneering porcelain. Individual split putty keys were then made using polyvinylsiloxane putty material (Express STD, 3M ESPE) which were relined with Exahiflex Injection type (GC America, Alsip, USA), to accurately capture the crown anatomy and indexing features. Molten blue modelling wax was poured into the moulds to produce the various crown forms on zirconia copings (figure 3-5 to 3-8).

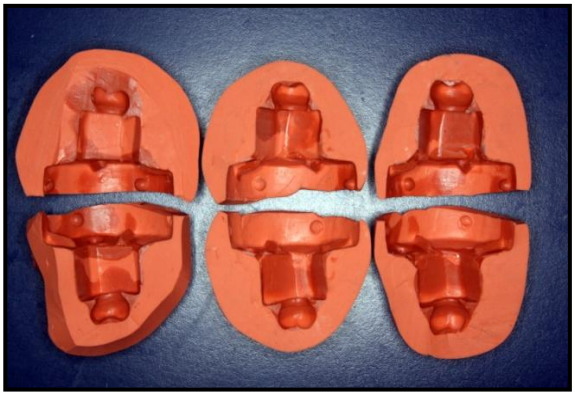

Figure 3-5: Split putty keys used to wax-up 1mm, 2mm and 3mm crowns (left to right)

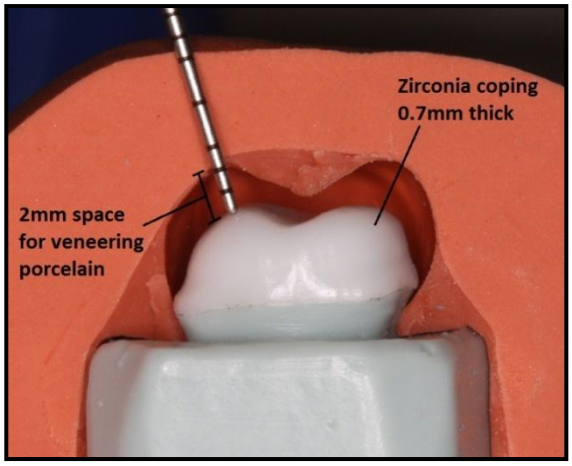

Figure 3-6: Split putty key used to wax-up the 2 mm cusped group

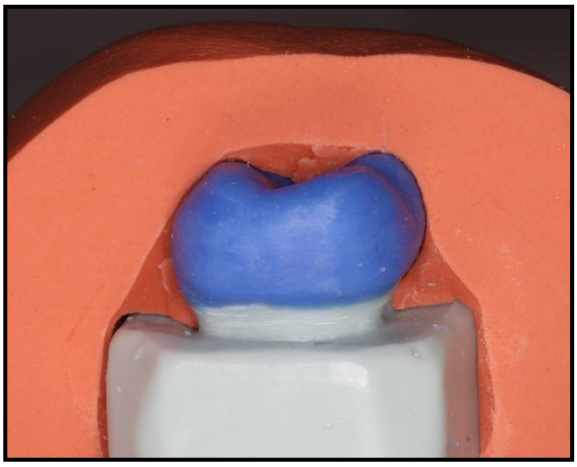

Figure 3-7: Completed waxed zirconia coping

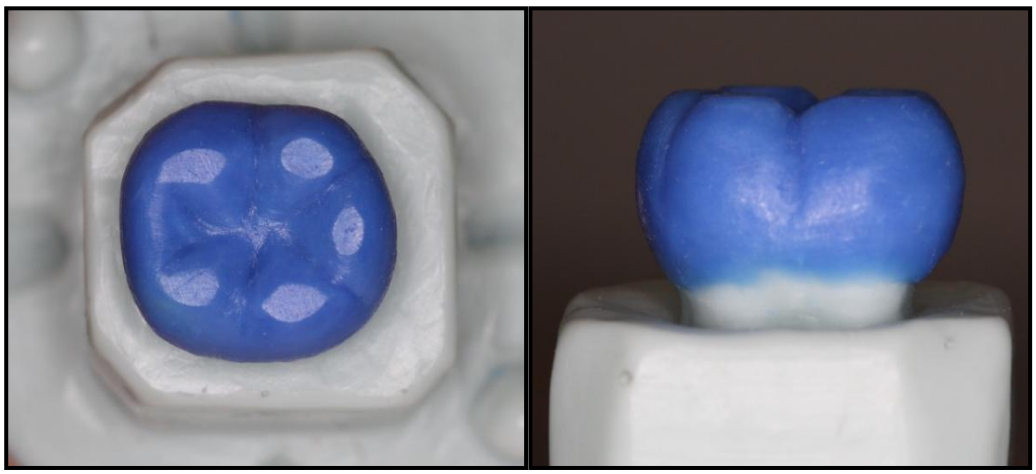

Figure 3-8: Zirconia coping waxed with flattened cusps anatomy

3.1.4 Veneering the zirconia copings

The zirconia copings were veneered with IPS e.max ZirPress (High translucency BL1, Lot K31321, Ivoclar Vivadent) pressable feldspathic porcelain, which were then hand-layered with a 0.5 mm thickness of IPS e.max Ceram (Dentin BL1, Lot L51615, Ivoclar Vivadent) to overcome a severe porosity problem that was noted on the surface of the pressed veneer (figure 3-9).

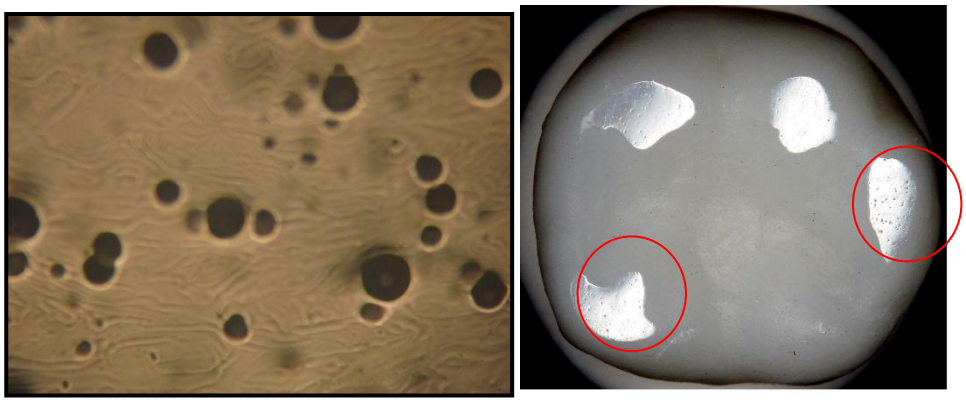

Figure 3-9: Porosities found on the surface of zirconia copings pressed with IPS e.max ZirPress, light microscopic view (left), porosity can also be seen without magnification (right)

IPS e.max ZirPress (pressing temperature 910 ^{o}C, CTE of 9.8 ± 0.25 ppm/^{o}K (100 – 400 ^{o}C), and Tg of 530 ± 10 ^{o}C [manufacturer data]) comes in an ingot form in various translucencies and shades (figure 3-10).

Figure 3-10: Sample of IPS e.max ZirPress ingots used in this study

The pressing procedure involved sprueing the waxed zirconia copings (figure 3-11) and investing using a 200g IPS Investment ring and IPS Press Vest Speed powder (Lot NL3046, Ivoclar Vivadent) with 32ml IPS Press Vest Speed Liquid (Lot NL3025, Ivoclar Vivadent) diluted with 22ml distilled water mixed to the manufacturer's instructions.

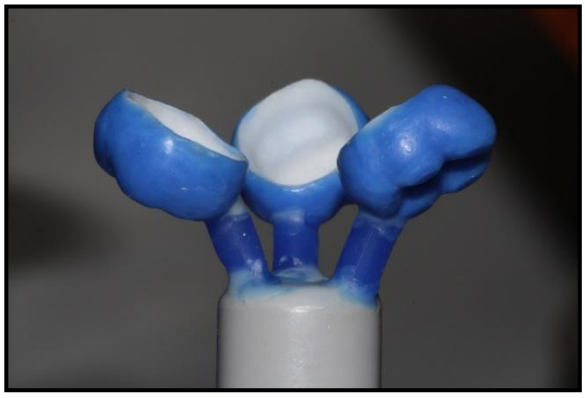

Figure 3-11: Three waxed zirconia copings sprued and ready for investment

After a setting time of 40 minutes, investment rings were transferred to a pre-heated burnout furnace at 850^{o}C and held for 1 hour. Upon completion of the preheating cycle, the investment rings were removed from the burnout furnace and two cold IPS e.max ZirPress ingots were placed into the investment rings and an alumina plunger (IPS Alox Plunger, Ivoclar Vivadent) was inserted before being transferred to a pre-heated Programat EP500 pressing machine (Ivoclar Vivadent) (figure 3-12).

Figure 3-12: Images of the Programat EP500 pressing machine (Ivoclar Vivadent)

Heat pressing was carried out according to the manufacturer's recommended parameters (table 3-1). After cooling the investment to room temperature, divesting was done in a sandblasting unit (EasyBlast, Bego Dental, Bermen, Germany) using 50µm glass beads at 2 bar pressure (Renfert, Hilzingen, Germany). The reaction layer formed during the pressing was removed by immersing the crowns into a hydrofluoric acid solution (IPS e.max Press Invex Liquid, Lot M72255, Ivoclar Vivadent) in an ultrasonic cleaner for 5 minutes. Subsequently the crowns were cleaned under running water for 2 minutes and dried under compressed air pressure. Sprues were cut using a high speed fine-grit diamond bur (Komet Diamonds) under copious water cooling.

Table 3-1: Firing temperature recommended by manufacturers

	Preheating temperature (^{O}C)	**Drying time (min)**	**Heating rate (^{O}C/min)**	**Firing temperature (^{O}C)**	**Holding time (min)**	**Vacuum V1/V2 (^{O}C)**
IPS e.max ZirLiner	403	4	40	960	1	450/ 959
IPS e.max Ceram	403	4	50	750	1	450/ 749
IPS e.max ZirPress	700	-	60	910	15	500/ -

The flat cusps on each pressed crown were cut back by 0.5mm using a high speed fine-grit pear-shaped diamond bur (Komet Diamonds) under water cooling to allow for a thin layer of IPS e.max Ceram veneer. This porcelain has a firing temperature of 750^{o}C, a CTE of 9.5 ppm/^{o}K (100 – 400^{o}C) and Tg of 490^{o}C. Slurry of porcelain powder mixed with modelling liquid (Wieland Dental & Technik GmbH & Co. KG, Pforzheim, Germany) was condensed on the cut-back cusp tips by a combination of blotting with absorbent paper and using an ultrasonic device (Ceramosonic II Condenser, Shofu Inc., Kyoto, Japan) to ensure minimal porosity development within the veneer surface. The hand-layered porcelain was sintered in an Ivoclar Vivadent furnace P500 as recommended by the manufacturer (table 3.1).

After sintering, the flat cusp tips were polished to a mirror finish using 1200, 2000 and 4000 grit silicon carbide rotary polishing discs (Struers Inc., Copenhagen, Denmark) in a TegraSystem polishing machine (Struers Inc.), while the remainder of the veneering

porcelain was polished using diamond impregnated rubber burs (OptraFine, Ivoclar-Vivadent). Figure 3-13 is an example of a polished crown.

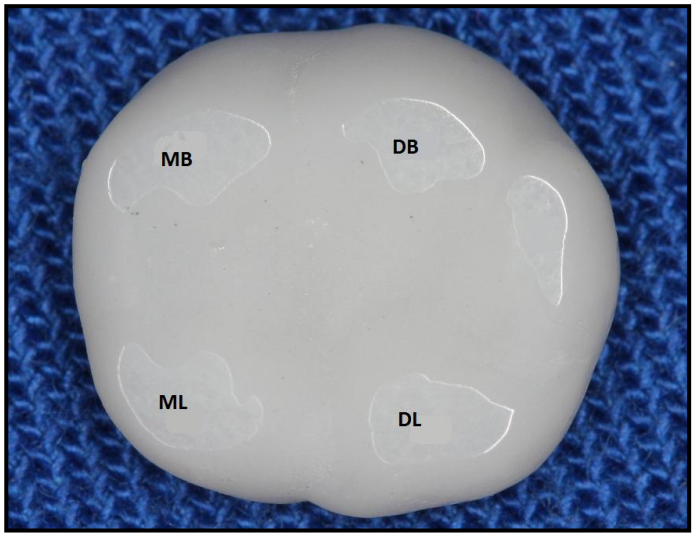

Figure 3.-13: Polished crown demonstrating flattened cusps for indentation; MB, mesio-buccal cusp; ML, mesio-lingual cusp; DB, disto-buccal cusp; DL, disto-lingual cusp

3.1.5 Fast and slow cooling protocols

Six fabricated zirconia crowns were divided into a fast and slow cooled group (figure 3-14).

Figure 3-14: 1mm, 2mm and 3mm cusped zirconia crown samples from left to right

Table 3-2: Codes given to each sample

CUSPS HEIGHT (mm)	FAST GROUP	SLOW GROUP
1	F1	S1
2	F2	S2
3	F3	S3

Each group was subjected to a final glaze cycle according to the firing protocols shown in table 3-3:

Table 3-3: Final glazing firing protocol for fast and slow cooled crowns

	Fast cooled group	**Slow cooled group**
Furnace used	Programat P500	Austromat D4
Preheating temperature (^{O}C)	403	403
Drying time (min)	1	1
Heating rate (^{O}C/min)	60	60
Firing temperature (^{O}C)	725	725
Holding time (min)	5	5
Vacuum (^{O}C)	50	725
Cooling protocol notes	Crowns immediately removed from furnace to bench cool at the end of the firing temperature holding time.	Cooling rate 20^{o}C/min from firing temperature until reached 400^{o}C, then held for 5 mins before crowns allowed to bench cool.

3.1.6 Composite cores

After the completion of glazing cycles, composite cores (Z100, 3M ESPE, Seefeld, Germany) were made for each crown ensuring that the base of the composite core was parallel to the flattened cusps. This was accomplished by using two glass microscope

slides (75mm X 25mm X 1.2mm) that were held apart using two rectangular bars (30mm X 12mm X 0.8mm) made of type III dental stone. Composite bases were built over the composite cores with the crowns inverted on their flat cusps touching the bottom slide, while the final composite cure was done with the top slide flattening the base parallel to the plane of the cusps.

3.1.7 Indentation fracture toughness testing

A total of 5 indentation cracks were made on each flattened cusp tip, resulting in a total of 20 indentations per sample (4 cusps per tooth, 5 indentations per cusp). To aid in crack visualisation and measurements, the samples were sputter coated with gold-palladium prior to indentation (figure 3-15). The indentations were made with a Vickers hardness indenter (Shimadzu Corp., Kyoto, Japan) using a standard 136^{o} pyramidal diamond indenter at a load of 10 N for 15 seconds (figure 3-15 and 3-16). Digital photographic images were taken immediately after each indentation using a digital camera (PowerShot A640, Canon, Tokyo, Japan) which was fixed onto an optical light microscope (Alphaphot-2 YS2, Nikon, Tokyo, Japan) (figure 3-16). Using Adobe Photoshop CS3 software (Adobe Systems Inc., San Jose, USA) each indentation was measured at a later date with minimal error of crack lengths due to continuing crack propagation in the presence of residual indentation stress and environmental moisture during direct crack measurements.

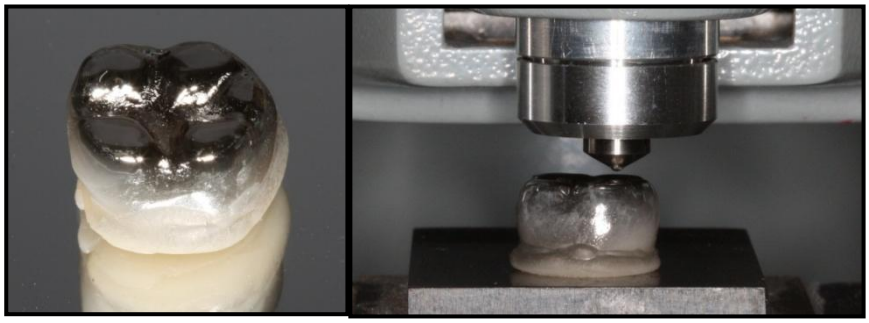

Figure 3-15: Close up image of a sputter coated zirconia crown (left); sample in Vickers indentation machine just before loading (right)

Figure 3-16: Vickers indentation machine (left); optical light microscope with digital camera fixed to the top viewer (right)

3.1.8 Residual stress calculation

In order to calculate the residual surface stresses on the various cusp tips using the indentation technique developed by Marshall and Lawn (1977), the fracture toughness or the critical stress intensity value (K_{IC}) for IPS e.max Ceram was first determined using the following equation:

$$K_{IC} = \kappa \left(\frac{E}{H} \right)^{0.5} \frac{P}{c^{3/2}} \qquad (4)$$

Where *E* is the elastic modulus of the material, *P* is the load applied, *H* is the hardness which is determined by dividing *P* with the measured indent length squared, *c* is the length of radial crack measure from centre of indent, and κ is a constant 0.016.

Discs of IPS e.max Ceram were made to determine its K_{IC} value. Porcelain samples were fabricated into pre-sintered discs of uniform size and shape using a Porcelain Sampler Kit Item No. 7015 shade tab maker (Smile Line, Courtelary, Switzerland) (figure 3-17). Slurry of IPS e.max Ceram powder mixed with modelling liquid (Wieland Dental & Technik GmbH & Co. KG, Pforzheim, Germany) was condensed into the shade tab maker by a combination of blotting with absorbent paper and using an ultrasonic device (Ceramosonic II Condenser, Shofu Inc., Kyoto, Japan) to ensure minimal porosity development within the porcelain discs. Six pre-sintered discs were fired in the Austromat D4 (Dekema Dental, Freilassing, Germany) furnace using the programme recommended by the manufacturer, with a slow cooling protocol to insure minimal residual stress development within the

discs. Sintered discs had a diameter of 10mm and thickness of 2.4mm. The discs were polished flat on both sides using a hand held polishing jig and the discs were attached using cyanoacrylate acid adhesive (Premabond 910, Pottstown, USA) . Polishing was done using 1000, 1200, 2000 and 4000 grit silicon carbide rotary polishing discs (Struers Inc.) in a TegraSystem polishing machine (Struers Inc.) under water irrigation.

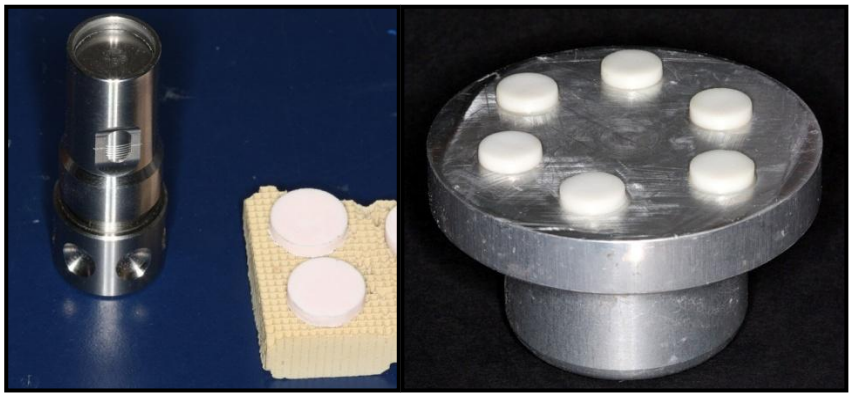

Figure 3-17: Smile Line shade tab maker and pre-sintered discs (left image), hand held polishing jig with 6 sintered discs attached (right image)

The fracture toughness of two IPS e.max Ceram discs were determined using the Vickers indentation technique described in section 3.1.6 and using equation 1.

Once the K_{IC} value for IPS e.max Ceram was determined, residual stress calculation was made for each indent on the flattened cusps by measuring the average crack lengths and indent sizes which were then inserted in the following equation:

$$K_{IC} = \kappa\left(\frac{E}{H}\right)^{0.5}\frac{P}{c^{3/2}} \pm \mathrm{Y}\sigma\sqrt{c} \qquad (5)$$

Where E is the elastic modulus of the material, P is the load applied, H is the hardness which is determined by dividing P with the measured indent length squared, c is the length of radial crack measure from the centre of the indent, and κ is a constant 0.016, Y is the factor for a half- penny surface crack (Y =1.985), σ is the applied or residual stress present. The second term in this equation may be positive or negative depending upon whether the stresses on the surface are tensile or compressive respectively. Figure 3-18 shows an example of how the crack length and indent size were determined. The above approach

was used to determine the residual tempering stresses developed in the veneering porcelains as a consequence of fast and slow cooling protocols for each group.

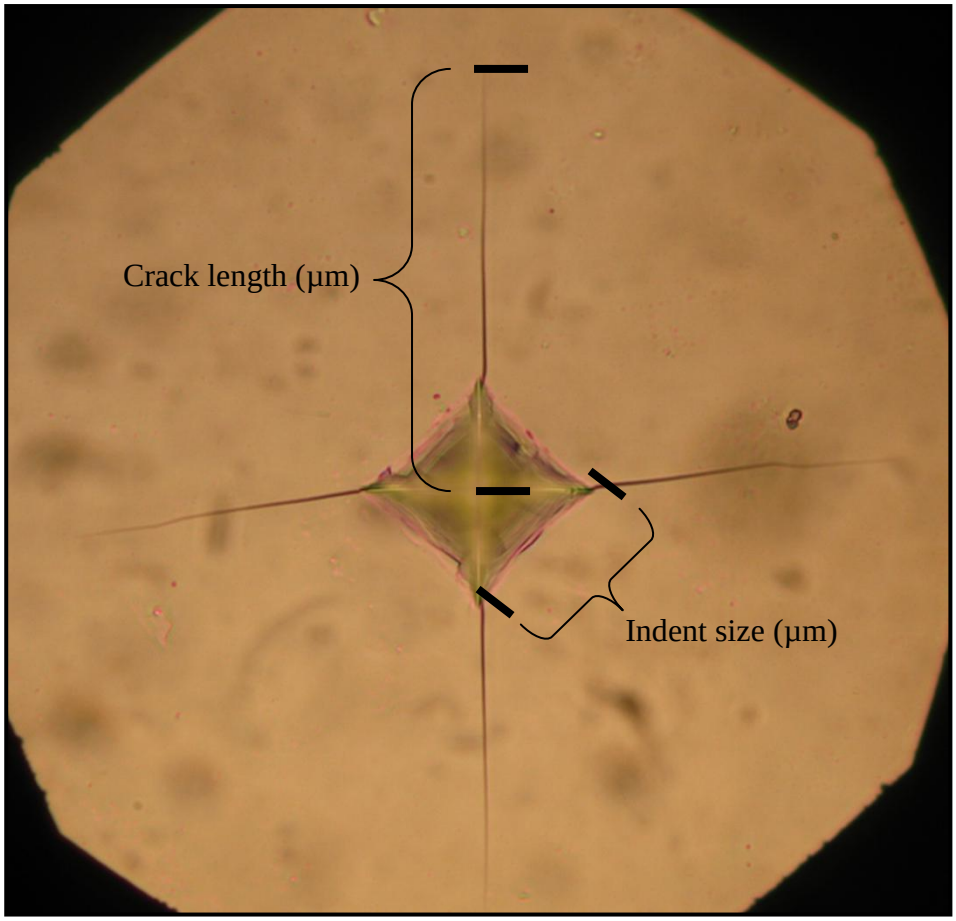

Figure 3-18: Example of crack length and indent size measurements for an indent, each indent had all 4 cracks and sides of indent measured and averaged

3.1.9 Statistical analysis

All statistical analyses were made using Statistical Package for Social Sciences for Windows (SPSS 17.0, SPSS Inc. Chicago, USA). To test for residual stresses normality distribution within each sample, the Kolmogorov-Smirnov & Shapiro-Wilk tests were used. One-way ANOVA tests was used to test for significance between the various cusp heights in the fast cooled group and the slow cooled group. Independent *t*-tests were used to evaluate significance between each cusp height group (1mm, 2mm and 3mm) with regards to the cooling protocols.

3.2 RESULTS

3.2.1 IPS e.max Ceram K_{IC} value

Crack lengths and indent measurements were made on two of the IPS e.max Ceram 2.2mm thick discs. The average crack length was 87.34µm, and indent size was 38.66µm. Using equation 4, the K_{IC} value for IPS e.max Ceram was calculated to be 610,968 $Pa.m^{1/2}$.

3.2.2 Residual stress on cusp tips

Figures 3-19 show examples of indents made on the various crown samples by the Vickers indenters that were used to measure average crack length and indent size to calculate the residual stress for each indent made.

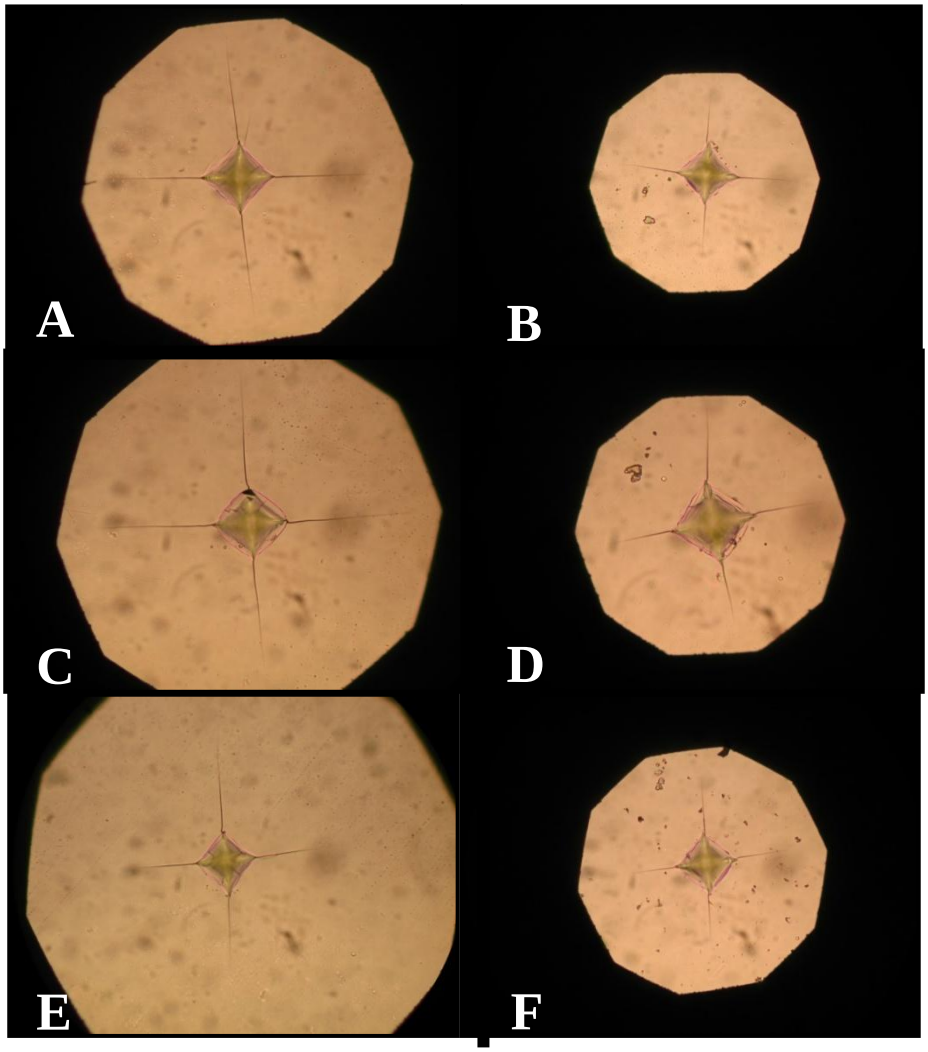

Figure 3-19: Example photographic images of indents on various samples; A: 1mm slow cooled; B, 1mm fast cooled; C, 2mm slow cooled; D, 2mm fast cooled; E, 3mm slow cooled; F, 3mm fast cooled, images are not to scale

For each crown, a total of 20 indents were made by making five indentations on each flattened cusp tip, with a total of four cusps per crown. Table 3-4 shows the average crack size, indent length, and calculated residual stresses with standard deviations for each sample.

Table 3-4: Average results for each sample with standard deviations in brackets

		Crack length (µm)	Indent size (µm)	Residual stress (MPa)
Slow cooled group	1mm	97.25 (4.53)	39.01 (0.56)	4.27 (1.75)
	2mm	101.81 (6.87)	39.27 (0.86)	5.63 (2.24)
	3mm	95.77 (5.68)	38.19 (0.68)	4.19 (2.07)
Fast cooled group	1mm	72.17 (3.94)	39.25 (1.19)	-13.07 (4.37)
	2mm	75.22 (3.79)	38.91 (0.70)	-9.46 (3.25)
	3mm	74.33 (3.08)	38.04 (0.90)	-9.23 (3.04)

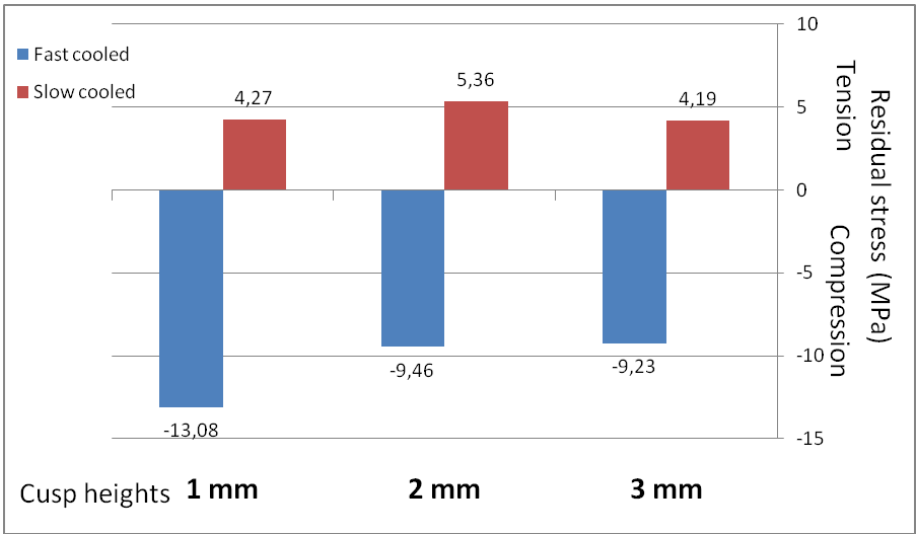

Figure 3-20: Residual stresses on fast and slow cooled 1mm, 2mm, and 3mm crowns

Residual surface compressive stresses were recorded for all fast cooled crowns. In contrast, residual surface tensile stresses were recorded on the cusp tips of all slow cooled zirconia crowns. Statistical normality testing for the residual stresses was done using the Kolmogorov-Smirnov & Shapiro-Wilk tests. Both the fast and slow cooled groups had

normally distributed results (table 3-4), thus one-way ANOVA and independent *t*-tests were used to determine statistical significance.

Within the varying veneering porcelain thicknesses in both groups, the 1mm fast cooled crown had a statistically significant higher compressive residual stresses compared to the 2mm and 3mm fast cooled samples ($P < 0.05$). Furthermore, there was a significant linear trend for residual stress to decrease with the thickness of the veneering porcelain in the fast cooled group ($P < 0.05$). However, there was no statistically significant difference between the 2mm fast cooled and 3mm fast cooled samples ($P > 0.05$). Similarly, the one-way ANOVA test for the means for the various cusp thicknesses in the slow cooled group, did not show any statistical significant differences ($P = 0.05$), moreover there was no significant linear trend with increasing veneering thickness ($P > 0.05$).

There was a statistically significant difference ($P < 0.05$) between the means of the fast and slow cooled crowns for each cusp height tested (1mm, 2mm and 3mm). As mentioned, each of the fast cooled crowns had compression on the surface of the flattened cusp tips, while the surface on the slow cooled crowns were in tension.

3.3 DISCUSSION

3.3.1 Residual stresses with various cusp heights in fast cooled group

Tempering of porcelain by fast cooling, incorporates residual compressive stresses on the surface of the porcelain, effectively toughening it (DeHoff et al. 1990; Asaoka et al. 1992). However compensating tensile stresses, reaching their maximum in the centre of the body, must balance the compressive stresses formed on the porcelain's surface, thus resulting in a net residual force of zero (Tada et al. 2000). It must follow then that in tempered bilayered dental crowns, the higher the residual surface compressive stresses are, the higher are the residual tensile stresses within the crown cusps and/or supporting framework. Furthermore, has been well established that for a monolayer, the thicker the porcelain is, the greater are the thermal gradients throughout the cooling porcelain resulting in higher residual stress formation than in thinner porcelain samples (Asaoka et al. 1989) and bilayered zirconia crown forms (Zhang et al. 2010b).

Residual surface stresses observed in the fast cooled group were all in compression (table 3-4). This corroborates other work on tempered bilayered porcelain flat samples using the indentation technique (Anusavice et al. 1989b; DeHoff et al. 1996), as well as the fracture mechanics approach (Taskonak et al. 2008b). However, increasing the thickness of the veneering porcelain did not result in higher compressive stresses. To the contrary, the 1mm cusped crown had statistically significantly ($P < 0.05$) higher residual compressive stress compared to the 2mm and 3mm crowns (-13.08, -9.46, and -9.23 MPa respectively). Furthermore, there was a significant linear trend for residual stress to decrease with increasing thickness of veneering porcelain in the fast cooled group ($P < 0.05$). However, there were no statistically significant differences between the 2mm and 3mm fast cooled samples in residual surface stresses ($P > 0.05$). Therefore we can reject the null hypothesis, that residual surface stresses in the fast cooled group are the same for all tested flattened cusp heights.

Residual stress profiles of porcelain bodies are geometry-dependent and are additive in nature (Anusavice et al. 1989a). Spherical and cylindrical geometries have been found to generate higher residual stress values than disc geometries (Nielsen et al. 1972; Walton et al. 1985; DeHoff et al. 2008). Using FEA, DeHoff and colleagues found that stress concentrations occurred at the edges of the cylindrical model compared to spheres when the CTE mismatch of the system was less than -0.61 ppm/^{o}K. Equally, residual stresses may vary at different locations in a restoration, due to irregular porcelain/core thickness ratios (Bertolotti 1980), and variations in the thermal properties of the porcelain resulting from different cooling rates (Coffey et al. 1988). Furthermore, abrupt changes in shape and thickness in the ceramic contours of a dental crown or FPD are reported to be areas of potential tensile stress raisers in the system that increase the risk of fracture of the veneering porcelain (Anusavice 2003; DeHoff et al. 2009). Changing the cusp heights in the test samples from 3mm to 1mm, effectively changed the various anatomical contours that influence residual stresses, and may have eliminated potential stress concentration zones in the 1mm crown, allowing the porcelain to contract evenly throughout the veneer. One limitation of this study was that indentation was done on flattened cusp regions, which does not allow for measurement of residual surface stresses at other locations, such as the fossa region where sharp "v" type notches exist between the cusps. It is possible that despite having lower residual compressive stresses on the surface of the cusp tips, stress concentrations existed for the thicker crowns in the fissure regions, influencing global hoop stress profiles on the cusps. Furthermore, despite a number of studies demonstrating that thicker porcelain develops higher residual stresses, in this study, increasing the veneering layer from 2mm to 3mm in the fast cooled crown samples did not develop different residual global surface stresses. Once again, the various complex anatomical features may have limited residual stress differences by directing stress concentrations away from the cusp tips.

It is also probable that the 1mm veneer was subjected to a combined effect from the positive CTE mismatch with the tempering process that caused it to develop higher compressive forces on the surface. According to the manufacturers product sheet, the CTE for IPS e.max Ceram and IPS e.max ZirPress at 100 – 400^{o}C are 9.5 ± 0.25 ppm/^{o}K and 9.75 ± 0.25 ppm/^{o}K respectively, while the CTE for Procera zirconia is reported to be 10.4 ppm/^{o}K at 500^{o}C. This insures a small positive CTE mismatch within the system that

further incorporates residual hoop compressive stresses in the veneering porcelain, while the core goes into tensile hoop stresses (Coffey et al. 1988). In comparison, the 2mm and 3mm veneered crowns were not influenced by the positive mismatch as much as the thin layer.

Part of the sample preparation process, was to produce highly polished crowns with flattened tips on all four cusps. Polishing was done using rotary carbide discs of various grits (see section 3.1.4), however, polishing porcelain has been shown to create a layer of compression on the surface (Tuan et al. 1999; Alkhiary et al. 2003), which may directly influence the indentation results. To overcome this problem, all samples were auto-glazed during the final glazing cycle for 5 minutes rather than the recommended 1 minute. Extended glazing was done for two reasons. First, it served to anneal the system and relax any surface compressive stresses created during the polishing process (Anusavice 2003). Annealing however, has been reported to be a complex procedure, and effective annealing temperature and duration is material specific (Fairhurst et al. 1992; Fischer et al. 2005). Therefore it is difficult to confirm that residual compressive stresses from the polishing process were removed by the 5 minute annealing time, however to establish this is beyond the scope of this research. Secondly, it allowed sufficient time for thorough heating of the entire sample at the glazing temperature before the cooling protocols were initiated. The recommended 1 minute glazing time may have not been long enough for the porcelain in the thickest regions to reach its visco-elastic state, thus influencing the final residual stresses in the thicker crowns.

3.3.2 Residual stresses with various cusp heights in slow cooled group

Residual surface stresses on the slow cooled crowns with various cusp heights did not show any statistically significant differences ($P = 0.05$). Moreover, there was no significant linear trend with increasing the veneering thickness such as that seen in the fast cooled group ($P > 0.05$). Furthermore, in contrast to the fast cooled group, the 1mm, 2mm, and 3mm slow cooled crowns demonstrated residual tensile stresses on the flattened cusp surfaces (4.27, 5.63, and 4.19 MPa respectively).

Studies investigating residual surface stresses created by various cooling rates on flat discs support these results. Using fracture mechanics to calculate residual stresses in zirconia bilayered disc samples, Taskonak et al. reported high residual tensile stresses for samples slow cooled from Tg, as well as several temperatures above and below Tg (Taskonak et al. 2008b). In comparison, all fast cooled samples exhibited residual compressive stresses. Tensile stresses have also been found using the Vickers indentation technique to measure residual surface stresses in slow cooled opaque porcelain-body porcelain discs (Anusavice et al. 1989b; Anusavice et al. 1991), and metal-porcelain discs (DeHoff et al. 1996). The residual tensile stresses reported by those studies ranged from 8.4 - 47.5 MPa, which was significantly higher than that observed in our results. This may be explained by the geometric influences in the crown anatomy, such as stress concentration zones and changing thickness ratios that were not present in the flat plate samples.

It is important to realise that the results in this study are limited to local residual surface stresses and do not report on maximum principle stresses existing within each system. Using mathematical modelling and FEA, authors are able to determine maximum principle stresses in various geometries. However these studies do so using many assumptions and therefore arbitrarily selected values (Asaoka et al. 1989; DeHoff et al. 2008; DeHoff et al. 2009). In a recent FEA study on various geometries, including molar crown and 3-unit FPD, De Hoff et al. found that maximum global tensile stresses were higher in FPD forms than in discs (44.0MPa and 5.4MPa, respectively). High tensile stresses occurred at the connector areas of the FPD, which supports the finding that all-ceramic FPDs fail clinically in the connector areas (Taskonak et al. 2006). Similarly, tensile stresses were higher at the core/veneer interface compared to those at the surface. This may explain the relatively low tensile stresses recorded at the surfaces of the slow cooled crowns in this study.

The Austromat D4 (Dekema Dental) porcelain furnace was used for the slow cooling protocol because of the accuracy of control of these furnaces in bringing the crowns down through the glass transformation temperature range. The firing table mechanism allows the table to exit the furnace in a vertical downwards direction so the crowns are subjected to high radiant heat from the furnace muffle resulting in even heating/cooling of the crown. However, this mechanism is limited when wanting to carry out a fast cooling cycle

because it takes too long for the table to exit the furnace muffle and the radiant heat from the muffle influences the rate of cooling through the Tg temperature. In contrast, the "clam" lid design of the Programat P500 furnaces (Ivoclar Vivadent) opens immediately at the end of the program so the crowns can be removed from the firing table, minimising exposure to radiant heat, allowing a fast cooling cycle. This design is less suitable for slow cooling because the opening of the "clam" lid muffle at an angle to the crowns on the firing table results in one side being subjected to radiant heat and the other side cooling faster with less control. Crowns in the slow group were cooled at the rate of 20^{o}C/min after the completion of the glazing cycle from 725^{o}C, to 400^{o}C. This slow cooling rate insured that the veneering porcelains in this system (IPS e.max ZirPress and IPS e.max Ceram) reached their glass transition temperatures at a slow rate throughout the entire thickness of the veneer. According to the manufacture's data sheets, the Tg values for IPS e.max ZirPress and IPS e.max Ceram are 530 ± 10^{o}C and 490 ± 10^{o}C respectively. If we were to take the lower value for each porcelain, then cooling from the 725^{o}C glazing temperature to Tg of IPS e.max ZirPress took just over 10 minutes, with a further 2 minutes for the temperature to reach the glass transition temperature of IPS e.max Ceram. The temperature was then held at 400^{o}C for further 5 minutes before crowns were removed from the furnace. Once again, this was to insure that the entire veneering layer reaches a temperature below Tg before the crowns are allowed to cool in ambient air. This thorough slow cooling protocol may account for the minimal difference in residual surface stresses recorded for 1mm, 2mm and 3mm crowns.

The three main influencing factors that determine residual stresses in bilayered dental restorations are reported to be differences in the coefficient of thermal expansion (CTE) between the core substructure and the veneering porcelain, cooling rate of the restoration to room temperature, and thickness of the veneering porcelain (Coffey et al. 1988; DeHoff et al. 1996; Swain 2009). It must then follow that the various cusp heights in this group, should have observed different residual stress magnitudes. However, it would appear that the last factor (thickness of the veneering porcelain) is only critical during *fast* cooling rates but not during slow cooling. This is because thermal gradients that influence the residual stresses can only be created during differential cooling in thicker porcelains. As a consequence, we would expect to see no significant differences in surface residual stresses in 1mm, 2mm and 3mm cusped crowns when they are slow cooled.

There was a statistically significant difference ($P < 0.05$) between the means of the fast and slow cooled crowns for each cusp height tested (1mm, 2mm and 3mm). As mentioned, each of the fast cooled crowns had compression on the surface of the flattened cusp tips, while the surface on the slow cooled crowns were in tension.

3.4 CONCLUSIONS

1. Fast cooled zirconia crowns exhibited residual surface compressive stresses on the cusp tips, while tensile stresses were recorded on the cusps of slow cooled crowns.
2. In the fast cooled group, there was a trend for residual surface stresses to decrease in compressive stresses with increasing veneering porcelain thickness from 1mm to 2mm, whereas an increase in thickness beyond 2mm did not have any further influence.
3. Increasing the veneering porcelain thickness in the slow cooled crowns did not have an influence on residual surface stresses at the cusp tips of zirconia crowns.

CHAPTER 4
INFLUENCE OF COOLING RATE ON STATIC LOAD-TO-FAILURE OF ZIRCONIA CROWNS

4.0 INTRODUCTION

The mechanical properties of zirconia have made it a suitable material for all-ceramic dental restorations for posterior teeth (Raigrodski 2004b). However, chipping of the veneering porcelain has been identified as one of its main problems, instigating a large number of studies (Al-Amleh et al. 2010). It is now believed that the development of high residual tensile stresses within the veneering porcelain caused by differential cooling of the porcelain around its glass transition temperature may result in an unstable bilayered system prone to chipping (Swain 2009). Zirconia is a very poor thermal conductor, and unlike other core materials, such as gold alloys, heat is trapped in the porcelain close to the zirconia core which leads to large thermal gradients within the veneer. This is exacerbated by rapidly cooling zirconia restorations from high porcelain sintering or glazing temperatures down to room temperature.

Direct evidence of residual tensile zones, or the accurate measurement of their magnitude in actual crown forms is not possible due to the trapped nature of these 3 dimensional residual stresses (Mainjot et al. 2011). Authors mostly rely on simple flat geometric models to study the interaction between residual stress influencing factors and the development of residual stresses (Taskonak et al. 2008b; Göstemeyer et al. 2010; Komine et al. 2010). Others have relied on the incidence of cracking in tempered bilayered zirconia spherical samples (Guazzato et al. 2010), or the maximum load to failure in fatigue tested zirconia crown forms (Rues et al. 2010). On the other hand, mathematical modelling and FEA studies are currently the only way to indirectly visualise these stresses, however, these methods rely on many assumptions that necessitate laboratory testing to verify results (DeHoff et al. 2008).

Static load-to-failure testing on crown forms without fatigue testing or thermocycling has been adopted by investigators due to its simplicity in sample preparation and data collection (Josephson et al. 1985; Burke 1999; Fischer et al. 2007). However, results do not replicate the failure mechanisms seen clinically, and has consequently been discouraged by some (Kelly 1999; Lawn et al. 2001; Thompson et al. 2004). Fractographic analyses of fractured samples not only identifies the origin of failure, but also reveals any variation in residual stresses at different regions of the fractured plane by analysing fractographic marking, such as compression curls and twist hackle lines (Quinn 2007).

This study uses fractographic analysis to confirm the presence or absence of residual stress differences in fractured fast cooled versus slow cooled zirconia crowns. The maximum load-to-failure for both groups will also be reported.

The null hypothesis is that the fractographic patterns and fracture mechanisms of fast cooled and slow cooled zirconia crowns are the same. Furthermore, maximum load-to-failure for both groups are no different.

4.1 MATERIALS AND METHODS

4.1.1 Zirconia crown samples

Ten Nobel Biocare Procera zirconia crown copings were used in this study. Fabrication of the copings was described in sections 3.1.1 and 3.1.2 in chapter 3. Figure 4-1 shows images of the designing process using the Procera Nobel Biocare software.

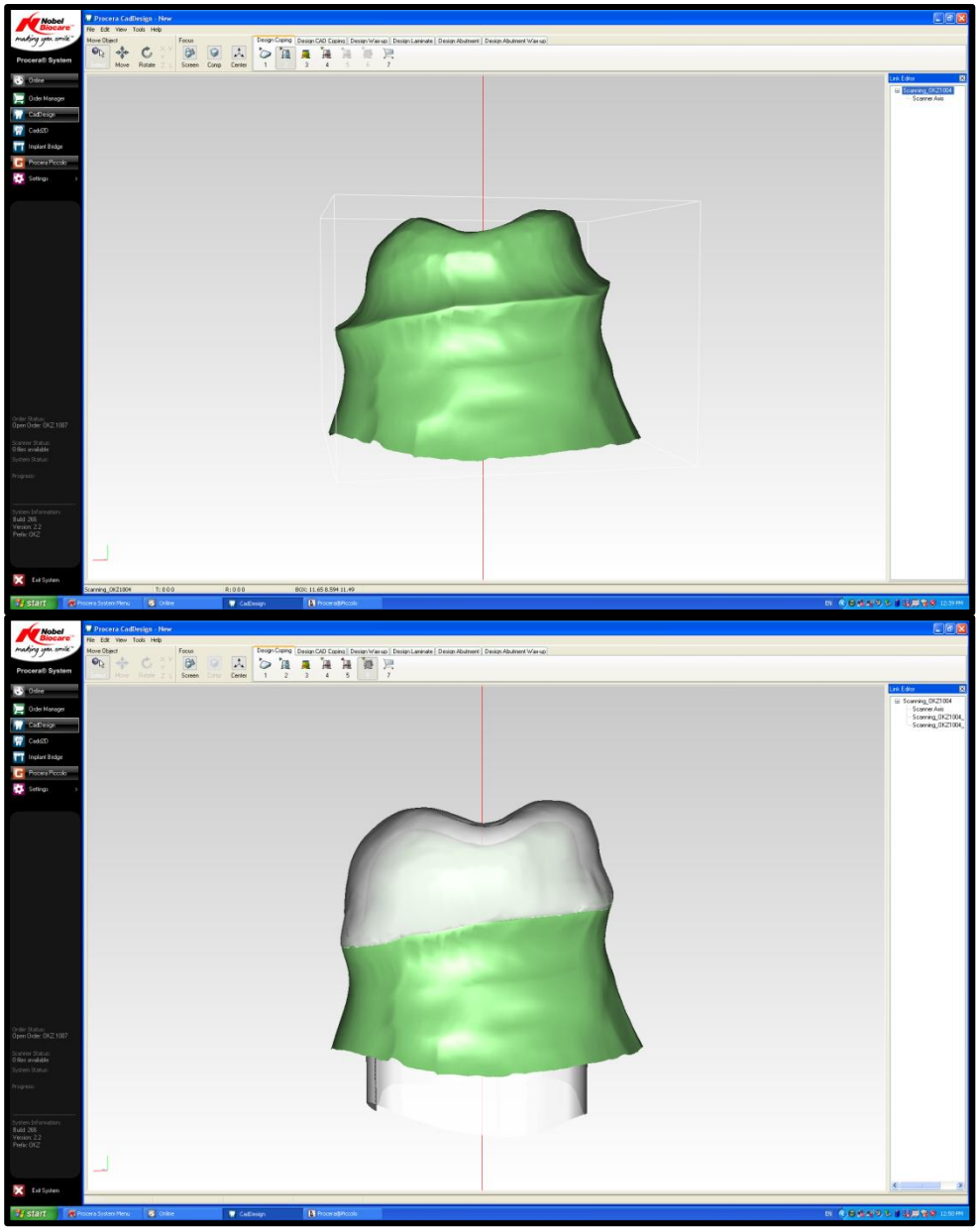

Figure 4-1: Images of the scanned master abutment and zirconia design by Procera Nobel Biocare software

4.1.2 Split putty key

Duplicate crowns were fabricated using a split putty key made of the test anatomical crown form using polyvinylsiloxane putty material (Express STD, 3M ESPE) which was relined with light body addition-silicone impression material (Exahiflex Injection Type, GC America, Alsip, USA). Cusp tips were left un-flattened, maintaining a more clinically realistic crown form compared to the flattened cusp tip zirconia crowns used in the residual stress study in chapter 3. Waxing the copings was also done as described in section 3.1.3.

4.1.3 Veneering the zirconia copings

The zirconia copings were veneered with IPS e.max ZirPress (High translucency BL1, Lot K31321, Ivoclar Vivadent) pressable feldspathic porcelain as described in section 3.1.4. No additional veneering was done using hand-layered porcelains. Each crown was polished to a high polish using diamond impregnated rubber burs (OptraFine, Ivoclar Vivadent).

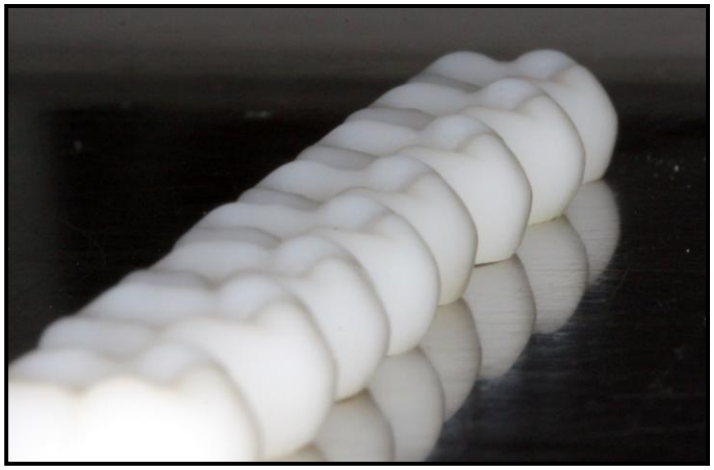

Figure 4-2: Duplicate crowns made using the split putty key and porcelain pressing techniques

4.1.4 Fast and slow cooling firing protocols

Ten pressed veneered zirconia crowns were divided into a fast and a slow cooled group. Table 4-1 shows details of the cooling protocols.

Table 4-1: Final glazing firing protocol for fast and slow cooled crowns

	Fast cooled group	Slow cooled group
Furnace used	Programat P500	Austromat D4
Preheating temperature (^{O}C)	403	403
Drying time (min)	1	1
Heating rate (^{O}C/min)	60	60
Firing temperature (^{O}C)	725	725
Holding time (min)	5	5
Vacuum (^{O}C)	50	725
Cooling protocol notes	Crowns immediately removed from furnace to bench cool at the end of the firing temperature holding time.	Cooling rate 20^{o}C/min from firing temperature until reached 400^{o}C, then held for 5 mins before crowns allowed to bench cool.

4.1.5 Acrylic abutments and cementation

Ten duplicate epoxy resin abutment jigs (Masterflow 622, Heavy Duty Epoxy Resin Grout, Degussa, Germany) were made using a silicone mould of the original full crown preparation resin model that was used for the scanning procedure and for the fabrication of the zirconia copings in section 4.1.1 (figure 4-3).

Figure 4-3: Prepared epoxy resin abutments ready for sample cementations

Each crown was cemented to a resin abutment using dual-cured resin cement (Rely-X Unicem, 3M ESPE) 24 hours prior to testing. No treatment of the zirconia at the intaglio surfaces of the crowns were done before cementation.

4.1.6 Simulated occlusal adjustment of the veneering porcelain

Before loading the crowns with a 4 mm diameter stainless steel ball, occlusal adjustment was carried out on each disto-lingual cusp to simulate clinical adjustment. Adjustments were made using a conventional air turbine high speed-handpiece (KaVo Super-Torque 640B, KaVo Dental, Biberach, Germany) and a pear-shaped fine-grit (46µm) diamond bur (Komet Diamonds, Product no #806 314, Brasseler GmbH & Co. KG, Lemgo, Germany) under water cooling. A new bur was used for each group. The exact site of adjustment for each crown was determined using the following two steps:

1. Using blue marking articulating paper (GC Co., Tokyo, Japan), the stainless steel ball was placed at the distal aspect of each crown to clearly mark the 3 points of contact on the disto-lingual cusp, disto-buccal cusp, and distal ridge (figure 4-4 and 4-5).

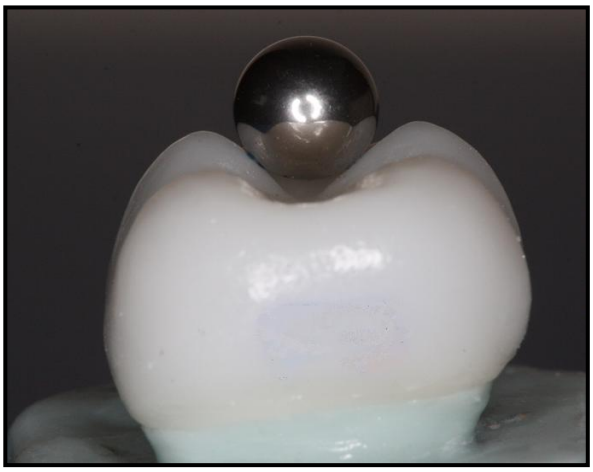

Figure 4-4: 4mm stainless steel ball sitting on the distal aspect of a test crown to demonstrate the area available for adjustment on the DL cusp

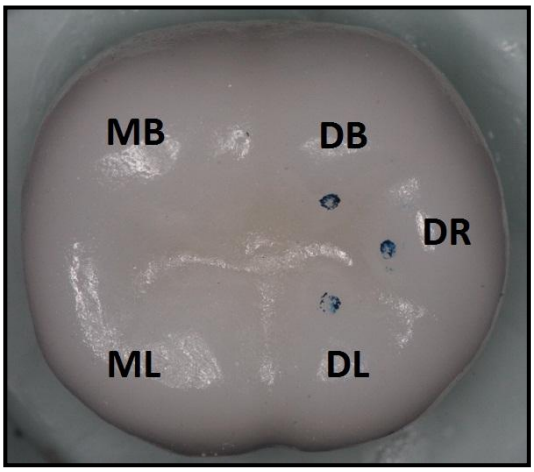

Figure 4-5: Marks made by the ball on the distal aspect of the crown using blue articulating paper

2. Occlusal adjustments were made just below the ball contact area on the disto-lingual cusp using a pear-shaped fine-grit diamond bur under copious water cooling, ensuring not to involve the contact area (figure 4-6). A count of five short strokes was repeated for each crown adjustment.

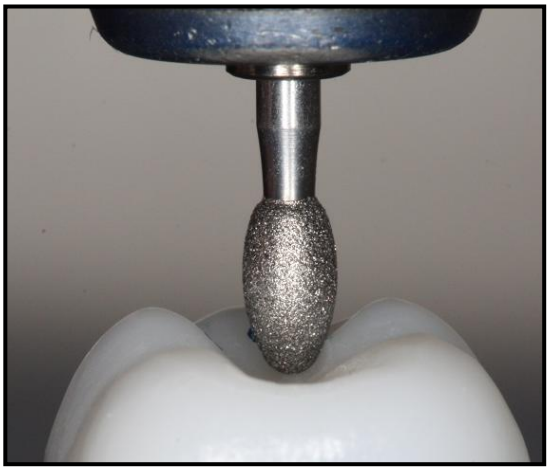

Figure 4-6: Image demonstrates the angle which the pear-shaped bur was held during the occlusal adustment

4.1.7 Static load-to-failure test

Following occlusal adjustment, the crowns were stored in sterile saline solution for 24 hours at room temperature before testing. Only the coronal 2/3 of the crowns was immersed in saline by inverting the crown and resin jig upside down in a small container, avoiding any soaking of the resin jig.

The static loading test was done using a 4 mm diameter stainless steel ball, which sat passively on the distal aspect of the crowns. The ball made contact with the disto-buccal cusp, disto-lingual cusp, and distal marginal ridge. Loading was carried out using an Instron 3369 Universal Testing Machine (Intron Corp, Canton, USA) (figure 4-7). Data was captured using the Bluehill 2 software programme (Version 2.3.359, Instron Corp, Canton, USA). A flat loading platform was used to load the samples at a cross-head speed of 0.1 mm per minute, and a 5kN load cell was used to measure forces. The maximum load-to-failure (N), as well as the flexure extension (mm) were recorded by the software programme. Testing was done under moist conditions by applying a drop of saline on the stainless steel ball before loading.

Figure 4-7: Sample set-up in the Instron testing machine

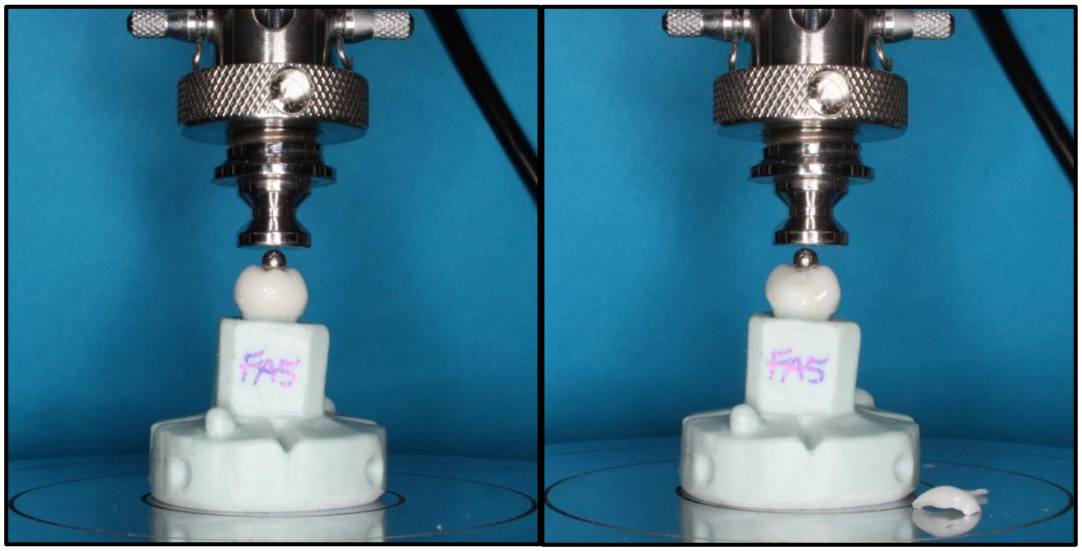

Figure 4-8: Example of one sample in place ready for loading-to-failure (left), and the fractured sample just after testing (right)

4.1.8 Fractographic analysis

Qualitative fracture analysis of each fractured sample was initially carried out by visual interpretation. Fiberoptic trans-illumination was used to aid in seeing the crack propagation path throughout the samples, in addition to illuminating any incidental peripheral cracks independent from the loaded fracture site which may have occurred. Failure was reported as chipping of the veneering porcelain or delamination, in addition to the extent of fracture involvement throughout the crown structure.

Two samples from each group were chosen to be examined under a scanning electron microscope (SEM). Samples were first sputter coated with gold-palladium alloy to a thickness of approximately 15 nm using an Emitech K575X Peltier cooled high resolution sputter coater (EM Technologies Ltd, Kent, UK) fitted with an Emitech 250X carbon coater (EM Technologies Ltd). A Cambridge Instrument S360 scanning electron microscope (Cambridge Instruments, Cambridge, UK) was used for SEM analyses. Images of the SEM scans were captured using a Dindima Image Slave frame grabber (Dindima Group Pty Ltd, Ringwood, Victoria, Australia). Images were 1024 x 768 pixels in size and in Tagged Image File Format (TIF files). A Back scatter Electron Detector (BSD) was utilised in some instances to confirm the exposure of the zirconia core by true delamination of the veneering porcelain. For each sample, at each of the ball points of contact, the occlusal adjustment and fractured porcelain were examined to establish the origin of fracture, path of crack propagation, and mode of failure by interpreting fractographic features such as, arrest lines, compression curls, twist hackle, wake hackle, and hackle lines. Fractography analyses and descriptions were based on the work of George Quinn (Quinn 2007). The aim of fractography was to identify any differences in fracture pattern between the fast and slow cooled samples caused by differences in the residual stress distribution within the veneering porcelain.

4.1.9 Statistical analysis

Independent sample *t*-tests were used to establish any statistical significance in the maximum load-to-failure between both groups. Statistical analyses were done using Statistical Package for Social Sciences for Windows (SPSS 17.0, SPSS Inc, Chicago, USA).

4.2 RESULTS

4.2.1 Maximum load-to-failure results

The load-to-failure recorded for each crown is listed in table 4-2:

Table 4-2: Maximum loads-to failure recorded for each sample

	Sample identification	Load-to-failure (N)
Fast group	FA 1	1060.21
	FA 2	778.82
	FA 3	818.18
	FA 4	884.40
	FA 5	966.07
	Average (SD)	901.54 (113.51)
Slow group	SA 1	882.08
	SA 2	1216.05
	SA 3	1114.58
	SA 4	1137.67
	SA 5	714.65
	Average (SD)	1013.00 (208.11)

The average maximum load-to-failure for the fast cooled group was only slightly lower than that of the slow cooled group (901.54 N and 1013.00 N respectively). There was no statistical difference between both groups ($P > 0.05$), and both the highest and lowest load-to-failure values were recorded in the slow cooled group.

4.2.2 Modes of failure

Figure 4-9 and 4-10 are photographic images of the loaded samples. Drawn on each image are the direction and extent of any cracks found via light trans-illumination.

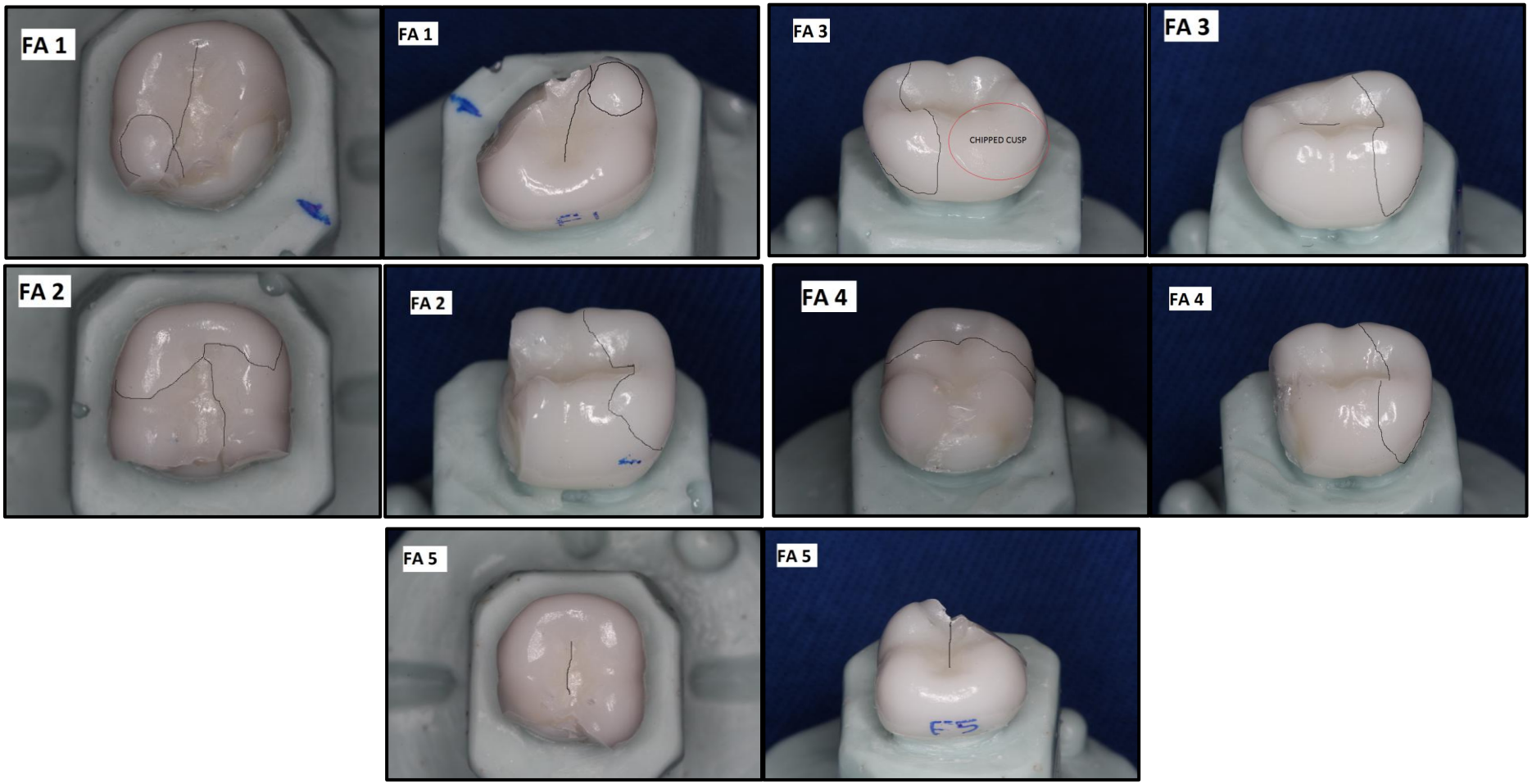

Figure 4-9: Images of loaded fast cooled samples showing modes of fracture and extent of cracks found via light transillumination drawn on (two images per sample)

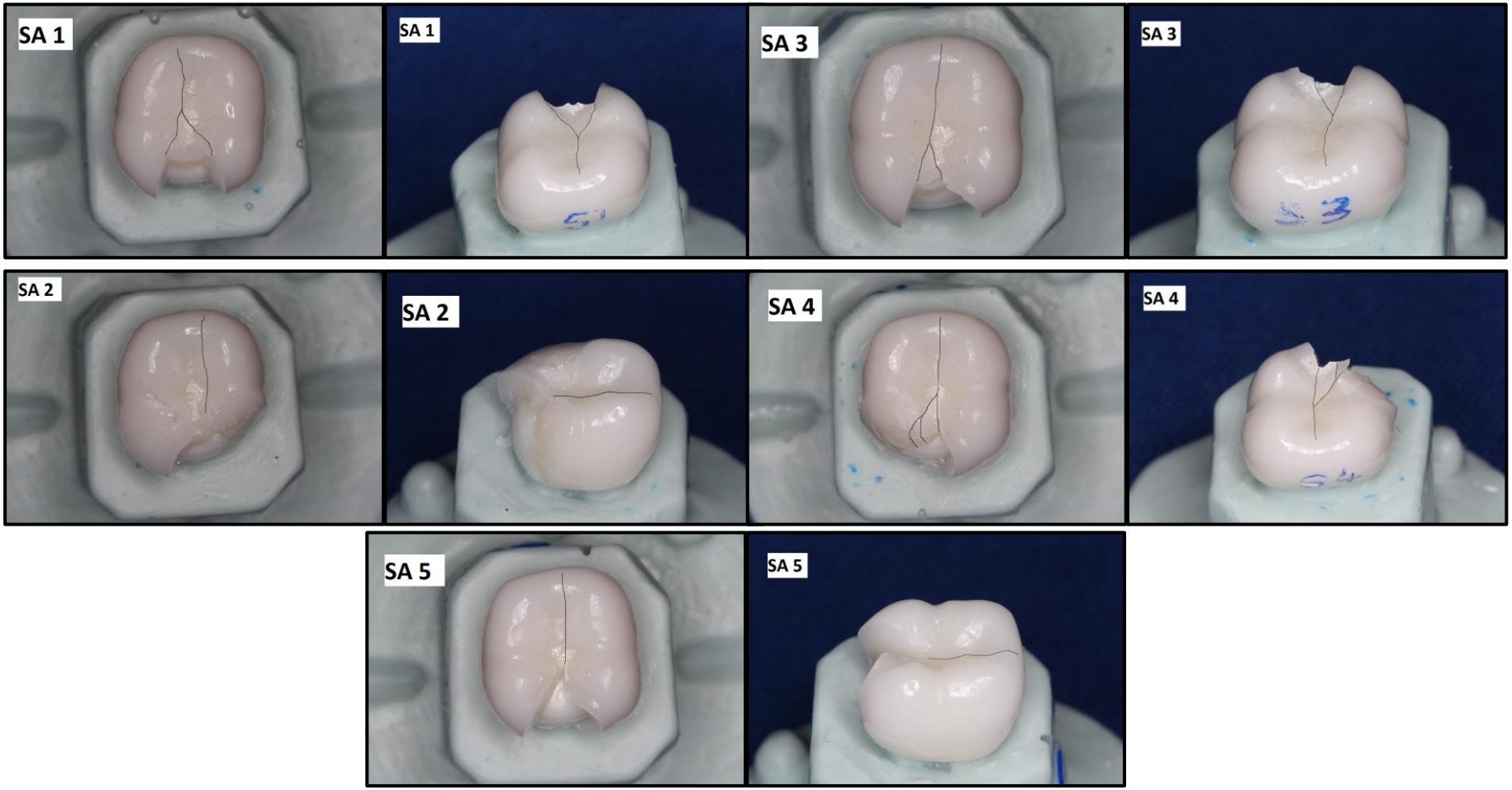

Figure 4-10: Images of loaded slow cooled samples showing modes of fracture and extent of cracks found via light transillumination drawn on (two images per sample)

Delamination fracture was the dominant mode of failure in both the fast and slow cooled groups, and almost exclusively involving the distal ridge of each crown (9 out of 10 samples). The fracture mode at the occlusally adjusted disto-lingual cusp was exclusively chipping fracture, occurring in 4/5 fast cooled crowns and 2/5 slow cooled crowns, with no delamination involving the DL cusp. In the mean time, no zirconia core fractures were observed in this study. Table 4-3 is a summary of the modes of fracture for each sample, as well as the load-to-failure value recorded for each sample.

Table 4-3: Modes of fracture and load-to-failure; DL, disto-lingual cusp; DR, distal ridge; DB, disto-buccal cusp; *, crack running through intact cusp

		Modes of fracture			Mesial cracks	Fissure cracks	Load to failure (N)
		DL	DR	DB			
Fast	FA 1	Chipped but attached	Delamination	Delamination	-	Yes	1060.21
	FA 2	Chipped	Delamination	Chipped	Yes	Yes	778.82
	FA 3	Chipped	Intact	Intact	Yes	Yes	818.18
	FA 4	Intact *	Delamination	Mixed	Yes	-	884.40
	FA 5	Chipped	Delamination	Intact	-	Yes	966.07
Slow	SA 1	Intact *	Delamination	Intact *	-	Yes	882.08
	SA 2	Chipped	Delamination	Mixed	-	Yes	1216.05
	SA 3	Intact *	Delamination	Intact	-	Yes	1114.58
	SA 4	Chipped	Delamination	Intact	-	Yes	1137.67
	SA 5	Intact	Delamination	Intact	-	Yes	714.65

Trans-illumination exposed peripheral cracks on the non-loaded mesial sides of 3 out of 5 samples in the fast cooled group only (figures 4-9, samples FA2, FA3 and FA4). On visual inspection, these cracks appeared to be independent from the primary distal fractures at the loaded sides. None of the slow cooled samples demonstrated similar cracking on the non-loaded sides. On the other hand midline fissure cracks running mesio-distally were noted on 90% of all samples (both fast and slow cooled). The pattern of fracture in 3 out of 5 slow cooled samples were almost identical, involving delamination of the distal ridges only (figure 4-10, samples SA1, SA3, and SA5), with no chipping or fractures involving either distal cusps. No correlation could be made between maximum load-to-failure and modes of failure in both groups.

4.2.3 Fractographic analysis

Two samples from each group were chosen for inspection under SEM. Images of the adjustment areas, each ball contact areas on the cuspal inclines, fractured veneer surfaces and delaminated areas were taken at various magnifications.

Fast cooled samples:

FA 3: load-to-failure: 818 N

This is the only sample that failed by pure chipping fracture of the disto-lingual cusp, which extended to the distal aspect of the mesio-lingual cusp (figure 4-11 to 4-19). The non-loaded mesial aspect of the crown had an encircling crack, in addition to a midline fissure crack which did not meet.

Figure 4-11: FA3 - Photographic image of fracture

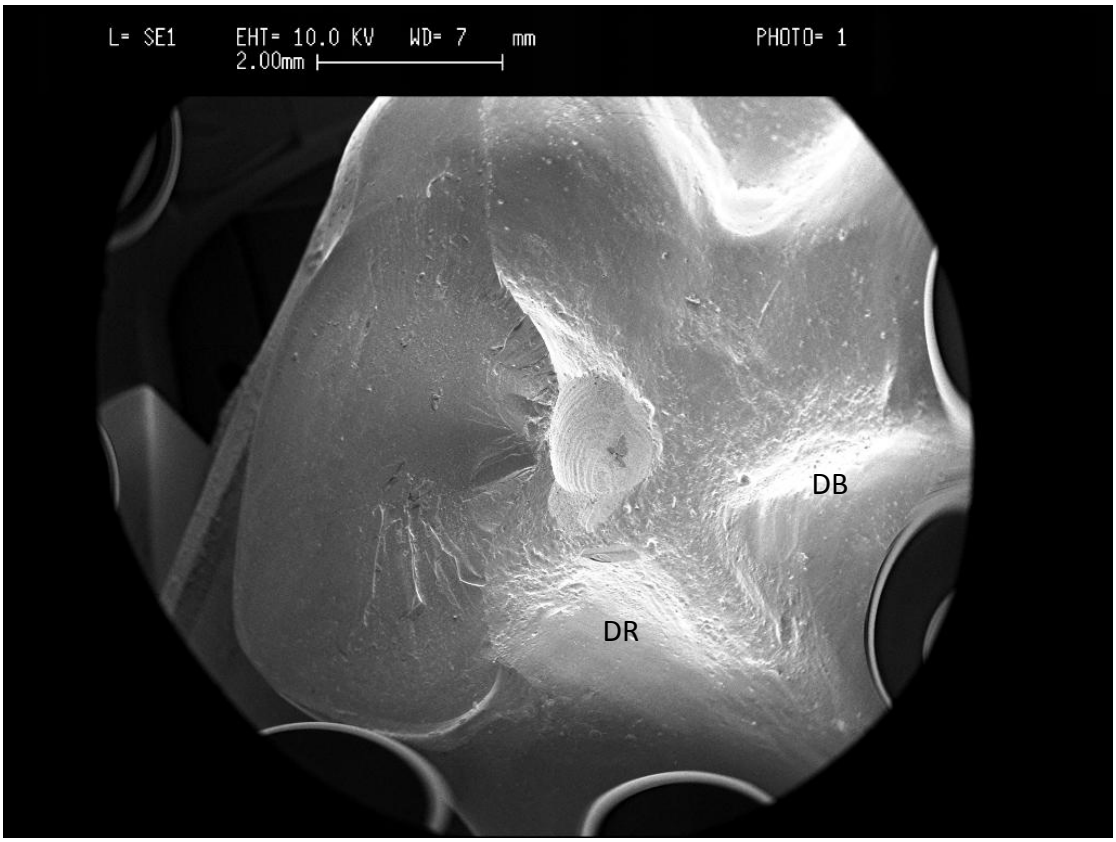

Figure 4-12: FA3 - Overview of chipped DL cusp over the occlusal adjustment; DB; disto-buccal cusp; DR, distal ridge [magnification x 10]

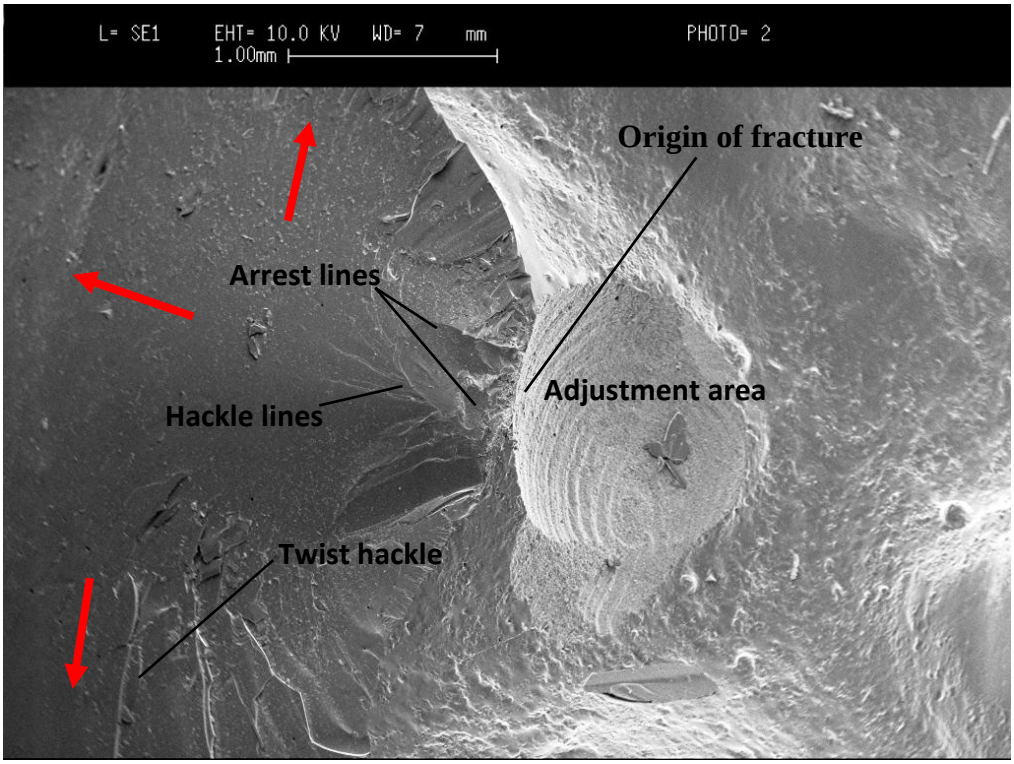

Figure 4-13: FA3 – Origin of fracture above occlusal adjustment, arrest line, hackle and twist hackel lines show patch of crack propagation (red arrows) [magnification x 50]

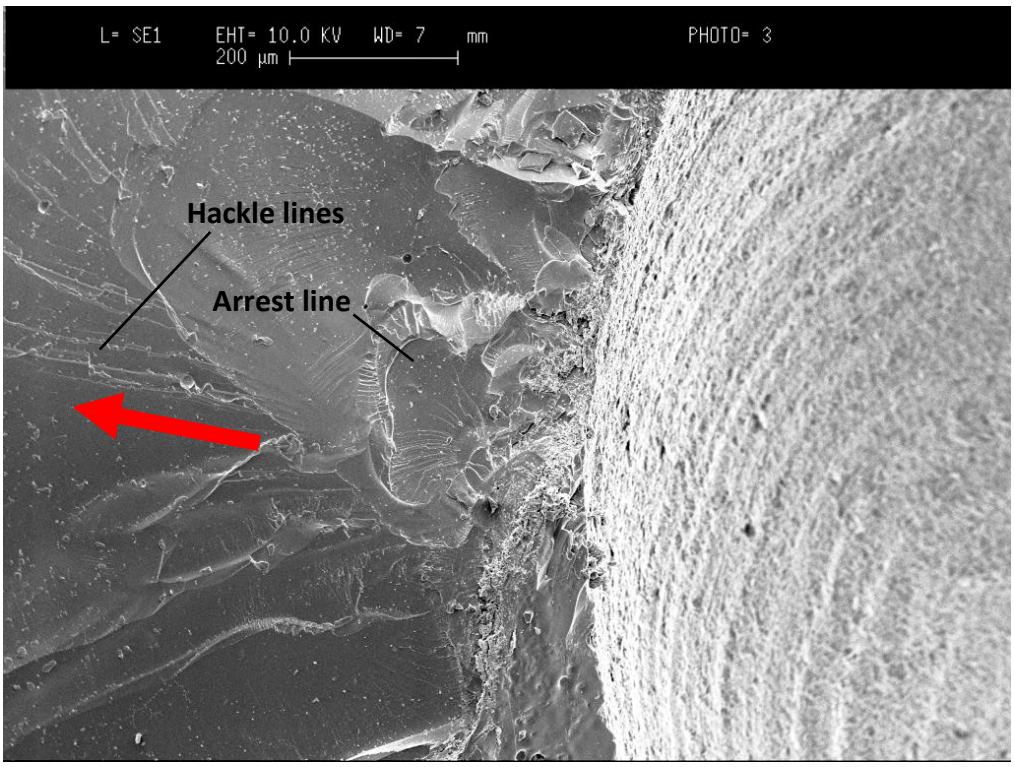

Figure 4-14: FA3 – Close-up of origin of fracture site showing crush zone at ball contact area above occlusal adjustment and arrest lines [magnification x 100]

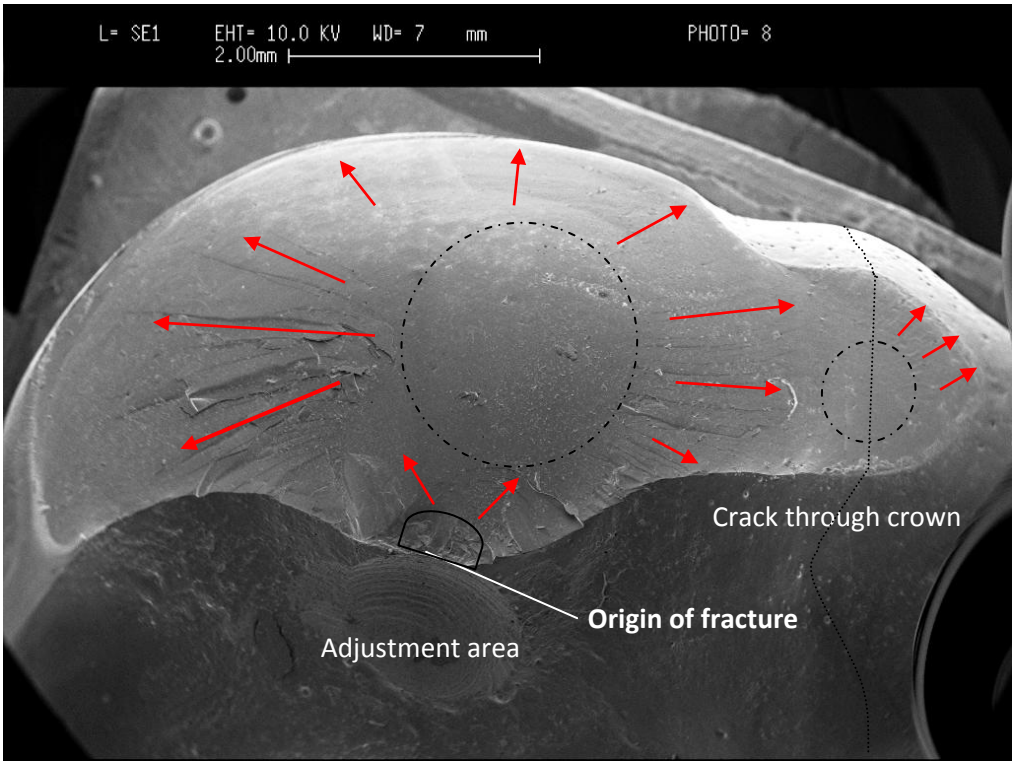

Figure 4-15: FA3 – Red arrows showing direction of crack propagation determined via twist hackle and hackle lines which correspond to superficial porcelain, while dotted circles outline featureless fracture planes corresponding to deeper porcelain zones, mesial crack marked by dotted line right of image [magnification x 15]

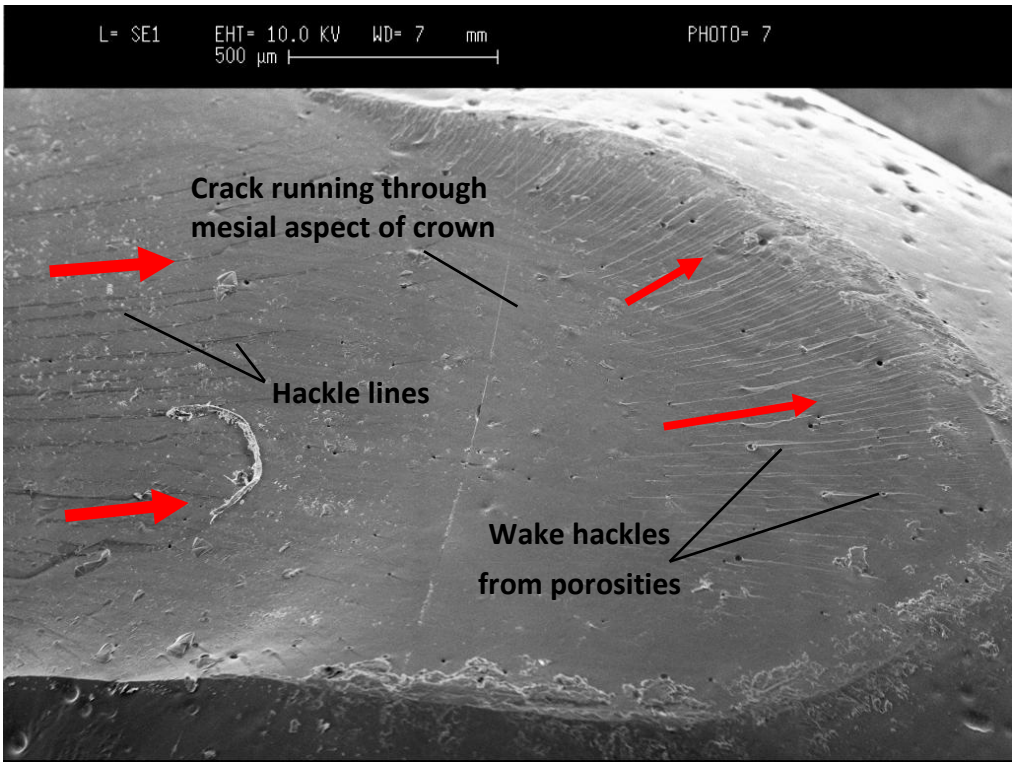

Figure 4-16: FA3 - Mesial extension of chip extending over to ML cusp [magnification x 50]

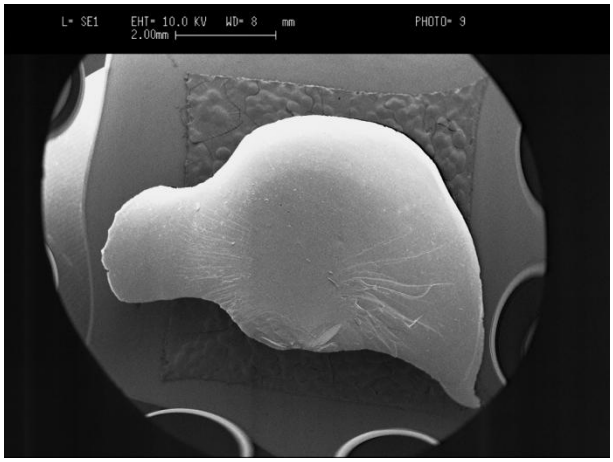

Figure 4-17: FA3 - SEM image of underside of chip [magnification x 10]

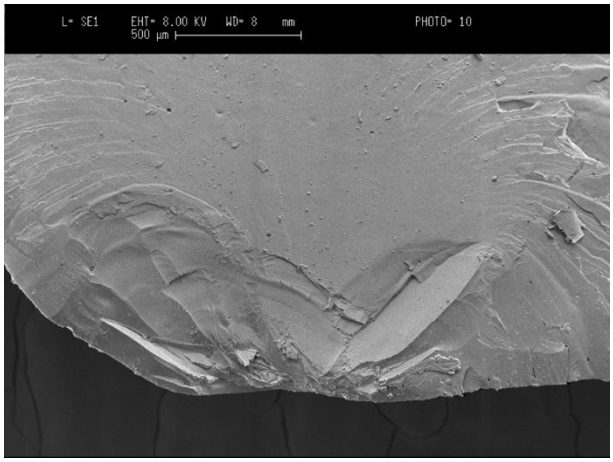

Figure 4-18: FA3 – Close-up image of origin of fracture site at underside of chip [magnification x 50]

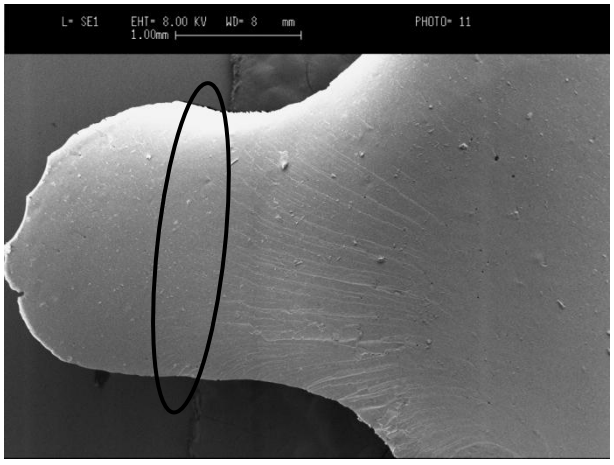

Figure 4-19: FA3 - Intact mesial side of chip above area on the crown where the mesial peripheral crack runs, oval marking correspond to crack location on the crown [magnification x 25]

This sample fractured by pure veneering porcelain chip involving the disto-lingual cusp and the distal aspect of the mesio-lingual cusp. The origin of fracture was located above the occlusal adjustment as can be seen from figures 4-12 to 4-15. Arrest lines seen on figures 4-13 and 4-14 represent momentarily hesitated cracks prior to resumption of crack propagation under altered stress configuration. The origin of fractures is always located on the concave side of any arrest lines, and therefore confirms the location to be from the adjustment area. Hackle lines point to the local direction of the cracking, as shown in figure 4-13 by the red arrows. Twist hackles on the outer rim of the fracture represent lateral rotation or twisting in the axis of principal tension as the crack surfaces out towards the compression zone in this fast cooled crown (figure 4-15). Note how twist hackle and hackle lines only appear at regions corresponding to superficial porcelain, disappearing in deeper zones at the middle of the chip at the disto-lingual cusp, and as the chip crosses over to the mesio-lingual cuspal region (figure 4-15 and 4-16).

The origin of fracture of the mesial crack which encircled the non-loaded aspect of the crown could not be established. The midline fissure crack does not involve the mesial crack.

FA 2 load-to-failure: 778 N

The entire distal aspect of this sample fractured with delamination of the zirconia core (figure 4-20 to 4-34). The fracture involves the distal half of the DB cusp, and distal 1/3 of the DL cusp. A midline fissure crack and a crack encircling the mesial non- loaded aspect of the crown were also observed.

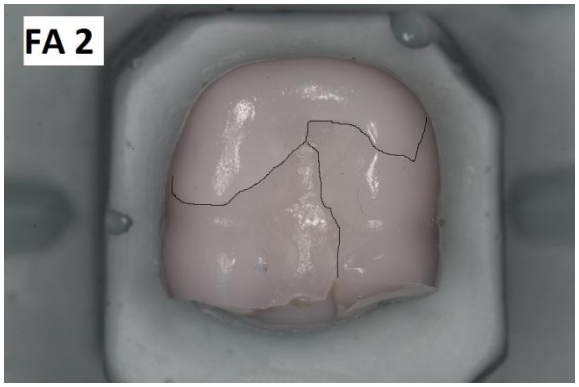

Figure 4-20: FA2 - Photographic image of fracture

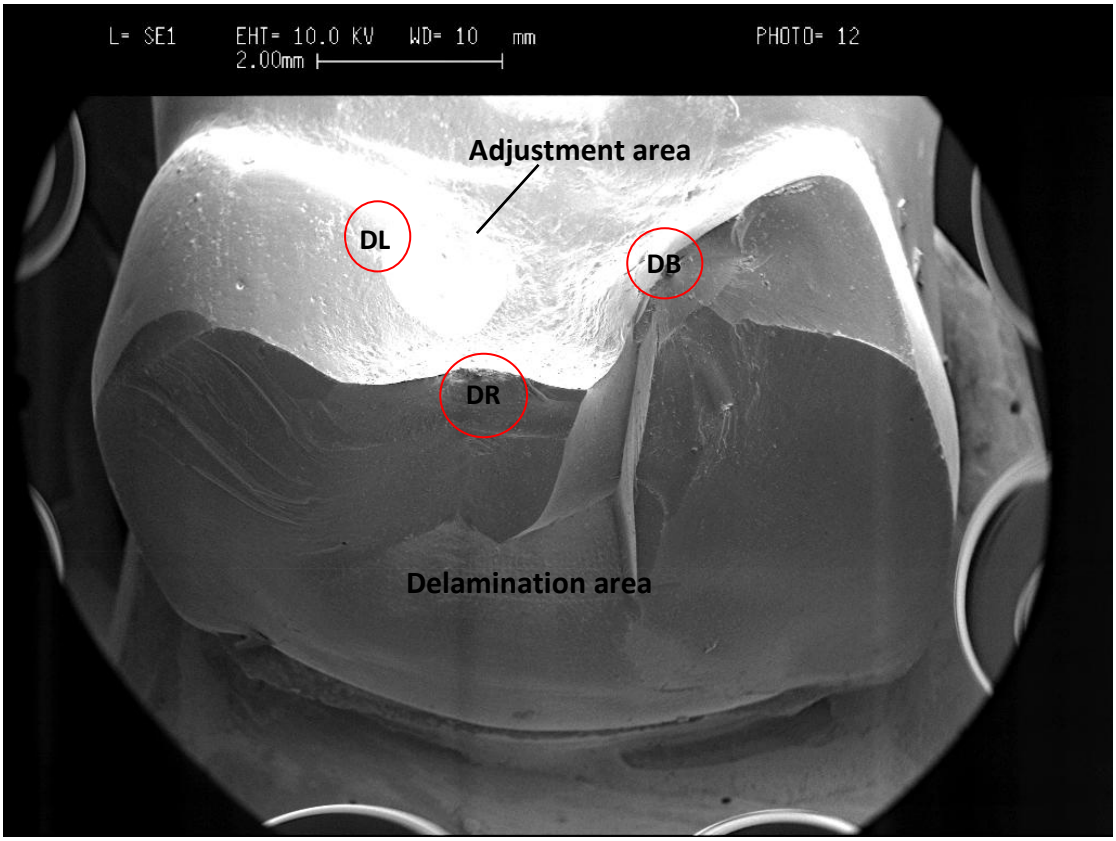

Figure 4-21: FA2 - Overview of distal fracture; ball contact areas are outlined in red circles [magnification x 10]

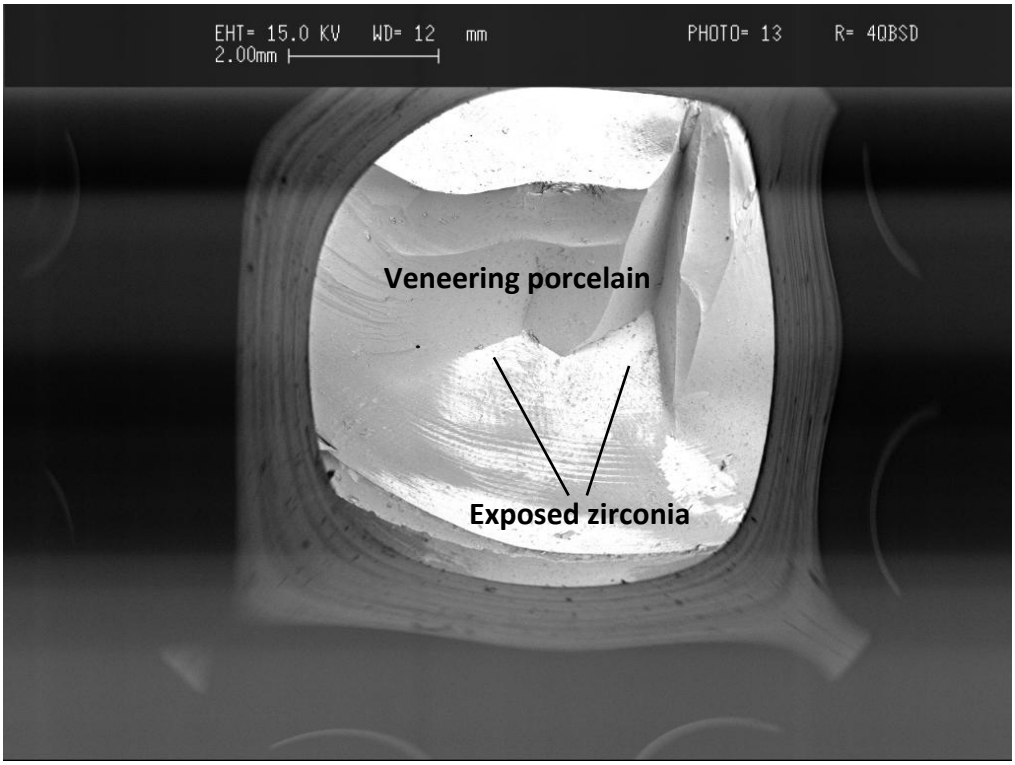

Figure 4-22: FA2 - Back scatter detector (BSD) confirms zirconia core delamination [magnification x 8]

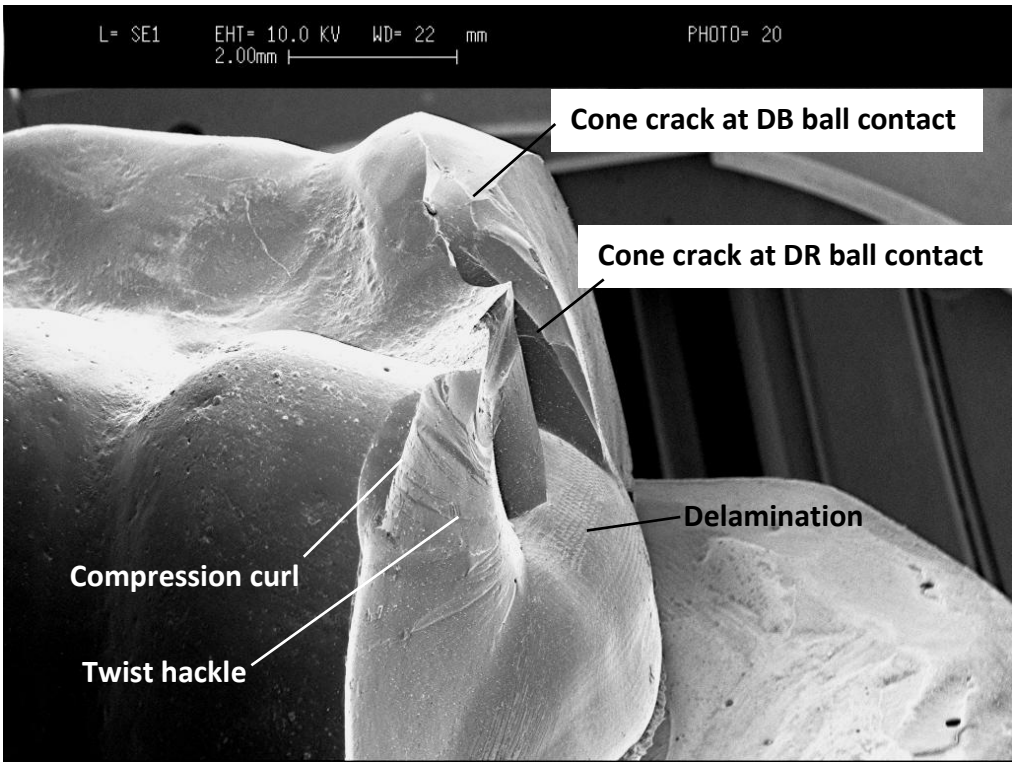

Figure 4-23: FA2 - Overview of distal fracture from the lingual side [magnification x 10]

DL cusp contact area:

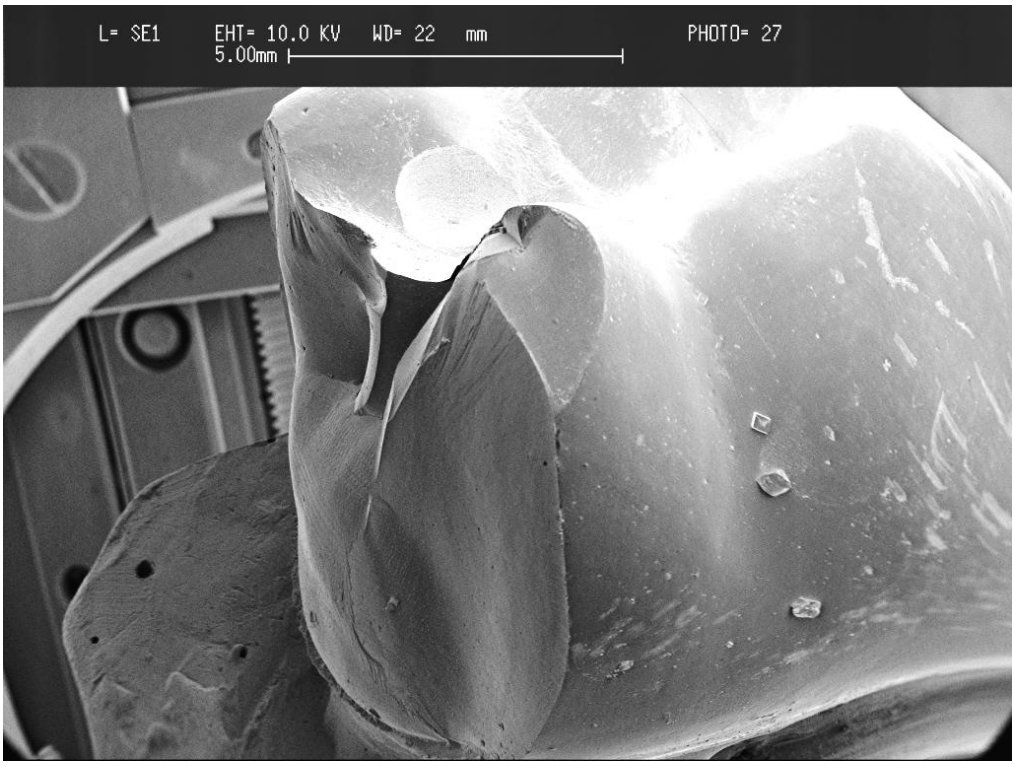

Figure 4-24: FA2 - Overview from the buccal aspect confirms fracture does not involve the occlusal adjustment at the DL cusp, note concave appearance of the DB fracture plane [magnification x 10]

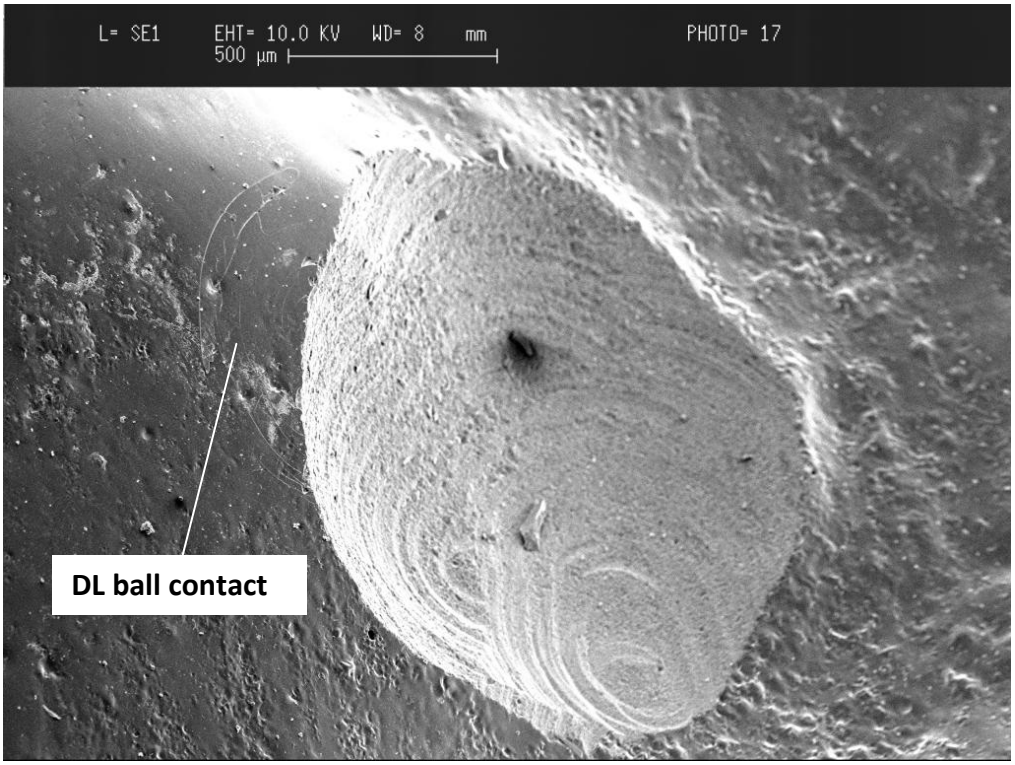

Figure 4-25: FA2 - Occlusal adjustment at DL cusp [magnification x 50]

DR ball contact area:

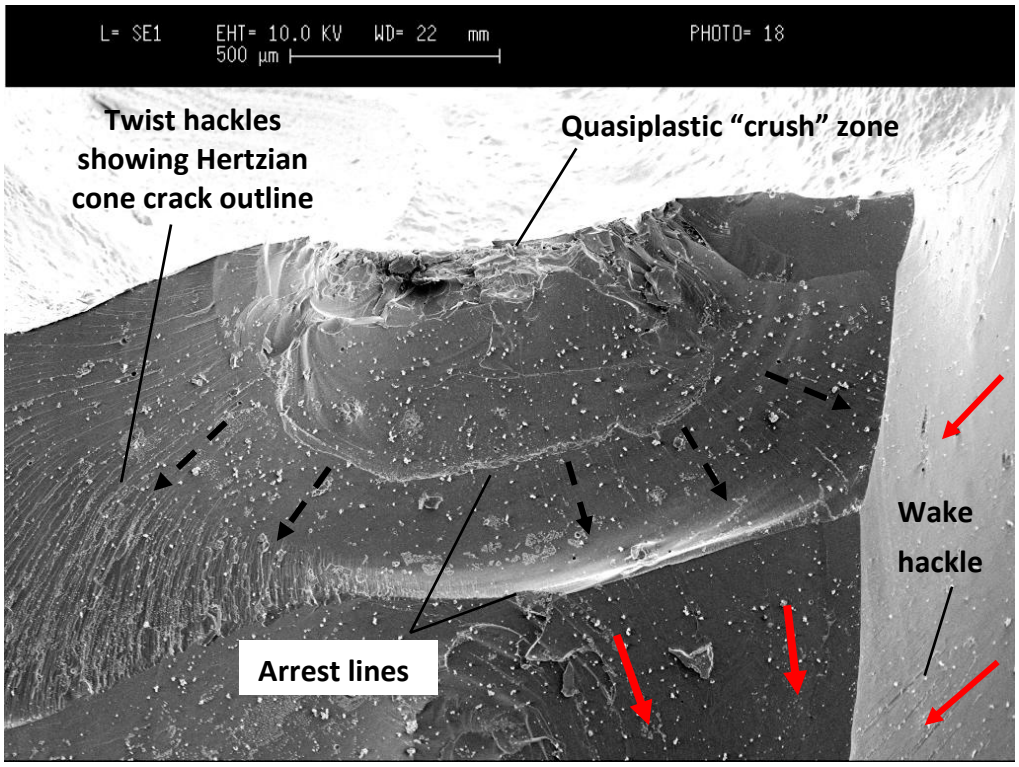

Figure 4-26: FA2 – Ball contact area on DR, wake hackle lines show direction of crack propagation (red arrows), dashed arrows show direction of cone crack propagation before changing direction [magnification x 50]

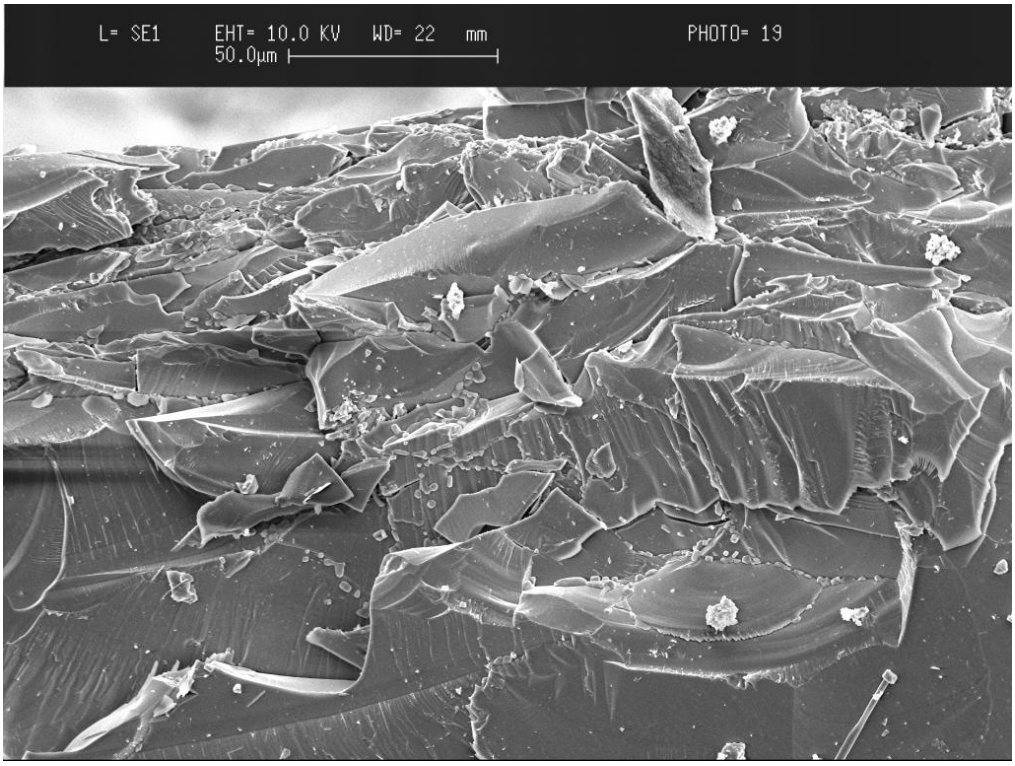

Figure 4-27: FA2 – Close-up of DR yield crush zone underneath ball contact [magnification x 500]

DB cusp contact area:

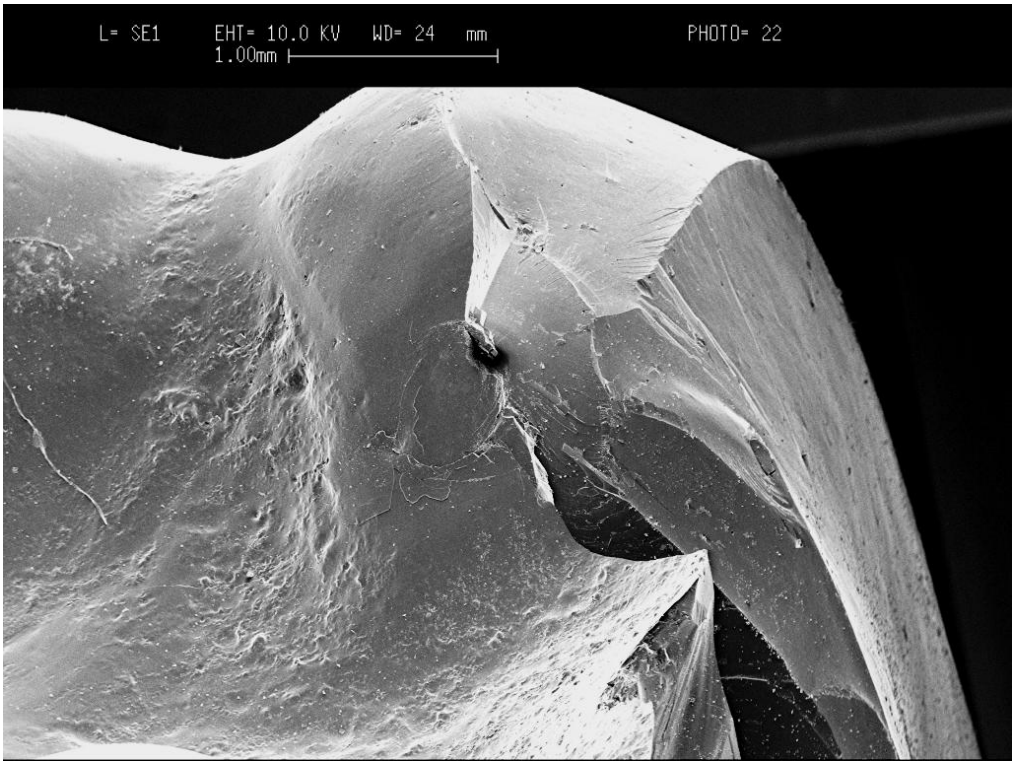

Figure 4-28: FA2 – An overview of the ball contact on the DB cusp with Hertzian cone crack formation [magnification x 25]

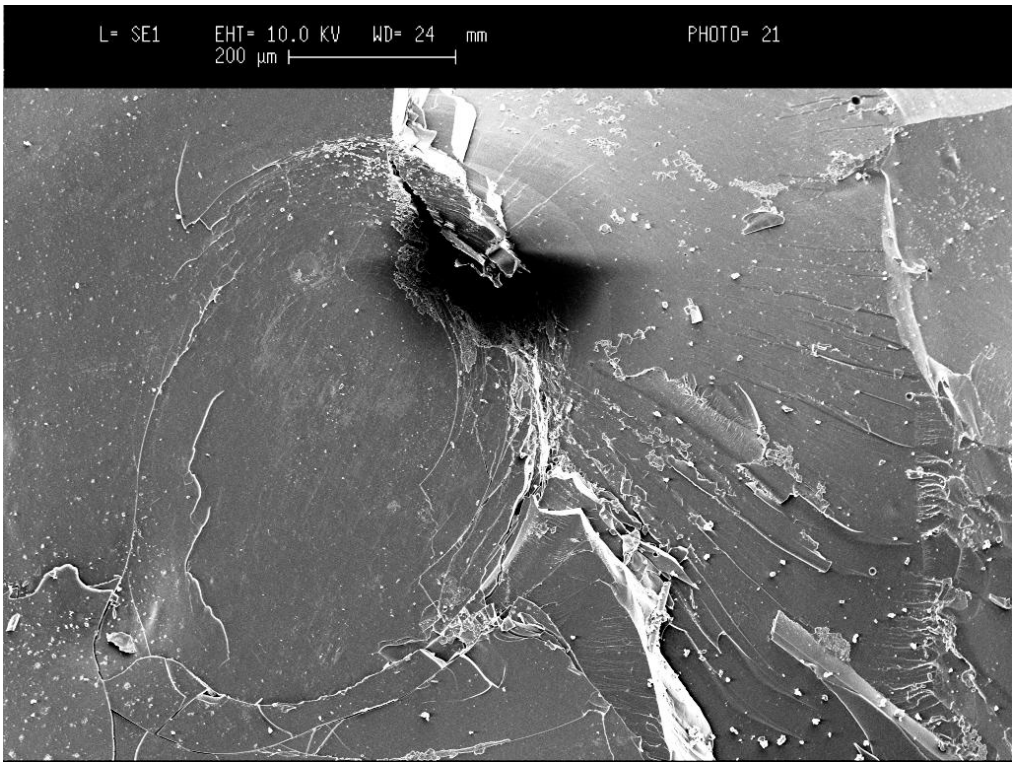

Figure 4-29: FA2 - Higher magnification of the DB ball contact area [magnification x 100]

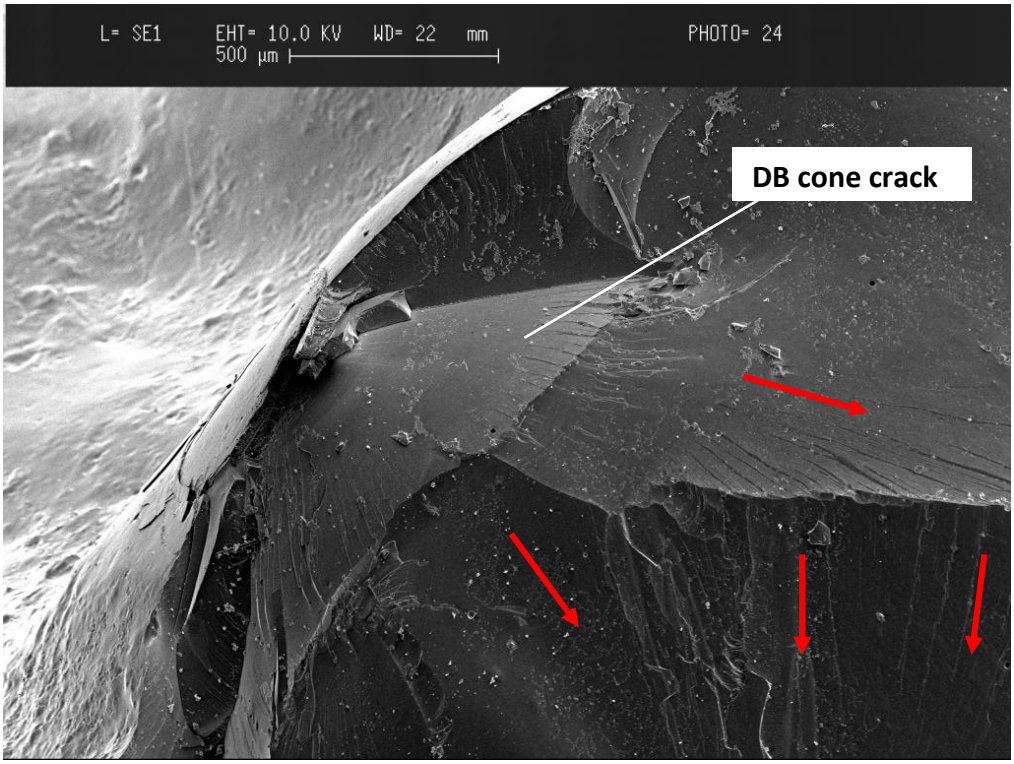

Figure 4-30: FA2 – Cone crack underneath DB ball contact area distal side view [magnification x 50]

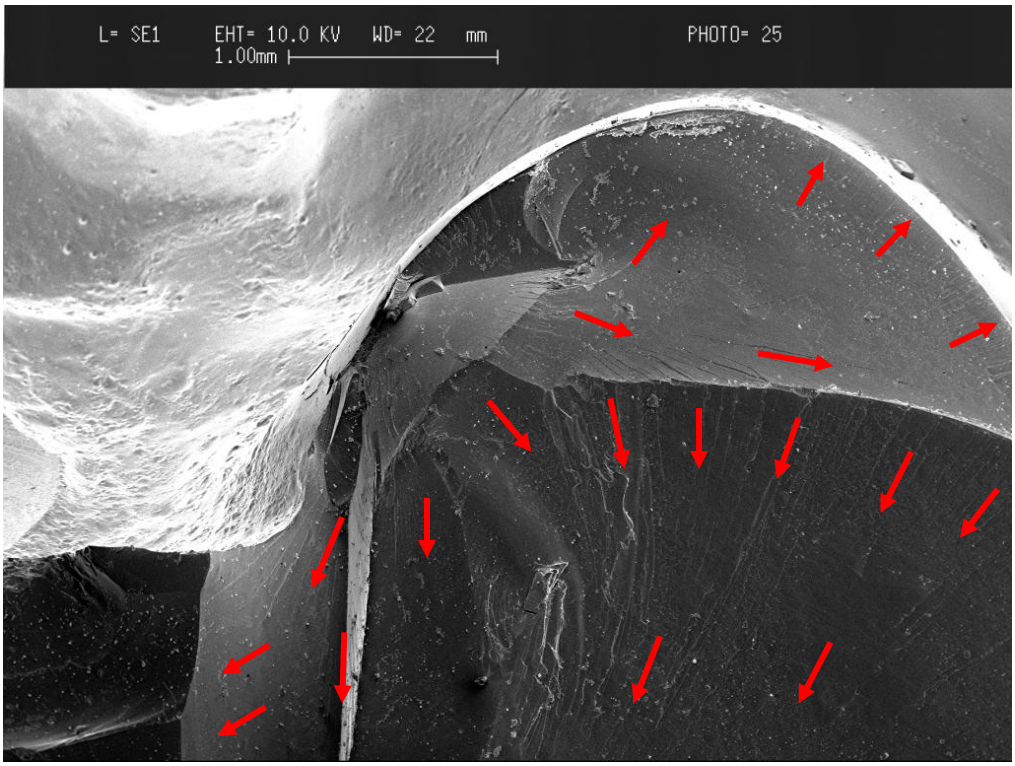

Figure 4-31: FA2 - Lower magnification of DB cone crack demonstrating steep changing planes of fracture path (red arrows) [magnification x 25]

Mesial crack and fissure crack:

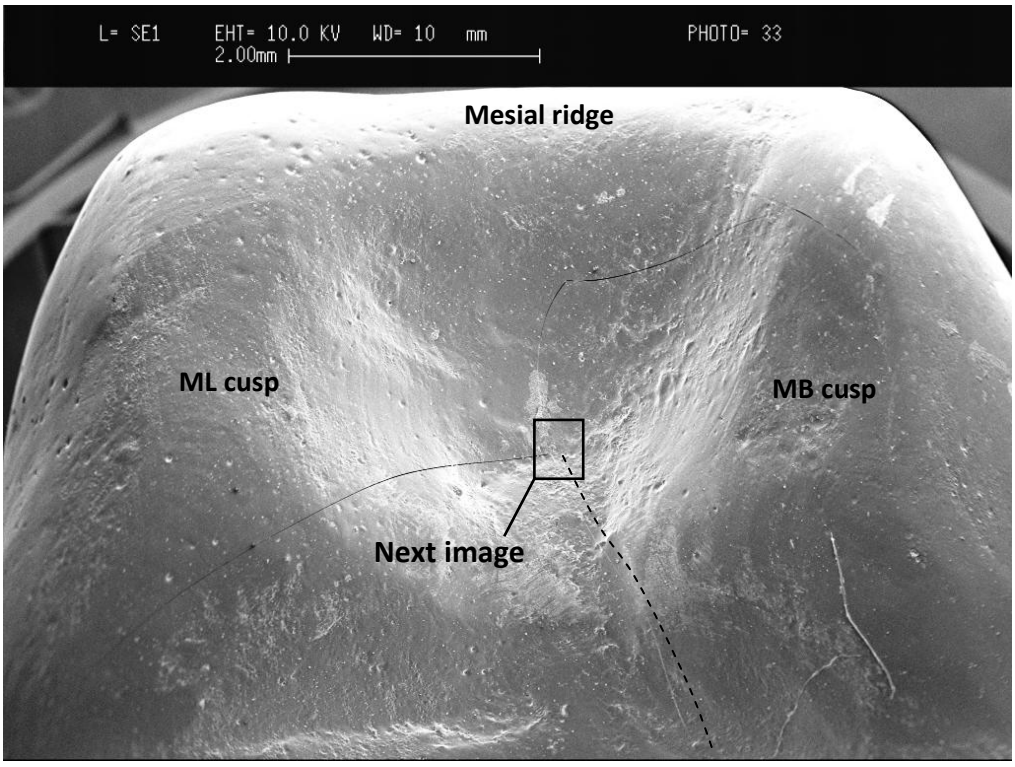

Figure 4-32: FA2 - Image of the crack encircling the mesial aspect of the crown and midline fissure crack, the later is drawn on (dashed line) [magnification x 15]

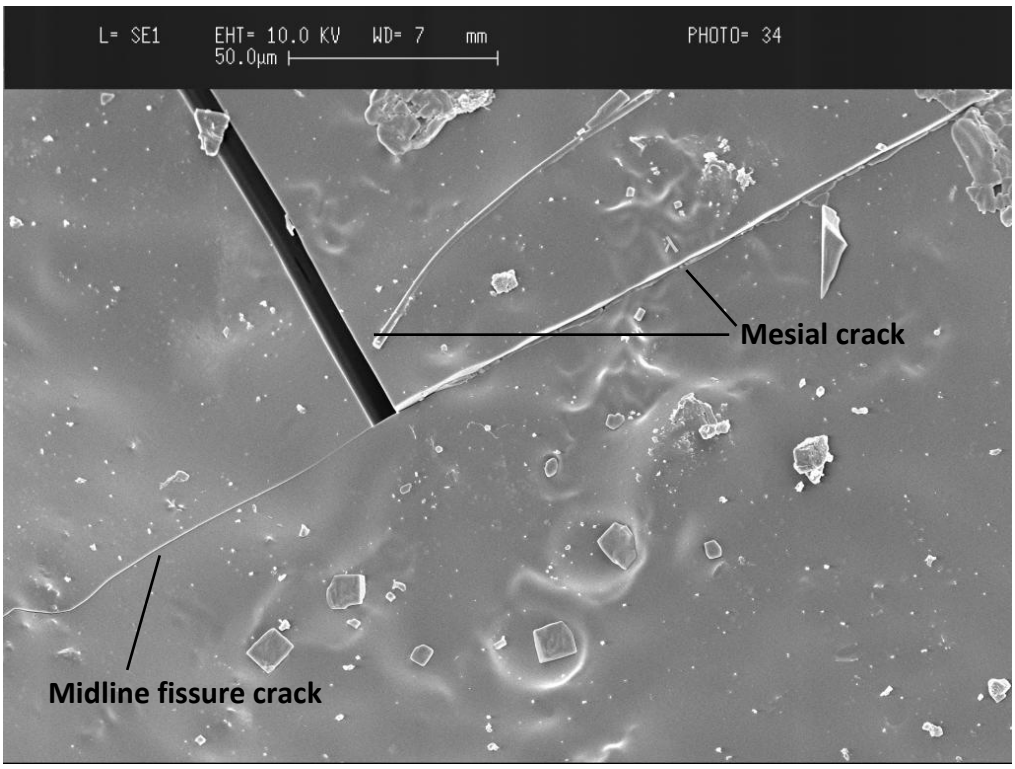

Figure 4-33: FA2 - Meeting point between midline fissure crack and mesial crack in the fossa, note change of mesial crack direction following the midline crack [magnification x 500]

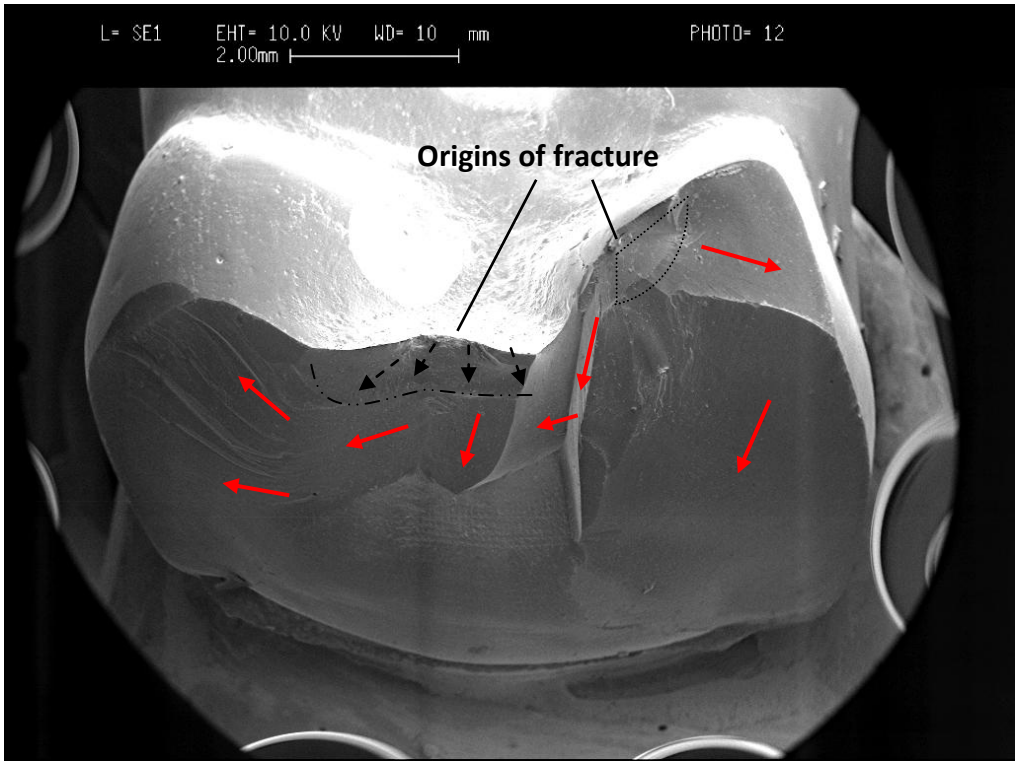

Figure 4-34: FA2 - Origin of fractures and path of crack propagations [magnification x 10]

In this loaded fast cooled sample, there are two origins of fractures that appear to have propagated independently but then join to cleave off the distal ¼ of the veneering porcelain. At the DB ball contact area, a crack appears to have emanated from a Hertzian cone crack which extended in a vertical plain until it reached the zirconia core starting the delamination process. Around the same time, cone cracks propagating from underneath the DR ball contact, which seemed to slowly grow under the increasing load, indicated by the stepwise arrest lines and high concentration of twist hackle lines (figure 4-26). The crack then takes a very sharp turn vertically, down to the core/veneer interface, finally turning towards the DL direction to surface out with large twist hackle lines and compression curls (figure 4-23 and 4-34).

Once again, it was not possible to determine the origin of the mesial crack.

Slow cooled samples:

SA 1: load-to-failure: 882 N

This sample fractured with delamination of the veneering porcelain limited to the DR only (figure 4-35 to 4-48). Fissure cracking was evident however with no cracking on the mesial aspect of the crown.

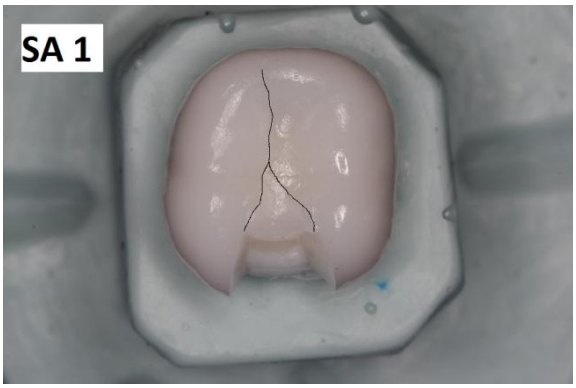

Figure 4-35: SA1 - Photographic image of fracture

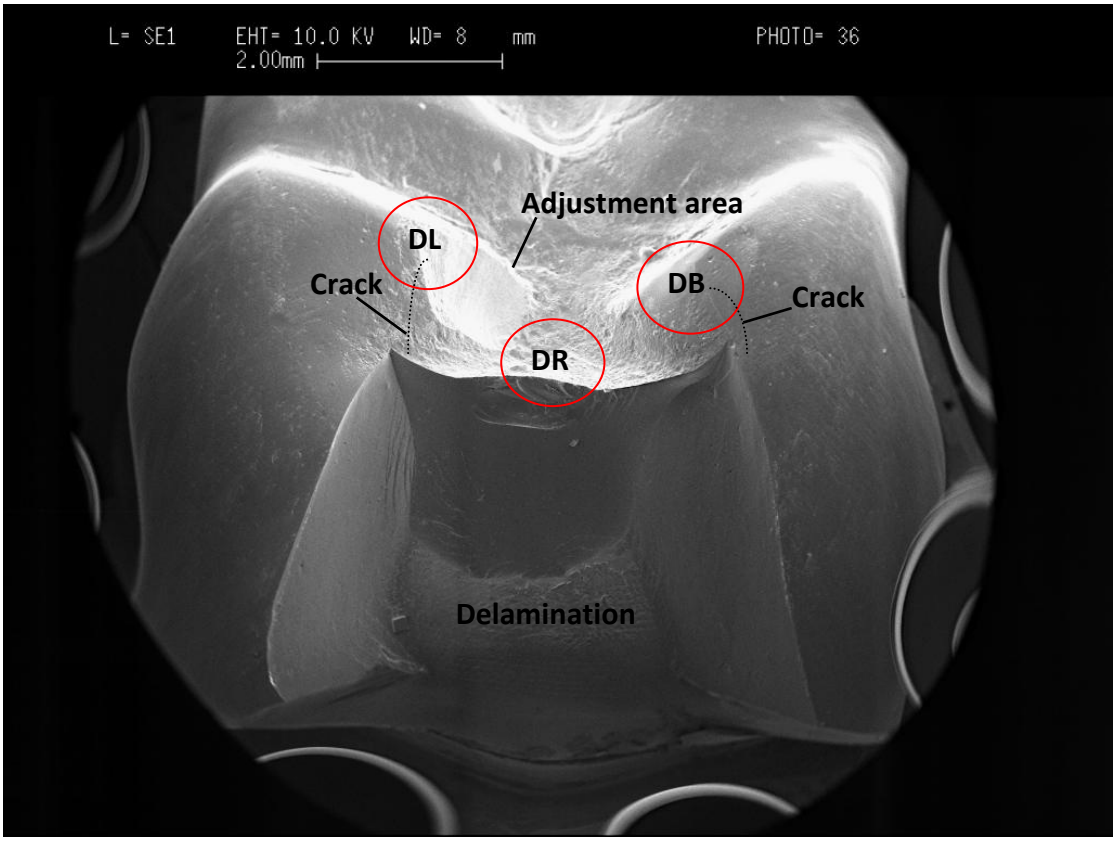

Figure 4-36: SA1 - Overview of distal fracture with contact areas and crack lines highlighted [magnification x 10]

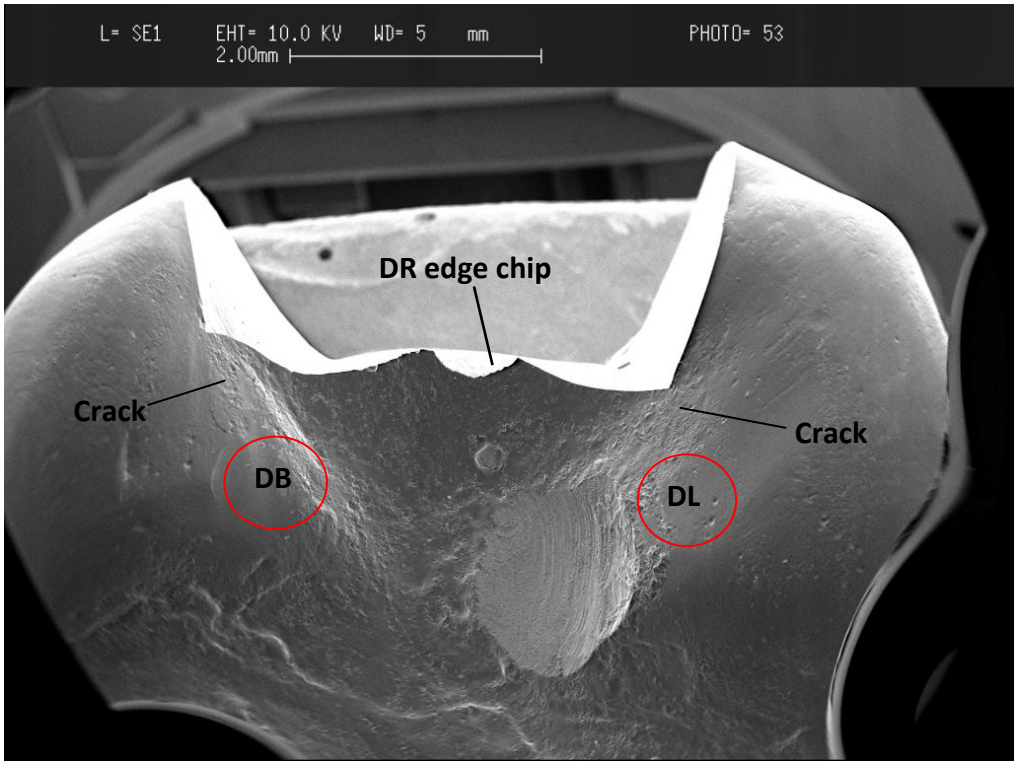

Figure 4-37: SA1 - Occlusal view of fracture [magnification x 15]

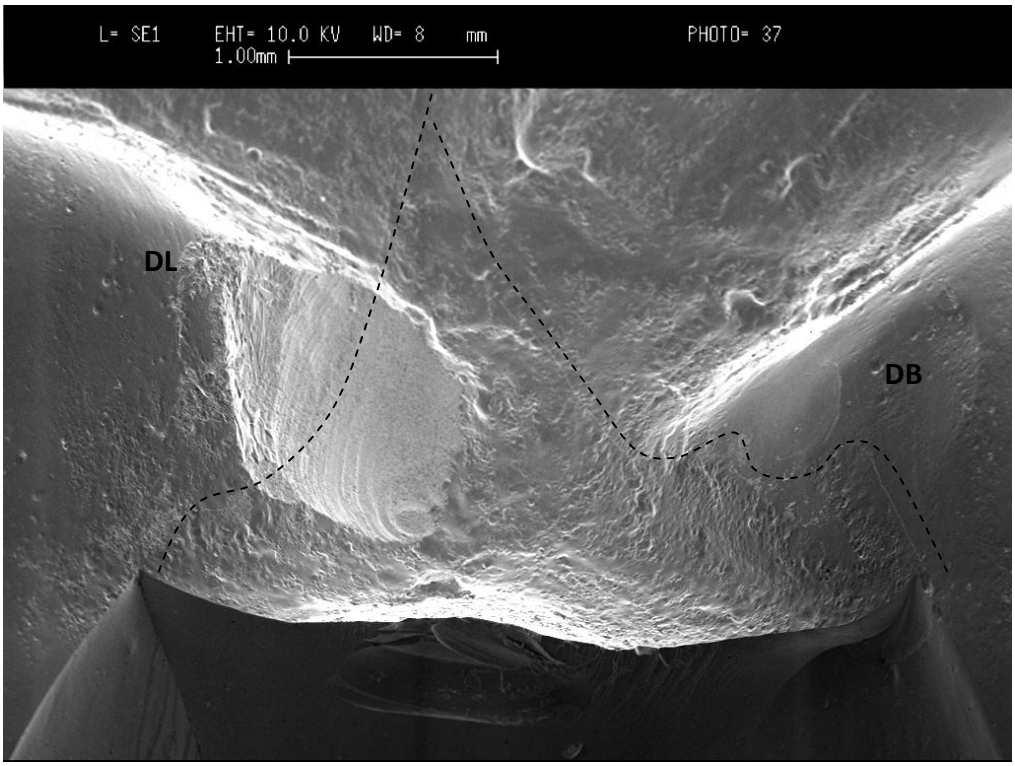

Figure 4-38: SA1 - Crack lines running mesially from DL and DB ball contact areas to meet forming a midline crack, and distally towards the fracture [magnification x 25]

DL cusp contact area:

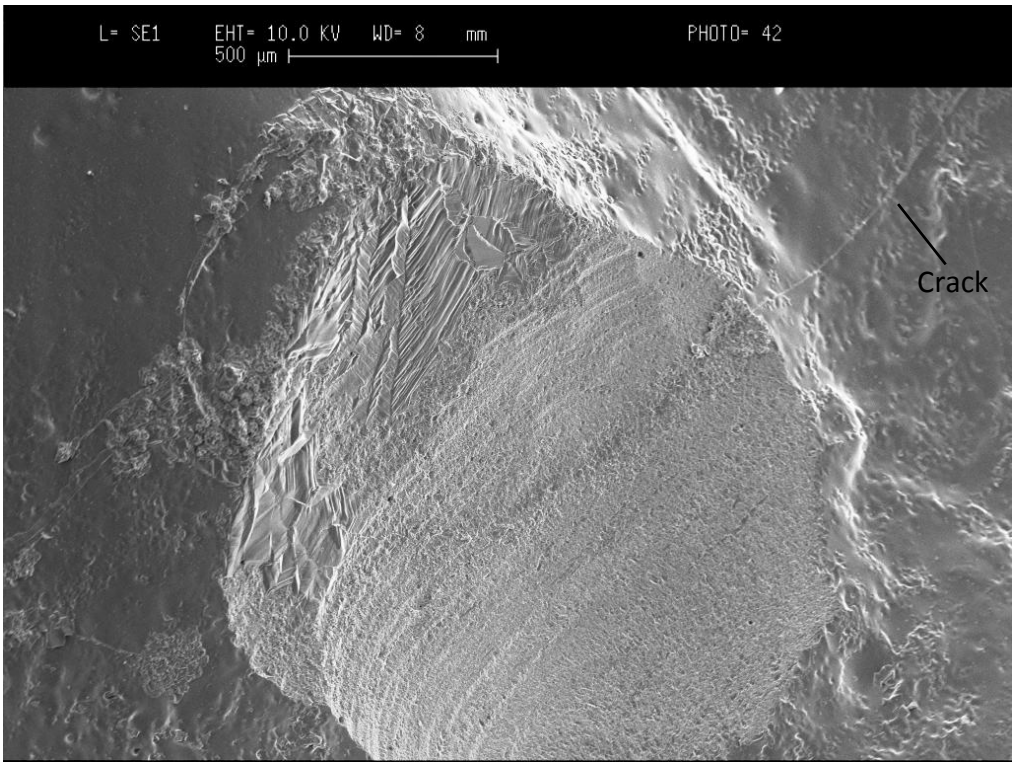

Figure 4-39: SA1 - Higher magnification of the occlusal adjustment at the DL cusp, a crack running through the middle of the adjustment can be seen on the image [magnification x 50]

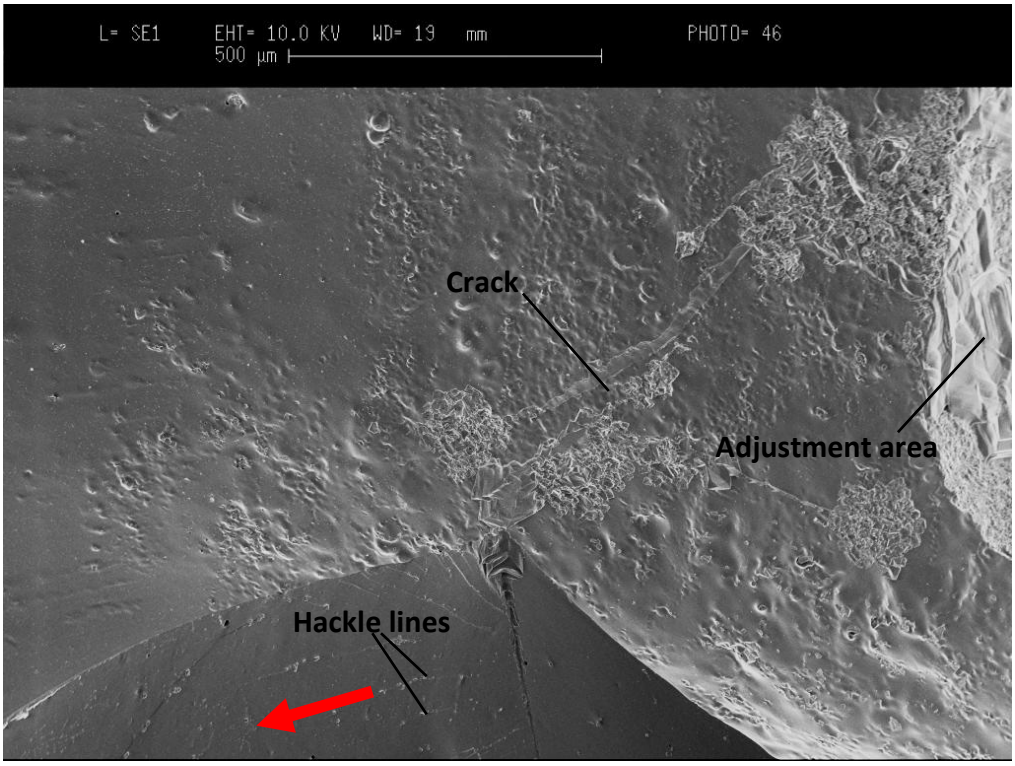

Figure 4-40: SA1 - Crack extending from the occlusal adjustment on the right, to the fracture at bottom centre of image [magnification x 75]

DR ball contact area:

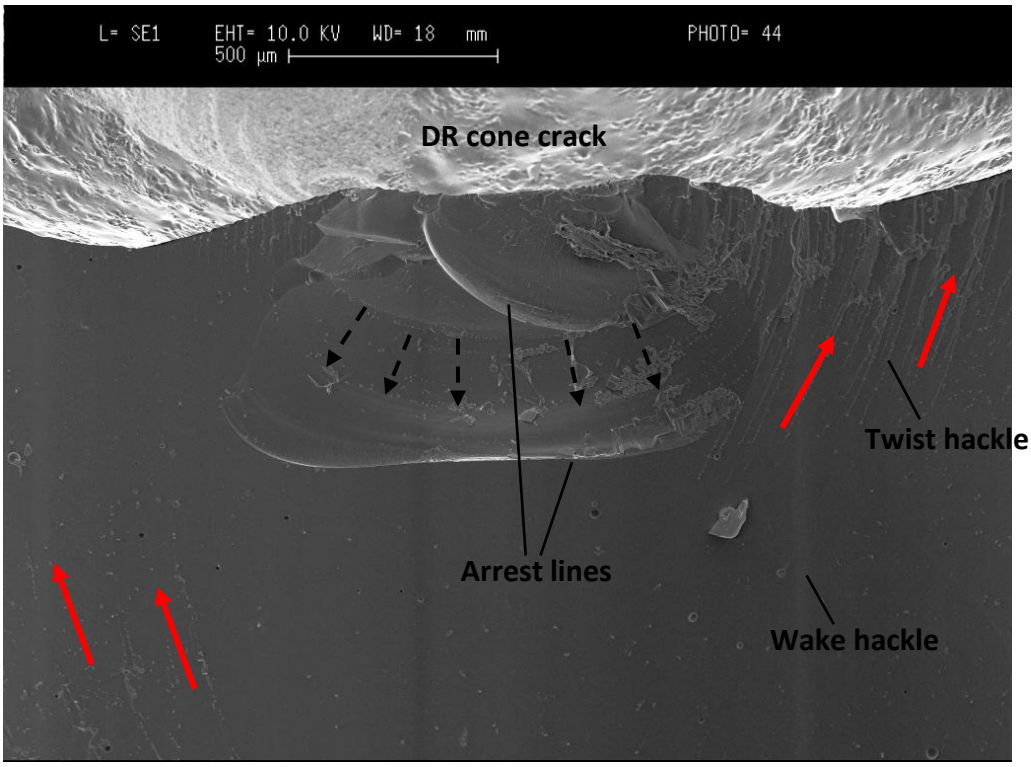

Figure 4-41: SA1 - DR contact area, dashed arrows point to direction of cone crack propagation were it stops at the bottom arrest line, red arrows point towards direction of main crack path [magnification x 75]

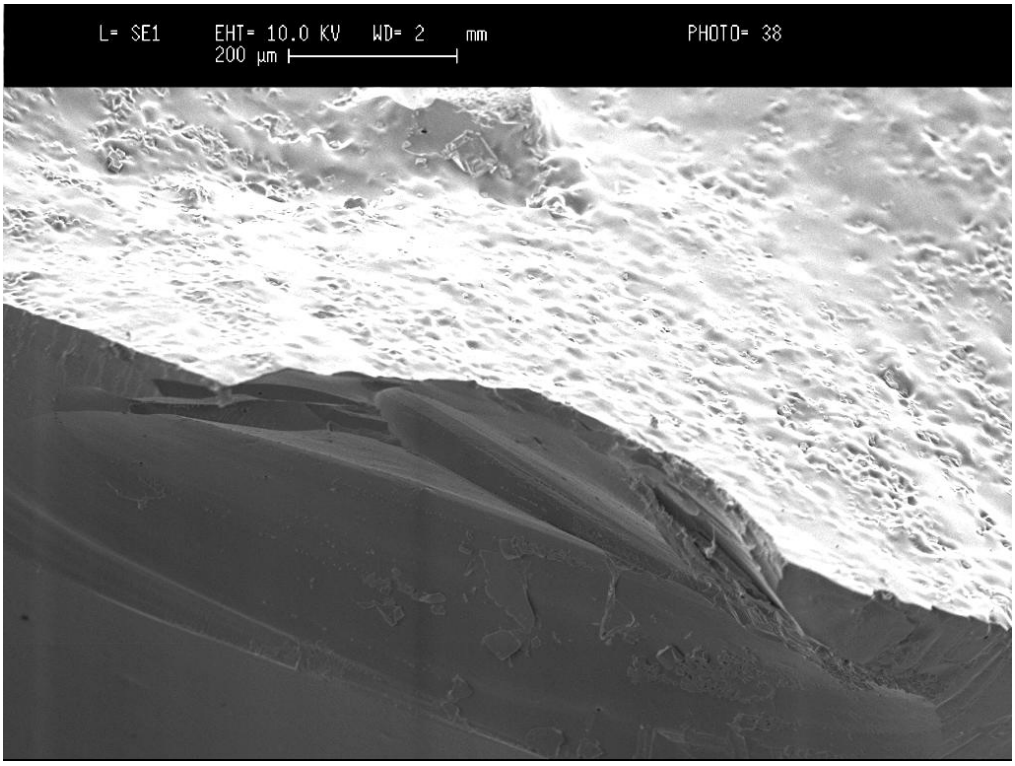

Figure 4-42: SA1 - Higher magnification of DR ball contact area and cone crack, note appearance similar to edge chip fractures by blunt contact [magnification x 100]

DB cusp contact area:

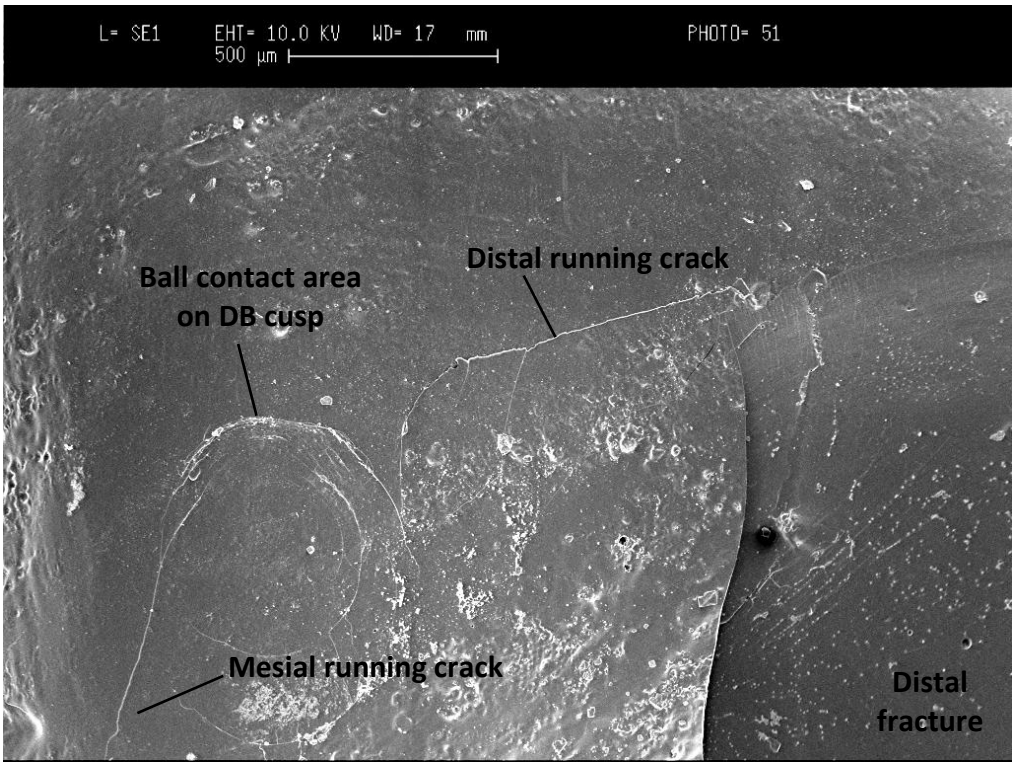

Figure 4-43: SA1 – Ring marks left by ball contact on DB cusp, with crack running towards distal fracture [magnification x 50]

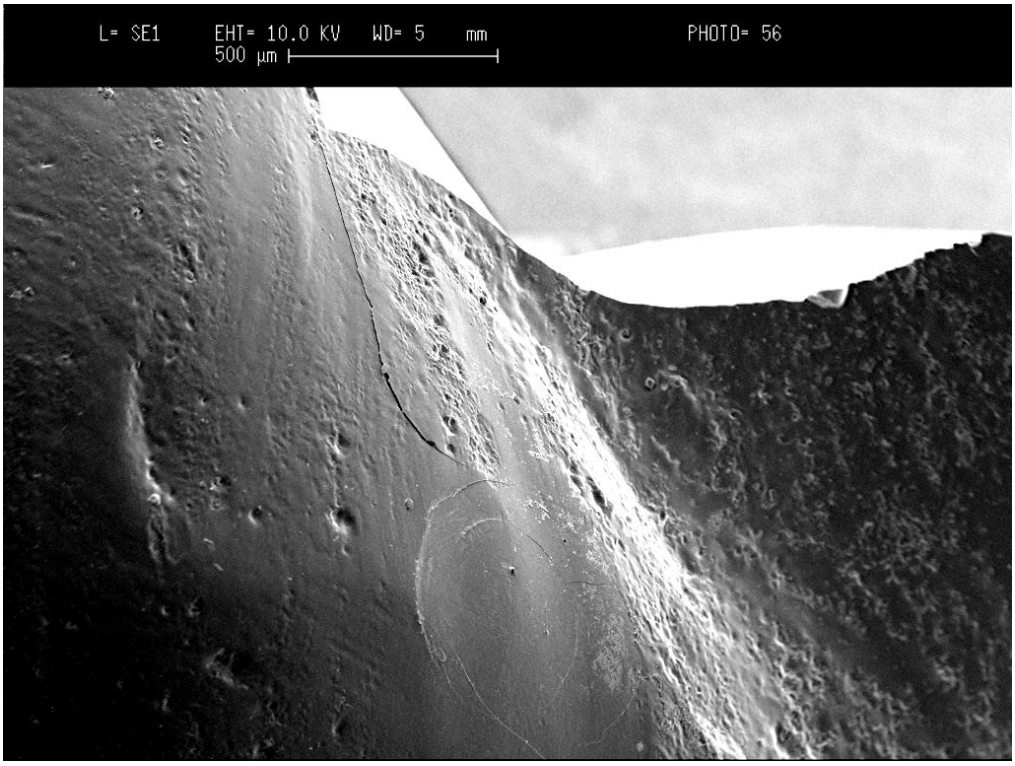

Figure 4-44: SA1 - Occlusal view of the distal running crack from DB ball contact zone to the fractured porcelain [magnification x 50]

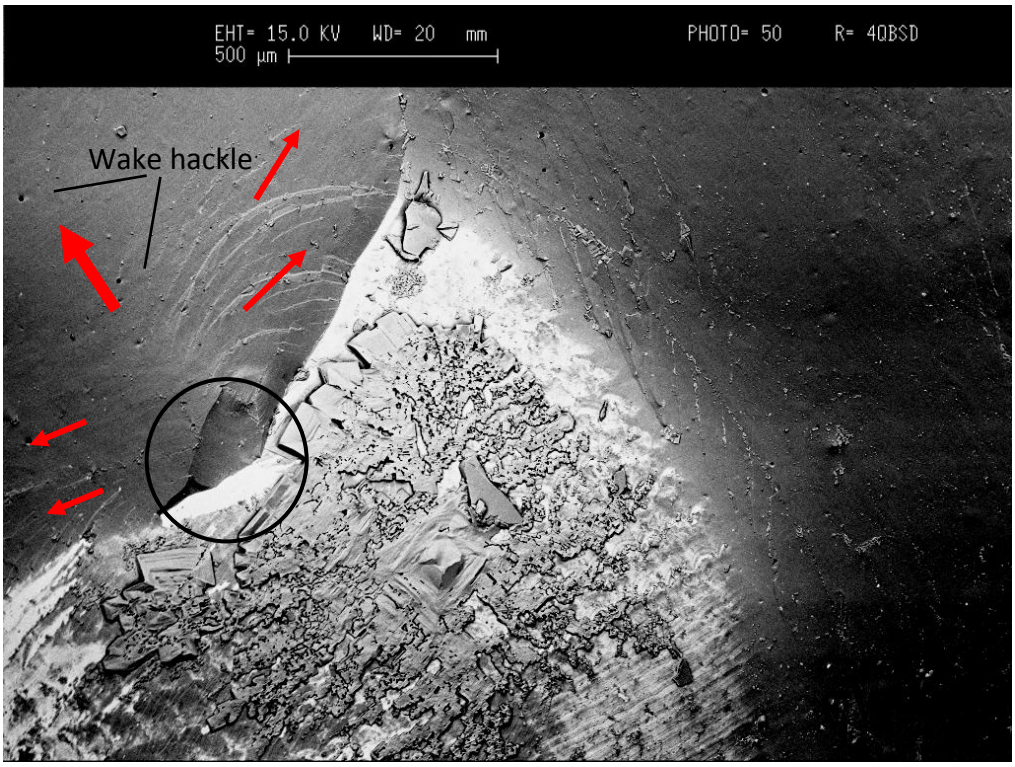

Figure 4-45: SA1 - Back scatter detector image of delamination zone shows primary origin of fracture at the base of veneering porcelain (black circle) [magnification x 50]

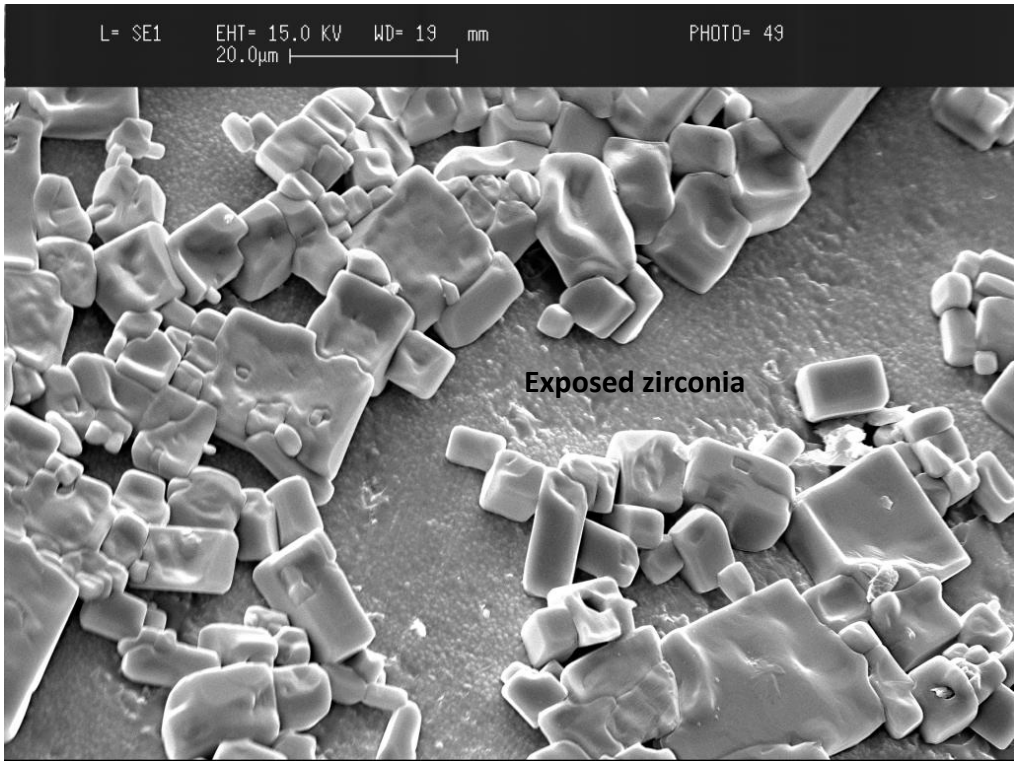

Figure 4-46: SA1 - Higher magnification confirms delamination of the zirconia with remnants of IPS e.max ZirLiner particles [magnification x 1000]

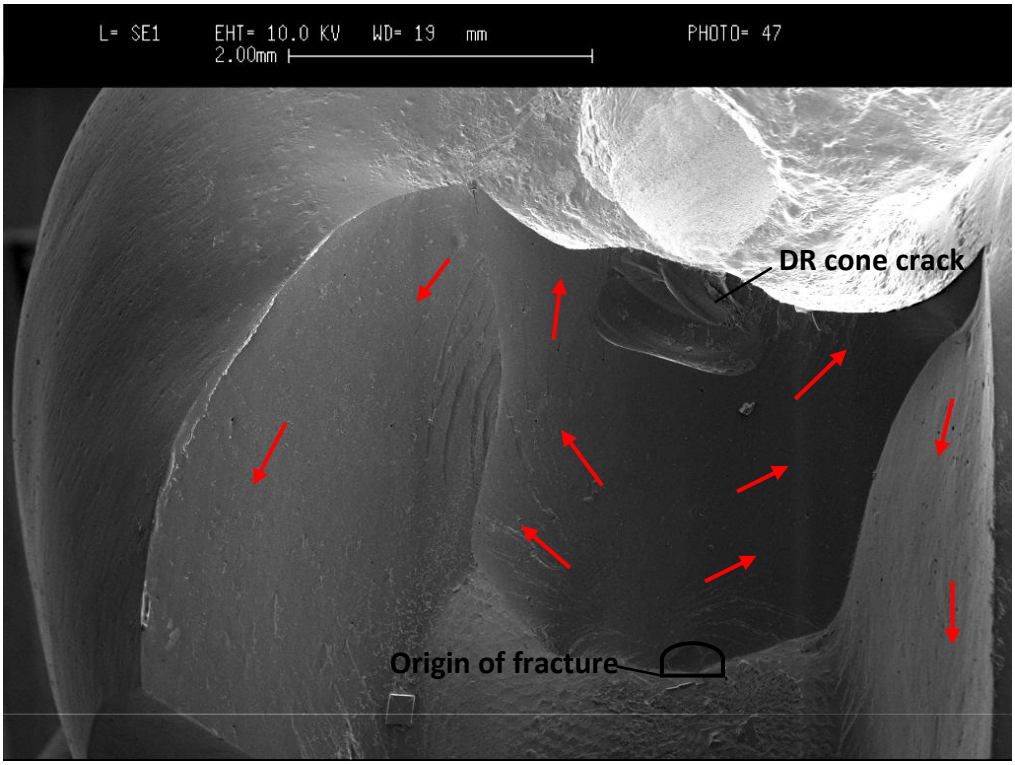

Figure 4-47: SA1 – Origin of fracture at the zirconia/veneer interface, which propagated radially towards the surface, note featureless and homogenous planes of fractured veneering porcelain with no sudden changes in direction of crack propagation [magnification x 18]

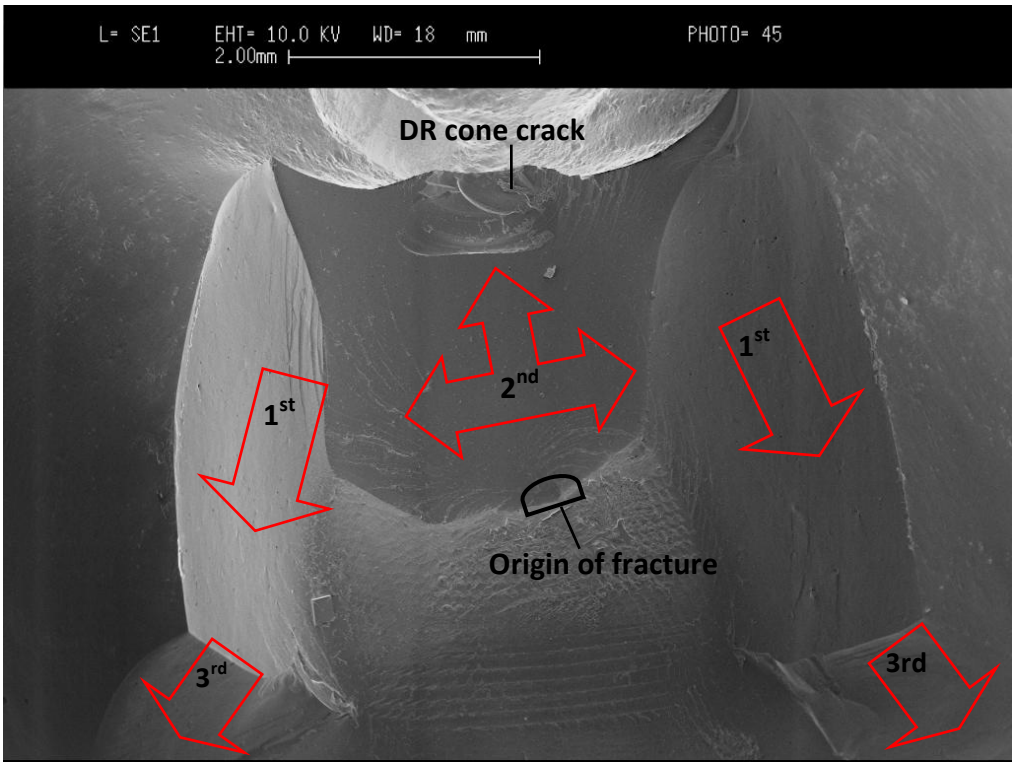

Figure 4-48: SA1: Order of crack planes propagations indicated by numbered arrows [magnification x 15]

The fracture origin in this slow cooled sample is the result of a combination of cracks that originated from the ball contact areas at DL and DB, and from delamination at the zirconia/veneer interface underneath the DR area.

A chip at the interface between the zirconia/veneer layers was the origin of fracture of the fracture plane underneath the DR ball contact area. The crack propagated vertically upwards (radially) and laterally to meet the DL and DB cracks on either side to cleave off the distal ridge. The DL and DB ball contact areas generated cone cracks that formed a midline fissure crack that ended at the mesial ridge. The cracks from the DL and DB contact areas appear to have extended distally first. This was followed by the ball exerting distal loading on the distal ridge that began with superficial cone cracking but ultimately failed because of radial crack propagation from delamination at the zirconia/veneer interface. As the distal ridge cleaved off continuing the delamination process, the DL and DB cracks make a sharp turn laterally as a result of the unsupported veneer cleaving off.

Compared to the fast cooled samples examined under SEM, the fracture planes appeared homogenous and featureless with no compression curls and minimal twist hackle lines appearing towards the superficial porcelain.

SA 5: load-to-failure: 715 N

This sample fractured with delamination of the veneering porcelain limited to the DR only (figure 4-49 to 4-62). Fissure cracking was evident however with no cracking on the mesial aspect of the crown.

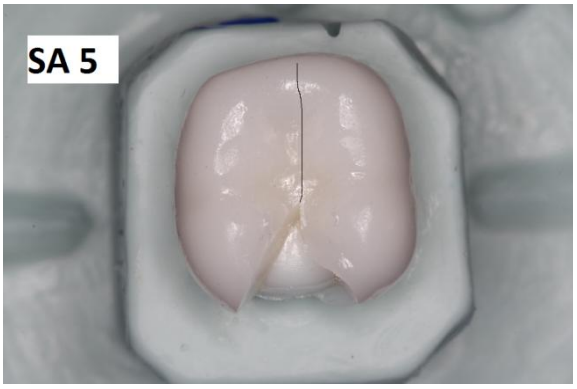

Figure 4-49: SA5 - Photographic image of fracture

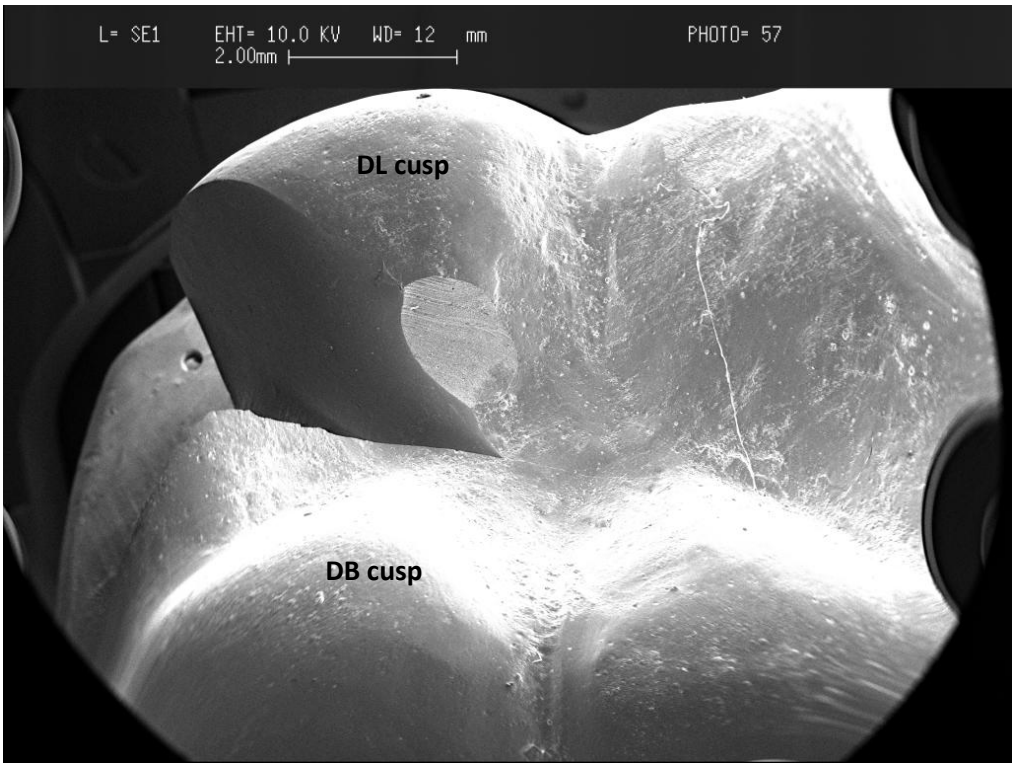

Figure 4-50: SA5 - Overview of distal fracture with occlusal adjustment centre of image [magnification x 10]

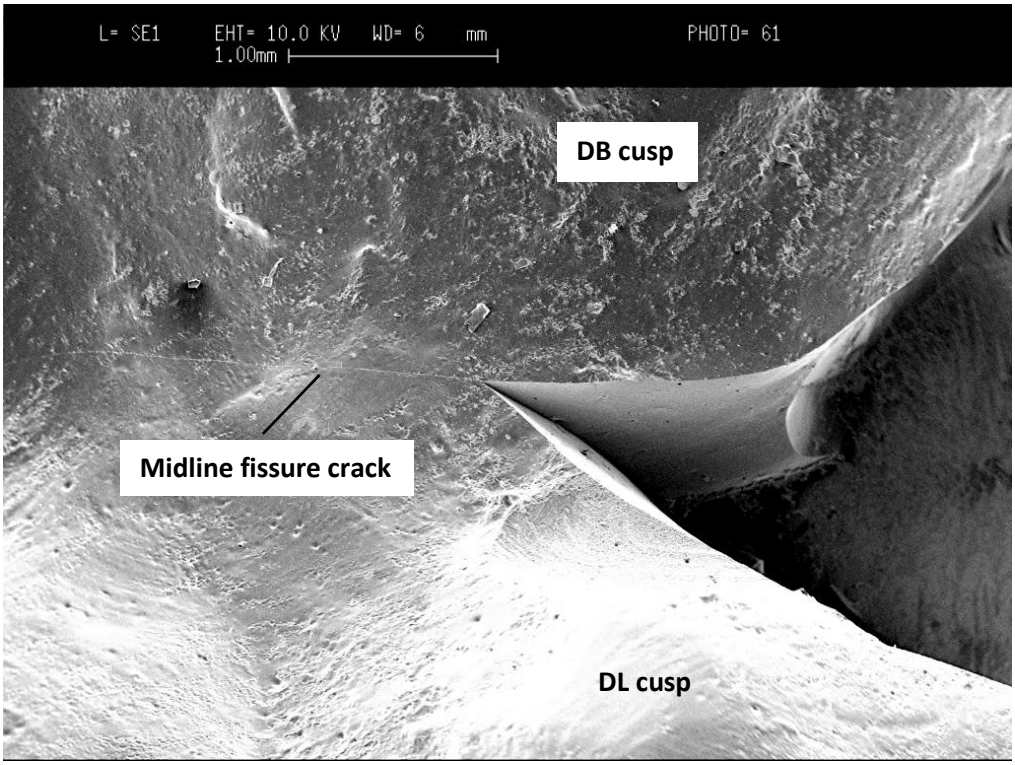

Figure 4-51: SA5 - Occlusal view of distal fracture on the right with midline fissure crack extending to the left of the image [magnification x 25]

DL cusp contact area:

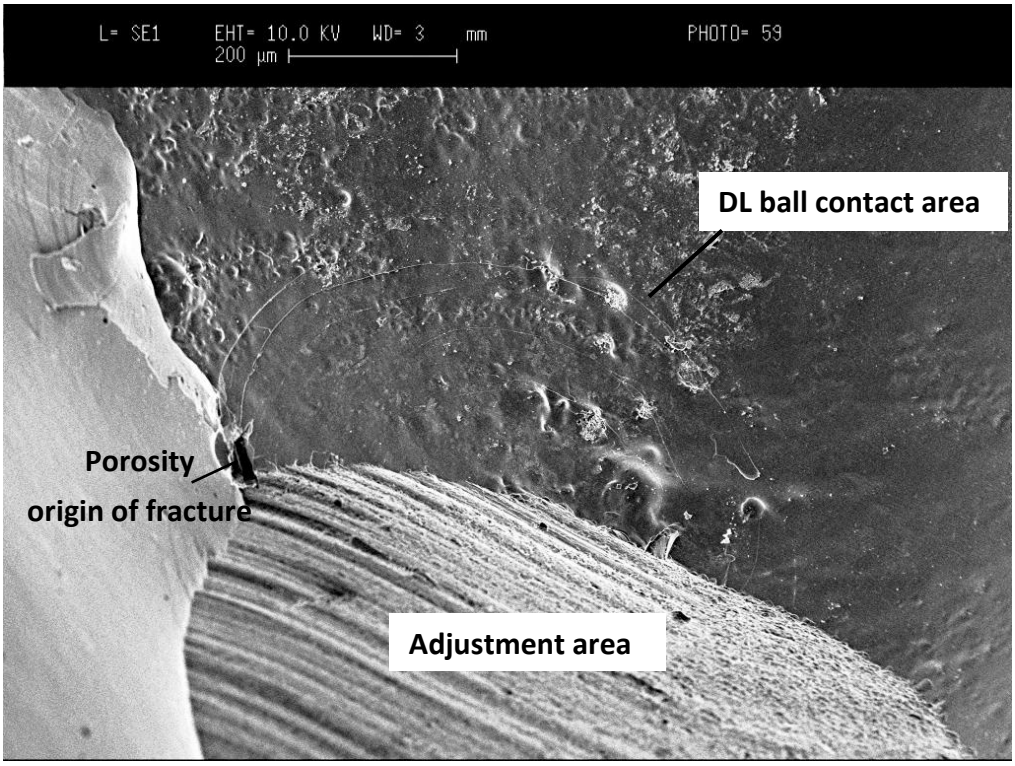

Figure 4-52: SA5 - Ball contact area above the adjustment with porosity at the apex of the adjustment [magnification x 100]

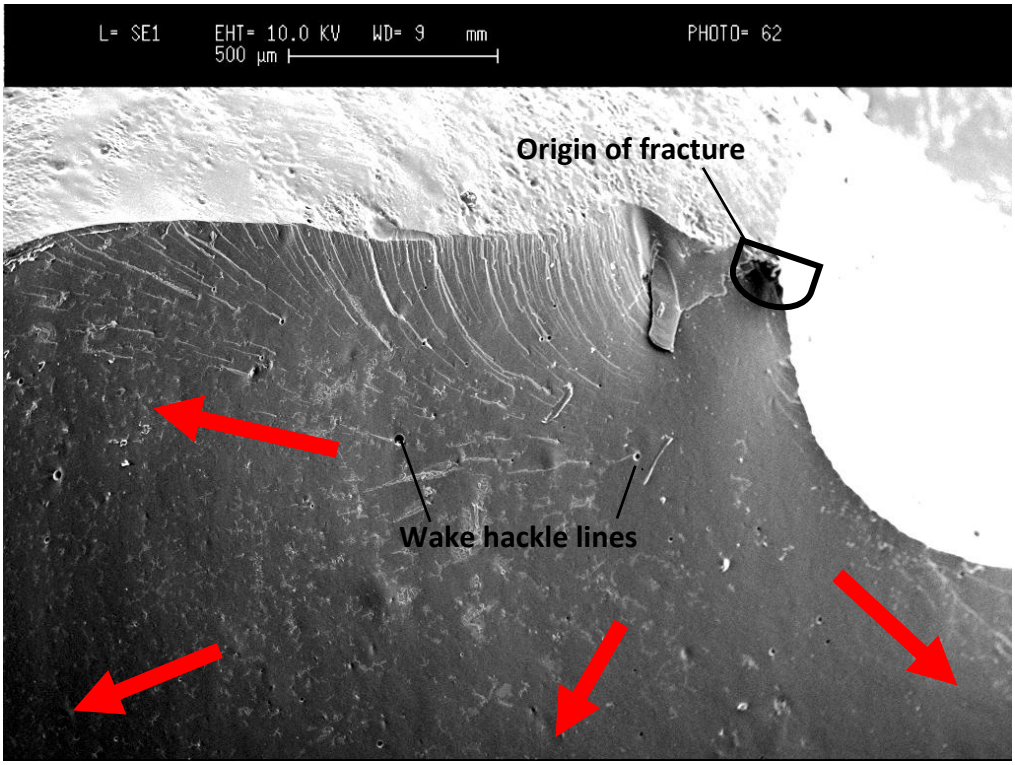

Figure 4-53: SA5 - Wake hackles lines showing direction of crack propagation (red arrows) [magnification x 50]

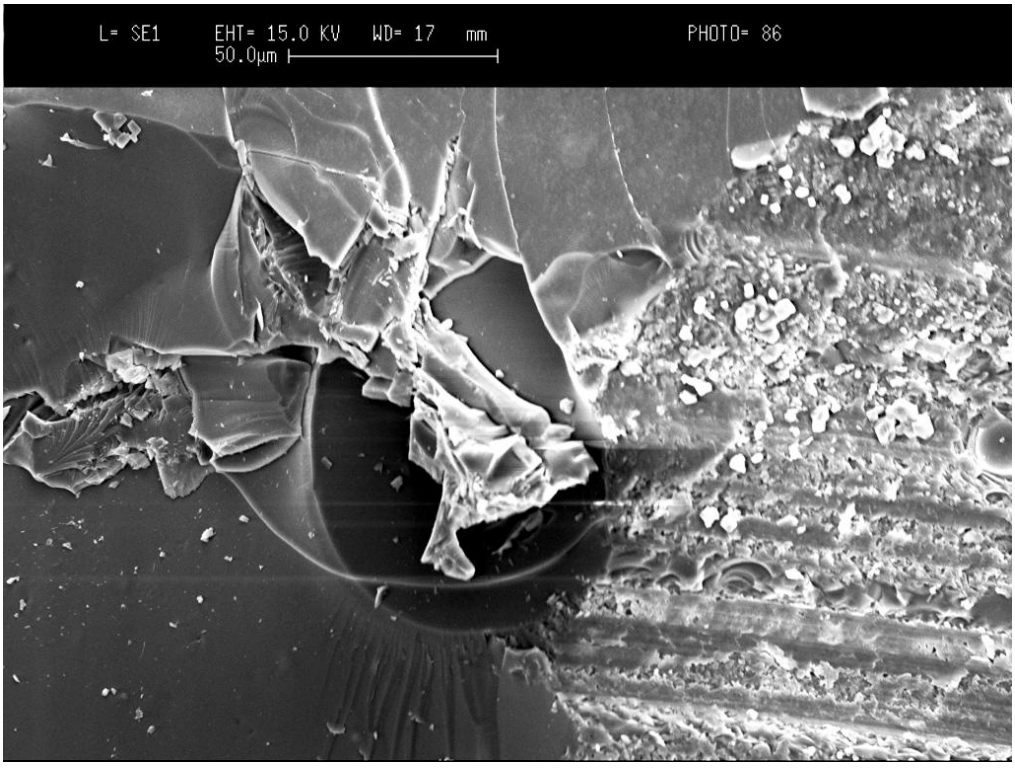

Figure 4-54: SA5 - Close-up image of the porosity at the DL cusp [magnification x 500]

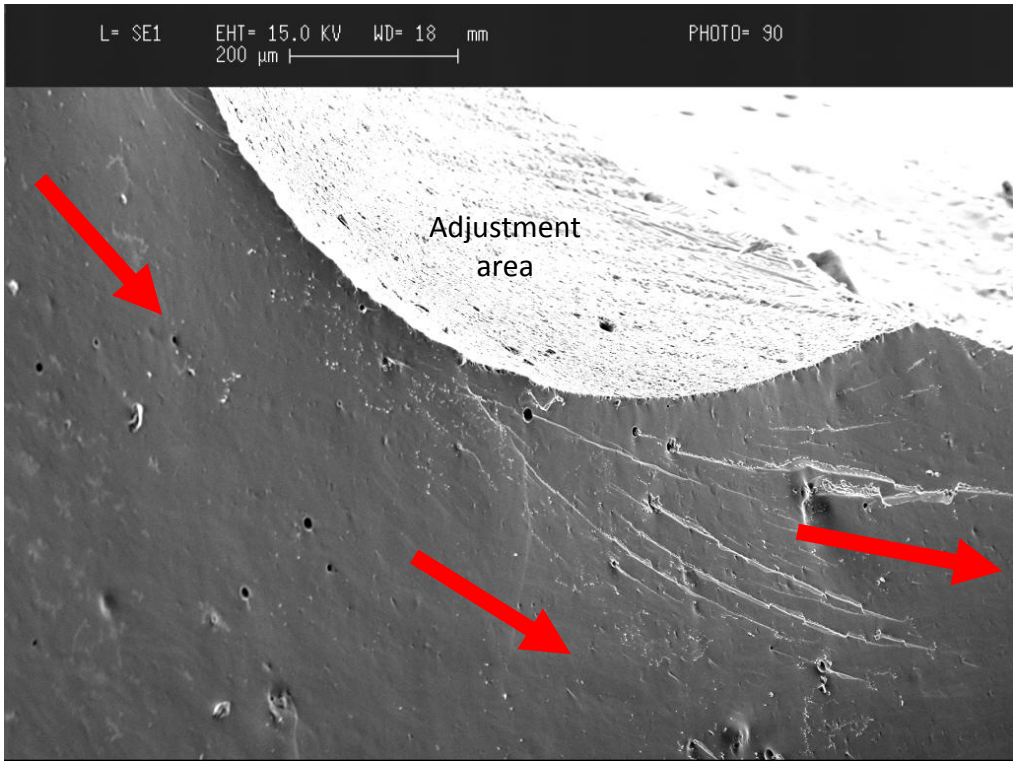

Figure 4-55: SA5 - Wake hackle lines underneath adjustment area running from the porosity at the top left (origin of fracture) towards the midline crack to the right of image [magnification x 100]

DR contact area:

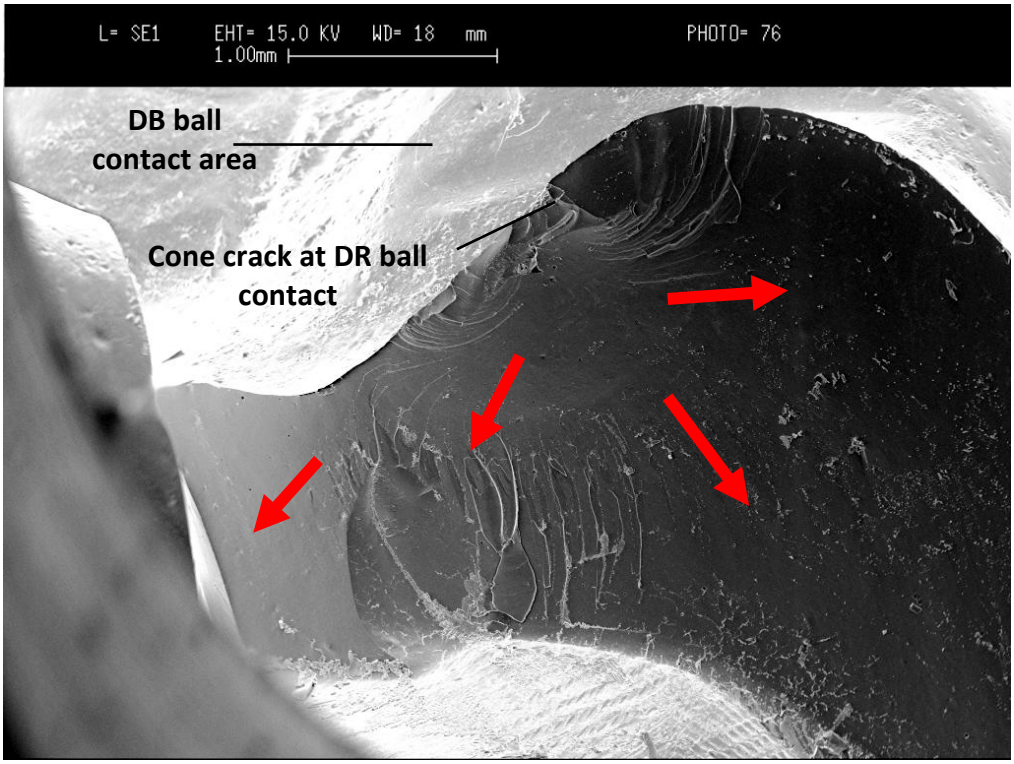

Figure 4-56: SA5 - DR origin of fracture at ball contact zone with direction of crack propagation [magnification x 25]

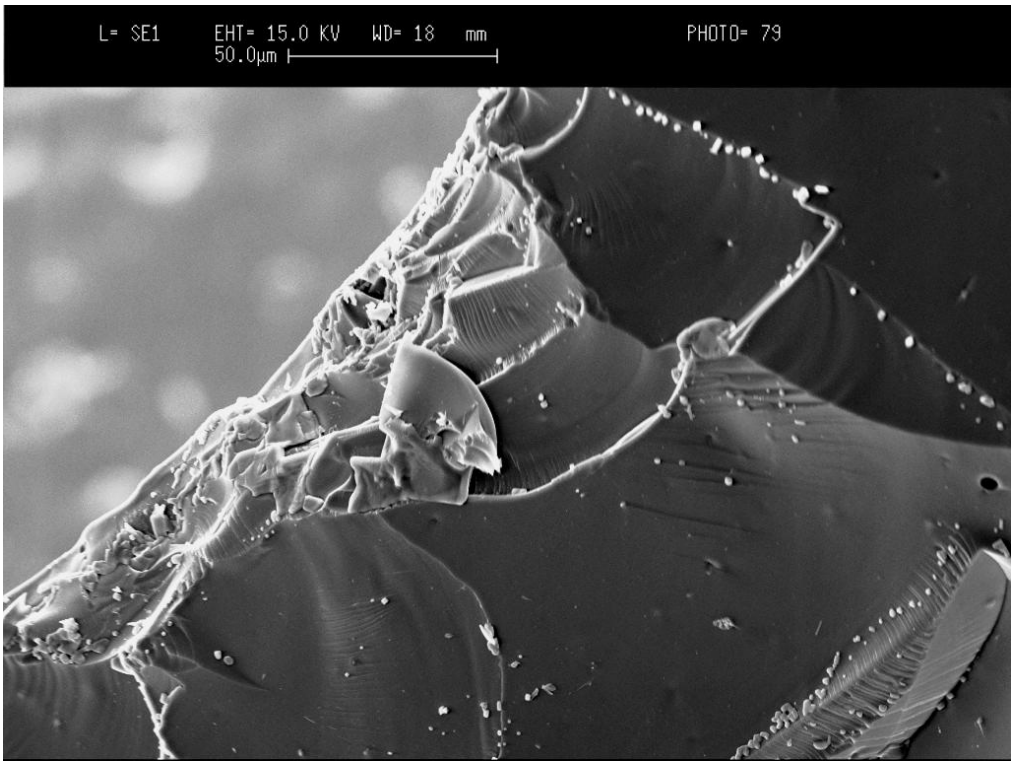

Figure 4-57: SA5 -Qasiplastic yield (crush zone) underneath ball contact at DR [magnification x 500]

DB cusp contact area:

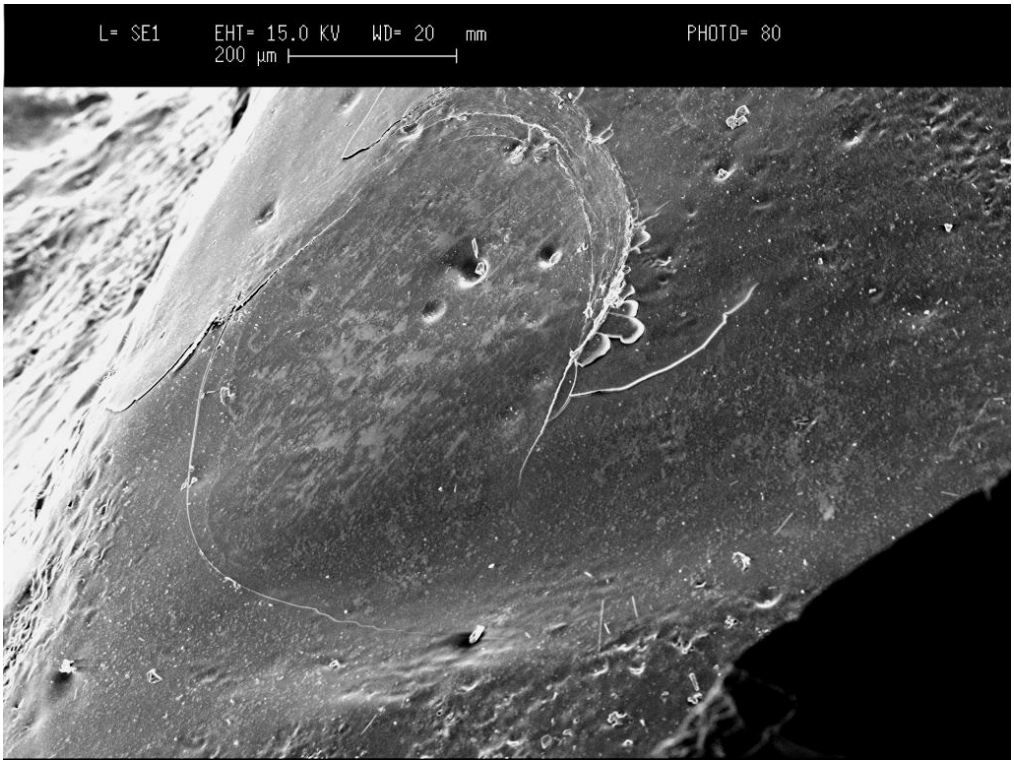

Figure 4-58: SA5 – DB cusp ball contact area [magnification x 100]

Delamination confirmed:

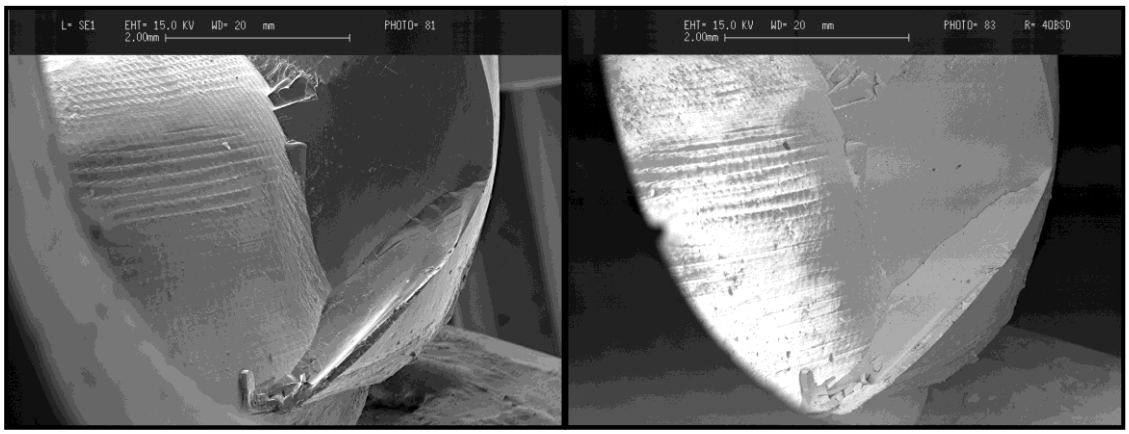

Figure 4-59: SA5 - Delamination confirmed using BSD (image on the right) [magnification x 20]

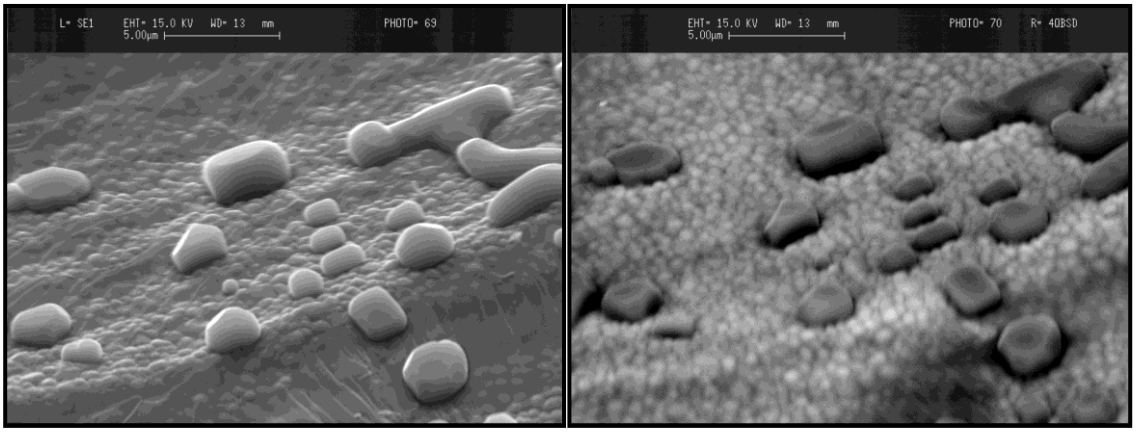

Figure 4-60: SA5 - Higher magnification combined with BSD (right image) confirm delamination and exposure of the zirconia core [magnification x 5000]

Figure 4-61: SA5 - Origins of fracture and directions of crack propagations joining at the midline fissure crack [magnification x 25]

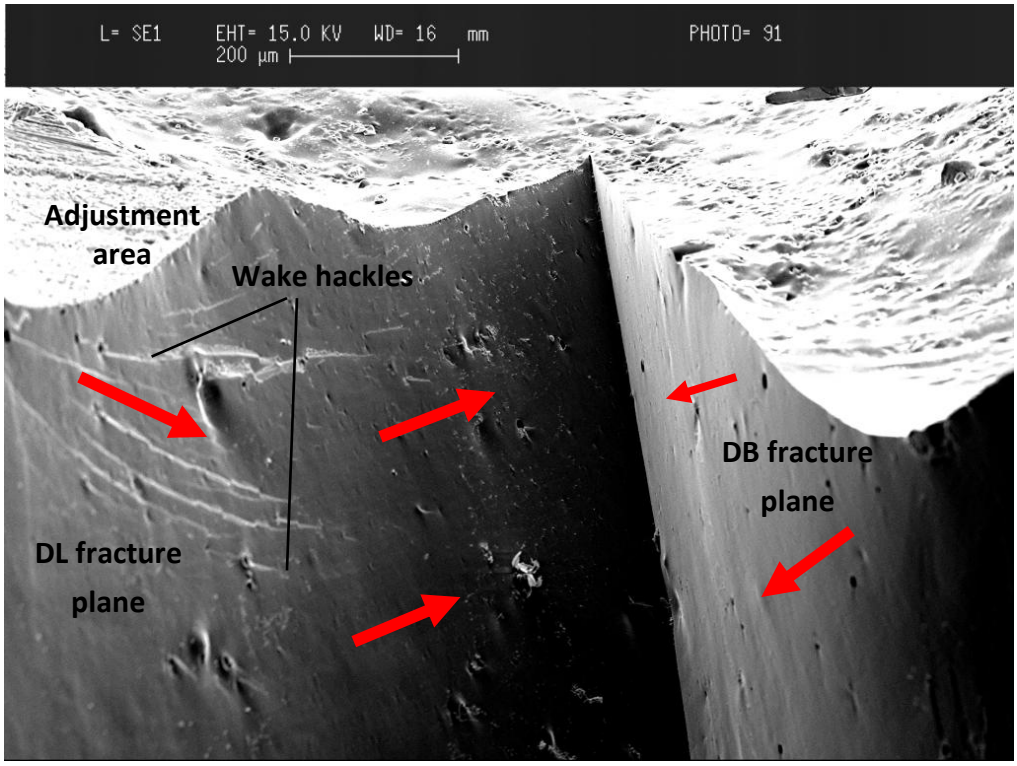

Figure 4-62: SA5 - Image of fractures propagating to join at the midline fissure crack [magnification x 100]

This slow cooled sample also fractured by the joining of two fractures to end in a midline fissure crack, similar to that at SA1. However in this sample, it was the DR ball contact area, rather than the DB contact that made the second fracture initiation site in addition to the DL site. Both fracture planes propagated vertically downwards to the zirconia/veneer interface, delaminating the zirconia core. Porosity at the corner of the occlusal adjustment was the origin of fracture at the DL ball contact (figure 4-53). The fracture planes appear featureless and spread in a mesial direction underneath the remaining area of occlusal adjustment at DL towards the midline, and distally surfacing out with no evidence of compression curls and minimal twist hackle lines. The hackle lines in the centre of the DB fracture plane are possibly due to further fragmentation of the veneering porcelain due to flaws such as porosities or contamination, however the cause of this fragment was undetermined.

The DB ball contact area showed ring compression marks by the loaded ball, however no cracks resulted from that contact and it does not seem to have affected the fracture of the distal ridge. The midline fissure crack ended at the mesial ridge without further surface propagation.

4.3 DISCUSSION

Five fast cooled and five slow cooled anatomical molar zirconia crowns were tested under static load-to-failure to qualitatively compare differences in failure mechanics and fracture features using fractographic analysis. Furthermore, quantitative assessment of the maximum loads-to-failure in both groups was also undertaken to establish any strengthening effects developed by the tempering process on the fast cooled zirconia crowns.

Despite the small sample size in this study, it was possible to establish that fracture features did differ between both groups, and that failure modes appeared consistent in samples within each group. The average maximum load-to-failure for the fast cooled group was slightly lower than that recorded for the slow cooled group (901.54 N and 1013.00 N respectively), however this difference was not statistically significant ($P > 0.05$). It is possible a larger sample size could have resulted in a significant difference between both groups. However, the null hypotheses for this study were partially rejected, in that the fracture mechanics between both groups were different, while the average maximum loads-to-failure were not.

4.3.1 Methodology

There are a number of reasons why a molar crown form was used in this study rather than an anterior or premolar tooth. The strength of zirconia has made it possible to use all-ceramic restorations to restore molar teeth (Raigrodski 2004b), and therefore would be the preferred material of choice in the posterior compared to the anterior of the mouth where other all-ceramic type restorations have been found to be successful (Fradeani et al. 2002; Fradeani et al. 2005). Furthermore, the dentition in the posterior mouth is subjected to greater and more complex occlusal loading (Devlin et al. 1986), and posterior teeth have been found to exhibit higher failure rates in all-ceramic systems compared to anterior teeth (Pjetursson et al. 2007). However, a premolar anatomy was not used in this study, because unlike the molar anatomy, a stainless steel ball could not sit passively on the occlusal anatomy made by the buccal and lingual cusps, and so therefore, a more complex loading set-up would have been needed, such as using an a bar type loader rather than a ball (Good et al. 2008).

The fracture strength and fracture modes in dental ceramics as reported in the literature, have been found to be greatly influenced by the testing parameters, such as the cross-head speed and type of indenter used (Kelly 1999; Lawn et al. 2001; Thompson et al. 2004). Thus after conducting a pilot study using a 6mm, and a 4mm diameter stainless steel ball to load fast cooled and slow cooled samples, the latter was chosen as the loading indenter for this study. This was done because contacts made by the 6mm ball were much higher on the cuspal inclines than the 4mm ball, and as a consequence the 6mm ball consistently produced small chipping type fractures restricted only to the DL cusps in both groups. On the other hand, the 4mm ball induced the desired type of fractures that involved the entire thickness of the veneering porcelain, extending to the zirconia cores, thus allowing fractographic analyses of thermal residual stresses within the veneering porcelain on a radial plane. The disto-occlusal aspect of the crown forms were used for the axial static loading, as opposed to the mesial aspects or the centre. This was because of the largely unsupported porcelain at the distal aspects, especially at the distal ridge, which would potentially develop higher thermal residual stresses, and thus have a higher risk of fracture compared to the mesial and the centre of the crowns. To allow the "locked-in" residual stresses to exert as much influence as possible on the fracture mechanisms in each system, a very slow cross-head speed was used (0.1mm/min). Finally, testing was done under moist conditions.

4.3.2 Delamination fractures

In general, delamination of the zirconia was the main mode of failure in both groups. Delamination was confirmed via SEM analysis (figures 4-46 and 4-90). However, under SEM examination, 100% delamination throughout the entire fractured surface did not occur. What appeared to be exposed zirconia under visual interpretation, seen as evidence of the trace lines produced during the CAD/CAM milling process, in fact was mostly covered by a thin layer of porcelain with only minor regions with actual exposed zirconia core material (figures 4-22, 4-45, 4-59). This finding highlights the limitation of clinical examination in determining true zirconia core delaminations and highlights the need for SEM confirmation.

Delamination fractures are not reported to be the main type of veneering porcelain fracture in clinical trials on zirconia restorations (Al-Amleh et al. 2010). However, static loading-to-failure tests do not produce failures similar to those seen clinically. Nevertheless, delamination of the distal aspect demonstrated particular trends for each group. In the fast cooled crowns, delamination fractures involved almost the entire distal aspect in 4 out of 5 samples, usually involving 1 or both distal cusps (figure 4-9, samples FA1, FA2, FA4, and FA5). Large areas of exposed zirconia could be seen, however, SEM confirmation was not done for all samples. In addition, despite the fact that all 5 samples in the slow cooled group also exhibited delamination type fractures, the pattern of fracture in 3 of 5 of these crowns were almost identical. The delamination fractures were limited to the distal ridge, with cracks joining the fracture on either side (buccal and lingual corners of the fracture) to a midline fissure crack which ended at the mesial ridge (figure 4-10, samples SA1, SA3, and SA5). In the other two samples, the distal ridge did fracture with evidence of delamination, however chipping of the adjusted DL cusp also occurred (samples SA2 and SA4). In the literature, fractographic analysis of clinically failed zirconia FPDs found that delaminations of the veneering porcelain were found in the failures (Taskonak et al. 2008a; Aboushelib et al. 2009). Fractures were found to initiate at the surface of the veneer, then they propagated to the zirconia core/veneer interface where they stopped, turned, and propagated along the interface to then reinitiate at stress concentration areas upon further loading (Taskonak et al. 2008a). Although the samples in this study were not subjected to cyclic fatigue type loading, a similar mechanism of fracture appears to have occurred in both the fast and slow cooled samples.

SEM analysis of the delaminated samples showed two types of fracture modes resulting in delamination. These were Hertzian cone cracks and radial cracks. The fracture sustained in the fast cooled sample FA2, was initiated from Hertzian cone cracks at the DB and DR ball contact areas (figure 4-34). Under SEM analysis, this sample provided good illustration of quasiplastic “crush” zones directly underneath the ball contact areas (figure 4-26 and 4-27), and Hertzian cone cracks (figure 4-30). It is difficult to determine from the SEM images whether inner or outer Hertzian cone cracks propagated vertically to the zirconia core, initiating the fracture. However, studies have shown that outer cone cracks are shallow and remain at low angles relative to the specimen surface (Kim et al. 2007). Furthermore they are usually considered to be less deleterious than inner cone cracks,

especially in sphere loaded flat specimens. On the other hand, inner cone cracks develop inside the contact area and quickly propagate at a relatively steep angle to initiate failure, and this normally precedes radial cracks by causing initial strength loss in the system (Kim et al. 1999). Inner cone cracks, however, have only been observed under cyclic loading in water (Kim et al. 1999; Zhang et al. 2005). It must follow then that inner cone cracks could not be the primary mode of failure, and raises the possibility of failures emanating from the less harmful outer cone cracks. On the other hand, Quinn described several outer cone crack geometries and angles possible in glass by a blunt contact depending on the angle of contact and type (static or sliding) (Quinn 2007).

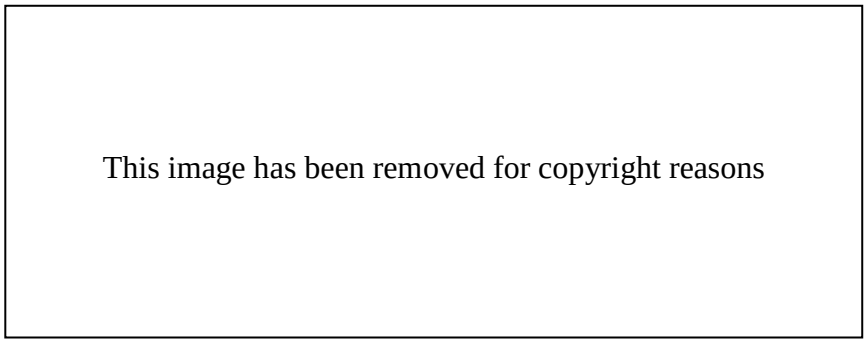

Figure 4-63: Blunt contact cone crack profiles, (a) static vertical contact, (b) static oblique contact (modified from Quinn 2007)

Figure 4-63 shows the difference between the cone profiles produced in glass underneath static loading a sphere at a perpendicular angle, and at an oblique angle. During vertical loading, ring cracks initially pop perpendicular to the surface but then turn and propagate with an internal angle between 125^{o} to 135^{o} (figure 4-63 a). Conditions are different if the contactor is loaded at non-perpendicular angles, so that the backside of the cone approaches the surface resulting in larger angles, while the front side penetrates deeper into the surface with smaller angles (figure 4-1 b) (Chaudhri et al. 1989). By measuring the cone angles created by the ball contact at the DB cusp of sample FA2, we can establish the angle at which the ball was exerting its load. The angle of the cone crack towards the midline is approximately 155^{o}, while on the buccal side it is measured at around 125^{o} (figure 4-64). Since the cone on the medial side approaches more to the surface relative to the buccal side, then an oblique type load was exerted by the ball on the cuspal inclines, as shown in figure 4-64 by the black arrow.

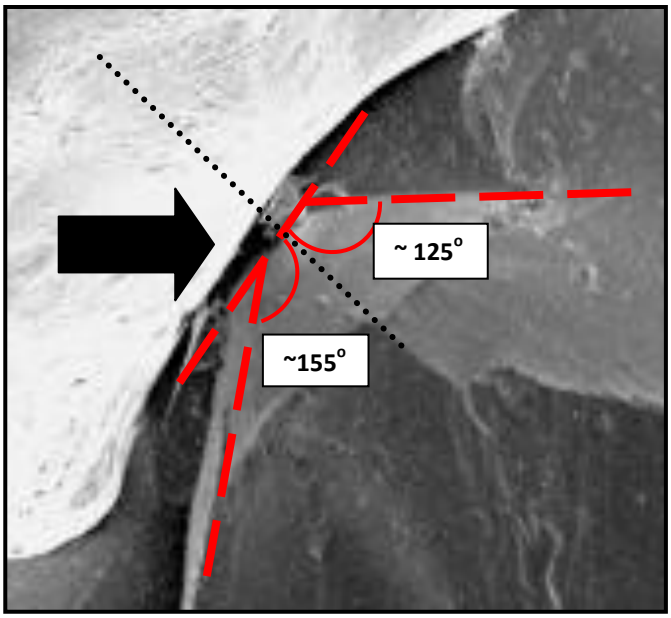

Figure 4-64: Outer cone crack at DB of FA2, angles measured on either side of the cone, dotted black line represents the perpendicular plane normal to the contact surface, black arrow shows the direction of loading exerted by the 4mm ball at the contact area

In this case, it appears that an outer cone crack grew by the oblique load to a critical size. It then spontaneously changed direction, and propagated vertically towards the zirconia core from the medial side, while the distal aspect cleaved off the distal aspect of the DB cusp (figure 4-34). A similar mode of fracture also occurred at the DR contact area of this sample (figure 4-26). The outer cone crack was found to propagate until it reached a new zone of stress where it abruptly changed direction following areas of tensile stress. The origin of fracture at the DR contact area of the slow cooled sample SA5 was also confirmed using SEM analysis to be from cone cracking underneath the ball contact, however the main fracture cleaved off flat, with no abrupt changes in crack propagation like that seen in sample FA2 (figure 4-56). These findings provide us with a better understanding of the materials behaviour in this bilayered crown system at a fundamental level, beyond the flat plane model, which will inevitably have geometric limitations. For instance, some studies have used flat trilayered zirconia plates subjected to 30^{o} off-axis cyclic loading conditions, in order to mimic cuspal inclines (Guess et al. 2009; Zhang et al. 2010a). They observed failure to occur as a result of the formation of partial cone cracking behind the sliding indenter, which then propagated towards the zirconia core/veneer interface (figure 4-65).

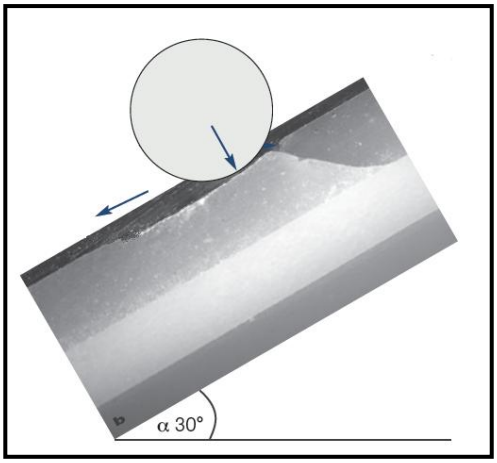

Figure 4-65: Cross-section view of fatigued IPS e.max ZirCAD/ IPS e.max ZirPress specimen at 140,000 cycles and 400 N with sliding cyclic load application at a 30^{o} angle with a tungsten carbide ball (diameter 3.18mm) (modified from Guess et al. 2009)

Despite the aforementioned studies having a more clinically relevant set-up in terms of cyclic-fatigue type testing conditions, using a plate model on an angle does not replicate the geometry at a cuspal incline. The zirconia core does not rise up along the incline, such as seen in figure 4-65, and in reality, the stiff core supporting the veneering porcelain is a distance away from the surface where the ball would be exerting its load. Therefore, despite being a simple geometry to test materials with, extrapolating clinically relevant information using flat angled specimens with a non-realistic layered system to mimic cuspal inclines may be misleading.

The other mode of failure resulting in delamination was found in slow cooled crown SA1, where radial cracking occurred through the veneering porcelain (figure 4-48). An outer cone crack at the DR contact area appeared to experience steady growth, as can be seen via the arrest lines in figure 4-41. However, delamination of the zirconia occurred beneath the DR contact, confirmed by wake hackle lines and twist hackles that show the crack propagation path from the core/veneer interface, to meet the growing cone crack at the DR contact area and two cracks running mesio-distally from DB and DL. As previously mentioned, cone cracks normally appear before radial cracks. This is because, as a cone crack grows, there is an increased load being applied at the core/veneer interface as the porcelain is loaded to its elastic limit. Zirconia has been found to require relatively low loads for the initiation of quasi-plastic yield, compared to loads needed for the onset of cone cracking (Rekow et al. 2005). As a result, Rekow and Thompson proposed that

excessive loading on bilayered zirconia restorations is likely to create a quasi-plastic yield zone in the zirconia just below the core/veneer interface, thus producing tensile stresses in the veneer, resulting in a radial crack in the veneer. This may explain the appearance of a chip like fragment that was located at the site of fracture origin in figure 4-45, and the upwards radial crack propagation.

Finally, based on four-point bending tests on notched bilayered zirconia samples, Göstemeyer and colleagues warned that slow cooling zirconia restorations may increase the risk of delamination failure at the core/veneer interface (Göstemeyer et al. 2010). The results in this study, however, do not agree with this claim, since both groups sustained mainly delamination type fractures under static loading. Another study conducted on fast cooled and slow cooled zirconia anterior crowns under both static loading and fatigue conditions, observed only chipping cohesive fractures in both groups, with no delamination fractures in either group (Rues et al. 2010). It may be that a reduction in strain energy was needed to fracture slow cooled notched samples compared with the fast cooled samples used by Göstemeyer and colleagues. Nevertheless, without incorporating the complex geometry of a bilayered restoration and fatigue conditions, the findings by Göstemeyer and colleagues are likely to have limited clinical implications in reality and need further research.

4.3.3 Chipping fractures

Only one crown sustained pure chipping fracture involving an adjusted cusp without delamination at the distal ridge region. This was a fast cooled crown (FA3) that had a fracture load of 818 N, just below the average load-to-failure found for the fast cooled group. SEM images of the fracture confirmed the origin of the fracture to involve the superior margin of the occlusal adjustment area (figure 4-14). Arrest lines seen on figures 4-13 and 4-14 represent momentarily hesitated cracks prior to resumption of crack propagation under altered stress configurations. Sudden redirection of the axis of principle tension can also appear as arrest lines without stopping crack propagation. In the mean time, the origin of fracture is always located on the concave side of any arrest lines (Quinn 2007), confirming the location of origin in this sample to come from the adjustment area. From the appearance of the origin of fracture, Hertzian cone cracking does not appear to

be the mode of failure in this fracture. Unlike the cone cracks observed in the other SEM samples examined, the fracture surface in sample FA3 started off flat and continued that way as it propagated through the cusp, with the exception of obvious arrest lines limited to the first 0.5mm region of the crack. The fracture appears to have resisted the initial load, as indicated by the arrest lines caused by the induced surface residual compression stresses, but then reached a high zone of tension within the cusp centre, where the crack propagated with ease, indicated by the featureless fracture plane. The crack then exited the crown with twist hackles at the edges, where the crack once again experienced a change in resultant stresses that slowed the crack down.

Furthermore, in deference to the other fracture modes observed, such as that seen for samples FA2 and SA5 (figures 4-26 and 4-57 respectively), this origin of fracture does not have a quasi-plastic yield zone limited to the ball contact area. Instead, a band of subsurface damage could be seen along the edge of the occlusal adjustment area beyond the origin of fracture. Occlusal adjustments were done on the DL cusps to simulate the clinical reality of post-cementation occlusal corrections. Studies have found that occlusal adjustments, or resurfacing glazed porcelain, induce high tensile stresses centred at the bur contact zones (Song et al. 2008; Song et al. 2010). Adjustments were found to cause subsurface damage in the porcelain; its depth was significantly influenced by the bur diamond grit size and rate of removal. Fine grit diamond burs (grit size 20 – 30μm) were found to produce subsurface damage in feldspathic porcelain between 7- 13μm, depending on the removal rates (Song et al. 2010). This subsurface damage was found with fine and with ultra-fine burs to be predominantly in the form of brittle fracture in feldspathic porcelain (Yin et al. 2006), while zirconia surfaces show plastic deformation and ductile cutting (Yin et al. 2003). It has also been found that brittle fractures result in surface residual micro-cracks and near-surface damage, thus reducing the residual flexural strength of the porcelain (Rekow et al. 2005). Brittle damage has been attributed to the low fracture toughness (K_{IC}) of feldspathic porcelains compared to other ceramics (table 1-1) (Schmidt et al. 2000). Furthermore, the depth of cut has also been shown to influence the final damage mode on porcelains (Yin et al. 2007). However, investigating these parameters was beyond the scope of this study, because to achieve accurate and controlled results, sophisticated load-controlled equipment such as that described by Dong et al. (2000) must be used. Nevertheless, in this study, occlusal adjustments in the 4 chosen samples was

thoroughly investigated using SEM for any evidence of microcracks that may have initiated fractures in the loaded crowns.

In general, most of the adjusted DL cusps sustained some form of damage during loading. Actual chipping of the DL cusps was a direct result of the adjustments and was seen in 3 of 5 of the fast cooled crowns (FA1, FA3 and FA5), and 2 out of 5 in the slow cooled crowns (SA2 and SA4). While crack lines running through the adjustment areas were seen in 2 samples (SA1 and SA3). However, crack lines and cusp fractures were also observed in the non-adjusted DB cusps at the ball contact areas in samples FA1, FA2, FA4, SA1, and SA2. From table 4-3, it would appear that the non-adjusted DB cusps were able to resist loads only slightly more than the DL adjusted cusps. This may be due to anatomical difference between both cusps within the volume of porcelain and cusp contours, and may not relate to the occlusal adjustment. On the other hand, the DL cusps may have sustained more fractures due to the loss of porcelain volume just underneath the ball contact area by the occlusal adjustment, thus changing the behaviour of the porcelain at the ball contact zones. There was no evidence of any microcracking seen with the adjusted porcelain that may have initiated cracks in any of the examined samples. Also, the presence of porosity in the porcelain adjacent to the adjustment was found to be the origin of fracture in sample SA5. In view of these results, it is inconclusive whether the occlusal adjustment created on the DL cusps had a major influence on the failure mechanism in both groups, however the incidence of chipping of the DL cusps was slightly higher than that seen with the DB non-adjusted cusps. Furthermore, it is not known what effect these adjustments had on the maximum loads-to-failures in both groups, and how they would compare to non-adjusted crowns. This could be part of future research on this test model.

4.3.4 Cracking on non-loaded side

Despite having a small sample size, 60% of the fast cooled crowns sustained cracking on the non-loaded mesial aspects, while the same was not observed in any of the slow cooled samples (figure 4-9). These cracks were almost identical in their path around the mesial aspect and did not cleave off the samples. The origin of fracture could not be established using SEM. In sample FA2, a midline fissure crack meets the mesial crack within the fossa, and therefore highlighting two possible scenarios for this fracture (figures 4-20, 4-32

and 4-33). The midline crack may have developed from the wedging effect of the loaded ball on the distal cusps, or from cone cracks that grew into fissure cracks. The crack then turned buccally to run around the mesial aspect of the crown to finally return back to the midline crack at a 90^{o} angle. Alternatively, the mesial crack may have initiated from the lingual aspect toward the midline fossa to meet a growing midline crack that travelled disto-mesially, changing its path of propagation. However, the other two samples with the mesial cracks (FA3 and FA4) did not join a midline fissure crack, therefore it is more likely that the two cracks were independent of each other.

SEM images of the underside of the chip from sample SA3 (figures 4-17 and 4-19) confirm that the mesial crack was independent from the chipping fracture, and occurred after the primary chipping crack had run through the crown, since the chip fragment was in one piece and had not been split by the crack.

It would therefore suggest that despite the fast cooled crowns having higher residual compressive stresses on the surface, as determined in chapter 3, high tensile zones within the cuspal regions may have influenced the development of cracks on the non-loaded side. This may have occurred as a result of a warping effect on the veneering porcelain layer by the high static loads applied, initiating the cracks from within the veneers. Fractures from non-load bearing areas have been reported in clinical trials, in the mesio-lingual cusps of mandibular second molars (Sailer et al. 2007), and the lingual aspect of FPD pontics (Schmitter et al. 2009). These studies report on 5-year and 2-year follow-up periods respectively, a considerable time before the realisation of the influence of cooling rates on the development of high residual tensile stresses within the veneering porcelain. We could therefore assume that meticulous slow cooling protocols were not followed during the manufacturing of restorations in these two studies, resulting in similar types of fractures occurring on non-loaded areas.

Based on our findings, a clinical recommendation could be made to clinicians and researchers using zirconia-based restorations, especially during retrospective studies. Trans-illumination should be used to look for cracks throughout the entire restoration, even at non-load bearing areas of the restoration, and not to limit fracture assessments to visual

interpretation without the aid of a light source. It is safe to assume that every dentist has a composite light-curing unit, which are often used to look for cracks in natural teeth (Liewehr 2001), and the same therefore, could be done with all-ceramic crowns especially zirconia, even when fractures are not obvious.

4.3.5 Fracture features in both groups

In this study, fractographic analysis has been used as a method for confirming the presence of tensile zones within the veneering porcelain of fast and slow cooled zirconia crowns. The Vickers indentation study in chapter 3, confirmed that fast cooling zirconia crowns does induce high residual compressive stresses on the surface of veneering porcelain. Compensating tensile stresses within veneering porcelain are unable to be physically measured, however, their presence exerts differential stresses on a passing crack that could be read using fractographic features. These features include twist hackles, and compression curls, as well as the overall appearance of a fractured plane (Quinn 2007).

The fracture planes left behind after loading to failure were of two general appearances. The fast cooled crowns exhibited fracture planes that had high concentrations of twist hackles, compression curls, abrupt and steep change in crack propagation paths, as well as curved planes of fracture. On the other hand, slow cooled samples had fracture planes that lacked high concentrations of twist hackles, and fracture planes were mostly featureless and flat.

Figure 4-26 is an SEM image of the outer cone crack produced by the ball contact at DR of fast cooled sample FA2. On this image, a high concentration of twist hackles underneath the ball contact can be seen, in addition to the arrest lines. These features are consistent with the presence of high compressive stresses on the surface of the veneering porcelain which the crack had to overcome, indicating interrupted growing crack extension. However, it appears that once the cone crack grew beyond a critical size, it spontaneously changed direction, twisting then turning downwards and to the lingual aspect, to cleave off with a final compression curl at the exit surface (figure 4-23). In contrast, the DR ball contact at sample SA1 (figure 4-41) produced a smaller cone crack with no twist hackles running in the same direction, such as those seen in sample FA2. In this case, the origin of

fracture was from delamination of the core/veneer interface below, where a radial crack propagated upwards leaving twist hackles pointing in the same direction, probably produced as a result of tensile stresses produced by contact induced bending. In comparison, the multi-plane fracture at the DB cusp of sample FA2 (figures 4-24 and 4-31) appears to have encountered steep stress profile changes within the veneer during its propagation. Furthermore, the smooth featureless zone in the middle of the cusp is a sign that the crack propagated effortlessly through this zone due to tensile stresses. A similar appearance was noted on the DL cusp chip in the fast cooled sample FA3. Here, twist hackles and hackle lines only appear at regions corresponding to superficial porcelain, disappearing at deeper zones in the middle of the chip in the disto-lingual cusp, and as the chip crosses over to the mesio-lingual cuspal region (figure 4-15 and 4-16). This is characteristic of superficial compressive stresses with subsurface tensile zones that help extend the cracks as soon as they are reached. Arrest lines at the origin of the fracture in this sample also indicate an initially slow growing crack, which is followed by a faster spontaneous-type fracture propagation, demonstrated by the featureless appearance.

The slow cooled samples fractured with mostly featureless flat planes, with minimal presence of twist and hackles (figures 4-47 and 4-50). This indicates that the fractures propagated at a steady rate, with no sudden change in stress profiles within the veneering porcelain. Nevertheless, twist hackles could be seen at the DR contact area fracture plane in sample SA5 (figure 4-61), presumed to be due to contamination or flaws within the veneer that caused further fragmentations. At the same time, twist hackles on the fracture planes that are close to the core/veneer interface, are likely to be due to compressive stresses developed by the positive CTE mismatch between the core and veneer, putting the core in tension and the veneer in compression. Despite that, fractures in this group did not seem to experience the same type of altering stress profiles that resulted in the multi-plane fractures. A more uniform stress profile seemed to exist in the veneering porcelain of the slow cooled zirconia crowns.

4.3.6 Maximum loads-to-failure

Fast cooling of crowns has been suggested for strengthening the veneering porcelain in metal-ceramic restorations, by developing residual compressive stresses on the surface of the veneer (DeHoff et al. 1990). However, in this study of fast and slow cooled zirconia crowns, the average maximum load-to-failure was not found to be significantly different between each group, in fact, the fast cooled group exhibited a slightly lower average of the two. According to the results in this study, fast cooling zirconia crowns does not improve their fracture resistance under static loading-to-failure.

4.4 CONCLUSIONS

1. Fracture modes and fracture features identified using fractographic analyse were different for fast cooled and slow cooled zirconia crowns.
2. Cracking on the non-loaded aspect of crowns were only observed in the fast cooled group.
3. The average maximum load-to-failure for fast cooled and slow cooled zirconia crowns were not statistically different under static loading-to-failure.

CHAPTER 5
GENERAL DISCUSSION & CONCLUSION

Similar to the strengthening of commercial glass (Rawson 1974), tempering of metal-ceramic restorations have been used for decades to induce a protective residual compressive stress layer on the surface of the veneering porcelain, thus strengthening and improving the clinical serviceability of restorations (DeHoff et al. 1990; Anusavice et al. 1991). This simple fast cooling process is usually done by removing the restoration from the furnace, after the completion of the final glazing cycle, and allowing the restoration to cool at ambient air from the high sintering temperature that are well above the glass transition temperature of porcelains. This practice may have certainly played a significant role in the clinical success of metal-ceramic restorations reported in the literature (Creugers et al. 1994; Tan et al. 2004), and therefore it is not surprising that dental technicians have continued this procedure for all-ceramic restorations when they were first introduced.

In chapter 2, the systematic review of clinical trials on zirconia restorations confirmed two important aspects in relation to the chipping problem: first, that cohesive chipping of the veneering porcelain is indeed a bane to zirconia-based restorations, and does appear at different rates in various studies. Secondly, early studies reported on restorations that were fabricated before the introduction of new recommendations for slow cooling that has been suggested by zirconia manufacturers, and reported in the literature. Therefore, if fast cooling zirconia restorations does indeed cause the development of high tensile zones within the veneering porcelain, then future clinical trials must address this aspect in their materials and methods.

In chapter 3, the development of residual surface compressive stresses from tempering zirconia crowns was confirmed using the microindentation technique, however, this induced compressive layer on the veneering porcelain did not strengthen the zirconia

crowns as it was intended, and failure occurred at loads similar to those seen in the slow cooled crowns (chapter 4). Using fractographic analyses of the loaded crowns, it can be seen that propagating cracks experienced different stress profiles throughout the veneering porcelains thickness, depending on the cooling rate of the crown. In the fast cooled samples, crack propagation appeared to encounter resistance at first, to then spontaneously change directions and spread throughout the veneering porcelain along various planes. On the other hand, slow cooled crowns had crack propagations that were not influenced by any changes in internal stress profiles such as those seen in the fast cooled group. Most importantly, average maximum load-to-failure was also slightly higher for the slow cooled group than the tempered group, albeit not statistically significant.

In the limited published clinical trials, chipping fractures have been reported in both single crowns and FPDs (Çehreli et al. 2009; Roediger et al. 2010). Chipping fractures were found at various rates and sizes, occasionally, necessitating the replacement of the entire restoration (Sailer et al. 2007; Örtorp et al. 2009; Groten et al. 2010). A large number of chipping events went undetected by the patients and were incidental findings during review appointments (Vult von Steyern et al. 2005; Larsson et al. 2006; Crisp et al. 2008). Furthermore, chipping fractures were also observed in non-loaded areas on some restorations (Sailer et al. 2007; Schmitter et al. 2009). It was presumed that high tensile zones within the veneering porcelain led to the cracking seen on the non-loaded side of 60% of the fast cooled crowns in chapter 4 (figure 4-9). Although superficial residual compression stresses are expected to protect the veneer during loading, these crowns demonstrated an affinity to cracking more than the slow cooled group. This may explain the high incidence of fractures observed in clinical trials, at times occurring at non-loaded areas. Furthermore, some of the cracks and chips in this study could not be detected by simple visual evaluation, and it was only with trans-illumination that an accurate visualisation of peripheral cracks was possible. Under these circumstances, it is quite possible that the reported chipping in the literature is a modest figure, since none of the clinical trials utilised any form of trans-illumination in their review appointments, and since patients are at times unable to detect chips and cracks.

It is well established that unsupported porcelain is prone to an increased risk of fracture (Miller 1977; Anusavice 2003). This is because feldspathic porcelain is unable to

withstand a deformation strain of more than 0.1 – 0.3% without fracture (Craig et al. 2002). Thus, in an attempt to offset the chipping problem, the design of zirconia core frameworks has been the topic of research in a number of recent *in vitro* studies, and so far no consensus on the best core design has been proposed (Bonfante et al. 2010; Lorenzoni et al. 2010; Rafferty et al. 2010; Kokubo et al. 2011; Silva et al. 2011). The aim of a modified core design is to minimise veneering porcelain bulk, and to improve the support for the veneering porcelain by mimicking metal-ceramic type framework designs, rather than "cap" type cores (Marchack et al. 2008). Nevertheless, chipping fractures have also been found in a clinical trial which utilised a modified core design (Tinschert et al. 2008). However once again, chipping in this study may have been related to high residual stresses caused by inappropriate cooling rates, and the modified core design may not have been sufficient to prevent chipping.

Furthermore, it has been found that increasing the thickness of porcelain, increases the residual stresses, especially during fast cooling rates (Asaoka et al. 1992; Guazzato et al. 2010). This however, was not observed when the cusp heights increased as reported in chapter 3 (figure 3-20). On the contrary, the 1mm cusp had significantly higher surface residual stresses compared to the 2mm and 3mm cusped crowns in the fast cooled group. These results could be explained by the change in anatomical contours, which are known to have a great influence on stress profiles within a bilayered system (Nielsen et al. 1972; Bertolotti 1980; DeHoff et al. 2008). The fact that there was no statistical difference between the 2mm and 3mm fast cooled crowns, might be due to the influence of cuspal anatomy and fissure regions that may have been the areas of stress raisers affecting the global stress profile within the system. This corroborates the finding of fissure cracks in 9 out of 10 crowns in the loaded crowns studied in chapter 4. These fissure cracks could be seen in both fast and slow cooled crowns with the aid of trans-illumination (figure 4-9 and 4-10). However, clinical trials do not report on fissure cracks in zirconia-based restorations. Chipping fracture mostly involves cusps and pontic regions (Larsson et al. 2007; Sailer et al. 2007). This is probably because of the vastly different loading conditions found between the oral cavity and *in vitro* studies such as statically loading a crown until fracture with a 4mm stainless steel ball (Thompson et al. 2004). For these reasons, it may be valuable to conduct a cyclic fatigue study on zirconia crowns with various cusp heights under fast and slow cooling protocols, to identify differences in

failure modes and fracture features influenced by the subtle change in anatomical contours. Furthermore, the theory of reducing residual stresses in the 2mm and 3mm cusp tips should also be investigated, since little is known about the effects of contours on the stress profile distribution in bilayered dental crowns (Mainjot et al. 2011).

In conclusion, the issue of chipping fractures of veneering porcelain in zirconia-based restorations is bound to be multi-factorial. It should not be assumed that modifying the cooling rates of veneering porcelains around the glass transition temperature to reduce residual tensile stresses within the veneer is the complete answer to this problem. There are many unanswered questions relating to all-ceramic systems, that are not an issue with metal-ceramics. As yet, there is no consensus on the best CTE mismatch for compatibility between zirconia core and veneering porcelains (DeHoff et al. 2009; Fischer et al. 2009a). In addition, the best core design which provides appropriate support for the veneering porcelain has not yet been established (Lorenzoni et al. 2010; Silva et al. 2011). The fact that metal-ceramic systems have an advantage which could not be imparted to all-ceramic restorations is a limitation that must be recognised, namely the ductility of metal alloys, versus the brittleness of ceramics. A number of authors cite the ductility of metal alloys used in metal-ceramics to be an influencing factor in their success, since ceramic copings are unable to accommodate high tensile stresses by plastic deformation that metal copings can tolerate (Kim et al. 2007; Donovan et al. 2009; Tholey et al. 2009; Silva et al. 2011). Zirconia as a core material is still under examination and is a developing product in dentistry (Fischer et al. 2007; Zhang et al. 2010a). It is likely that the Y-TZP we use today, may be replaced by a “newer” and “better” zirconia which would have to go through clinical and laboratory trials before being recommended for long-term dental clinical use. In the mean time, efforts must be made to reduce residual tensile stresses within veneering porcelains of zirconia-based restorations by appropriately slow cooling the restorations following the final glazing cycle that takes into account the Tg of the veneering porcelain.

5.1 SUMMARY OF RESEARCH FINDINGS:

Within the limitations of this *in vitro* study several conclusions can be made.

1. Published clinical trials on zirconia-based restorations confirm that there is a high incidence of chipping of veneering porcelain. This occurs with every brand of zirconia, in both single crowns and fixed partial dentures.

2. Clinical trials up to this point are based on restorations fabricated before the implementation of modified slow cooling protocol for zirconia-based restorations. Future trials should consider this issue in their materials and methods, and ideally, the studies should be based on randomised controlled trials on slow cooled vs. tempered restorations to determine the clinical relevance of residual tensile stresses on fracture chipping, (although it is appreciated that there may be ethical issues with this approach).

3. In the present study, tempering of zirconia molar crowns induced residual surface compressive stresses in the veneering porcelain; however that did not improve fracture resistance under static loading-to-failure.

4. Increasing the thickness of veneering porcelain in zirconia molar crowns did not result in an increase in the residual surface stresses. Furthermore, a reverse trend was found decreasing the thickness from 2mm to 1mm at cusp tips in fast cooled crowns.

5. The anatomical contours of the veneering porcelain has a major influence on the resulting residual stress profile, so that increasing the veneering thickness from 2mm to 3mm does not greatly affect the final residual stress profile at the cusp tips.

6. Fractographic analyses confirmed the presence of a differential residual stress profiles in the veneering porcelains of tempered zirconia crowns by the presence of high concentrations of twist hackles, compression curls, and multi-plane fractures,

which were not observed in the slow cooled zirconia crowns. Crack propagation and fracture patterns were highly influenced by the cooling protocol used.

7. Occlusal adjustment had some influence on the fracture mode of some samples, however their direct effect was inconclusive. This is because loss of volume underneath the loading area or anatomical differences between the cusps may have contributed to the increase chipping that occurred with the adjusted cusps. In addition, no evidence of microcracking was found in the porcelain at the occlusal adjustments areas.

5.2 HYPOTHESES

The null hypotheses proposed in section 1.6.3 are addressed as follows:

Null hypothesis 1:

Residual surface stresses on cusp tips of zirconia crowns are not influenced by the thickness of the veneering porcelain.

This null hypothesis is partially rejected for the fast cooled group, but accepted for the slow cooled group. In the fast cooled group, residual surface stresses on the cusp tips were not influenced by an increase from 2mm to 3mm, however 1mm cusps had significantly higher stresses values compared to the 2mm and 3mm. The thickness of veneering porcelain did not have an influence on residual stresses in the slow cooled crowns.

Null hypothesis 2:

Residual surface stresses on cusp tips of zirconia crowns are not influenced by the cooling rate of the restoration during the final firing cycle.

The second null hypothesis was rejected. The cooling rate of the restorations significantly influenced the residual stresses on the cusp tip, fast cooling induced compressive stresses, while slow cooling induced tensile stresses.

Null hypothesis 3:

The fracture mechanisms and fracture features of fast and slow cooled zirconia crowns are the same during static load-to-failure testing.

This null hypothesis was rejected.

5.3 AREAS OF FUTURE RESEARCH

1. Residual stresses on the cusp tip surfaces of zirconia crowns in this study where not influenced by an increase in porcelain thickness as expected. Metal-ceramics are still considered to be the gold-standard when it comes to fixed prosthodontic restorations. Investigating the influence of veneer thickness on the magnitude of the residual stresses on the cusp tips using the microindentation technique in both metal-ceramic and zirconia crowns could show the effect of conductivity of the core material on the residual stress profiles. However, it must be ensured that the CTE mismatch between both systems are similar.

2. Similarly, it is not known if differences in the fracture modes and fracture features would occur when comparing a metal core with a zirconia core, on anatomical crown forms under various cooling rates. Both a cyclic fatigue-type loading and static loading-to-failure study using duplicates of metal-ceramic and zirconia crowns, under fast and slow cooling protocols, will identify whether the low conductivity of the zirconia cores has a negative effect of inducing high tensile zones within the veneer, thus increasing the risk of chipping fracture.

3. Studies should focus on the influences of various anatomical contours on global residual stresses in the dental bilayered system, in particular to the fissure regions in molar crowns where stress concentration is possible.

5.4 CLINICAL RECOMMENDATIONS

When using zirconia-based restorations in fixed prosthodontics, attention must be directed towards the veneering process. Only recommended zirconia veneering porcelains should be used, and until conclusive research can provide specific recommendations, a slow cooling protocol should be used in the final glazing cycle that takes into account the veneering porcelains Tg. This will avoid the development of high residual tensile zones within the veneering porcelain that may drive crack propagation, once a crack has passed through the superficial tempered compression layer on the ceramic.

Chipping and cracking can occur in the veneering porcelain at both loaded and non-loaded sides. Chipping and cracking is hard to visualise in veneering porcelain due to its translucency. During routine review appointments, trans-illumination should be used to aid when checking for these cracks, and to accurately identify failures and/or potential failures. This will also ensure that chipping and cracking will be detected clinically, and will allow more accurate reporting of this problem in the literature in the future.

REFERENCES

Aboushelib, M.N., Kleverlaan, C.J., and Feilzer, A.J. (2006), 'Microtensile bond strength of different components of core veneered all-ceramic restorations. Part II: Zirconia veneering ceramics', *Dent Mater*, 22, 857-863.

Aboushelib, M. N., Kleverlaan, C. J., and Feilzer, A. J. (2008), 'Microtensile bond strength of different components of core veneered all-ceramic restorations. Part 3: Double veneer technique', *J Prosthodont*, 17, 9-13.

Aboushelib, M. N., Feilzer, A. J., and Kleverlaan, C. J. (2009), 'Bridging the gap between clinical failure and laboratory fracture strength tests using a fractographic approach', *Dent Mater*, 25, 383-391.

Aboushelib, M. N., de Jager, N., Kleverlaan, C. J., and Feilzer, A. J. (2005), 'Microtensile bond strength of different components of core veneered all-ceramic restorations', *Dent Mater*, 21, 984-991.

Akesson, J., Sundh, A., and Sjogren, G. (2009), 'Fracture resistance of all-ceramic crowns placed on a preparation with a slice-formed finishing line', *J Oral Rehabil*, 36, 516-523.

Al-Amleh, B., Lyons, K., and Swain, M. (2010), 'Clinical trials in zirconia: A systematic review', *J Oral Rehabil*, 37, 641-652.

Albakry, M., Guazzato, M., and Swain, M.V. (2003), 'Biaxial flexural strength, elastic moduli, and x-ray diffraction characterization of three pressable all-ceramic materials', *J Prosthet Dent*, 89, 374-380.

Al-Dohan, H.M., Yaman, P., Dennison, J. B., Razzoog, M.E., et al. (2004), 'Shear strength of core-veneer interface in bi-layered ceramics', *J Prosthet Dent*, 91, 349-355.

Alkhiary, Y.M., Morgano, S.M., and Giordano, R.A. (2003), 'Effects of acid hydrolysis and mechanical polishing on surface residual stresses of low-fusing dental ceramics', *J Prosthet Dent*, 90, 133-142.

Anusavice, K.J. and Gray, A.E. (1989a), 'Influence of framework design, contraction mismatch, and thermal history on porcelain checking in fixed partial dentures', *Dent Mater*, 5, 58-63.

Anusavice, K.J. and Hojjatie, B. (1992), 'Tensile stress in glass-ceramic crowns: Effect of flaws and cement voids', *Int J Prosthodont,* 5, 351-358.

Anusavice, K.J., Dehoff, P.H., Twiggs, S.W., and Lockwood, P.C. (1983), 'Thermal shock resistance of porcelain discs', *J Dent Res,* 62, 1082-1085.

Anusavice, K.J., Dehoff, P.H., Gray, A., and Lee, R.B. (1988), 'Delayed crack development in porcelain due to incompatibility stress', *J Dent Res,* 67, 1086-1091.

Anusavice, K.J., Ringle, R.D., Morse, P.K., Fairhurst, C.W., et al. (1981), 'A thermal shock test for porcelain-metal systems', *J Dent Res,* 60, 1686-1691.

Anusavice, K.J. (2003), Phillips' science of dental materials (11 ed.; St. Louis, Missouri Saunders Amsterdam).

Anusavice, K.J. and Hojjatie, B. (1991), 'Effect of thermal tempering on strength and crack propagation behavior of feldspathic porcelains', *J Dent Res,* 70, 1009-1013.

Anusavice, K.J., Dehoff, P.H., and Fairhurst, C.W. (1980), 'Comparative evaluation of ceramic-metal bond tests using finite element stress analysis', *J Dent Res*, 59, 608-613.

Anusavice, K.J., DeHoff, P.H., Hojjatie, B., and Gray, A. (1989b), 'Influence of tempering and contraction mismatch on crack development in ceramic surfaces', *J Dent Res,* 68, 1182-1187.

Asaoka, K. and Tesk, J.A. (1989), 'Transient and residual stresses in dental porcelains as affected by cooling rates', *Dent Mater J,* 8, 9-25.

Asaoka, K., Kuwayama, N., and Tesk, J.A. (1992), 'Influence of tempering method on residual stress in dental porcelain', *J Dent Res,* 71, 1623-1627.

Ashkanani, H.M., Raigrodski, A.J., Flinn, B.D., Heindl, H., et al. (2008), 'Flexural and shear strengths of ZrO2 and a high-noble alloy bonded to their corresponding porcelains', *J Prosthet Dent,* 100, 274-284.

Bagby, M., Marshall, S.J., and Marshall, G.W. (1990), 'Metal ceramic compatibility: A review of the literature', *J Prosthet Dent,* 63, 21-25.

Baran, G.R. (1985), 'Selection criteria for base metal alloys for use with porcelains', *Dent Clin North Am,* 29, 779-787.

Becher, P.F. and Swain, M.V. (1992), 'Grain-size-dependent transformation behavior in polycrystalline tetragonal zirconia', *J Am Ceram Soc,* 75, 493-502.

Bertolotti, R.L. (1980), 'Calculation of interfacial stress in porcelain-fused-to-metal systems', *J Dent Res*, 59, 1972-1977.

Bertolotti, R.L. and Fukui, H. (1982), 'Measurement of softening temperatures in dental bake-on porcelains', *J Dent Res*, 61, 480-483.

Beuer, F., Edelhoff, D., Gernet, W., and Sorensen, J.A. (2009a), 'Three-year clinical prospective evaluation of zirconia-based posterior fixed dental prostheses (FDPs)', *Clin Oral Investig,* 13, 445-451.

Beuer, F., Edelhoff, D., Gernet, W., and Naumann, M. (2008), 'Effect of preparation angles on the precision of zirconia crown copings fabricated by CAD/CAM system', *Dent Mater J,* 27, 814-820.

Beuer, F., Schweiger, J., Eichberger, M., Kappert, H.F., et al. (2009b), 'High-strength CAD/CAM-fabricated veneering material sintered to zirconia copings: A new fabrication mode for all-ceramic restorations', *Dent Mater*, 25, 121-128.

Boaretto, E., Wu, X., Yuan, J., Bar-Yosef, O., et al. (2009), 'Radiocarbon dating of charcoal and bone collagen associated with early pottery at Yuchanyan Cave, Hunan Province, China', *Proc Natl Acad Sci*, 106, 9595-9600.

Bonfante, E.A., Rafferty, B., Zavanelli, R.A., Silva, N.R.F.A., et al. (2010), 'Thermal/mechanical simulation and laboratory fatigue testing of an alternative yttria tetragonal zirconia polycrystal core veneer all ceramic layered crown design', *Eur J Oral Sci*, 118, 202-209.

Bornemann, G. (2003), 'Prospective clinical trial with conventionally luted zirconia-based fixed partial dentures:18-month results', *J Dent Res*, 82 (Sp issue B), 117.

Bulpakdi, P., Taskonak, B., Yan, J., and Mecholsky, J.J., Jr. (2009), 'Failure analysis of clinically failed all-ceramic fixed partial dentures using fractal geometry', *Dent Mater*, 25, 634-640.

Burke, F.J. (1999), 'Fracture resistance of teeth restored with dentin-bonded crowns constructed in a leucite-reinforced ceramic', *Dent Mater*, 15, 359-362.

Callister, W.D. (2007), Materials science and engineering: An introduction (7th ed.; New York: John Wiley & Sons New York).

Cao, X.Q., Vassen, R., and Stoever, D. (2004), 'Ceramic materials for thermal barrier coatings', *J Eur Ceram Soc*, 24, 1-10.

Capon, W.A. (1927), 'Porcelain: Its properties', *J. Am. Dent. Assoc*, 14, 1459-1463.

Cascone, P.J. (1979), 'Effect of thermal properties on porcelain-to-metal compatibility', *IADR Progr & Abst*, 58, No. 683.

Çehreli, M.C., Kökat, A.M., and Akça, K. (2009), 'CAD/CAM Zirconia vs. slip-cast glass-infiltrated alumina/zirconia all-ceramic crowns: 2-year results of a randomized controlled clinical trial', *J Appl Oral Sci*, 17, 49-55.

Chadwick, B. (2004), 'Good short-term survival of IPS-Empress crowns', *Evid Based Dent*, 5, 73.

Chang, P.P., Henegbarth, E.A., and Lang, L.A. (2007), 'Maxillary zirconia implant fixed partial dentures opposing an acrylic resin implant fixed complete denture: A two-year clinical report', *J Prosthet Dent*, 97, 321-330.

Chaudhri, M. and Liangyi, C. (1989), 'The orientation of the Hertzian cone crack in soda-lime glass formed by oblique dynamic and quasi-static loading with a hard sphere', *J Mat Sci*, 24, 3441-3448.

Chevalier, J., Cales, B., and Drouin, J.M. (1999), 'Low temperature aging of Y TZP ceramics', *J Am Ceram Soc*, 82, 2150-2154.

Chevalier, J. (2006), 'What future for zirconia as a biomaterial?', *Biomaterials*, 27, 535-543.

Christel, P., Meunier, A., Heller, M., Torre, J.P., et al. (1989), 'Mechanical properties and short-term in-vivo evaluation of yttrium-oxide-partially-stabilized zirconia', *J Biomed Mater Res*, 23, 45-61.

Cibirka, R.M., Nelson, S.K., Lang, B.R., and Rueggeberg, F.A. (2001), 'Examination of the implant-abutment interface after fatigue testing', *J Prosthet Dent*, 85, 268-275.

Coelho, P.G., Silva, N.R., Bonfante, E.A., Guess, P.C., et al. (2009a), 'Fatigue testing of two porcelain-zirconia all-ceramic crown systems', *Dent Mater*, 25, 1122-1127.

Coelho, P.G., Bonfante, E.A., Silva, N.R.F., Rekow, E.D., et al. (2009b), 'Laboratory simulation of Y-TZP all-ceramic crown clinical failures', *J Dent Res*, 88, 382-386.

Coffey, J.P., Anusavice, K.J., DeHoff, P.H., Lee, R.B., et al. (1988), 'Influence of contraction mismatch and cooling rate on flexural failure of PFM systems', *J Dent Res,* 67, 61-65.

Conrad, H.J., Seong, W., and Pesun, I.J. (2007), 'Current ceramic materials and systems with clinical recommendations: A systematic review', *J Prosthet Dent,* 98, 389-404.

Craig, R.G. and Powers, J.M. (2002), Mechanical properties in restorative dental material (11th ed.; New York, Mosby).

Creugers, N.H., Kayser, A.F., and van 't Hof, M.A. (1994), 'A meta-analysis of durability data on conventional fixed bridges', *Community Dent Oral Epidemiol,* 22, 448-452.

Crisp, R.J., Cowan, A.J., Lamb, J., Thompson, O., et al. (2008), 'A clinical evaluation of all-ceramic bridges placed in UK general dental practices: First-year results', *Br Dent J,* 205, 477-482.

Crispin, B.J. and Watson, J.F. (1981), 'Margin placement of esthetic veneer crowns. Part I: Anterior tooth visibility', *J Prosthet Dent,* 45, 278-282.

DeHoff, P.H. and Anusavice, K.J. (2009), 'Viscoelastic finite element stress analysis of the thermal compatibility of dental bilayer ceramic systems', *Int J Prosthodont,* 22, 56-61.

DeHoff, P.H., Anusavice, K.J., and Gray, A.E. (1990), 'Tempering as a means to strengthen porcelain-fused-to-metal restorations', *Biomed Sci Instrum,* 26, 167-174.

DeHoff, P.H., Anusavice, K.J., and Vontivillu, S.B. (1996), 'Analysis of tempering stresses in metal-ceramic disks', *J Dent Res,* 75, 743-751.

DeHoff, P.H., Barrett, A.A., Lee, R.B., and Anusavice, K.J. (2008), 'Thermal compatibility of dental ceramic systems using cylindrical and spherical geometries', *Dent Mater,* 24, 744-752.

DeLong, R. and Douglas, W. H. (1983), 'Development of an artificial oral environment for the testing of dental restoratives: bi-axial force and movement control', *J Dent Res*, 62, 32-36.

Denry, I. and Kelly, J.R. (2008), 'State of the art zirconia for dental applications', *Dent Mater*, 24, 299-307.

Devigus, A. and Lombardi, G. (2004), 'Shading Vita YZ substructures: influence on value and chroma, part I', *Int J Comput Dent*, 7, 293-301.

Devlin, H. and Wastell, D.G. (1986), 'The mechanical advantage of biting with the posterior teeth', *J Oral Rehab*, 13, 607-610.

Dodd, A. and Murfin, D. (1994), Dictionary of ceramics (3rd edn.; London, Institute of Materials).

Dong, J.K., Luthy, H., Wohlwend, A., and Schärer, P. (1992), 'Heat-pressed ceramics: technology and strength', *Int J Prosthodont*, 5, 9-16.

Dong, X., Yin, L., Jahanmir, S., Ives, LK, et al. (2000), 'Abrasive machining of glass-ceramics with a dental handpiece', *Mach Sci Tech*, 4, 209-233.

Donovan, T.E. and Chee, W.W. (2004), 'Cervical margin design with contemporary esthetic restorations', *Dent Clin North Am*, 48, 417-431.

Donovan, T.E. and Swift, E.J. (2009), 'Porcelain-fused-to-metal (PFM) alternatives ', *J Esthet Restor Dent*, 21, 4-6.

Drummond, J.L., Novickas, D., and Lenke, J.W. (1991), 'Physiological aging of an all-ceramic restorative material', *Dent Mater*, 7, 133-137.

Dunn, D.B. (2008), 'The use of a zirconia custom implant-supported fixed partial denture prosthesis to treat implant failure in the anterior maxilla: a clinical report', *J Prosthet Dent*, 100, 415-421.

Edelhoff, D., Florian, B., Florian, W., and Johnen, C. (2008), 'HIP zirconia fixed partial dentures: Clinical results after 3 years of clinical service', *Quintessence Int,* 39, 459-471.

El-Mowafy, O. and Brochu, J.F. (2002), 'Longevity and clinical performance of IPS-Empress ceramic restorations: A literature review', *J Can Dent Assoc,* 68, 233-237.

Etemadi, S. and Smales, R.J. (2006), 'Survival of resin-bonded porcelain veneer crowns placed with and without metal reinforcement', *J Dent,* 34, 139-145.

Fairhurst, C.W., Hashinger, D.T., and Twiggs, S.W. (1981), 'Glass transition temperatures of dental porcelain', *J Dent Res,* 60, 995-998.

Fairhurst, C.W., Hashinger, D.T., and Twiggs, S.W. (1989), 'The effect of thermal history on porcelain expansion behavior', *J Dent Res,* 68, 1313-1315.

Fairhurst, C.W., Lockwood, P.E., Ringle, R.D., and Thompson, W.O. (1992), 'The effect of glaze on porcelain strength', *Dent Mater,* 8, 203-207.

Fischer, H., Weber, M., and Marx, R. (2003), 'Lifetime prediction of all-ceramic bridges by computational methods', *J Dent Res,* 82, 238-242.

Fischer, H., Hemelik, M., Telle, R., and Marx, R. (2005), 'Influence of annealing temperature on the strength of dental glass ceramic materials', *Dent Mater,* 21, 671-677.

Fischer, J. and Stawarczyk, B. (2007), 'Compatibility of machined Ce-TZP/Al2O3 nanocomposite and a veneering ceramic', *Dent Mater,* 23, 1500-1505.

Fischer, J., Stawarczyk, B., and Hämmerle, C.H.F. (2008), 'Flexural strength of veneering ceramics for zirconia', *J Dent,* 36, 316-321.

Fischer, J., Stawarzcyk, B., Trottmann, A., and Hammerle, C.H. (2009a), 'Impact of thermal misfit on shear strength of veneering ceramic/zirconia composites', *Dent Mater,* 25, 419-423.

Fischer, J., Stawarczyk, B., Trottmann, A., and Hammerle, C.H. (2009b), 'Impact of thermal properties of veneering ceramics on the fracture load of layered Ce-TZP/A nanocomposite frameworks', *Dent Mater,* 25, 326-330.

Fradeani, M. and Redemagni, M. (2002), 'An 11-year clinical evaluation of leucite-reinforced glass-ceramic crowns: A retrospective study', *Quintessence Int,* 33, 503-510.

Fradeani, M., D'Amelio, M., Redemagni, M., and Corrado, M. (2005), 'Five-year follow-up with Procera all-ceramic crowns', *Quintessence Int,* 36, 105-113.

Garvie, R.C. (1965), 'The occurrence of metastable tetragonal zirconia as a crystallite size effect', *J Phys Chem,* 69, 1238-1243.

Ghazy, M.H. and Madina, M.M. (2006), 'Fracture resistance of metal- and galvano-ceramic crowns cemented with different luting cements: In vitro comparative study', *Int J Prosthodont,* 19, 610-612.

Giordano, R. (2006), 'Materials for chairside CAD/CAM-produced restorations', *J Am Dent Assoc,* 137, 14S-21S.

Glauser, R., Sailer, I., Wohlwend, A., Studer, S., et al. (2004), 'Experimental zirconia abutments for implant-supported single-tooth restorations in esthetically demanding regions: 4-year results of a prospective clinical study', *Int J Prosthodont,* 17, 285-290.

Gökçen-Röhlig, B., Saruhanoglu, A., Çifter, E.D., and Evlioglu, G. (2010), 'Applicability of zirconia dental prostheses for metal allergy patients', *Int J Prosthodont,* 23, 562-565.

Gong, W.B., Sha, C.K., Sun, D.Q., and Wang, W.Q. (2006), 'Microstructures and thermal insulation capability of plasma-sprayed nanostructured ceria stabilized zirconia coatings', *Surf Coat Technol,* 201, 3109-3115.

Good, M.L., Orr, J.F., and Mitchell, C.A. (2008), 'In vitro study of mean loads and modes of failure of all-ceramic crowns cemented with light-cured or dual-cured luting cement, after 1 and 30 d of storage', *Eur J Oral Sci,* 116, 83-88.

Gorman, C.M., McDevitt, W.E., and Hill, R.G. (2000), 'Comparison of two heat-pressed all-ceramic dental materials', *Dent Mater,* 16, 389-395.

Göstemeyer, G., Jendras, M., Dittmer, M.P., Bach, F.W., et al. (2010), 'Influence of the cooling rate on the zirconia/veneer interfacial adhesion', *Acta Biomater,* 6, 4532-4538.

Groten, M. and Huttig, F. (2010), 'The performance of zirconium dioxide crowns: A clinical follow-up', *Int J Prosthodont,* 23, 429-431.

Guazzato, M., Albakry, M., Swain, M.V., and Ironside, J. (2002), 'Mechanical properties of In-Ceram Alumina and In-Ceram Zirconia', *Int J Prosthodont* 15, 339-346.

Guazzato, M., Quach, L., Albakry, M., and Swain, M.V. (2005), 'Influence of surface and heat treatments on the flexural strength of Y-TZP dental ceramic', *J Dent,* 33, 9-18.

Guazzato, M., Albakry, M., Ringer, S.P., and Swain, M.V. (2004a), 'Strength, fracture toughness and microstructure of a selection of all-ceramic materials. Part II. Zirconia-based dental ceramics', *Dent Mater,* 20, 449-456.

Guazzato, M., Albakry, M., Ringer, S.P., and Swain, M.V. (2004b), 'Strength, fracture toughness and microstructure of a selection of all-ceramic materials. Part I. Pressable and alumina glass-infiltrated ceramics', *Dent Mater,* 20, 441-448.

Guazzato, M., Proos, K., Quach, L., and Swain, M.V. (2004c), 'Strength, reliability and mode of fracture of bilayered porcelain/zirconia (Y-TZP) dental ceramics', *Biomaterials,* 25, 5045-5052.

Guazzato, M., Walton, T. R., Franklin, W., Davis, G., et al. (2010), 'Influence of thickness and cooling rate on development of spontaneous cracks in porcelain/zirconia structures', *Aust Dent J,* 55, 306-310.

Guerini, V. (1909), A history of dentistry (Philadelphia, Lea & Febiger).

Guess, P.C., Kulis, A., Witkowski, S., Wolkewitz, M., et al. (2008), 'Shear bond strengths between different zirconia cores and veneering ceramics and their susceptibility to thermocycling', *Dent Mater,* 24, 1556-1567.

Guess, P.C., Zhang, Y., and Thompson, V.P. (2009), 'Effect of veneering techniques on damage and reliability of Y-TZP trilayers', *Eur J Esthet Dent,* 4, 262-276.

Gupta, P.K. and Jubb, N.J. (1981), 'Post indentation slow growth of radial cracks in glasses', *J Am Ceram Soc,* 64, 112-114.

Hadavi, F., Hey, J.H., Ambrose, E.R., Louie, P.W., et al. (1993), 'The effect of dentin primer on the shear bond strength between composite resin and enamel', *Oper Dent,* 18, 61-65.

Hjerppe, J., Narhi, T., Froberg, K., Vallittu, P.K., et al. (2008), 'Effect of shading the zirconia framework on biaxial strength and surface microhardness', *Acta Odontol Scand,* 66, 262-267.

ISO-Standard (1995), '6872, Dental ceramic', International Organization for Standardization; Geneva, Switzerland.

ISO- Standard (1999), '9693, Metal-ceramic bond characterisation (Schwickerath crack initiation test)', International Organization for Standardization; Geneva, Switzerland.

Johnston, J.F., Dykema, R.W., and Cunningham, D.M. (1958), 'Porcelain veneers bonded to gold castings: A progress report', *J Prosthet Dent,* 8, 120-122.

Jones, D.W. (1985), 'Development of dental ceramics: An historical perspective', *Dent Clin North Am,* 29, 621-644.

Jones, D.W. and Sutow, E.J. (1987), 'Stress corrosion failure of dental porcelain', *Br Ceram Trans J,* 86, 40-43.

Josephson, B.A., Schulman, A., Dunn, Z.A., and Hurwitz, W. (1985), 'A compressive strength study of an all-ceramic crown', *J Prosthet Dent,* 53, 301-303.

Jung, Y.G., Peterson, I.M., Kim, D.K., and Lawn, B.R. (2000), 'Lifetime-limiting strength degradation from contact fatigue in dental ceramics', *J Dent Res,* 79, 722-731.

Kelly, J.R. (1995), 'Perspectives on strength', *Dent Mater,* 11, 103-110.

Kelly, J.R. (1999), 'Clinically relevant approach to failure testing of all-ceramic restorations', *J Prosthet Dent,* 81, 652-661.

Kelly, J.R. and Denry, I. (2008a), 'Stabilized zirconia as a structural ceramic: An overview', *Dent Mater,* 24, 289-298.

Kelly, J.R., Campbell, S.D., and Bowen, H.K. (1989), 'Fracture-surface analysis of dental ceramics', *J Prosthet Dent,* 62, 536-541.

Kelly, J.R., Tesk, J.A., and Sorensen, J.A. (1995), 'Failure of all-ceramic fixed partial dentures in vitro and in vivo: Analysis and modeling', *J Dent Res,* 74, 1253-1258.

Kelly, J. R., Giordano, R., Pober, R., and Cima, M.J. (1990), 'Fracture surface analysis of dental ceramics: clinically failed restorations', *Int J Prosthodont,* 3, 430-440.

Kelly, J.R. (2004), 'Dental ceramics: current thinking and trends', *Dent Clin N Am,* 48, 513- 530.

Kelly, J.R. (2008), 'Dental ceramics: What is this stuff anyway?', *J Am Dent Assoc,* 139, 4S-7S.

Kelly, J.R. and Denry, I. (2008b), 'Stabilized zirconia as a structural ceramic: An overview', *Dent Mater,* 24, 289-298.

Kim, B., Zhang, Y., Pines, M., and Thompson, V.P. (2007), 'Fracture of porcelain-veneered structures in fatigue', *J Dent Res,* 86, 142-146.

Kim, D.K., Jung, Y.G., Peterson, I.M., and Lawn, B.R. (1999), 'Cyclic fatigue of intrinsically brittle ceramics in contact with spheres', *Acta Materialia,* 47, 4711-4725.

Kittel, C. (1986), Introduction to solid state physics (8 edn.; New York: Wiley).

Knap, F.J. and Ryge, G. (1966), 'Study of bond strength of dental porcelain fused to metal', *J Dent Res,* 45, 1047-1051.

Kobayashi, K., Kuwajima, H., and Masaki, T. (1981), 'Phase change and mechanical properties of ZrO2-Y2O3 solid electrolyte after aging', *Solid State Ion,* 3, 489-493.

Kokubo, Y., Tsumita, M., Kano, T., and Fukushima, S. (2011), 'The influence of zirconia coping designs on the fracture load of all-ceramic molar crowns', *Dent Mater J,* 30, 281-285.

Komine, F., Saito, A., Kobayashi, K., Koizuka, M., et al. (2010), 'Effect of cooling rate on shear bond strength of veneering porcelain to a zirconia ceramic material', *J Oral Sci,* 52, 647-652.

Kosmac, T., Oblak, C., Jevnikar, P., Funduk, N., et al. (1999), 'The effect of surface grinding and sandblasting on flexural strength and reliability of Y-TZP zirconia ceramic', *Dent Mater,* 15, 426-433.

Krejci, I., Lutz, F., and Reimer, M. (1994), 'Wear of CAD/CAM ceramic inlays: restorations, opposing cusps, and luting cements', *Quintessence Int,* 25, 199-207.

Lange, F.F., Dunlop, G.L., and Davis, B.I. (1986), 'Degradation during aging of transformation toughened ZrO_2 $Y2O_3$ materials at 250 ^{o}C', *J Am Ceram Soc,* 69, 237-240.

Larsson, C., Vult von Steyern, P., Sunzel, B., and Nilner, K. (2006), 'All-ceramic two- to five-unit implant-supported reconstructions. A randomized, prospective clinical trial', *Swed Dent J,* 30, 45-53.

Larsson, C., Holm, L., Lovgren, N., Kokubo, Y., et al. (2007), 'Fracture strength of four-unit Y-TZP FPD cores designed with varying connector diameter. An in-vitro study', *J Oral Rehabil,* 34, 702-709.

Lawn, B.R. and Marshall, D.B. (1977), 'Contact fracture resistance of physically and chemically tempered glass plates--a theoretical model', *Phy Chem Glass,* 18, 7-18.

Lawn, B.R., Deng, Y., and Thompson, V.P. (2001), 'Use of contact testing in the characterization and design of all-ceramic crownlike layer structures: A review', *J Prosthet Dent,* 86, 495-510.

Li, J.F., Watanabe, R., Zhang, B.P., Asami, K., et al. (1996), 'X ray photoelectron spectroscopy investigation on the low temperature degradation of 2 mol% Y_2O_3 ZrO_2 ceramics', *J Am Ceram Soc,* 79, 3109-3112.

Liewehr, F.R. (2001), 'An inexpensive device for transillumination', *J Endodont,* 27, 130-131.

López, M.V., Martínez, M.A., Mañes, J.F., Amigó, V., et al. (2010), 'Bond strength evaluation of the veneering-core ceramics bonds', *Med Oral Patol Oral Cir Bucal,* 15, 919-923.

Lorenzoni, F.C., Martins, L.M., Silva, N.R.F.A., Coelho, P.G., et al. (2010), 'Fatigue life and failure modes of crowns systems with a modified framework design', *J Dent,* 38, 626-634.

Lughi, V. and Sergo, V. (2010), 'Low temperature degradation-aging-of zirconia: A critical review of the relevant aspects in dentistry', *Dent Mater,* 26, 807-820.

Luthardt, R.G., Sandkuhl, O., and Reitz, B. (1999), 'Zirconia-TZP and alumina--advanced technologies for the manufacturing of single crowns', *Eur J Prosthodont Restor Dent,* 7, 113-119.

Luthardt, R.G., Holzhuter, M., Sandkuhl, O., Herold, V., et al. (2002), 'Reliability and properties of ground Y-TZP-zirconia ceramics', *J Dent Res*, 81, 487-491.

Luthy, H., Filser, F., Loeffel, O., Schumacher, M., et al. (2005), 'Strength and reliability of four-unit all-ceramic posterior bridges', *Dent Mater*, 21, 930-937.

Mainjot, A.K., Schajer, G.S., Vanheusden, A.J., and Sadoun, M.J. (2011), 'Residual stress measurement in veneering ceramic by hole-drilling', *Dent Mater*, 27, 439-444.

Malament, K.A. and Socransky, S.S. (2001), 'Survival of Dicor glass-ceramic dental restorations over 16 years. Part III: Effect of luting agent and tooth or tooth-substitute core structure', *J Prosthet Dent*, 86, 511-519.

Malament, K.A. and Socransky, S.S. (2010), 'Survival of Dicor glass-ceramic dental restorations over 20 years: Part IV. The effects of combinations of variables', *Int J Prosthodont*, 23, 134-140.

Marchack, B.W., Futatsuki, Y., Marchack, C.B., and White, S.N. (2008), 'Customization of milled zirconia copings for all-ceramic crowns: A clinical report', *J Prosthet Dent*, 99, 169-173.

Marshall, D.B. and Lawn, B.R. (1977), 'An indentation technique for measuring stresses in tempered glass surfaces', *J Am Ceram Soc*, 60, 86-87.

McLean, J.W. and Hughes, T.H. (1965), 'The reinforcement of dental porcelain with ceramic oxides', *Br Dent J*, 119, 251-267.

McLean, J.W. and von Fraunhofer, J.A. (1971), 'The estimation of cement film thickness by an in vivo technique', *Br Dent J*, 131, 107-111.

Meyenberg, K.H., Luthy, H., and Scharer, P. (1995), 'Zirconia posts: A new all-ceramic concept for nonvital abutment teeth', *J Esthet Dent*, 7, 73 - 80.

Michalske, T.A. and Freiman, S.W. (1982), 'A molecular interpretation of stress corrosion in silica', *Nature,* 295, 511-512.

Miller, L.L. (1977), 'Framework design in ceramo-metal restorations', *Dent Clin North Am,* 21, 699-716.

Molin, M.K. and Karlsson, S.L. (2008), 'Five-year clinical prospective evaluation of zirconia-based Denzir 3-unit FPDs', *Int J Prosthodont,* 21, 223-227.

Myers, M.L., Ergle, J.W., Fairhurst, C.W., and Ringle, R.D. (1994), 'Fatigue failure parameters of IPS-Empress porcelain', *Int J Prosthodont,* 7, 549-553.

Nam, J., Raigrodski, A.J., and Heindl, H. (2008), 'Utilization of multiple restorative materials in full-mouth rehabilitation: a clinical report', *J Esthet Restor Dent,* 20, 251-263; discussion 264-265.

Nielsen, J.P. and Tuccillo, J.J. (1972), 'Calculation of interfacial stress in dental porcelain bonded to gold alloy substrate', *J Dent Res,* 51, 1043-1047.

NIST, Bureau of Weights and Measures International (2008), 'The international system of units (SI)' (8 edn.; Gaithersburg: National Institute of Standards and Technology).

O'Brien, W.J. and Ryge, G. (1964), 'Relation between molecular force calculations and observed strengths of enamel-metal interfaces', *J Am Ceram Soc,* 47, 5-8.

Oh, W., Gotzen, N., and Anusavice, K.J. (2002), 'Influence of connector design on fracture probability of ceramic fixed-partial dentures', *J Dent Res,* 81, 623-627.

Ohlmann, B., Gabbert, O., Schmitter, M., Gilde, H., et al. (2005), 'Fracture resistance of the veneering on inlay-retained zirconia ceramic fixed partial dentures', *Acta Odontol Scand,* 63, 335-342.

Ohlmann, B., Rammelsberg, P., Schmitter, M., Schwarz, S., et al. (2008), 'All-ceramic inlay-retained fixed partial dentures: Preliminary results from a clinical study', *J Dent,* 36, 692-696.

Ohlmann, B., Marienburg, K., Gabbert, O., Hassel, A., et al. (2009), 'Fracture-load values of all-ceramic cantilevered FPDs with different framework designs', *Int J Prosthodont,* 22, 49-52.

Olsson, K.G., Fürst, B., Andersson, B., and Carlsson, G.E. (2003), 'A long-term retrospective and clinical follow-up study of In-Ceram Alumina FPDs', *Int J Prosthodont,* 16, 150-156.

Örtorp, A., Kihl, M.L., and Carlsson, G.E. (2009), 'A 3-year retrospective and clinical follow-up study of zirconia single crowns performed in a private practice', *J Dent,* 37, 731-736.

Ozkurt, Z., Kazazoglu, E., and Unal, A. (2010), 'In vitro evaluation of shear bond strength of veneering ceramics to zirconia', *Dent Mater J,* 29, 138-146.

Pallis, K., Griggs, J.A., Woody, R.D., Guillen, G.E., et al. (2004), 'Fracture resistance of three all-ceramic restorative systems for posterior applications', *J Prosthet Dent,* 91, 561-569.

Peitl, O., Serbena, F.C., Mastelaro, V.R., and Zanotto, E.D. (2010), 'Internal residual stress measurements in a bioactive glass–ceramic using Vickers indentation', *J Am Ceram Soc,* 93, 2359-2368.

Piconi, C. and Maccauro, G. (1999), 'Zirconia as a ceramic biomaterial', *Biomaterials,* 20, 1-25.

Pittayachawan, P., McDonald, A., Petrie, A., and Knowles, J.C. (2007), 'The biaxial flexural strength and fatigue property of Lava Y-TZP dental ceramic', *Dent Mater,* 23, 1018-1029.

Pjetursson, B.E., Sailer, I., Zwahlen, M., and Hämmerle, C.H.F. (2007), 'A systematic review of the survival and complication rates of all ceramic and metal–ceramic reconstructions after an observation period of at least 3 years. Part I: single crowns', *Clin Oral Impl Res,* 18, 73-85.

Pospiech, P.R., Rountree, P.R., and Nothdurft, F.P. (2003), 'Clinical evaluation of zirconia-based all-ceramic posterior bridges: two-year results', *J Dent Res,* 82, 114

Proos, K.A., Swain, M.V., Ironside, J., and Steven, G.P. (2002), 'Finite element analysis studies of an all-ceramic crown on a first premolar', *Int J Prosthodont,* 15, 404-412.

Quinn, G.D. (2007), 'Fractography of ceramics and glasses', NIST recommended practice guide; Special Publication 960-16 (Washington DC: National Institute of Standards and Technology).

Quinn, G.D. and Bradt, R.C. (2007), 'On the Vickers indentation fracture toughness test', *J Am Ceram Soc,* 90, 673-680.

Quinn, J.B., Sundar, V., Parry, E.E., and Quinn, G.D. (2010), 'Comparison of edge chipping resistance of PFM and veneered zirconia specimens', *Dent Mater,* 26, 13-20.

Rafferty, B.T., Janal, M.N., Zavanelli, R.A., Silva, R.F., et al. (2010), 'Design features of a three-dimensional molar crown and related maximum principal stress. A finite element model study', *Dent Mater,* 26, 156-163.

Raigrodski, A.J., Chiche, G.J., Potiket, N., Hochstedler, J.L., et al. (2006), 'The efficacy of posterior three-unit zirconium-oxide-based ceramic fixed partial dental prostheses: a prospective clinical pilot study', *J Prosthet Dent,* 96, 237-244.

Raigrodski, A.J. (2004a), 'Contemporary materials and technologies for all-ceramic fixed partial dentures: a review of the literature', *J Prosthet Dent,* 92, 557-562.

Raigrodski, A.J. (2004b), 'Contemporary all-ceramic fixed partial dentures: a review', *Dent Clin North Am,* 48, 531-544.

Rawson, H. (1974), 'Physics of glass manufacturing processes', *Physics Technol,* 5, 91-114.

Reich, S., Kappe, K., Teschner, H., and Schmitt, J. (2008), 'Clinical fit of four-unit zirconia posterior fixed dental prostheses', *Eur J Oral Sci,* 116, 579-584.

Rekow, D. and Thompson, V.P. (2005), 'Near-surface damage-a persistent problem in crowns obtained by computer-aided design and manufacturing', *Proc IME H J Eng Med,* 219, 233-243.

Rekow, D. and Thompson, V.P. (2007), 'Engineering long term clinical success of advanced ceramic prostheses', *J Mater Sci Mater Med,* 18, 47-56.

Reuter, J.E. and Brose, M.O. (1984), 'Failures in full crown retained dental bridges', *Br Dent J,* 157, 61-63.

Roediger, M., Gersdorff, N., Huels, A., and Rinke, S. (2010), 'Prospective evaluation of zirconia posterior fixed partial dentures: four-year clinical results', *Int J Prosthodont,* 23, 141-148.

Roesler, F. (1956), 'Brittle fracture near equilibrium', *Proc Phy Soc B,* 69, 981-992.

Rosenstiel, S.F., Land, M.F., and Fujimoto, J. (2006), Contemporary fixed prosthodontics (4th edn.; St Louis, Mosby Elsevier).

Rosentritt, M., Behr, M., Thaller, C., Rudolph, H., et al. (2009), 'Fracture performance of computer-aided manufactured zirconia and alloy crowns', *Quintessence Int,* 40, 655-662.

Rues, S., Kröger, E., Müller, D., and Schmitter, M. (2010), 'Effect of firing protocols on cohesive failure of all-ceramic crowns', *J Dent,* 38, 987-994.

Sailer, I., Zembic, A., Jung, R.E., Siegenthaler, D., et al. (2009), 'Randomized controlled clinical trial of customized zirconia and titanium implant abutments for canine and

posterior single-tooth implant reconstructions: preliminary results at 1 year of function', *Clin Oral Implants Res,* 20, 219-225.

Sailer, I., Feher, A., Filser, F., Gauckler, L.J., et al. (2007), 'Five-year clinical results of zirconia frameworks for posterior fixed partial dentures', *Int J Prosthodont,* 20, 383-388.

Sailer, I., Feher, A., Filser, F., Luthy, H., et al. (2006), 'Prospective clinical study of zirconia posterior fixed partial dentures: 3-year follow-up', *Quintessence Int,* 37, 685-693.

Sato, T. and Shimada, M. (1985a), 'Transformation of yttria doped tetragonal ZrO2 polycrystals by annealing in water', *J Am Ceram Soc,* 68, 356-356.

Sato, T. and Shimada, M. (1985b), 'Transformation of ceria-doped tetragonal zirconia polycrystals by annealing in water', *Am Ceram Soc Bull,* 64, 1382-1384.

Savage, G. (1965), Porcelain through the ages (2nd edn.; London, Penguin Books).

Scherrer, S.S., de Rijk, W.G., Belser, U.C., and Meyer, J.M. (1994), 'Effect of cement film thickness on the fracture resistance of a machinable glass-ceramic', *Dent Mater,* 10, 172-177.

Schmidt, C. and Weigl, P. (2000), 'Machinability of IPS Empress 2 framework ceramic', *J Biomed Mater Res,* 53, 348-352.

Schmitt, J., Wichmann, M., Holst, S., and Reich, S. (2010), 'Restoring severely compromised anterior teeth with zirconia crowns and feather-edged margin preparations: A 3-year follow-up of a prospective clinical trial', *Int J Prosthodont,* 23, 107-109.

Schmitter, M., Mussotter, K., Rammelsberg, P., Stober, T., et al. (2009), 'Clinical performance of extended zirconia frameworks for fixed dental prostheses: two-year results', *J Oral Rehabil,* 36, 610-615.

Shell, J.S. and Nielsen, J.P. (1962), 'Study of the bond between gold alloys and porcelain', *J Dent Res,* 41, 1424-1437.

Silva, N., Bonfante, E.A., Rafferty, B.T., Zavanelli, R.A., et al. (2011), 'Modified Y-TZP core design improves all-ceramic crown reliability', *J Dent Res*, 90, 104-108.

Song, X.F. and Yin, L. (2010), 'The quantitative effect of diamond grit size on the subsurface damage induced in dental adjustment of porcelain surfaces', *Proc IMecE Part H: J Eng. Med*, 224, 1185-1194.

Song, X., Yin, L., Han, Y., and Li, J. (2008), 'Finite element analysis of subsurface damage of ceramic prostheses in simulated intraoral dental resurfacing', *J Biomed Mater Res B: Appl Biomater*, 85, 50-59.

Spear, F.M. (2001), 'The metal-free practice: Myth? Reality desirable goal? ', *J Esthet Restor Dent*, 13, 59-67.

Stichert, W. and Schüth, F. (1998), 'Influence of crystallite size on the properties of zirconia', *Chem Mater*, 10, 2020-2026.

Studart, A. R., Filser, F., Kocher, P., and Gauckler, L. J. (2007), 'In vitro lifetime of dental ceramics under cyclic loading in water', *Biomaterials*, 28, 2695-2705.

Sundh, A. and Sjogren, G. (2004), 'A comparison of fracture strength of yttrium-oxide-partially-stabilized zirconia ceramic crowns with varying core thickness, shapes and veneer ceramics', *J Oral Rehabil*, 31, 682-688.

Sundh, A. and Sjogren, G. (2006), 'Fracture resistance of all-ceramic zirconia bridges with differing phase stabilizers and quality of sintering', *Dent Mater*, 22, 778-784.

Sundh, A. and Sjogren, G. (2008), 'A study of the bending resistance of implant-supported reinforced alumina and machined zirconia abutments and copies', *Dent Mater*, 24, 611-617.

Swain, M.V. (2009), 'Unstable cracking (chipping) of veneering porcelain on all-ceramic dental crowns and fixed partial dentures', *Acta Biomater*, 5, 1668-1677.

Tada, H., Paris, P.C., and Irwin, G.R. (2000), The stress analysis of cracks handbook (3rd edn., New York: ASME press).

Tan, K., Pjetursson, B.E., Lang, N.P., and Chan, E.S.Y. (2004), 'A systematic review of the survival and complication rates of fixed partial dentures (FPDs) after an observation period of at least 5 years', *Clin Oral Impl Res*, 15, 654-666.

Taskonak, B., Mecholsky, J.J., and Anusavice, K.J. (2006), 'Fracture surface analysis of clinically failed fixed partial dentures', *J Dent Res*, 85, 277-281.

Taskonak, B., Yan, J., Mecholsky, J.J., Jr., Sertgoz, A., et al. (2008a), 'Fractographic analyses of zirconia-based fixed partial dentures', *Dent Mater*, 24, 1077-1082.

Taskonak, B., Borges, G.A., Mecholsky, J.J., Jr., Anusavice, K.J., et al. (2008b), 'The effects of viscoelastic parameters on residual stress development in a zirconia/glass bilayer dental ceramic', *Dent Mater*, 24, 1149-1155.

Taskonak, B., Griggs, J.A., Mecholsky, J.J., Jr, and Yan, J. (2008c), 'Analysis of subcritical crack growth in dental ceramics using fracture mechanics and fractography', *Dent Mater*, 24, 700-707.

Tatarko, P., Lojanová, Š., Dusza, J., and Šajgalík, P. (2009), 'Fracture toughness of Si_3N_4 based ceramics with rare-earth oxide sintering additives', *Key Eng Mater*, 409, 377-381.

Tholey, M.J., Swain, M.V., and Thiel, N. (2009), 'SEM observations of porcelain Y-TZP interface', *Dent Mater*, 25, 857-862.

Thompson, J.Y., Anusavice, K.J., Naman, A., and Morris, H.F. (1994), 'Fracture surface characterization of clinically failed all-ceramic crowns', *J Dent Res*, 73, 1824-1832.

Thompson, V.P. and Rekow, D.E. (2004), 'Dental ceramics and the molar crown testing ground', *J Appl Oral Sci*, 12, 26-36.

Timoshenko, S. (1925), 'Analysis of bi-metal thermostats', *J. Opt. Soc. Am*, 11, 233-255.

Tinschert, J., Schulze, K.A., Natt, G., Latzke, P., et al. (2008), 'Clinical behavior of zirconia-based fixed partial dentures made of DC-Zirkon: 3-year results', *Int J Prosthodont,* 21, 217-222.

Tsalouchou, E., Cattell, M.J., Knowles, J.C., Pittayachawan, P., et al. (2008), 'Fatigue and fracture properties of yttria partially stabilized zirconia crown systems', *Dent Mater,* 24, 308-318.

Tsukuma, K. (1986), 'Mechanical properties and thermal stability of CeO/sub 2/containing tetragonal zirconia polycrystals', *Am Ceram Soc Bull,* 65, 1386-1389.

Tuan, W.H. and Kuo, J.C. (1999), 'Contribution of residual stress to the strength of abrasive ground alumina', *J Eur Ceram Soc,* 19, 1593-1597.

Tuccillo, J.J. and Nielsen, J.P. (1972), 'Shear stress measurements at a dental porcelain-gold bond interface', *J Dent Res,* 51, 626-633.

Vagkopoulou, T., Koutayas, S.O., Koidis, P., and Strub, J.R. (2009), 'Zirconia in dentistry: Part 1. Discovering the nature of an upcoming bioceramic', *Eur J Esthet Dent,* 4, 130-151.

Vult von Steyern, P., Ebbesson, S., Holmgren, J., Haag, P., et al. (2006), 'Fracture strength of two oxide ceramic crown systems after cyclic pre loading and thermocycling', *J Oral Rehabil,* 33, 682-689.

Vult von Steyern, P., Carlson, P., and Nilner, K. (2005), 'All-ceramic fixed partial dentures designed according to the DC-Zirkon technique. A 2-year clinical study', *J Oral Rehabil,* 32, 180-187.

Vult von Steyern, P., Jönsson, O., and Nilner, K. (2001), 'Five-year evaluation of posterior all-ceramic three-unit (In-Ceram) FPDs', *Int J Prosthodont,* 14, 379-384.

Walton, T.R. (2002), 'An up to 15-year longitudinal study of 515 metal-ceramic FPDs: Part 1. Outcome', *Int J Prosthodont,* 15, 439-445.

Walton, T.R. and O'Brien, W.J. (1985), 'Thermal stress failure of porcelain bonded to a palladium-silver alloy', *J Dent Res,* 64, 476-480.

Walton, T.R. (1999), 'A 10-year longitudinal study of fixed prosthodontics: clinical characteristics and outcome of single-unit metal-ceramic crowns', *Int J Prosthodont,* 12, 519-526.

Wang, H., Aboushelib, M.N., and Feilzer, A.J. (2008), 'Strength influencing variables on CAD/CAM zirconia frameworks', *Dent Mater,* 24, 633-638.

Wenz, H.J., Bartsch, J., Wolfart, S., and Kern, M. (2008), 'Osseointegration and clinical success of zirconia dental implants: A systematic review', *Int J Prosthodont,* 21, 27 - 36.

Wiskott, H.W., Nicholls, J.I., and Belser, U.C. (1995), 'Stress fatigue: Basic principles and prosthodontic implications', *Int J Prosthodont,* 8, 105-116.

Wolfart, S. and Kern, M. (2006), 'A new design for all-ceramic inlay-retained fixed partial dentures: a report of 2 cases', *Quintessence Int,* 37, 27-33.

Wolfart, S., Harder, S., Eschbach, S., Lehmann, F., et al. (2009), 'Four year clinical results of fixed dental prostheses with zirconia substructures (Cercon): end abutments vs. cantilever design', *Eur J Oral Sci,* 117, 741-749.

Yin, L., Jahanmir, S., and Ives, L.K. (2003), 'Abrasive machining of porcelain and zirconia with a dental handpiece', *Wear,* 255, 975-989.

Yin, L., Han, Y. G., Song, X. F., Li, J., et al. (2007), 'In vitro study on high rotation deep removal of ceramic prostheses in dental surgery', *J Biomed Mater Res B: Appl Biomater,* 82B, 334-345.

Yin, L., Song, X.F., Qu, S.F., Han, Y.G., et al. (2006), 'Surface integrity and removal mechanism in simulated dental finishing of a feldspathic porcelain', *J Biomed Mater Res B: Appl Biomater,* 79B, 365-378.

Yuodelis, R.A., Weaver, J.D., and Sapkos, S. (1973), 'Facial and lingual contours of artificial complete crown restorations and their effects on the periodontium', *J Prosthet Dent*, 29, 61-66.

Zahran, M., El-Mowafy, O., Tam, L., Watson, P.A., et al. (2008), 'Fracture strength and fatigue resistance of all-ceramic molar crowns manufactured with CAD/CAM technology', *J Prosthodont*, 17, 370-377.

Zallat, J. (2006), 'Optimal configurations for imaging polarimeters: impact of image noise and systematic errors', *J Optic Pure Appl Optic*, 8, 807- 814.

Zarone, F., Sorrentino, R., Traini, T., Di lorio, D., et al. (2007), 'Fracture resistance of implant-supported screw- versus cement-retained porcelain fused to metal single crowns: SEM fractographic analysis', *Dent Mater*, 23, 296-301.

Zembic, A., Sailer, I., Jung, R.E., and Hämmerle, C.H. (2009), 'Randomized-controlled clinical trial of customized zirconia and titanium implant abutments for single-tooth implants in canine and posterior regions: 3-year results', *Clin Oral Implants Res*, 20, 802-808.

Zhang, Y. and Kim, J.W. (2010a), 'Graded zirconia glass for resistance to veneer fracture', *J Dent Res*, 89, 1057-1062.

Zhang, Y., Song, J.K., and Lawn, B.R. (2005), 'Deep-penetrating conical cracks in brittle layers from hydraulic cyclic contact', *J Biomed Mater Res B Appl Biomater*, 73, 186-193.

Zhang, Y., Lawn, B.R., Rekow, D.E., and Thompson, V.P. (2004), 'Effect of sandblasting on the long-term performance of dental ceramics', *J Biomed Mater Res B Appl Biomater*, 71B, 381-386.

Zhang, Z., Li, Q., Li, W., and Swain, M.V. (2009), 'Transient modelling of thermal processing for ceramic prostheses', *J Aust Ceram Soc* 45, 40-48.

Zhang, Z.P., Zhou, S.W., Li, Q., Li, W., et al. (2010b), 'Residual stresses in fabrication of core-veneered ceramic prostheses', *Adv Mater Res*, 97- 101, 2241-2244.

APPENDIX

Poster presentation:

International College of Prosthodontists,

14th Biennial meeting,

Big Island of Hawaii, September 8th – 12th 2011

Al-Amleh B, Waddell N, Lyons K, Jansen Van Vuuren L, He C, Swain M.V.

Influence of cusp veneering porcelain thickness and cooling rate on residual stresses in zirconia crowns

Purpose: Chipping of the veneering porcelain has been recognised as the main disadvantage of zirconia restorations, believed to be due to its propensity to develop large thermal gradients within the veneering porcelain layer. This occurs when the porcelain cools from above to below the glass transition temperature during the final firing cycle resulting in high residual tensile zones within the veneering porcelain. In addition to the cooling rate, thickness of the veneering porcelain has also been identified as a contributing factor by further increasing thermal gradients. So far there are no studies that have integrated the relationship between veneering porcelain thickness, cooling rate, and differences in surface residual stresses on anatomical zirconia crowns.

Methods & Materials: Six identical Procera zirconia copings (Procera, Nobel Biocare) were pressed with IPS e.max ZirPress (Ivoclar Vivadent) and layered with IPS e.max Ceram (Ivoclar Vivadent) based on a mandibular molar form, were divided into 3 groups to the following flattened cusp heights: 1mm, 2mm, and 3mm. Half the samples were slow-cooled during the final glazing cycle and the other half fast-cooled. To determine the residual surface stresses, 4 cusps on each crown were indented using a Vickers microhardness indenter under a load of 10N; crack measurements were made immediately after each indentation using an optical light microscope.

Results: All fast-cooled crowns exhibited residual surface compressive stresses, while on the slow group tensile stresses were recorded. The highest residual compressive stresses were found on fast-cooled 1mm thick porcelain cusps (-12.75 MPa) which was significantly higher than 2mm and 3mm fast-cooled crowns. The highest residual tensile stresses were recorded for slow-cooled 2 mm cusps (5.89 MPa), however there were no significant statistical differences in the later group.

Conclusion: The results confirm that residual surface compressive stresses at the cusp tips were significantly higher in the fast-cooled crowns than the slow-cooled crowns. No correlation was found between residual surface compressive stresses with increasing veneering porcelain thickness.